ISBN 978-82-326-6077-3 (printed ver.)
ISBN 978-82-326-6007-0 (electronic ver.)
ISSN 1503-8181 (printed ver.)
ISSN 2703-8084 (electronic ver.)

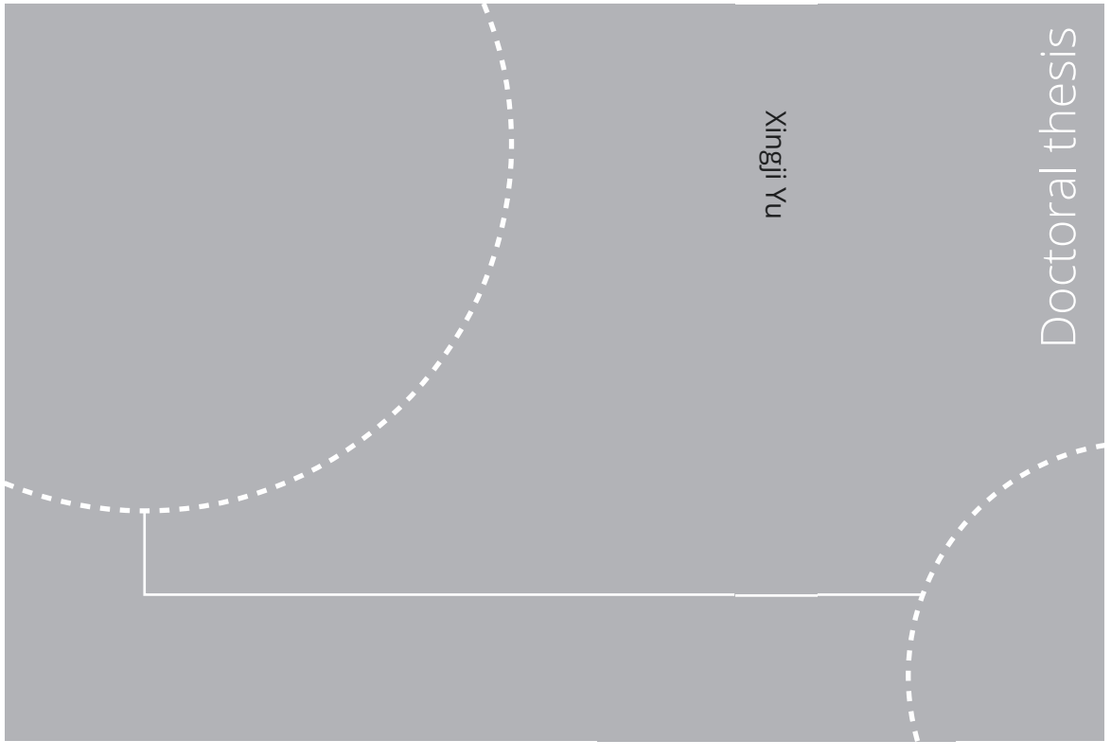

Doctoral theses at NTNU, 2022:324

Xingji Yu

Grey-box modeling of the building thermal dynamics for MPC applications

The case of residential space-heating

Doctoral theses at NTNU, 2022:324

NTNU
Norwegian University of Science and Technology

NTNU
Norwegian University of Science and Technology
Thesis for the degree of Philosophiae Doctor
Faculty of Engineering
Department of Energy and Process Engineering

NTNU
Norwegian University of Science and Technology

Xingji Yu

Grey-box modeling of the building thermal dynamics for MPC applications

The case of residential space-heating

Thesis for the degree of Philosophiae Doctor

Trondheim, "OCT" "2022"

Norwegian University of Science and Technology
Faculty of Engineering
Department of Energy and Process Engineering

NTNU
Norwegian University of
Science and Technology

NTNU
Norwegian University of Science and Technology

Thesis for the degree of Philosophiae Doctor

Faculty of Engineering
Department of Energy and Process Engineering

ISBN 978-82-326-6077-3 (printed ver.)
ISBN 978-82-326-6007-0 (electronic ver.)
ISSN 1503-8181 (printed ver.)
ISSN 2703-8084 (electronic ver.)

Doctoral theses at NTNU, 2022:324

PRINTED IN NORWAY
NO - 1598

NORDIC SWAN ECOLABEL
Printed matter
2041 0731

Printed by Skipnes Kommunikasjon AS

PREFACE

This thesis is submitted to the Norwegian University of Science and Technology in partial fulfillment of the requirements for the degree of Doctor of Philosophy (PhD).

I have carried out this work at the Department of Energy and Process Engineering, NTNU. The work was under the main supervision of Associate Professor Laurent Georges from NTNU and the co-supervision of Professor Lars Imsland and Igor Sartori from NTNU and SINTEF Community, respectively.

This PhD project was under financial support from the internal fund from the Department of Energy and Process Engineering of NTNU.

Trondheim, April 2022

Xingji Yu

ABSTRACT

The transition from a conventional energy system to a decarbonized energy system requires an increasing penetration of intermittent renewable energy sources, which brings more fluctuations to the electricity grid. Therefore, increased flexibility is required on the demand side.

This thesis focuses on the energy flexibility of residential buildings by activating their thermal mass. Model predictive control (MPC) is acknowledged to be an appropriate control method for this purpose. The thesis addresses MPC using grey-box linear models of the building thermal dynamics. The research is split into two main parts, namely modeling and control. The modeling part can also be further split into data collection and model identification subsections.

In the data collection part, the experiments for collecting the data are designed for both virtual and field experiments. The experimental design includes the selection of the excitation signal, the training period, and for field experiments, the influence of the sensor location and dynamics. Thus, different experiments with various excitation signals and training periods have been executed. The results show that the identified parameters are strongly dependent on the types of excitation and the training period for deterministic grey-box models. On the contrary, the identified parameters are less dependent on the excitation signal for stochastic grey-box models. Furthermore, there is no specific period of the space-heating season that is more suited to train a linear time invariant (LTI) grey-box model since weather conditions including solar radiation vary significantly during the entire space-heating season.

In the model identification part, a suitable model structure is first investigated using different resistance-capacitance (RC) networks based on existing standards for building energy modeling (like the EN13790 and VDI 6007 standards) and the knowledge of building physics. The model selection is based on the structural and practical identifiability, the physical plausibility and the prediction performance of the grey-box model. The results show that for a mono-zone grey-box model, the second-order model is an appropriate trade-off between overfitting or poor model fidelity. The optimizer for the training of the model parameters is also investigated by comparing the parameters identified using traditional gradient-based optimization routines and global optimization routines. Results reveal that global optimization performs better than gradient-based optimization. The influence of data pre-processing on the grey-box modeling is investigated by using a low-pass filter as well as the influence of input data alignment using anti-causal shift (ACS). Results show that the pre-processing of data does not have a large influence on deterministic models. However, for stochastic models, the parameter values are significantly influenced by the data pre-processing. The identified parameters are strongly correlated with the sampling time (T_s). ACS can prevent the parameter value and variance from getting non-physical for large Ts. Pre-filtering only has a limited

influence with ACS, while the pre-filtering influence without ACS does not have a clear trend. Some research is done in this thesis to compare the performance between grey-box and black-box models in the case of deterministic models. Results show that the second-order black-box model shows a similar performance to the second-order grey-box model. However, the physical interpretation of the hidden states and parameters is unknown for black-box models.

In the control part, the performance of conventional MPC based on LTI models and adaptive MPC that are able to recalibrate the model parameters during operation is compared. The adaptive MPC is designed to overcome the influence of varying weather conditions during the heating season. Two different candidates for this adaptive control are investigated. Partially Adaptive MPC only updates the effective window area of the grey-box model. The Fully Adaptive MPC updates all the parameters of the grey-box model. Results show that the Partially Adaptive MPC is not able to deliver satisfactory prediction performance due to the limited number of parameters updated. The Fully Adaptive MPC outperforms the conventional MPC based on LTI models, especially in avoiding thermal discomfort. Different types of models (e.g., ARX, NARX, SVM) are also compared in an MPC experiment in a supporting paper of this thesis. Results show that the seven states black-box state-space model has the best performance among the MPCs in the study. Using multi-step ahead prediction error as the objective function when training the model is beneficial for guaranteeing its prediction performance.

Keywords

Energy flexibility; demand response; demand side flexibility; model predictive control; model complexity; data pre-processing; time varying electricity prices; co-simulation

ACKNOWLEDGMENTS

It is a great pleasure for me to finish the journey of this PhD. I have met so many kind and inspiring people during this journey. It has been a wonderful experience for me in the last four years.

First and foremost, I want to express my deep gratitude to my main supervisor Laurent Georges, for all his support, patience, personal advice and scientific guidance during my PhD study. I highly appreciate the relaxed work environment that you created for me. The open-door policy and the flexible working time make our relationship friendly instead of a stricter teacher-student interaction, which helped me to get rid of much stress from my PhD study. All our discussions, your encouragement and your instructions help me to go through all the difficulties of this project and shape my PhD research.

I would like to acknowledge my co-supervisor Lars Imsland. His high efficiency and professional knowledge significantly improved the quality of my research. This PhD work would not be achievable without your supervision and feedback.

I wish to thank my co-supervisor Igor Sartori at SINTEF Community for introducing me to the FME ZEN project, to a first research question and IEA EBC Annex 81, which allowed me to learn new knowledge from researchers of different advanced research institutes.

I want to say thanks to the researchers involved in Annex 71 for the inspiring and innovative meetings and discussions. Special thanks to Arash Erfani from KU Leuven, Kristian Skeie from NTNU and Michael Dahl Knudsen from Aarhus University for the joyful collaboration during my PhD project. I would also thank all my coauthors with whom I had the pleasure to cooperate.

Thanks to my office mates Vegard Heide, Elyas Larkermani, Martin Thalfeldt and John Clauß for the good atmosphere and your friendliness and tolerant attitudes. Thanks also to my close friends Zhengru Ren, Yuemin Ding, Haoshui Yu, Jinping Gu and Xin Li for the support, discussion and wonderful moments that we went through together.

Last but not least, to my most important family. I would like to thank my parents, Menghong Yu and Yuxing Pan, for supporting and encouraging me to pursue my goal. A special thanks to my girlfriend Qi Zhu for all your support, patience and understanding throughout the period of my PhD study.

LIST OF PAPERS

Paper 1:

Yu X, Georges L, Knudsen MD, Sartori I, Imsland L. Investigation of the Model Structure for Low-Order Grey-Box Modelling of Residential Buildings. *Proceedings of Building Simulation 2019 16th Conference IBPSA*, International Building Performance Simulation Association (IBPSA), 2nd-4th September 2019, Rome, Italy.

Paper 2:

Yu X, Georges L. Influence of Data Pre-Processing Techniques and Data Quality for Low-Order Stochastic Grey-Box Models of Residential Buildings. *International Conference Organised by IBPSA-Nordic*, 13th–14th October 2020, Oslo, Norway. BuildSIM-Nordic 2020 (BSN2020). Selected papers. SINTEF Academic Press.

Paper 3:

Yu X, Georges L, Imsland L. Data pre-processing and optimization techniques for stochastic and deterministic low-order grey-box models of residential buildings. *Energy and Buildings*. 2021; 236: 110775.

Paper 4:

Yu X, Skeie KS, Knudsen MD, Ren Z, Imsland L, Georges L. Influence of data pre-processing and sensor dynamics on grey-box models for space-heating: Analysis using field measurements. *Building and Environment*, 2022; 108832.

Paper 5:

Yu X, Georges L, Imsland L. Adaptive linear grey-box models for Model Predictive Controller of Residential Buildings. Accepted to *International Conference Organised by IBPSA-Nordic*, 22nd-23rd August 2022, Copenhagen, Denmark. BuildSIM-Nordic 2022 (BSN2022).

Paper 6:

Yu X, Ren Z, Georges L, Imsland L. Comparison of Time-Invariant and Adaptive Linear Grey-box Models for Model Predictive Control of Residential Buildings. Submitted to *Applied Energy*

Paper 7:

Erfani A, Yu X, Kull TM, Bacher P, Jafarinejad T, Roels S, Saelens D. Analysis of the impact of predictive models on the quality of the model predictive control for an experimental building. *Proceedings of Building Simulation 2021 17th Conference IBPSA*, International Building Performance Simulation Association (IBPSA), 1st-3rd September 2021, Bruges, Belgium.

ABBREVIATIONS

ACS	Anti-causal shift
AMS	Advanced metering system
AHU	Air-handling units
BMS	Building management system
BPS	Building performance simulation
Det	Deterministic model
DSM	Demand side management
DS	Direct sampling
DR	Demand response
EMPC	Economic model-predictive control
FHS	Full heating season
FIR	Finite impulse response
GA	Genetic algorithm
HC	Heat capacitance
HVAC	Heating, ventilation and air-conditioning
HTC	Heat transfer coefficient
LTI	Linear time-invariat
KPI	Key performance indicator
MA	Moving average
MBE	Mean bias error
MPC	Model-predictive control
MSPE	Multi-Step ahead prediction error
NRMSE	Normalized root mean squared error
P	Proportional
RC	Resistance and capacitance
PH	Passive house
PI	Proportional integral
PID	Proportional integral derivative
PRBC	Predictive rule-based control
PRBS	Pseudo-random binary signal
PSO	Particle swarm optimization
RES	Renewable energy sources

ABBREVIATIONS

SNR	Signal to noise ratio
SH	Space heating
Sto	Stochastic model
TABS	Thermally activated building systems
ZEB	Zero emission building

LIST OF CONTENTS

PREFACE ..... **i**

ABSTRACT ..... **ii**

ACKNOWLEDGMENTS ..... **iv**

LIST OF PAPERS ..... **v**

ABBREVIATIONS ..... **vi**

LIST OF CONTENTS ..... **viii**

LIST OF TABLES ..... **x**

LIST OF FIGURES ..... **xi**

1 INTRODUCTION **1**

1.1 Background and motivation 1

1.2 Research questions and research tasks 5

1.3 Structure of the thesis 7

1.4 List of publications 7

2 RESEARCH CONTEXT AND BACKGROUND **11**

2.1 Demand response with MPC 11

2.2 Review of grey-box modeling for building thermal dynamics 12

3 METHODOLOGY **28**

3.1 Description of experiments 28

3.1.1 ZEB Living Lab and corresponding experiments 28

3.1.2 IDA ICE building model and corresponding experiments 32

3.2 System identification for the building 35

3.2.1 Grey-box modeling 35

3.2.2 Structural and practical identifiability 40

3.2.3 Key performance indicators 41
3.3 MPC experiments setup 42
3.3.1 Optimal Control Problem Formulation 43
3.3.2 Conventional and Adaptive MPC 45
4 RESULTS AND DISCUSSION 49
4.1 Modeling (data collection) 49
4.2 Modeling (train parameters) 62
4.3 Control (MPC) 66
4.3.1 LTI grey-box MPC vs adaptive grey-box MPC 66
4.3.2 Other Types of MPC 79
5 CONCLUSIONS AND FUTURE RESEARCH 83
5.1 Concluding remarks 83
5.2 Limitations 86
5.3 Future research 87
BIBLIOGRAPHY 89
RESEARCH PUBLICATIONS 97

LIST OF TABLES

Table 1-1: Relation between research questions and papers. 10

Table 2-1: Summary of grey-box models for the building thermal dynamics. 25

Table 3-1: Summary of the four experiments. “Full set” means all measurements of volume-averaged, single sensor (no casing), wall-mounted sensor are available. ... 30

Table 3-2: Weather conditions in four PRBS experiments. 34

Table 3-3: Description of the datasets and their corresponding abbreviation. 35

Table 3-4: The physical interpretation of the parameters of all grey-box models. . 37

Table 3-5: Cases summary of experiments. 47

Table 4-1: Description of the datasets and their corresponding abbreviations from ZEB Living Lab. 52

Table 4-2: The values and the corresponding variance of C_e. 64

Table 4-3: Optimizer leading to the lowest prediction error: each cell of the table has two symbols, one for the case without ACS (left) and the other with ACS (right); the symbol “D” means default greyest, “G” means global optimization and “$\approx$” means equal performance. 65

Table 4-4: Trained parameter values of the LTI models 67

Table 4-5: Summary of the MPC performance for the energy saving case 67

Table 4-6: Results summary of MPC controllers' performance for energy cost saving (EMPC) case 70

Table 4-7: Results summary of MPC controllers' performance for energy cost saving (EMPCPR) case. 74

LIST OF FIGURES

Figure 1-1: Research questions grouped by categories. 7

Figure 1-2: Interconnections of the papers included in this thesis. 10

Figure 2-1: Thermal network representation of the used grey-box model [60]. 13

Figure 2-2: 5R3C Grey-box model structures: (a) Model I: model trained from detailed building simulation tools, and (b) Model II: model modified from ISO 13790 [63]. 13

Figure 2-3: Modified RC network of the model used in ISO 13790 [37]. 14

Figure 2-4: Model structures depicted as RC-networks. Red text denotes inputs, blue highlights the assumptions made for third-order models [66]. 15

Figure 2-5: Schematic of the grey-box thermal model of residential buildings (5R4C) [38]. 15

Figure 2-6: RC-analogy of reduced-order building models [67]. 16

Figure 2-7: Model structure of the 3R2C model and 4R2C model [19]. 17

Figure 2-8: Model structure of the 1R1C model and 8R3C model [19]. 17

Figure 2-9: RC thermal network models in the study: (a) R1C1, (b) R3C3, (c) R5C4 [68]. 18

Figure 2-10: Thermal network representation of the four tested grey-box models [69]. 19

Figure 2-11: Simplified representation of the solar radiation model [70]. 20

Figure 2-12: The R3C2 thermal network model [71]. 20

Figure 2-13: RC model of a single-room building [30]. 20

Figure 2-14: Heat dynamics RC-network of the PowerFlexHouse3 [10]. 21

Figure 2-15: Grey-box model structures used for the forward selection [72]. 22

Figure 2-16: Example of a centralized three-zone grey-box building model [72]. 23

Figure 2-17: RC Model for a boundary wall [73]. 23

Figure 2-18: RC network structure for a two-zone building [74]. 24

Figure 2-19: (a) The complex three-zone model structure, and (b) the simplified three-zone model structure [75]. 24

Figure 3-1: The appearance and floor plan of the ZEB Living Lab. 28

Figure 3-2: Wireless temperature sensors (a) and wall-mounted temperature sensors (b). 31

Figure 3-3: Comparison of different indoor temperature sensors, global solar irradiation on a horizontal plane and heating power of the electric heater for Experiment 4. 31

Figure 3-4: 3D geometry of the building model in IDA ICE (showing the southwest facade). 32

Figure 3-5: Floor plan of the test building (ducts for the supply air are in blue and in red for extraction). 33

Figure 3-6: Structure of the 5R3C model. 36

Figure 3-7: Flow chart of the optimization procedure to identify the model parameters. 39

Figure 3-8: co-simulation experiment setup between IDA ICE and MATLAB. 43

Figure 3-9: Electricity and Peak Hour Penalty Cost Profile. 45

Figure 4-1: Identified HTC of the 3R2C deterministic model for the cases 1,2,3,4 and 14, different sampling times and pre-filtering techniques; cases with ACS are shown by triangles in lighter colors. 49

Figure 4-2: Identified C_e of the 3R2C deterministic model for the cases 1,2,3,4 and 14, different sampling times and pre-filtering techniques; cases with ACS are shown by triangles in lighter colors. 50

Figure 4-3: Identified C_e of the 3R2C deterministic model for cases 9 to 13, different sampling times and pre-filtering techniques; cases with ACS are shown by triangles in lighter colors. 50

Figure 4-4: Identified C_e of the 3R2C stochastic model for the cases 1,2,3,4 and 14, different sampling times and pre-filtering techniques; cases with ACS are shown by triangles in lighter colors. 51

Figure 4-5: Identified C_i of the 3R2C stochastic model for the cases 1,2,3,4 and 14, different sampling times and pre-filtering techniques; cases with ACS are shown by triangles in lighter colors. 51

Figure 4-6: Comparing the HTC of the 3R2C deterministic (det) and stochastic (sto) models using Experiment 4 and different types of temperature measurement (5min). 53

Figure 4-7: Comparing the Ce of the 3R2C deterministic (det) and stochastic (sto) models using Experiment 4 and different types of temperature measurement (5 min). 54

Figure 4-8: Cumulative periodogram of the residuals of the model 3R2C for different types of indoor temperature measurement. 54

Figure 4-9: Comparing the one-day ahead prediction of the 3R2C stochastic (sto) models with different types of temperature measurement, trained using Experiment 4 and validated using Experiments 2, 3. 55

Figure 4-10: HTC and C_e for the 3R2C stochastic model using Experiment 5 and different data pre-processing techniques..... 56

Figure 4-11: Identified HTC, Ce and Ai of the 3R2C deterministic model for Experiment 4 with different types of temperature, data pre-processing techniques. 57

Figure 4-12: Identified HTC of the 3R2C stochastic model for the cases 1,2,3,4 and 14, different sampling times and pre-filtering techniques; cases with ACS are shown by triangles in lighter colors. 58

Figure 4-13: Identified C_e of the 3R2C stochastic model for the cases 1,2,3,4 and 14, different sampling times and pre-filtering techniques; cases with ACS are shown by triangles in lighter colors. 59

Figure 4-14: Identified C_i of the 3R2C stochastic model for the cases 1,2,3,4 and 14, different sampling times and pre-filtering techniques; cases with ACS are shown by triangles in lighter colors. 59

Figure 4-15: Comparison of the simulation performance of the deterministic and stochastic 3R2C models trained on the dataset 14 without ACS and validated using the other datasets. 60

Figure 4-16: Comparison of the simulation performance of the stochastic 3R2C model with and without ACS, trained with the dataset 14 and validated with datasets 1 to 4. 61

Figure 4-17: Cumulative periodogram of the residuals for the stochastic models. 64

Figure 4-18: Indoor temperature profile under the operation of different MPC controllers with energy saving objective ($L = 10^8$)..... 68

Figure 4-19: Close-up of the indoor temperature profile under the operation of different MPC controllers with energy savings objective (Upper figure corresponding to 10^6, Lower figure corresponding to 10^8)..... 69

Figure 4-20: *Indoor temperature profile under the operation of different MPC controllers with energy cost saving objective ($L = 10^8$).* 71

Figure 4-21: Close-up of the indoor temperature profile under the operation of different MPC controllers with energy cost saving objective (Upper figure corresponding to 10^6, Lower figure corresponding to 10^8). 72

Figure 4-22: Indoor temperature profile under the operation of different MPC controllers with energy cost saving and peak reduction ($L = 10^8$). 75

Figure 4-23: Close-up of the indoor temperature profile under the operation of different MPC controllers with energy cost saving and peak reduction (Upper figure corresponding to 10^6, Lower figure corresponding to 10^8). 76

Figure 4-24: Profile of the emitted power by the electric radiators for the different MPC controllers and the energy cost saving and peak reduction objective ($L = 10^8$). 77

Figure 4-25: History of the HTC value update. 78

Figure 4-26: History of the A_i value update..... 78

Figure 4-27: History of the C_{total} value update. 79

Figure 4-28: R^2(%) of models against test dataset. 80

Figure 4-29: KPIs deploying different predictive models. 80

Figure 4-30: Building's temperature profile due to MPC. 81

Figure 4-31: Electricity use against electricity price. 82

1 INTRODUCTION

The transition of the current conventional energy system to a decarbonized energy system leads to more volatility in the power grid as power generated from renewable energy sources (RES) is often decentralized and intermittent. The power imbalance on the supply and demand sides can have severe implications for power quality and reliability [1]. Therefore, more flexibility is needed from the demand side to enable increasing penetration of intermittent RES. An important energy consumer on the demand side is buildings. They could play a very important role in providing energy flexibility and better utilizing the energy generated from RES. Model predictive control (MPC) enables operating the energy system close to an optimal way by shifting some load to synchronize more with the RES generation.

1.1 Background and motivation

The energy consumed by buildings accounts for 20% to 40% of the total energy used in developed countries and the proportion is still increasing at the rate of 0.5% to 5% every year [2]. The proportion of the building sector accounts for 36% of the energy consumption in Norway. Electricity is the dominant energy carrier since most of the buildings use direct electric heating [3] and the heating season is long and relatively cold.

In Norway, 96% of domestic electricity is generated by hydropower plants [3]. The Scandinavian power system is strongly integrated, allowing electricity trading between bidding zones in Scandinavia and the continental European power grid. In general, Norway plays the role of a net exporter, but it also imports energy from other countries at various times (e.g., during the period when wind energy production from Denmark is very high). Thus, the fluctuating electricity price of the market becomes an important driver for optimally operating the building energy system. In cold climate countries like Norway, space heating is dominant compared to cooling demands, which makes the optimal control of space heating an important approach to provide flexibility to the grid.

Demand response (DR) is the interaction and responsiveness from the demand side end-users based on a penalty signal (e.g., price signal, CO_2 intensity factor for electricity signal) [4,5]. DR is closely related to the concept of energy flexibility defined by the IEA EBC Annex 67 as the ability of a building to manage its demand and generation according to local climate conditions, user needs and grid requirements [6]. It provides flexibility for smart grids [7], which enables higher exploitation of the electricity generated from intermittent RES. Building thermal mass can be considered as short-term heat storage, which makes it appropriate to perform DR [8–10]. Deploying DR with building thermal mass requires the heating system to be operated optimally while keeping the indoor temperature comfortable constraint for the occupants. Model predictive control (MPC) is an advanced method

of control that is used to control a system while satisfying a set of constraints, which perfectly fits the requirements of performing DR in buildings.

In MPC applications in buildings, the dynamic model in the MPC controller is used to predict the thermal response of the building exposed to the prediction of future boundary conditions (e.g., weather forecast and energy usage). The optimal control sequence is then calculated based on future prediction and system constraints. Thus, the MPC controller performance strongly relies on the accuracy of the prediction model. Models of poor quality could cause undesired control results (e.g., increased energy cost, violation of thermal comfort). Due to the complex implementation procedure and hardware requirements, MPC is currently only applied to a limited number of existing buildings. Therefore, the cost of identifying the prediction model should be limited, especially for small residential buildings where the investment into an MPC should be low to make it cost-efficient. There are two main parts for reducing the cost. One part is to reduce the hardware cost for implementing MPC in buildings. The ongoing implementation of smart meters, like the Advanced Metering System (AMS) in Norway [11] and the rule "Key principles for the package of ordinances governing smart grids" in Germany" [12], makes the implementation of MPC in buildings in a large scale with lower cost more feasible in the future. The emergence of small, low-cost and wireless sensors with data collection functions in recent years [13] will also accelerate the implementation of MPC in buildings. The other part is the most time-consuming part of implementing MPC in a building, which is identifying an appropriate prediction model for MPC [14,15]. Thus, the model identification process should also be made more automated to reduce the cost.

Dynamic control-oriented models can be divided into three main categories, namely white-, black- and grey-box models. White-box models are based on physical laws (e.g., mass-, energy- and momentum balance equations), which require exhaustive information about the building including underlying physical processes and parameters. It is generally mathematically complex but has high accuracy. This type of model is widely used in building performance simulation (BPS) software like Modelica[16], EnergyPlus [17] and IDA[18]. White-box models are generally the most time-consuming among the three modeling methods, which need detailed information on the parameters and need to be updated during the lifetime of the building. Further, the mathematical complexity of white-box models requires extensive computational power [19], which makes the white-box models not suitable for MPC implementation of buildings in many cases. Black-box models are pure data-driven methods based on measured time-series data from the system. Statistical regression and artificial neural network (ANN) are common mathematical techniques for black-box modeling [20], which requires sufficient training data to guarantee the quality of the model [21]. The quality of the data can also significantly affect the black-box model performance. A grey-box model is a combination of a white-box and a black-box model. It takes the dominant physical process of the system to build

up the model structure and then the model parameters are fitted with measurement data. In the building engineering field, lumped resistance and capacitance models (i.e., RC models) are a common approach to creating the structure of grey-box models, which means that the building thermal dynamics are expressed using an electric circuit analogy [22,23]. It is claimed that grey-box models have better extrapolation properties compared to black-box models [24]. They have been widely applied to solve recent problems in building science, such as building load estimation, optimal control, and building-grid integration [25,26].

This thesis uses grey-box models to investigate the DR of heating systems in energy-flexible residential buildings. The thesis focuses on two main applications of grey-box models, which are MPC and the characterization of the thermal properties of buildings using field measurements [25,27].

1. Model predictive control (MPC) is considered a suitable advanced optimal control method to perform DR in a building [14,26] or to activate the building energy flexibility [6]. This study uses the building thermal mass as short-term thermal energy storage (e.g., by pre-heating of the building thermal mass) by controlling the operation of the space-heating system optimally using MPC [8,19,28–30]. The exploitation of such thermal storage requires the indoor temperature to stay within the thermal comfort limits for occupants. Existing studies have confirmed the significant DR potential of MPC activating the thermal mass of residential buildings [31–33]. The grey-box models should enable adequate prediction to achieve decent control performance.
2. Developing a proper grey-box model with physically plausible (i.e., interpretable) parameters is beneficial for evaluating the real building performance based on field measurements during the operational phase [29]. Physically plausible parameters in grey-box models could contribute to characterizing the thermal properties of a building using field experiments, such as its overall heat transfer coefficient (HTC).

Electric heating is the most common space-heating strategy for residential buildings in Norway. The time constant of the electric radiator is relatively short, so its thermal mass can be neglected for the time steps used in this thesis (i.e., typically 15 minutes). Thus, the research mainly focuses on modeling the building thermal dynamics, not the dynamics of the space-heating system.

1.2 Knowledge gap

Grey-box models have already been used in the literature to activate the building thermal mass using MPC. Several model structures have been used [28,34–38], but limited studies have been performed in Norway. As the model performance depends on the construction type, most often in lightweight wooden structures in Norway, and the climate (including the latitude for the solar gains), it is worth investigating the best grey-box model structures for small residential buildings in the Norwegian

context. Secondly, many studies identified the grey-box models using an ideal excitation signal, typically a PRBS signal. As will be explained in the thesis, a PRBS signal can lead the indoor temperature to deviate outside the thermal comfort limits for the occupants. Therefore, these signals may not be applicable over a long period with occupancy, limiting their practical implementation. It is therefore worth investigating if normal operating conditions corresponding to comfortable conditions for the occupants can excite the building dynamics in a sufficient way to identify reliable grey-box models.

In reality, the temperature field in a room is not uniform. Two important effects should be considered. Firstly, the room air can present significant temperature stratification, especially when the heat emitter is close to maximum power. Secondly, the sensors are usually mounted on a wall in a casing. For sudden changes in the indoor temperature, the measured value with a wall-mounted sensor may thus differ from the real air temperature. The thermal dynamics of the sensor due to the casing can also be seen as a form of implicit data pre-treatment if the sensor dynamics are not modeled. Thus, the influence of temperature sensor location and thermal dynamics on the grey-box model results needs to be investigated so that a reliable grey-box model can be developed.

Data pre-processing (or data pre-treatment) is acknowledged to have a key influence on the model identification results [39]. However, this topic has hardly been addressed in the field of grey-box models for buildings. Ljung and Wills [40] revealed several issues when applying a long sampling time to estimate continuous-time models with stochastic disturbances. However, the analysis of Ljung and Wills is illustrated using a theoretical example. Therefore, this thesis also investigates the influence of long sampling times in building applications.

Creating a suitable model is acknowledged to be the most important and time-consuming part of MPC implementation [15]. For the grey-box models, the model structure should not be too simple so that the model accuracy can be guaranteed. On the other side, the model structure should not also be too complicated to ensure the identifiability of the model and save computational costs for the MPC. Hence, the appropriate grey-box model structure is investigated in this thesis.

In the parameter identification stage, the default function (*greyest*) in the MATLAB identification toolbox uses gradient-based optimizers. Consequently, the optimizer may converge to a local optimum if the problem is not convex. As shown in Arendt et al. [41], Genetic Algorithm (GA) combined with a gradient-based method could be used to solve non-convex optimization problems used to identify the parameters of grey-box models. The influence of the optimizer on the grey-box modeling results is also inspected in this thesis.

In existing buildings' MPC research, it has been demonstrated that linear time-invariant (LTI) models can approximate the heat dynamics of buildings with

sufficient accuracy for MPC [42–46]. Thus, the prediction performance of grey-box models is compared to black-box models (e.g., ARX, NARX) under the MPC operation (virtual experiments). However, the limitation of MPC with an LTI model is that a model trained from one period is not able to provide decent prediction in another period due to time-varying weather conditions throughout the year. The performance of the MPC controller cannot be guaranteed when using an LTI model over a long period of time. Consequently, developing an adaptive MPC controller that updates the parameters during operation becomes a potential solution. Adaptive MPC has been widely applied in engineering in general, but it has surprisingly been rarely investigated in building energy control. Yang et al. [47] developed an adaptive robust model predictive control for indoor climate optimization, and the model is based on a detailed grey-box model and updates the parameters every 24 hours. Yang et al. [48] also introduced an adaptive machine-learning-based model for building control based on an artificial neural network (ANN). Fux et al. [49] used an extended Kalman filter-based self-adaptive thermal model for passive house demand prediction with the model updating the parameters at each time step. Choi et al. [50] used an adaptive neural network model to perform the optimal control for a data center. Maree et al. [51] proposed an adaptive control for heating demand-response in buildings that incorporates a reinforcement learning (RL) strategy. Zhang et al. [52] proposed a time-dependent solar aperture estimation method based on B-splines, which could be considered an adaptive grey-box model of buildings. Merema et al. [34] and Wolisz et al. [53] also applied adaptive control strategies for long-period control, which updates the coefficients of ARX models during operation. Therefore, this thesis also compares the performance of a conventional MPC based on an LTI grey-box model to the adaptive MPC using virtual experiments (i.e., co-simulation).

This thesis focuses on residential buildings. The defined research questions are considered to contribute to filling the knowledge gaps to enable the deployment of MPC using grey-box models in real buildings.

1.3 Research questions and research tasks

The context thesis is the use of residential buildings to provide flexibility so that the penetration of renewable energy can be increased and the current energy system becomes more sustainable. In order to achieve this goal, this thesis focuses on the thermal dynamics modeling of residential buildings and the implementation of MPC for the heating system of residential buildings. Grey-box models and related modeling techniques are mainly investigated in this study. The following original research questions are investigated:

Q 1: Which type, period and duration of the excitation signal are suitable for grey-box model identification of residential buildings?

Task 1.1: Different types of excitation signals are applied to the heating system in the experiment.

Task 1.2: Different periods and durations of data are taken to train the model parameter of models.

Q 2: What is the influence of temperature sensor location and thermal dynamics on the grey-box model results?

Task 2.1: The grey-box models trained using the volume-averaged indoor temperature, a single indoor temperature sensor and the temperature measurement of exhaust air are compared.

Task 2.2: The grey-box models trained using a single wall-mounted sensor with casing and a single sensor in the air without casing are compared.

Q 3: What is the influence of data pre-processing on the grey-box modeling results?

Task 3.1: Training datasets with different data pre-processing are taken to investigate the influence of sampling time and data alignment (here using anti-casual shift) on the performance of grey-box models.

Task 3.2: Training datasets with different low-pass filters are taken to investigate the influence of pre-filtering on the performance of grey-box models.

Q 4: What are the most suitable grey-box model structures for residential buildings?

Task 4.1: Develop a set of grey-box model structures with different levels of complexity.

Task 4.2: Evaluate the model performance based on the trade-off between model accuracy and complexity.

Q 5: What is the influence of the optimizer on the grey-box modeling results?

Task 5.1: Compare the model performance of grey-box models trained using traditional gradient-based optimization and global optimization routines.

Q 6: Prediction performance of grey-box compared to black-box models?

Task 6.1: The prediction performance of grey-box and black-box models is compared.

Q 7: What is the performance MPC using LTI and adaptive grey-box models and other types of data-driven models?

Task 7.1: The performance of MPC controller with conventional LTI grey-box models and adaptive grey-box models are compared.

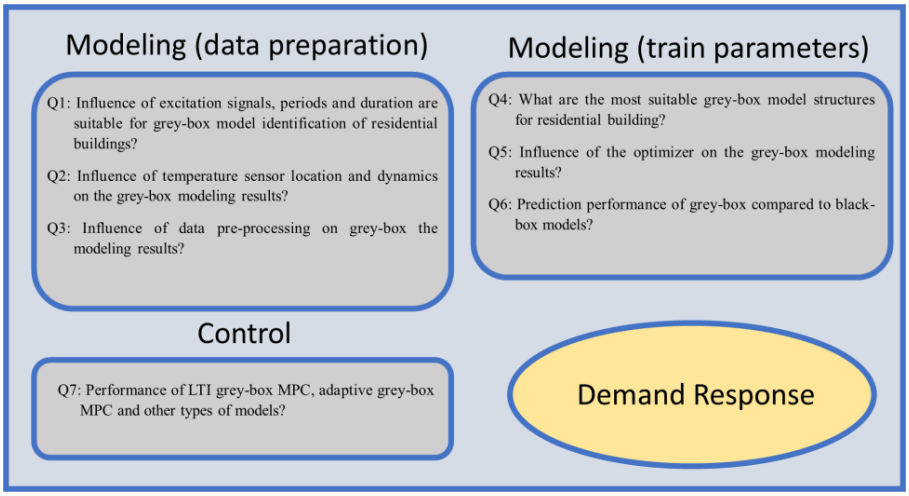

Figure 1-1: *Research questions grouped by categories.*

Figure 1-1 puts the above research questions connected logically in context to the different sections.

1.4 Structure of the thesis

The remainder of the thesis is structured as follows. Chapter 2 presents the research methodology, including a review of grey-box modeling for residential buildings and the data pre-processing, optimization methods and other setups of grey-box modeling used in the PhD research work. Chapter 3 illustrates the setup for the MPC implementation and control scenarios of the case studies. The main results of the papers are presented, explained, and discussed in Chapter 4. Chapter 5 outlines the main conclusions, addresses the limitations of current work and gives recommendations for future research.

1.5 List of publications

Three journal papers and four conference papers construct this PhD thesis. An overview of the papers is presented in Table 1-1 and Figure 1-2. The papers are distinguished between primary papers and one supporting paper. The primary papers address and answer the main research questions of the thesis, and the supporting paper presents preparative and supporting work for the primary papers. The papers included in this thesis are listed below, together with my personal contribution to each paper.

Primary papers:

Paper 1:

Yu X, Georges L, Knudsen MD, Sartori I, Imsland L. Investigation of the Model Structure for Low-Order Grey-Box Modelling of Residential Buildings. *Proceedings of Building Simulation 2019 16th Conference IBPSA*, International Building Performance Simulation Association (IBPSA), 2019 Rome, Italy.

Contribution: The conceptualization was done together with Laurent Georges and Igor Sartori. I structured the data and developed the methodology in collaboration with Laurent Georges and Michael Dahl Knudsen. The results were analyzed and visualized by me. I wrote the majority of the paper draft. Revision and editing were done in collaboration with all co-authors.

Paper 2:

Yu X, Georges L. Influence of Data Pre-Processing Techniques and Data Quality for Low-Order Stochastic Grey-Box Models of Residential Buildings. *International Conference Organised by IBPSA-Nordic*, 13th–14th October 2020, OsloMet. BuildSIM-Nordic 2020 (BSN2020). Selected papers. SINTEF Academic Press.

Contribution: I did the conception and virtual experiment design of the paper together with Laurent Georges. I also did the modeling work, data processing and analysis for the paper and wrote the original draft of the paper. Editing and revision were done in collaboration with Laurent Georges.

Comment: This contribution got the best conference paper award of BSN2020.

Paper 3:

Yu X, Georges L, Imsland L. Data pre-processing and optimization techniques for stochastic and deterministic low-order grey-box models of residential buildings. *Energy and Buildings*. 2021; 236: 110775.

Contribution:

This paper is based on Paper 2, which is an extension by adding more case studies and explanations. Regarding the extended part, I developed the models, analyzed the data, visualized the results and wrote the original draft of the article. Conceptualization and methodology were done in collaboration with Laurent Georges. Editing and revision were done in collaboration with Laurent Georges.

Paper 4:

Yu X, Skeie KS, Knudsen MD, Ren Z, Imsland L, Georges L. Influence of data pre-processing and sensor dynamics on grey-box models for space-heating: Analysis using field measurements. *Building and Environment*, 2022; 108832.

Contribution: This paper is a continuation work of Paper 3 by moving from virtual experiments to field experiments to validate the conclusions from Paper 3. Most of

the research methodology originates from Paper 3. The additional conception and design part was done together with Laurent Georges. Revision and editing were done in collaboration with all co-authors.

Paper 5:

Yu X, Georges L, Imsland L. Adaptive linear grey-box models for Model Predictive Controller of Residential Buildings. Accepted to *International Conference Organised by IBPSA-Nordic*, 22nd-23rd August 2022, CopenhagenMet. BuildSIM-Nordic 2022 (BSN2022).

Contribution: The conceptualization and virtual experiment design was done together with Laurent Georges. I also did the modeling work, MPC controller design and wrote the original draft of the paper. Revision and editing were done in collaboration with all co-authors.

Paper 6:

Yu X, Ren Z, Georges L, Imsland L. Comparison of Time-Invariant and Adaptive Linear Grey-box Models for Model Predictive Control of Residential Buildings. Submitted to *Applied Energy*

Contribution: This paper is based on Paper 5, which is an extension by adding more case studies and scenarios. I did the conception and design of the paper together with Laurent Georges. I also wrote the initial draft of the paper. Revision and editing were done in collaboration with all co-authors.

Supporting paper:

Paper 7:

Erfani A, Yu X, Kull TM, Bacher P, Jafarinejad T, Roels S, Saelens D. Analysis of the impact of predictive models on the quality of the model predictive control for an experimental building. *Proceedings of Building Simulation 2021 17th Conference IBPSA*, International Building Performance Simulation Association (IBPSA), 2021 Bruges, Belgium.

Contribution: I did part of the modeling work in this paper and worked together on the MPC controller. Revision and editing were done in collaboration with all co-authors with A. Erfani as the main writer.

The thesis is written in the form of a collection of articles. The interconnections of all the papers included in this PhD thesis are shown in Table 1-1 and Figure 1-2.

Table 1-1: *Relation between research questions and papers.*

	Involving Papers	Experiment Type	Topic
Q1	Paper 3	Virtual Experiment	Modeling
Q2	Paper 2 and Paper 4	Field Experiment	Modeling
Q3	Paper 3 and Paper 4	Virtual and Field Experiment	Modeling
Q4	Paper 1 and Paper 4	Field Experiment	Modeling
Q5	Paper 2 and Paper 3	Virtual Experiment	Modeling
Q6	Paper 1	Field Experiment	Modeling
Q7	Paper 5, Paper 6 and Paper 7	Virtual Experiment	MPC

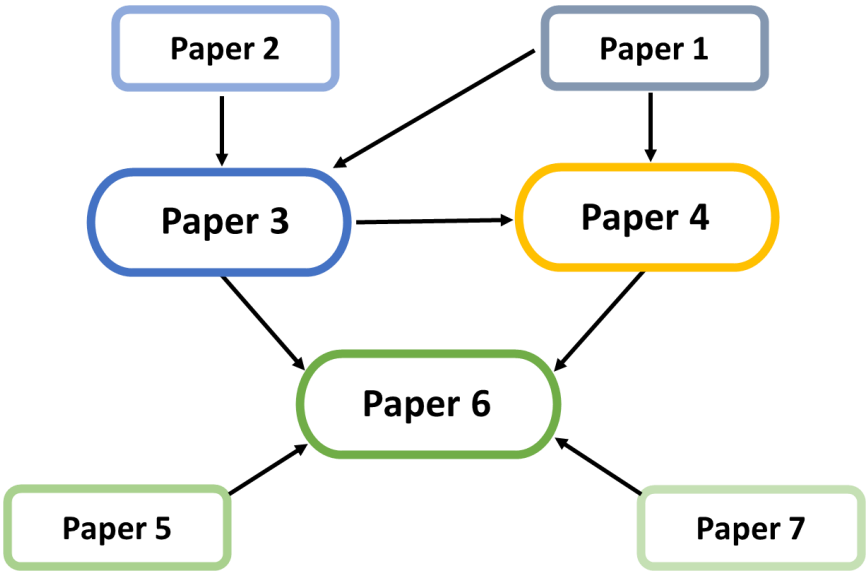

Figure 1-2: *Interconnections of the papers included in this thesis.*

2 RESEARCH CONTEXT AND BACKGROUND

This chapter introduces the research context and background of this thesis. Section 2.1 introduces the existing research on applying DR with MPC in buildings. Section 2.2 gives a review of the existing literature for the grey-box modeling of the building thermal dynamics.

2.1 Demand response with MPC

In building automation, MPC is a more advanced control strategy to perform DR compared to the conventional ones such as predictive rule-based control (PRBC). It is a promising approach for DR strategies in buildings with different control objectives such as peak shaving and load shifting.

A large number of existing researches have investigated the potential of performing DR in buildings using MPC. Knudsen et al. [43] propose an economic model predictive control strategy (EMPC) for the heating system with solar shading as an additional control variable. An experimental test of a black-box EMPCfor residential building space heating has been carried out in [54]. Results show that MPC with black-box models and constrained excitation signals for training can also provide good indoor air temperature control. Freund et al. [29] implement MPC in a large-sized, low-energy office building by controlling the supply temperature of heating circuits for thermally activated building systems (TABS). Awadelrahman et al. [33] deploy EMPC with a stratified thermal energy storage tank in the smart building. Wang et al. [30] use data-driven models which have universal approximation ability by utilizing a hybrid optimization algorithm, namely BSAS-LM, for the MPC implementation. Hedegaard et al. [55] use a grey-box model as the prediction model for an EMPC of space heating in residential buildings for multi-market demand response. Coninck et al. [56] also use a grey-box model-based MPC for an office building in Brussels. The results show that the MPC controller can provide a similar or better thermal comfort than the reference control and reduce energy costs by more than 30%. Prívara et al. [57] use the subspace black-box approach to obtain the model for the MPC controller. Hazyuk et al. [36] present a comparison of conventional PID and MPC, and the MPC also uses a grey-box model. The results show that MPC can reduce occupant discomfort by up to 97% and energy consumption by up to 18%. Pedersen et al. [58] present a scenario-based MPC of space heating in residential buildings taking a two-state grey-box model as the base. The above researches prove the benefits of using MPC in buildings to perform DR in the current grid system. In conclusion, all these studies demonstrate the large DR potential using MPC in buildings.

However, the investment in implementing MPC is more expensive. The model identification part is acknowledged as the most critical and time-consuming part of deploying an MPC [14]. All measures to reduce the modeling part of the MPC are

thus of prime importance. Therefore, the thesis aims to increase the knowledge of control-oriented modeling for MPC in buildings. Smart meters and the building management system (BMS) for signals collection and communication are also prerequisites for deploying MPC in buildings. More and more communication technologies, sensing, and computing devices at affordable prices have emerged on the market in recent years. The ongoing projects, like the Advanced Metering System (AMS) in Norway [11] and the rule "*Key principles for the package of ordinances governing smart grids*" in Germany" [12], make the implementation of MPC in residential buildings in a large scale a reachable target in the future. Thermal energy storage is commonly adopted to exploit the flexibility of residential buildings. Water storage tanks and the building thermal mass are the typical thermal storage. This study mainly focuses on utilizing the building thermal mass with MPC. In Nordic countries like Norway, the space-heating season is long and relatively cold, which makes the heating system a suitable candidate for performing DR. The thermal mass of the building is temporarily loaded to higher temperatures or unloaded by letting the indoor temperature decrease to maximize the control objective. Increasing the indoor temperature above the minimal temperature providing an equivalent thermal comfort usually leads to increased energy use for heating, but the summed objective function is decreased (e.g., the energy costs). The thermal comfort under a dynamic thermal environment is investigated in Favero et al. [59].

This operation is the aforementioned DR with buildings. It requires a proper model and appropriate control design so that the DR target can be approached, which are the main two parts of this thesis.

2.2 Review of grey-box modeling for building thermal dynamics

The performance of an MPC controller is significantly related to the prediction model accuracy of the control-oriented model. As the thesis focuses on MPC with a grey-box model as the prediction model, a short literature review of grey-box modeling of thermal dynamics of the building is given in this section. The review starts with mono-zone models and then considers multi-zone models.

Freund et al. [60] describe the thermal zone by a grey-box model consisting of three capacitances and four resistances (R4C3 model). The model is extended by a thermally activated building system (TABS) model with one capacitance and two resistances and a resistance for the air-handling units (AHU) (Figure 2-1).

The heat exchange between the external walls and the outdoor environment is evaluated using an equivalent outdoor temperature defined by the VDI 6007 standard [61], which takes the influence of short-wave radiation into consideration.

$$T_{a,eq} = T_a + Q_{irrad} \frac{a_f}{\alpha_A} \tag{2-1}$$

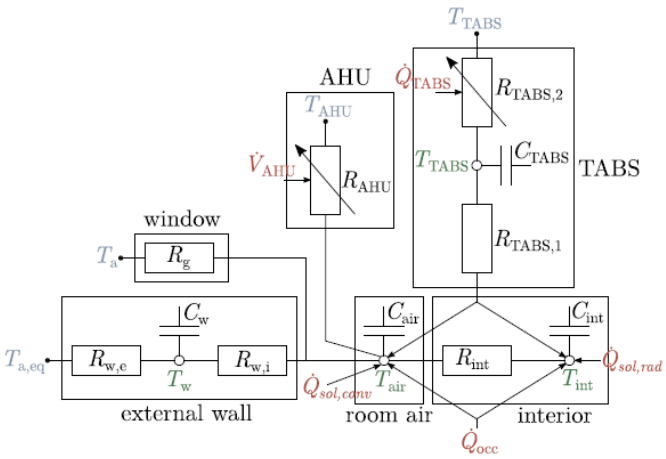

Figure 2-1: *Thermal network representation of the used grey-box model* [60].

The short-wave absorption coefficient of the exterior surface a_f is set to 0.5 and the exterior heat transfer coefficient α_A is set to 25 W/(m2K). The coefficients are determined according to DIN 6946 [62]. The solar heat gains Qsol are determined by

$$Q_{sol} = f_{sol} \bullet I_{GH} \tag{2-2}$$

where f_{sol} is a factor that should be estimated during the identification process. f_{sol} is usually interpreted as the effective window area, which translates how much of the outdoor total solar irradiation on a horizontal plane is converted into solar gains. The internal gains are calculated by multiplying the occupancy signal, which is detected by presence sensors, and a constant internal heat gain Q_{occ}, which is part of the identification. The convective part of internal gains is assumed to be 40 %. The model was applied in one office building in the city of Hamburg in Northern Germany. The model showed a decent prediction performance for the indoor temperature with a TABS system.

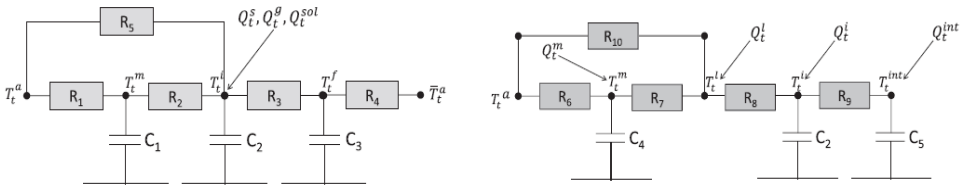

Figure 2-2: *5R3C Grey-box model structures: (a) Model I: model trained from detailed building simulation tools, and (b) Model II: model modified from ISO 13790* [63].

Two different single-zone 5R3C models are presented in [63]. The model structures are shown in Figure 2-2. The first model structure (Model I) is trained from detailed building simulation tools. The solar gains and internal gains are directly accessible from the building simulation. The second model structure (Model II) is a modification

of the ISO13790 standard [64]. Solar and internal gains are distributed amongst different temperature nodes as described in the standard [64]. The model was applied to a cluster of representative Belgian residential buildings to investigate the aggregated load flexibility.

Hedegaard et al. [65] present a 4R2C model to predict the response of the building for operating the heating system. The model structure of this study includes two lumped capacities: one for room air and another for building construction. The internal heat gains and solar heat gains are directly accessible from the simulation in Energy Plus.

Hedegaard et al. [37] introduce a modified model based on the standard ISO 13790 (Figure 2-3). An additional node corresponding to the interior thermal inertia (for the room air, furniture, etc.) is added to the original massless air temperature node according to ISO 13790 with the thermal capacity (C_i). The results indicate that the modification significantly improves the model prediction ability under dynamic operating conditions.

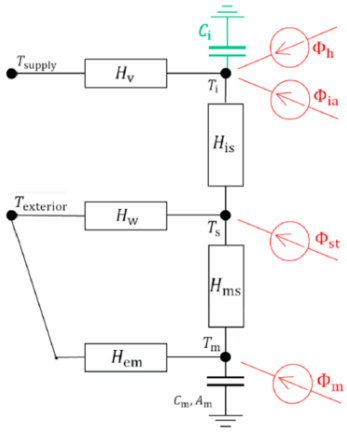

Figure 2-3: *Modified RC network of the model used in ISO 13790* [37].

Hedegaard et al. [66] propose several model structures to estimate the grey-box model parameters to characterize the thermal properties of buildings (see Figure 2-4). The initial model is a 2R2C model, which considers the thermal inertia of the wall and air. The solar gains are calculated by the effective window area times the solar irradiance. The heat gain from the heating system is directly injected into the air node. The 3R2C model adds one transmission heat loss resistance based on the 2R2C model. The 4R3C model contains an interior capacity representing the internal elements that only interact with zone air. The 4R3Cw model adds the third thermal mass node in the envelope to better model the distribution of capacity in the envelope. Mathematical dependencies between the parameters were introduced to the third-order models to ensure identifiability. The results show that the 2R2C model is not able to estimate individual heat loss coefficients due to the structures. It is also clear that the 4R3C model lack consistency and accuracy. The 3R2C and the 4R3Cw models show close

estimates of all characteristics, and the accuracy and consistency across all datasets are decent.

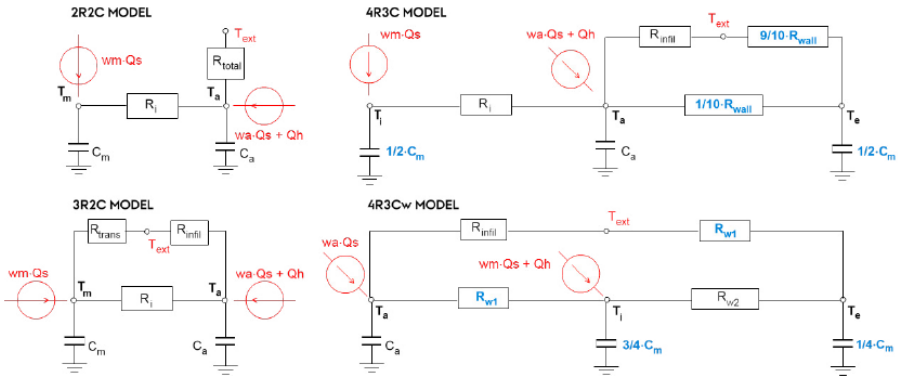

Figure 2-4: *Model structures depicted as RC-networks. Red text denotes inputs, blue highlights the assumptions made for third-order models* [66].

Hu et al. [38] use a 5R4C grey-box model to predict the temperature of the room (Figure 2-5). The model contains more physical principles of the room thermal dynamics. The building's external building envelope is made up of opaque walls and transparent windows. Because of the climate of Hong Kong, most residential structures are made of lightweight wall and roof materials. Therefore, the external wall was considered as one thermal resistance and two equal thermal capacitances. Another two capacitances are for the nodes of indoor air and the internal mass. For the solar radiation, $Q_{solar,w}$, $Q_{solar,i}$, and $Q_{solar,m}$ are solar heat gains absorbed by external wall surface, indoor air and internal mass, respectively. For the internal gains, $Q_{inter,i}$, $Q_{inter,m}$ are internal heat gains absorbed by indoor air and internal mass, respectively. All the heat gains information and splitting factor is a prior knowledge in this study. Only the R and C are free parameters to be identified in this study.

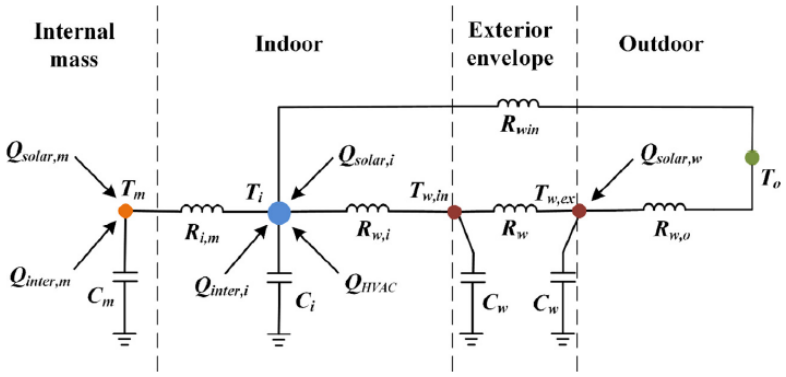

Figure 2-5: *Schematic of the grey-box thermal model of residential buildings (5R4C)* [38].

$$Q_{solar,w} = \alpha A_w I_{solar} \tag{2-3}$$

$$Q_{solar,m} = SHGC \bullet f_{solar,m} \bullet A_{win} I_{solar} \tag{2-4}$$

$$Q_{solar,i} = SHGC \bullet f_{solar,i} \bullet A_{win} I_{solar} \tag{2-5}$$

$$Q_{inter,m} = f_{inter,m} Q_{inter} \tag{2-6}$$

$$Q_{inter,i} = f_{inter,i} Q_{inter} \tag{2-7}$$

Reynders et al. [67] investigate the quality of grey-box models of different levels of complexity with data generated from the energy assessment simulation (IDEAS) package in Modelica (Figure 2-6). They take the different components of the building envelope (e.g., walls and windows) into account. Measurements of the indoor air temperature and the heat flux to the different building components are accessible for this study. The ambient air temperature, the heat emitted by the radiators, the effective internal and solar gains are used as inputs. Solar and internal gains are also modeled based on more realistic measurements like the global horizontal irradiation for solar gains or the electricity consumption from a smart meter for internal gains. The distribution coefficients for the solar gains, internal gains and heating are assumed to be constant and are identified as part of the parameter identification process. Reynders claims that 1st order models are unable to describe the thermal conditions in buildings under dynamic operating conditions. The 3rd order is the highest order leading to acceptable performance if only the indoor temperature is measured and included in the model. Above 3rd, the 4th and 5th order models require the measurements of the heat flux through the building components to improve the identifiability of the model.

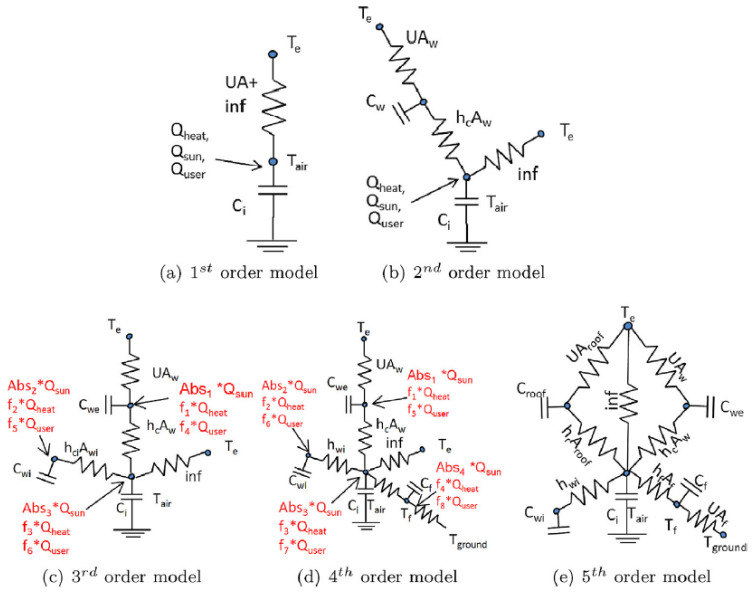

Figure 2-6: *RC-analogy of reduced-order building models* [67].

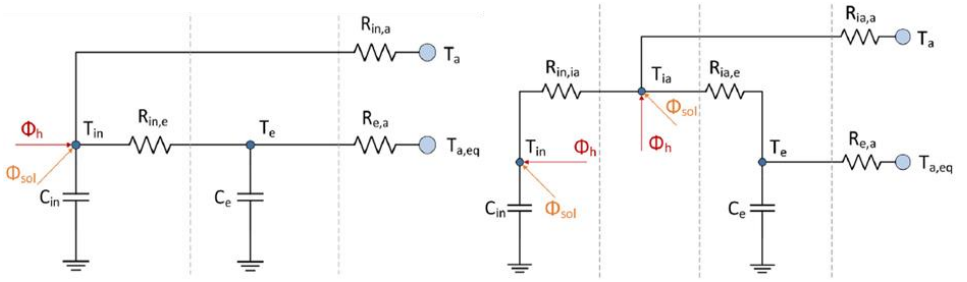

Figure 2-7: *Model structure of the 3R2C model and 4R2C model* [19].

Harb et al. [19] propose several grey-box models for predicting the thermal response of occupied buildings (see Figure 2-7). The heat exchange between the interior and the exterior environment and the solar heat gains is described as the same equations below based on the standard VDI 6007 standard [2]. For the 3R2C model, the solar gain and heat gains are directly injected into the interior node. The 4R2C model extends the 3R2C by considering the indoor air as a separate temperature node with no thermal capacity. According to the EN ISO13790 standard [64], the convective contribution of the solar heat gains can be assumed at f_{conv}= 9%. The allocation of the heat gain on different nodes is carried out according to the following equations.

$$\phi_{h,ia} = \phi_h \bullet (1 - f_{heat,rad}) \tag{2-8}$$

$$\phi_{h,in} = (\phi_h - \phi_{h,ia}) \bullet (1 - f_{heat,rad,ext}) \tag{2-9}$$

$$\phi_{h,e} = (\phi_h - \phi_{h,ia}) \bullet f_{heat,rad,ext} \tag{2-10}$$

with $f_{heat,rad}$ being the radiation contribution of the heat flux from the heater (with a value of 0.2) and $f_{heat,rad,ext} = \alpha_{e,floor}/\alpha_{in,floor}$ being the share of the radiation contribution to the exterior walls. $\alpha_{e,floor}$ and $\alpha_{in,floor}$ are empirical values which are 2.5 and 1.5, respectively.

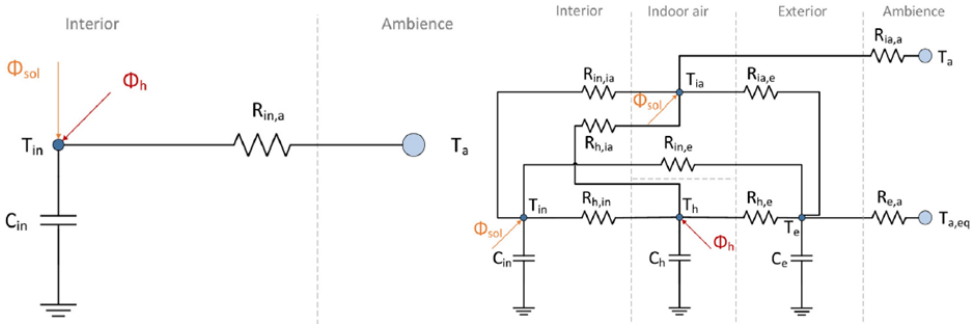

Figure 2-8: *Model structure of the 1R1C model and 8R3C model* [19].

In addition to the second-order models, the simple 1R1C model and a more complicated model 8R3C are also proposed in this paper (see Figure 2-8). This last

model is an extension of the 4R2C model by considering the heating system with a separate thermal capacity C_h and a temperature node T_h. The model considering the heating system as a separate thermal capacity is reasonable due to the high thermal inertial of the underfloor heating system. Thus, the heating system not only transmits heat to the interior and exterior through the radiative thermal resistances $R_{h,in}$ and $R_{h,e}$ but also to the indoor air through convection resistance $R_{h,ia}$.

The model comparison results revealed that the two capacity model with an additional mass-less node of indoor air (4R2C) perfectly integrated the accurate prediction performance (mean forecast error of 0.2 K) and the clear physical interpretation of the assessed parameters within constraints.

Blum et al. [68] compare three grey-box model structures in their study (see Figure 2-9). The extra resistance is in parallel with the wall for model 5R4C to account for infiltration and window conduction gains separately. The model inputs, like the radiative and convective internal heat gains $q_{occ,r}$, $q_{occ,c}$ [W/m2], the HVAC heating (q_h) and cooling (q_c) power $q_{hvac} = q_h - q_c$ [W] are directly accessible in this study. Regarding the solar gains of the building, it is calculated as the total global horizontal irradiance H_{glo} [W/m^2] incident on the floor α, and exterior walls (for 3R3C and 5R4C), α_e. The results show that 3R3C model performs best among the three models considering 1-day and 7-day validation periods. In addition, the 5R4C model shows a lower training error than the 1R1C model but a higher 1-day and 7-day validation error. It indicates that the 5R4C model maybe overfitted for the training data.

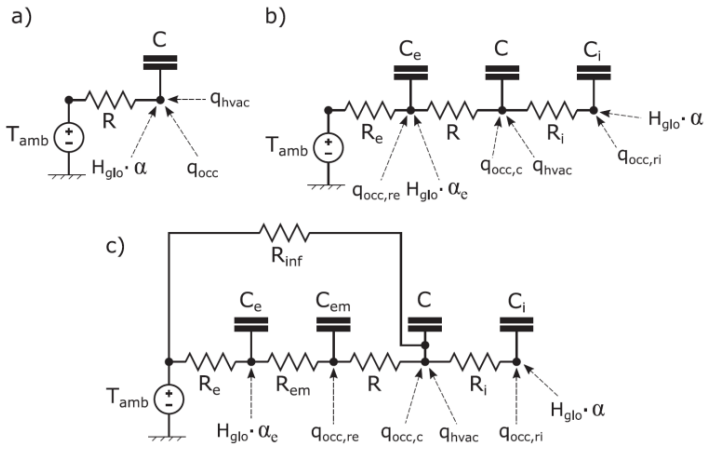

Figure 2-9: *RC thermal network models in the study: (a) R1C1, (b) R3C3, (c) R5C4* [68].

Berthou et al. [69] propose four grey-box models to predict the heating and cooling demand and indoor air temperature (Figure 2-10). The study used the data from a multi-zone building simulation (TRNSYS). Thus, all the related physical inputs, the occupancy heat gains and the ventilation mass flow are accessible. The 4R2C model is an extension of the normal 3R2C model with a supplementary resistance. The additional resistance is used to characterize variable airflow ventilation. The model

has the disadvantage of not being able to capture the solar flux coming on external walls, which is problematic during the summer. The 6R2C, 6R3C and 7R3C use the additional nodes (T_h and T_s) to enable the split of the solar heat flux into two parts. The split solar gains are calculated with the adopted Kasten model [70]. The simplified representation of the solar gain model is presented in Figure 2-11.

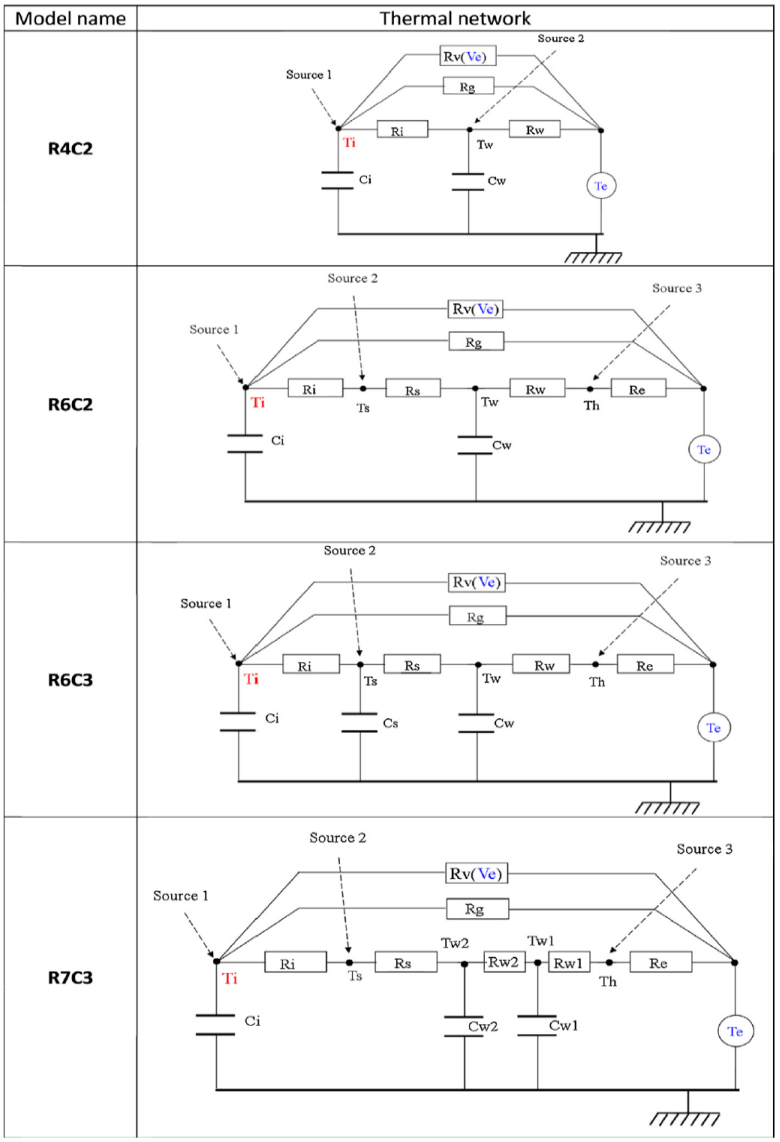

Figure 2-10: *Thermal network representation of the four tested grey-box models* [69].

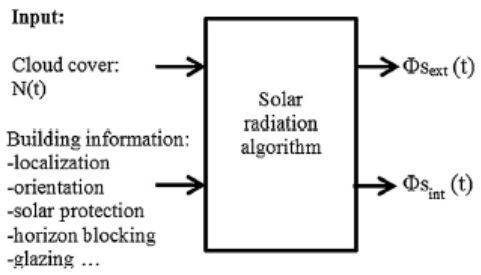

Figure 2-11: *Simplified representation of the solar radiation model* [70].

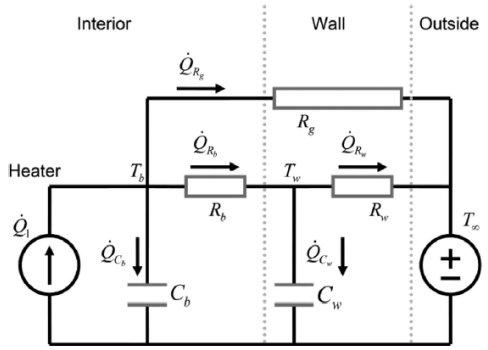

Figure 2-12: *The R3C2 thermal network model* [71].

Brastein et al. [71] use the randomized initial parameter value to investigate the dispersion of parameter estimates (see Figure 2-12). Results show that there is a significant dispersion in the parameter estimates when using randomized initial conditions. The 3R2C model is used in this paper. The results show that when the parameter R_g is set to a fixed value, the identifiability of the model is significantly improved. This conclusion can be observed from the shape of the Monte Carlo simulations in the parameter space. Further, the parameters show much better convergence for the case of 5 degrees freedom compared to the case of 4 degrees freedom when randomized initial parameters are applied.

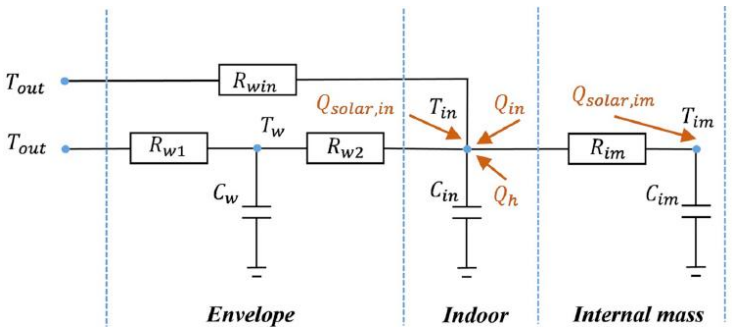

Figure 2-13: *RC model of a single-room building* [30].

Wang et al. [30] use the RC model of Figure 2-13 as the control model for the MPC. The model is very similar to the other 4R3C models in the literature. The solar radiation is assumed to be absorbed by the air node and interior thermal mass (for internal walls and furniture). A split coefficient α (ranging from 0 to 1) is used to determine how the heat flux of solar radiation is distributed between the T_{in} and T_{im} nodes.

$$Q_{solar} = Q_{solar,in} + Q_{solar,im} \tag{2-11}$$

$$Q_{solar} = \alpha \bullet Q_{solar} \tag{2-12}$$

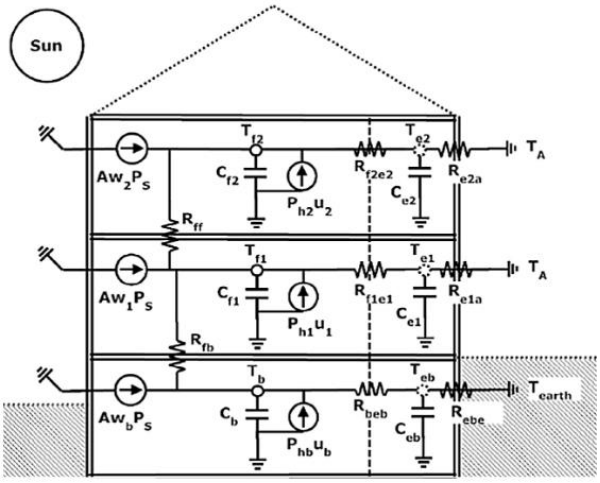

Figure 2-14: *Heat dynamics RC-network of the PowerFlexHouse3 [10].*

Zong et al. [10] propose a multi-zone grey-box model for a residential building in Denmark called PowerFlexHouse3 (Figure 2-14). The model takes a second-order model as the basic structure for each floor. The inputs of the model include the ground temperature (for the basement), ambient temperature, heating power from the electric heater and the solar heat gain from the solar radiation. The heat gain from solar radiation is also modeled using an effective window area times the solar irradiance. The results show that the second-order model can provide a relatively detailed knowledge of the building thermal dynamics of each floor for the EMPC controller design.

Arroyo et al. [72] presented a method to identify multi-zone grey-box building models (Figure 2-15). A forward selection process increasing the model complexity is implemented at the first stage to select the most suitable model for each individual zone without any coupling with the other zones. The inputs of each individual zone include the heat released to each zone, the internal gains, ambient temperature and the global horizontal irradiation. For the centralized case (see Figure 2-16), the obtained grey-box model for each zone is merged and coupled together. For the

decentralized case, the zone model works independently without interaction among zones. The simulation performance of the models shows that the centralized multi-zone model slightly outperforms the decentralized model and has similar accuracy to the single-zone model. Regarding the control performance of the MPC controller, the centralized model performs much better than the decentralized model by achieving minimum comfort violations. The single-zone model also shows a surprisingly good performance. The results of this study show that the thermal interactions among zones should be modeled properly. The single-zone models can also be suitable if the heat distribution to the zones is balanced correctly.

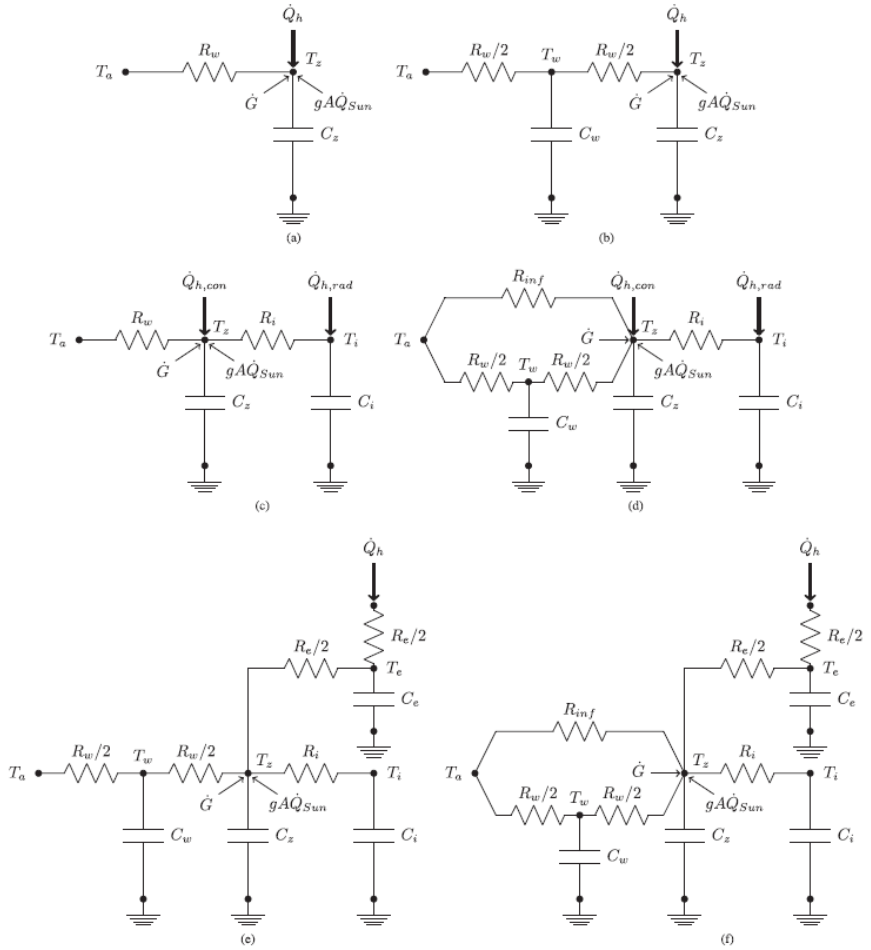

Figure 2-15: *Grey-box model structures used for the forward selection* [72].

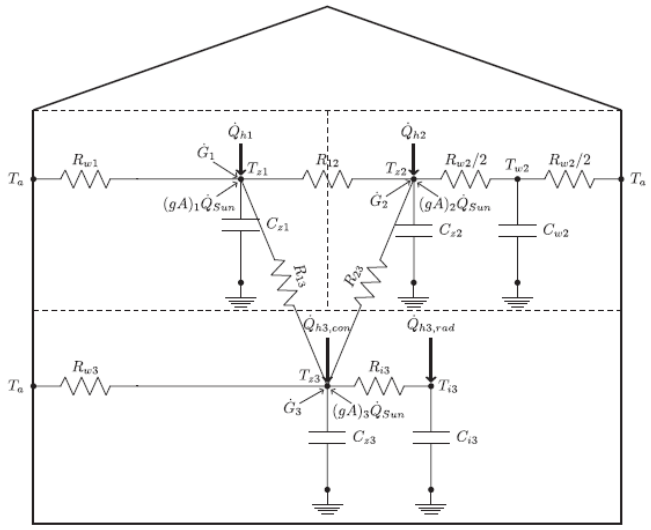

Figure 2-16: *Example of a centralized three-zone grey-box building model* [72].

Agbi et al. [73] discuss the parameter identifiability for multi-zone grey-box models (see Figure 2-17). Each zone has a thermal capacity to represent the thermal mass of the zone. Unlike Arroyo et al. [72], the interaction between zones is not simply represented by thermal resistances. An additional thermal capacity is added to the partition walls to account for the thermal mass.

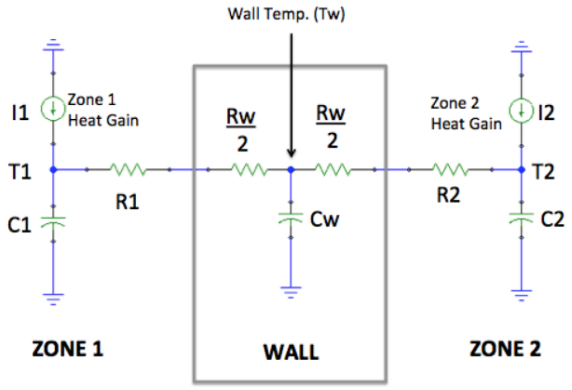

Figure 2-17: *RC Model for a boundary wall* [73].

Kim et al. [74] also propose a similar approach as [10] and [73] to identify a suitable grey-box model for multi-zone buildings. The second-order model is used as the base model for each zone. Figure 2-18 is the example RC network for a two-zone system. Each zone has two thermal capacitances and two thermal resistances. The two zones are connected at the zone air nodes with a single thermal resistance $R_{zz,12}$.

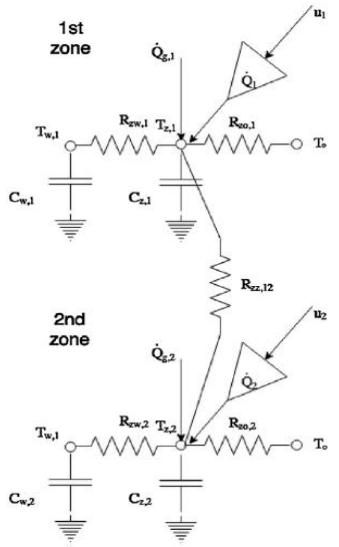

Figure 2-18: *RC network structure for a two-zone building* [74].

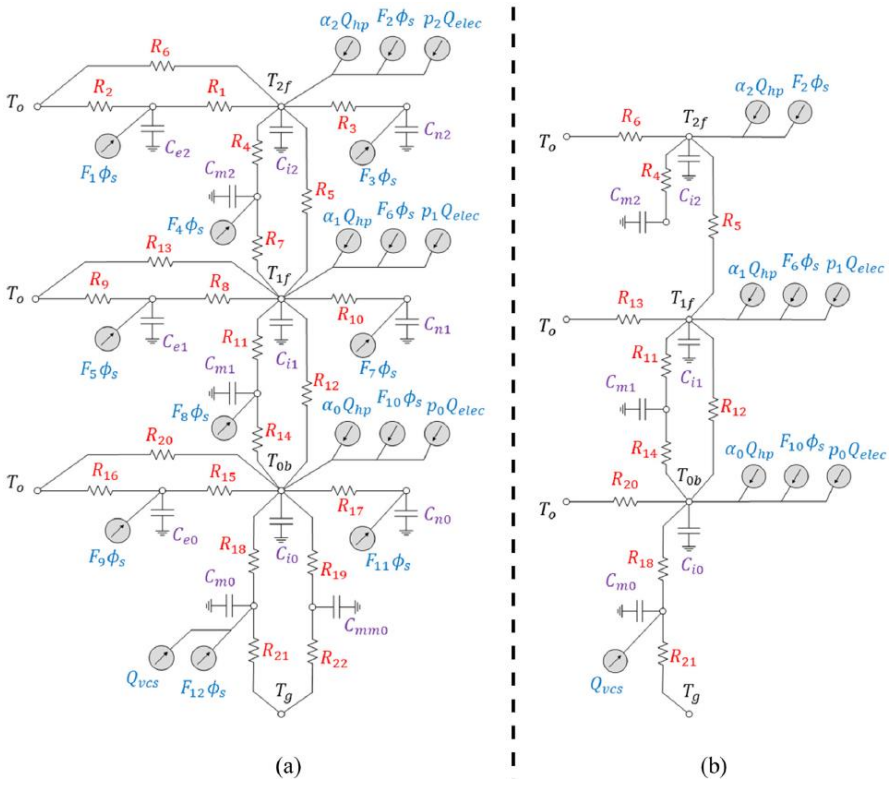

Figure 2-19: *(a) The complex three-zone model structure, and (b) the simplified three-zone model structure* [75].

Wang et al. [75] propose a multi-zone RC model for the thermal dynamics analysis in buildings by model structure simplification method. A complex model structure based on physical principles is first created and then simplified by progressively removing parameters. The genetic algorithm is employed during the training phase to obtain satisfactory fitting ability for large model structures. In the model simplification stage, the asymptotic standard errors are used to quantify the identifiability of the parameters. The original complex model is a 22R13C (see Figure 2-19 (a)) for the three-floor residential buildings, and the model is progressively simplified to a 10R6C (see Figure 2-19 (b)) model by removing the non-identifiable parameters. The results show that the simplification does not cause a significant loss of training or validation accuracy in terms of RMSE and Fitting. Further, the results also show that the simplified model is able to capture the temperature differences between adjacent zones.

The review gives a review of the state-of-the-art of existing grey-box models of the building thermal dynamics, which covers both single-zone and multi-zone situations. All the models in this review are summarized in the table below.

Table 2-1: *Summary of grey-box models for the building thermal dynamics.*

RC Model	application	Solar gains	Internal gains	Other Standards used	Multi-zone or single-zone	Reference
4R3C	office buildings	$Q_{sol} = f_{sol} \cdot I_{GH}$ DIN 52016	DIN 18599 construction data	DIN 6946 VDI6007	single-zone	[60]
5R3C(1)	residential buildings (cluster)	precalculated	precalculated	-	single-zone	[63]
5R3C(2)	residential buildings (cluster)	precalculated	precalculated	EN13790	single-zone	[63]
4R2C	dormitry	precalculated (simulation)	precalculated (simulation)	-	single-zone	[65]
5R4C	residential buildings	$Q_{sol,w} = \alpha A_w I_{solar}$ $Q_{solar,m} = SHGC \cdot f_{solar,m} \cdot A_{win} I_{solar}$ $Q_{solar,i} = SHGC \cdot f_{solar,i} \cdot A_{win} I_{solar}$	$Q_{inter,m} = f_{inter,m} \cdot Q_{inter}$	ASHRAE Handbook	single-zone	[38]
1R1C	residential buildings	precalculated	precalculated domestic electricity	EN12831 NBN50-001	single-zone	[67]
3R2C	residential buildings	precalculated	precalculated domestic electricity	EN12831 NBN50-001	single-zone	[67]
4R3C	residential buildings	precalculated $Q_{sol} = f_{sol} \cdot I_{GH}$ $Q_{sol} = f_{sol} \cdot Iov$	precalculated domestic electricity	EN12831 NBN50-001	single-zone	[67]

6R4C	residential buildings	precalculated $Q_{sol} = f_{sol} \cdot I_{GH}$ $Q_{sol} = f_{sol} \cdot Iov$	precalculated domestic electricity	EN12831 NBN50-001	single-zone	[67]
8R5C	residential buildings	precalculated	precalculated domestic electricity	EN12831 NBN50-001	single-zone	[67]
5R2C	residential buildings	precalculated	precalculated	ISO13790	single-zone	[37]
3R2C	residential and office buildings	$Q_{sol} = f_{sol} \cdot I_{GH}$	not included	-	single-zone	[19]
4R2C	residential and office buildings	$Q_{sol} = f_{sol} \cdot I_{GH}$	not included	-	single-zone	[19]
4R2C	office buildings	adopted Kasten model	precalculated	-	single-zone	[69]
6R2C	office buildings	adopted Kasten model	precalculated	-	single-zone	[69]
6R3C	office buildings	adopted Kasten model	precalculated	-	single-zone	[69]
7R3C	office buildings	adopted Kasten model	precalculated	-	single-zone	[69]
2R2C	residential buildings	$Q_{sol} = W_a \cdot Q_s$	not included	ISO13790	single-zone	[66]
3R2C	residential buildings	$Q_{sol} = W_a \cdot Q_s$	not included	ISO13790	single-zone	[66]
4R3C	residential buildings	$Q_{sol} = W_a \cdot Q_s$	not included	ISO13790	single-zone	[66]
4R3Cw	residential buildings	$Q_{sol} = W_a \cdot Q_s$	not included	ISO13790	single-zone	[66]
1R1C	office buildings	$Q_{sol} = H_{glo} \cdot \alpha_e$ $Q_{sol} = H_{glo} \cdot \alpha_e$	precalculated	-	single-zone	[68]
3R3C	office buildings	$Q_{sol} = H_{glo} \cdot \alpha_e$ $Q_{sol} = H_{glo} \cdot \alpha_e$	precalculated	-	single-zone	[68]
5R4C	office buildings	$Q_{sol} = H_{glo} \cdot \alpha_e$ $Q_{sol} = H_{glo} \cdot \alpha_e$	precalculated	-	single-zone	[68]
4R3C	buildings	precalculated	precalculated	-	single-zone	[30]
4R3C	buildings	-	-	-	multi-zone	[73]
3R2C	residential buildings	-	-	-	single-zone	[71]
8R6C	residential buildings	$Q_{sol} = A_w \cdot I_{GH}$	-	-	multi-zone	[10]
36R20C	residential buildings	$Q_{sol} = gA \cdot I_{GH}$	precalculated	-	multi-zone	[72]
18R18C	residential buildings	$Q_{sol} = gA \cdot I_{GH}$	precalculated	-	multi-zone	[72]
10R6C	residential buildings	$Q_{sol} = f_{sol} \cdot I_{GH}$	precalculated	-	multi-zone	[75]
22R13C	residential buildings	$Q_{sol} = f_{sol} \cdot I_{GH}$	precalculated	-	multi-zone	[75]

Most studies select a single-zone model for the MPC implementation due to the consideration of computational cost (high computation cost requires more expensive hardware). The results of those studies show that a first-order model is not enough to capture the thermal dynamics of the building. The second-order and third-order model models are the most popular selection for the single-zone case. The main difference between the second-order model and the third-order model is the additional capacitance for the internal thermal mass (e.g., furniture and internal walls). The model order selection also depends on the availability of the measurement data in the field. Higher-order models (i.e., higher than third-order) with insufficient measurements could easily cause overfitting problems.

For multi-zone models, most studies take the second-order model as the base model for each thermal zone. Thermal resistances and sometimes capacitances are then used to connect those thermal zones. The combination of thermal resistances and capacitances to connect the thermal zones also depends on the availability of the measurement data. For the same order, different model structures present good prediction performance. This indicates that there is some flexibility in the model structure selection due to variable building types and structures. The model structures reviewed in this study are a good reference for the model selection in grey-box modeling work of the thesis. This grey-box modeling work is presented in Paper 1, Paper 2, Paper 3 and Paper 4.

3 METHODOLOGY

This chapter briefly explains the experimental platform and setup. Furthermore, the modeling and control methods are also introduced in this section. The description of the experiments platform is given in Section 3.1. Section 3.2 presents the system identification process of the thesis. Section 3.2 introduces the setup for the MPC using virtual experiments.

3.1 Description of experiments

This thesis has one physical experimental building called the ZEB Living Lab and one virtual experimental building implemented in the building performance simulation (BPS) packaged IDA ICE. This section introduces the details of the two experimental platforms and their corresponding experiments.

3.1.1 ZEB Living Lab

The ZEB Living Lab is a Norwegian residential single-family, zero-emission house with a heated floor area 105 m² located on the Gløshaugen campus in Trondheim (Norway). The appearance and the internal floor plan are shown in Figure 3-1. The building has a highly-insulated envelope with lightweight timber construction with mineral wool inside external walls. It is also equipped with energy-efficient windows (glazing ratio equals 0.2). Furthermore, the ZEB LivingLab contains phase change material in the ceiling to limit peak indoor temperatures. The space heating can be floor heating, a single radiator, or ventilation air. The ventilation system is equipped with a heat recovery unit. By closing the doors in the building, four zones can be created (i.e., the bedroom west, bedroom east, the bathroom and living areas).

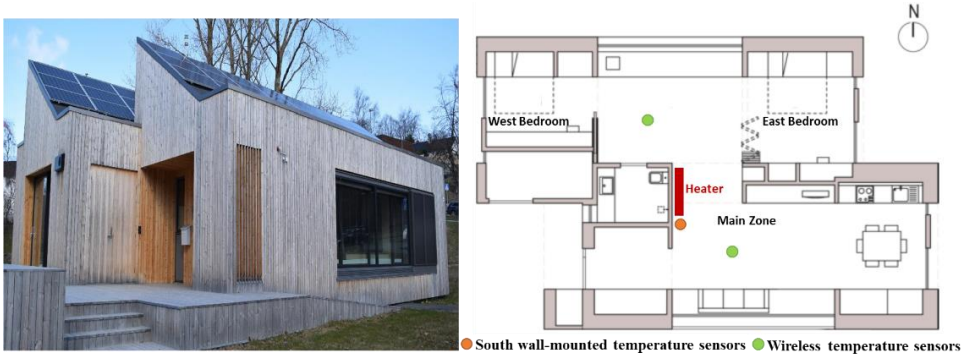

(a) *(b)*

Figure 3-1: *The appearance and floor plan of the ZEB Living Lab.*

This thesis mainly uses two sets of experiments done in this building with different space-heating emission systems and different periods of the space-heating season.

Data using two different heat emitters are used to make the conclusions more general.

The first set of experiments (from the 18th April to 15th May 2017) used an electric heater for space heating. Detailed information on the measurement setup and data can be found in previous work [46,76]. The corresponding length of these three experiments are 6 days, 11 days and 7 days, respectively. The electric heater of 2.6 kW was placed in the center of the building (the heater is marked in red in Figure 3-1 (b)). A pseudo-random binary signal (PRBS) has been applied to the electric heater to excite the thermal dynamics of the building. PRBS is a periodic and deterministic signal which has white noise properties and no correlation with other inputs. The PRBS signal activates the dynamic system at a broad range of frequencies with a high signal-to-noise ratio (SNR). The basic period of the signal is λ and the maximum length sequence N ($N = 2^n-1$) with the total duration of the PRBS signal is $T = N \lambda$. Four experiments were carried out, and only the last three were successful. The successful experiments are named Experiments 2, 3, and 4 (i.e., Experiment 1 was discarded). The dataset has a time interval of 5 minutes. The measurements include the outdoor temperature, indoor air temperatures, global solar irradiation and electricity consumption, including the radiator power (Q_h). To avoid modeling the air-handling unit (AHU), the ventilation losses from the mechanical ventilation are introduced as one input. These ventilation losses are explicitly pre-calculated with the measured temperature difference between the supply and exhaust ventilation air combined with the measured airflow rate (constant air volume, CAV). The electric heating system has negligible thermal inertia compared to the building envelope, so it is assumed that the dynamics of the radiators play a limited role. Experiments 2 and 4 were conducted with internal doors opened, which theoretically should lead to a more uniform spatial distribution of the air temperature inside the building while all the doors were closed in Experiment 3. Air was pre-heated using a heating coil in Experiment 4 only. The building is unoccupied in all the experiments, but electric dummies operated by a control schedule have been used leading to realistic internal gains.

The experiment with the hydronic radiator was initially performed to investigate cost-effective MPC implementation (E-MPC) in a Norwegian zero-emission building (Living Lab) [54]. The experiment lasted for approximately one month (from mid-February to mid-March 2019, with an 18-day excitation phase and an E-MPC operation phase of two weeks. A randomly generated binary signal switching the radiator temperature set-point between 21 °C and 24 °C was created to excite the thermal dynamics of the building and collect measurements for training the model. This new training dataset is based on six days in February and is named here as Experiment 5. The dataset has a time interval of 5 minutes. The hydronic radiator has a rated power of 4.7 kW (at a rated temperature 75 °C/65 °C) and is in the same place as the electric heater of the first set of experiments. The supply water temperature was maintained at about 55 °C leading to a maximum radiator power of 2.5 kW. The

thermostatic valve in the radiator adjusts the mass flow using a proportional-integral (PI) controller to track the set-point temperature. Compared to the electric heater, the thermal mass of the hydronic radiator with 113 kg of steel cannot be neglected. The power delivered to the hydronic radiator (Q_h) is measured by an energy meter based on the difference between supply and return temperatures. When the hydronic radiator is switched on, the initial water temperature in the radiator is close to the indoor air temperature. Due to the thermal mass of the radiator, it takes time for the return temperature to heat up and reach steady-state (when the power delivered to and emitted by the radiator is equal). This makes a large difference in supply and returns temperatures at the beginning, leading to a very high start-up peak for Q_h. The maximum emitted power of the radiator in steady-state is around 2.5 kW, while the maximum delivered power during start-up periods is around 4.0 kW. This confirms that the thermal dynamics of the hydronic radiator are significant.

Table 3-1: *Summary of the four experiments. "Full set" means all measurements of volume-averaged, single sensor (no casing), wall-mounted sensor are available.*

Experiments	Radiator	Door	Sampling time	Period	Use	Temperature Sensor
2	Electric	Open	5 min	18/04-24/04 (2017)	Validation	Full set
3	Electric	Closed	5 min	27/04-08/05 (2017)	Validation	Full set
4	Electric+AHU	Open	5 min	08/05-15/05 (2017)	Training	Full set
5	Hydronic	Open	5 min	22/02-27/02 (2019)	Training	Wall-mounted

In the experiments with the electric heater, PT100 sensors with an accuracy of ± 0.1 K are placed at different locations in the building; see details in [76]. This leads to the definition of three datasets:

- Two available datasets correspond to different placements of PT100 temperature sensors without casing and with wireless transmitters. They are placed in a vertical bar in the middle of the two living rooms (see green dots in Figure 3-1 (b) and Figure 3-2 (a)). For each bar, the height of the six sensors is 0.18 m, 0.95 m, 1.6 m, 1.7 m, 2.3 m and 3.4 m, respectively. The volume-averaged temperature of the building is calculated using the measurement from all the sensors placed in the vertical bars and evaluated using the volume average at each horizontal layer. The single sensor without casing dataset corresponds to the measurement at 1.6 m in the living room south. The height of 1.6 m is close to the middle height of the building, where the influence of stratification is expected to be minimal (meaning that the measured temperature at 1.6 m is the closest to the volume-averaged temperature).

- The third dataset is based on PT100 sensors mounted on the wall in a casing (see the orange dot in Figure 3-1 (b) and Figure 3-2 (b)). The height of the wall-mounted sensors is 0.1 m, 0.8 m, 1.6 m, 2.4 m and 3.2 m, respectively. The third dataset corresponds to the measurement of a single wall-mounted sensor mounted in the south of the living room at the height of 1.6 m.

In the experiments with the hydronic radiator, only the temperature measurements from the wall-mounted temperature sensor are available.

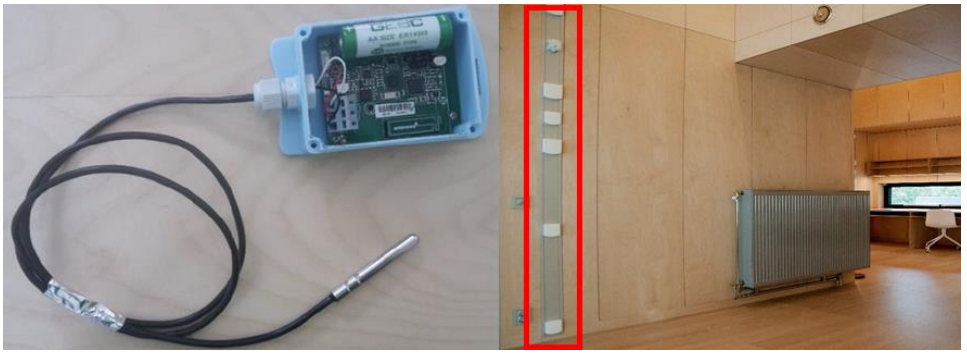

(a) *(b)*

Figure 3-2: *Wireless temperature sensors (a) and wall-mounted temperature sensors (b).*

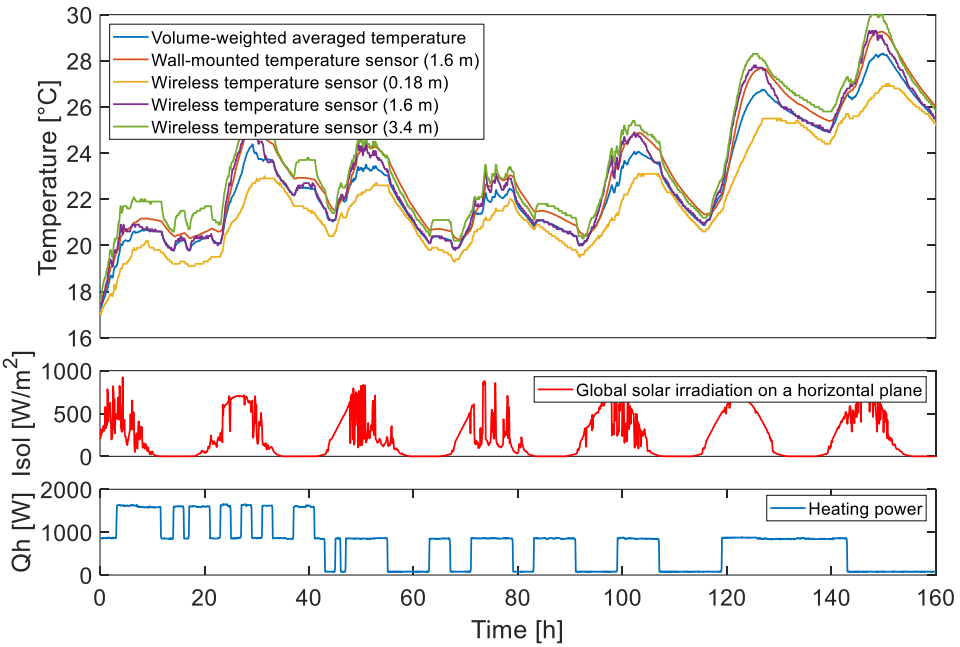

Figure 3-3: *Comparison of different indoor temperature sensors, global solar irradiation on a horizontal plane and heating power of the electric heater for Experiment 4.*

Figure 3-3 shows the temperature reading from the wireless temperature sensors with different heights (0.18 m, 1.6 m and 3.4 m) and the wall-mounted temperature sensor (1.6 m) against the volume-averaged temperature. The stratification of the temperature of the wireless temperature sensors at different heights can be observed. The stratification gets larger when the solar radiation or the radiator power is large. The reason for choosing the sensor in the south was to capture the influence of solar radiation. The thermal dynamics of the wall-mounted sensor can also be observed. The reading from the wall-mounted sensor is smoother compared to the volume-averaged temperature and the readings from the single wireless temperature sensors.

3.1.2 IDA ICE building model and corresponding experiments

IDA ICE is a detailed dynamic simulation tool to study the indoor environment and the energy consumption of buildings. In this thesis, an IDA ICE building model is used as a virtual experiment to generate data for system identification. It is a two-story detached house located in Oslo with a heated floor area of 160 m². The building is constructed in wood, meaning a lightweight construction, and complies with the requirement of the Norwegian passive house standard, NS 3700 [77]. The three-dimensional geometry of the building is shown in Figure 3-4. The building is equipped with balanced mechanical ventilation with a heat recovery unit. A cascade ventilation strategy is applied. This heat exchanger is modeled using constant effectiveness of 85% without bypass (like a plate heat exchanger) to promote the linearity of the model. This is done because the research focuses on the thermal dynamics of the building envelope and does not aim at modeling the air handling unit (AHU) in detail. Other detailed information regarding the BPS software model can be found in [78].

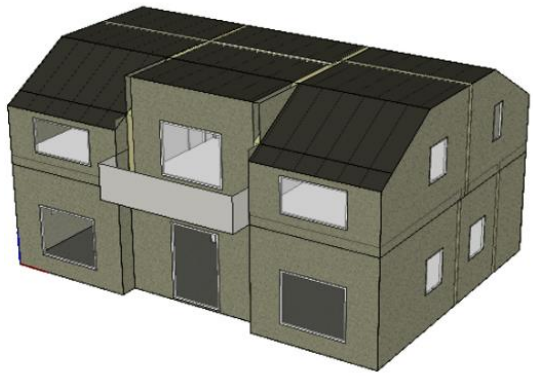

Figure 3-4: *3D geometry of the building model in IDA ICE (showing the southwest facade).*

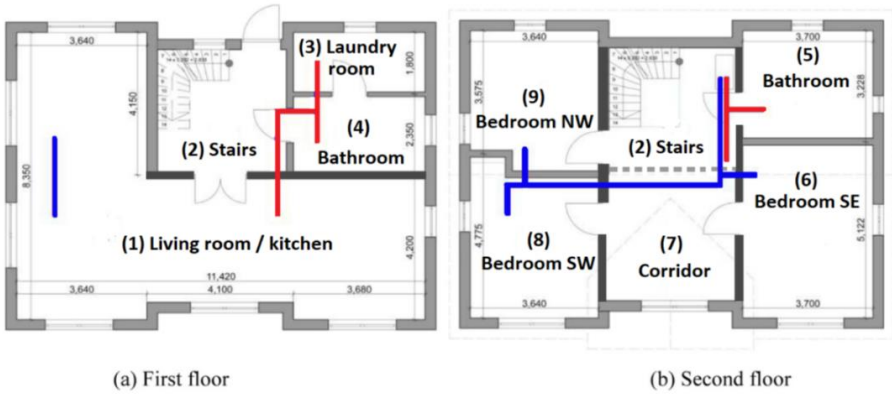

Figure 3-5: *Floor plan of the test building (ducts for the supply air are in blue and in red for extraction).*

The detailed building model is multi-zone and the zoning follows the floor plan presented in Figure 3-5. For the sake of simplicity, the grey-model models considered in our study are mono-zone to ensure that the model performance is not polluted by other phenomena, such as overfitting or poor model fidelity. Consequently, the indoor temperature in our virtual experiments should be as uniform as possible. This is done by opening all the internal doors inside the building. IDA ICE has an embedded ventilation network model, which accounts for the large bidirectional airflow through open doorways. Thus, the air temperature inside the building computed by IDA ICE is relatively uniform due to the large convective heat transfer between rooms. The volume-averaged temperature is selected to represent the measured indoor air temperature. The mean air temperature of the extract ventilation air is also a common choice. However, based on preliminary investigations, the volume-averaged temperature proved to give better grey-box models for this test case. The building is heated using electric radiators as these are the most common space-heating systems for residential buildings in Norway [79]. This heating system has smaller thermal inertia than the building envelope, so the dynamics of the radiators are expected to play a limited role. Hourly profiles for internal gains generated by artificial lighting, electric appliances and occupancy are taken from the Norwegian technical standard TS3031:2016 [80]. The typical meteorological year (TMY) of Oslo with a resolution of one hour is used for the IDA ICE simulations. Like internal gains, solar gains thus have a resolution of one hour.

The Pseudo-Random Binary Signal (PRBS) is also used to activate the heating system in the virtual experiments. The excitation signal is simultaneously applied to all the electric radiators in the BPS model. Following the guidelines of the IEA EBC Annex 58 [27], the excitation signal is in fact the combination of the two PRBS signals. One sequence to identify the short-time dynamics with a period (T) of 10 minutes and with an order (n) of 8. The second sequence aims at identifying the long time constant of

the building with a period (T) of 3.5 hours and n equals 5. The PRBS signal can be applied to four different weeks in the space-heating season. These weeks are characterized by different weather conditions, as described in Table 3-2.

Table 3-2: *Weather conditions in four PRBS experiments.*

Type	Outdoor Temperature	Sky	Date	Duration
Very Cold	-10 °C	Clear sky	12/13/2019	One week
Cold	0 °C	Overcast	12/24/2019	One week
Cold	0 °C	Clear sky	3/23/2019	One week
Mild	5 °C	Overcast	11/23/2019	One week

However, it is not always desirable to apply a PRBS signal to the space-heating system as large variations of the indoor temperature may occur and lead to thermal discomfort for the occupants. Therefore, conventional controls of heating systems are also investigated. Intermittent heating with a temperature setpoint changing between daytime and night-time is considered (i.e., a night setback). Two different local controllers are tested to track the set-point temperature in each room: a Proportional-Integral (PI) control and an on-off control (with a differential of 1K). The last one is the most common control strategy for electric radiators in buildings. When a PRBS signal is applied over a long period of time (i.e., longer than one week), it is difficult to design the signal so that the indoor temperature is kept within comfortable temperature limits for the occupants. By definition, conventional heating controls enable to have normal occupancy of the building during the experiments used to collect data for model identification. It is thus possible to collect data over a longer period of time than one week without impacting the thermal comfort of building users. The full space-heating season (FHS) starting in November and finishing at the end of March can be used to train the model. However, it is also interesting to test whether a shorter training period of one month would be sufficient to train the grey-box models. It is also interesting to check whether specific months are more suited for this task. Therefore, the model parameters are also identified using each of five different months of the space-heating season (i.e., Month 1 to 5). 20 different datasets have been generated using different excitation signals, duration of the experiment and weather data. The detailed description of each case can be found in Table 3-3 below. IDA ICE assumes that variables are piecewise linear during one-time step. The model equations are integrated numerically using a variable time-step so that data is not generated at constant time intervals. Consequently, conservative interpolation has been used to interpolate IDA ICE data on a uniform grid of 2.5 min. This time step is significantly smaller than the shortest period of the PRBS (i.e., 10 min).

Table 3-3: *Description of the datasets and their corresponding abbreviation.*

Case (dataset)	Case description (excitation)	Period/ Duration	Abbreviation
1	PRBS1	Week 1	W1-PRBS
2	PRBS2	Week 2	W2-PRBS
3	PRBS3	Week 3	W3-PRBS
4	PRBS4	Week 4	W4-PRBS
5	Intermittent on-off	Week 1	W1-Inter I/O
6	Intermittent on-off	Week 2	W2-Inter I/O
7	Intermittent on-off	Week 3	W3-Inter I/O
8	Intermittent on-off	Week 4	W4-Inter I/O
9	Intermittent on-off	Month 1	M1-Inter I/O
10	Intermittent on-off	Month 2	M2-Inter I/O
11	Intermittent on-off	Month 3	M3-Inter I/O
12	Intermittent on-off	Month 4	M4-Inter I/O
13	Intermittent on-off	Month 5	M5-Inter I/O
14	Intermittent on-off	Full heating season	FHS-Inter I/O
15	Intermittent PI	Month 1	M1-PI
16	Intermittent PI	Month 2	M2-PI
17	Intermittent PI	Month 3	M3-PI
18	Intermittent PI	Month 4	M4-PI
19	Intermittent PI	Month 5	M5-PI
20	Intermittent PI	Full heating season	FHS-PI

3.2 System identification for the building

3.2.1 Grey-box modeling

3.2.1.1 Grey-box model structure

The structure of the grey-box models is derived from the conservation of energy. The physics modeled by the grey-box models is the heat transfer between the building and its outdoor environment, the solar radiation and internal gains.

In this thesis, a mono-zone model structure is taken to fit the ZEB Living Lab and IDA ICE data for the following reasons. In IDA ICE virtual experiments, the air temperature inside the building computed by IDA ICE is relatively uniform due to large bidirectional airflow through open doorways and the large convective heat transfer between rooms. In the ZEB Living Lab experiments, the building is super-insulated with an efficient heat recovery of the ventilation air. These two points lead

to limited temperature differences between rooms [33] (compared to the temperature difference between indoor and outdoor air) even if internal doors are closed. Consequently, the ZEB Living Lab can be modeled as one thermal zone (i.e., the mono-zone model with a unique node to represent the indoor temperature). The studies [29,32,34] confirmed that a mono-zone grey-box model is able to make an accurate prediction of the air temperature in the ZEB Living Lab, for closed and open internal doors.

An example model structure 5R3C is shown in Figure 3-6. Other model structures are presented in Paper 1, Paper 3, Paper 4 and Paper 6. The physical meaning of the model parameters is listed in Table 3-4.

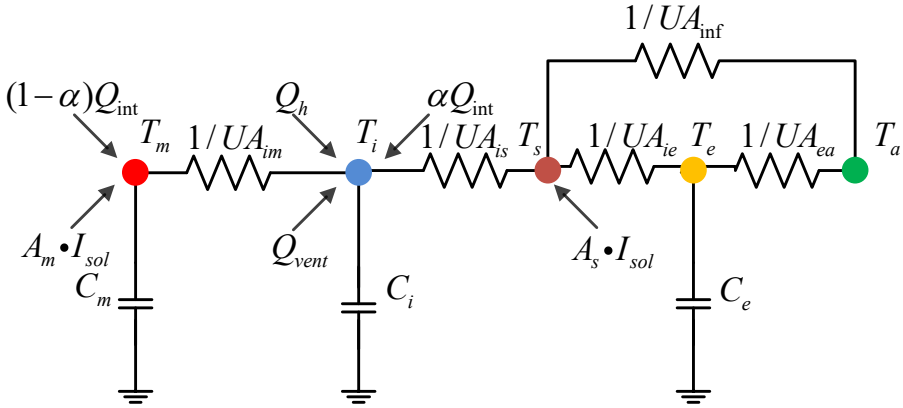

Figure 3-6: *Structure of the 5R3C model.*

The corresponding state-space model of Figure 3-6 is given by:

$$\begin{bmatrix} \dot{T}_e(t) \\ \dot{T}_i(t) \\ \dot{T}_m(t) \end{bmatrix} = \begin{bmatrix} -\frac{(UA_{ie}+UA_{ea})}{C_e} + \frac{UA_{ie}^{\,2}}{C_e \bullet (UA_{is}+UA_{ie}+UA_{\inf})} & \frac{UA_{ie} \bullet UA_{is}}{C_e \bullet (UA_{is}+UA_{ie}+UA_{\inf})} & 0 \\ \frac{UA_{ie} \bullet UA_{is}}{C_i \bullet (UA_{is}+UA_{ie}+UA_{\inf})} & -\frac{(UA_{im}+UA_{is})}{C_i} + \frac{UA_{is} \bullet UA_{is}}{C_i \bullet (UA_{is}+UA_{ie}+UA_{\inf})} & \frac{UA_{im}}{C_i} \\ 0 & \frac{UA_{im}}{C_m} & -\frac{UA_{im}}{C_m} \end{bmatrix} \begin{bmatrix} T_e(t) \\ T_i(t) \\ T_m(t) \end{bmatrix}$$

$$+ \begin{bmatrix} \frac{UA_{ea}}{C_e} + \frac{UA_{ie} \bullet UA_{\inf}}{C_e \bullet (UA_{is}+UA_{ie}+UA_{\inf})} & \frac{UA_{ie} \bullet UA_{\inf}}{C_e \bullet (UA_{is}+UA_{ie}+UA_{\inf})} & 0 & 0 & 0 \\ \frac{UA_{is} \bullet UA_{ie}}{C_i \bullet (UA_{is}+UA_{ie}+UA_{\inf})} & \frac{UA_{is} \bullet A_s}{C_i \bullet (UA_{is}+UA_{ie}+UA_{\inf})} & \frac{\alpha}{C_i} & \frac{\alpha}{C_i} & \frac{1}{C_i} \\ 0 & \frac{A_m}{C_m} & \frac{1-\alpha}{C_m} & \frac{1-\alpha}{C_m} & 0 \end{bmatrix} \begin{bmatrix} T_a(t) \\ I_{sol}(t) \\ Q_{int}(t) \\ Q_{vent}(t) \\ Q_h(t) \end{bmatrix} \quad (3\text{-}1)$$

$$y(t) = \begin{bmatrix} 0 & 1 & 0 \end{bmatrix} \begin{bmatrix} T_e(t) \\ T_i(t) \\ T_m(t) \end{bmatrix} \tag{3-2}$$

Table 3-4: *The physical interpretation of the parameters of all grey-box models.*

Parameters	Physical interpretation and unit
T_i	Temperature of the internal node (i.e., indoor air, furniture) [°C].
T_e	Temperature of the external walls [°C].
T_s	Temperature of the internal wall surfaces of external walls [°C].
T_m	Temperature of the internal walls [°C].
T_a	The outdoor (or outdoor) temperature [°C].
C_i	Heat capacity including the thermal mass of the air, the furniture [kWh/K].
C_e	Heat capacity of the node external wall for the second-order and third-order models [kWh/K].
C_m	Heat capacity of the node internal wall for the third-order model [kWh/K].
UA	Overall heat transfer coefficient (HTC) between T_i and T_a [kW/K].
UA_{ie}	Heat conductance between the building envelope and the interior [kW/K].
UA_{ea}	Heat conductance between the outdoor and the building envelope [kW/K].
UA_{inf}	Heat conductance between the outddoor and the interior node (components with negligible thermal mass, like windows and doors) [kW/K].
UA_{im}	Heat resistance between the internal thermal mass and the interior node [kW/K].
UA_{is}	Heat resistance between the indoor wall surface and the interior node [kW/K].
Q_{int}	Internal heat gain from artificial lighting, people and electric appliances [kW].
Q_h	Heat gain delivered to the heat emitter [kW].
Q_{vent}	Heat gain from the ventilation (pre-computed using measurements) [kW].
I_{sol}	Global solar irradiation on a horizontal plane [W/m^2].
A_i	The effective window area of the building corresponding to T_i [m^2].
A_e	The effective window area of the building corresponding to T_e [m^2].
A_m	The effective window area of the building corresponding to T_m [m^2].
A_s	The effective window area of the building corresponding to T_s [m^2].
α	Fraction of internal gains injected to the internal node.

3.2.1.2 Model identification tool and method

The MATLAB system identification toolbox is used in this thesis. Madsen et al. [27] illustrated how stochastic models could be formulated as an extension of deterministic models. In the stochastic form, a system noise (or noise term) is added to the deterministic model equations to better account for the modeling approximations, unrecognized inputs and measurement of inputs corrupted by noise. The generic equations of the stochastic linear state-space model in innovation form can be expressed as:

$$\frac{dx}{dt} = Ax(t) + Bu(t) + Ke(t) \tag{3-3}$$

$$y(t) = Cx(t) + e(t) \tag{3-4}$$

where x is the state vector, A, B and C are the system matrices, u is the input vector (i.e., $T_{a,eq}$, Q_{solar}, Q_{int}, Q_h) and y is the output (i.e., indoor temperature, T_i). K is the disturbance matrix of the innovation form (Kalman gain) [81]. The matrices A, B, C and K are functions of the model parameters (θ). The continuous-time model is first discretized so that discrete measurement data can be used to identify the model parameters. Unlike IDA ICE, the time discretization in the MATLAB identification toolbox assumes piecewise-constant input data during each time interval (i.e., zero-order hold).

At the beginning of the identification procedure, the initial guess of the model parameters and their region of feasibility (i.e., lower and upper bounds for each parameter) should be defined by the user as input parameters. Then, the optimizer iterates within the feasibility region to find the value of the parameters that minimize the prediction error criterion $f(x)$

$$f(x) = \sum_{k=1}^{N} \| y_k - \hat{y}_k(\theta) \|^2 \tag{3-5}$$

where y_k is the measurement output while $\hat{y}_k(\theta)$ is the one-step ahead prediction.

The default function (*greyest*) in the MATLAB identification toolbox uses gradient-based optimizers. Four different iterative search methods are used in sequence. Consequently, the optimizer may converge to a local optimum if the problem is not convex. As shown in Arendt et al. [41], Genetic Algorithm (GA) combined with a gradient-based method could be used to solve non-convex optimization problems used to identify the parameters of grey-box models. Likewise, a global optimization algorithm has been implemented in our work to avoid a local optimum. A metaheuristic Particle Swarm Optimization (PSO) is applied at the first stage, followed by the default *greyest* function to refine results during the second stage. The PSO algorithm begins by creating the initial particles and assigning them initial velocities. It evaluates the objective function at each particle location and determines

the best (lowest) function value and the best location. In the next step, new velocities are chosen based on the current velocity, the particles' individual best locations, and the best locations of their neighbors. The optimizer then iterates the particle locations, velocities, and neighbors until the algorithm reaches a stopping criterion. Detailed information on the PSO algorithm can be found in [82,83]. For each test case, both optimization procedures are used in sequence: the default *greyest* and the global optimization. The method giving the lowest error for the prediction error criterion is selected to provide the model parameters. The flow chart of the identification routine is summarized in Figure 3-7.

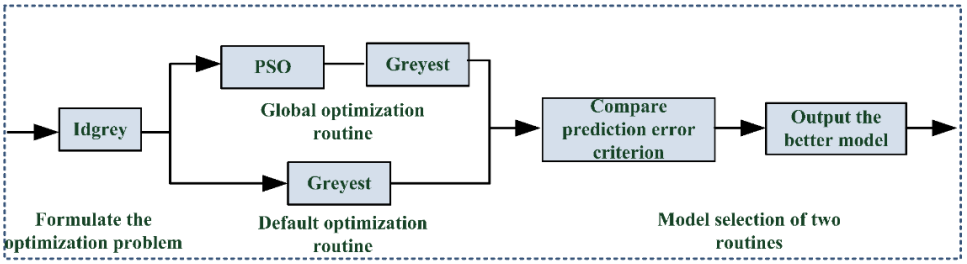

Figure 3-7: *Flow chart of the optimization procedure to identify the model parameters.*

3.2.1.3 Data pre-processing techniques

Extended sampling time (T_s) can lead to a non-physical value and variance for the identified parameters of grey-box models (see e.g., [40]). In real-life applications, it can seldom be guaranteed that measurement data is recorded at a sampling time (T_s) shorter than the shortest time of the system (T_{min}). Thus, three distinct data pre-treatments are investigated in this thesis. They are sampling, low-pass filtering and anti-causal shift (ACS). The original dataset has a sampling time (T_s) that is always faster than the highest frequency of the input signal (T_{min}), such as the PRBS signal. Ljung et al. [40] demonstrated that longer sampling time with $T_s > T_{min}$ can lead to non-physical value and variance for the identified parameters. To investigate this effect, sampling times of increasing duration are considered in our investigations, namely 15, 30 and 60 minutes. Before resampling the data, a low-pass filter can be applied. This leads to three scenarios:

- The first approach is direct sampling (DS) at T_s without pre-filtering. This may cause a high aliasing error.
- The second approach applies a moving-average (MA) filter of length T_s before sampling. With MA, the aliasing error is significantly decreased but, in theory, it can still occur.
- The third approach applies a finite impulse response (FIR) filter with a cut-off frequency of $1/T_s$ before sampling. The FIR would lead to negligible aliasing error (if it is designed in a sufficient order).

By analyzing the performance of the three methods, it is possible to understand the influence of aliasing. It is known that these low-pass filters introduce a time delay [39]. Therefore, The low-pass filters are applied to all input and output variables in the dataset. Thus, theoretically, no delay will be introduced in the dataset, which could influence the final results. The conclusion would be different if the low-pass filter was applied to a subset of the input and output data.

Finally, time labeling plays a role in aligning inputs and outputs for the identification application [40]. As shown by Ljung et al. [40], a time shift, called anti-causal shift (ACS), of the input (Input Delay = $-T_s$) is beneficial for model identification with large T_s. However, the study of Ljung et al. is theoretical and uses a generic example. This effect has been barely analyzed in the context of buildings.

3.2.1.4 Sensor dynamics

Figure 3-3 shows that the wall-mounted sensors have non-negligible thermal dynamics. Consequently, the grey-box model structures introduced in Section 3.1 should be adapted to account for the effect of the time constant of sensor dynamics and thus avoid potential mistakes in the model identification process. As proposed in Bacher et al. [45], it is possible to add an additional node for the temperature sensor, leading to an extra resistance (R_s) and capacitance (C_s). However, the authors also pointed out that it was not possible to give a physical interpretation of the value of C_s. This was also found in our preliminary tests based on our data. Therefore, we rather introduced an adaptation of the model with a single additional parameter, the time constant of the sensor $\tau = R_s C_s$. The model decreased the number of parameters compared to the version in the study [45] to increase the identifiability of the model. The dynamics for the sensor node are expressed by the following equation:

$$\frac{dT_{sensor}}{dt} = \frac{1}{\tau}(T_i - T_{sensor}) \tag{3-6}$$

where T_i is the temperature of the internal node, T_{sensor} is the temperature measurement from the wall-mounted temperature sensors.

3.2.2 Structural and practical identifiability

Checking structural identifiability is the prerequisite in the model identification process [84–86], which refers to the theoretical possibility of determining the parameter values from the input and output data. This property guarantees that the parameters can be uniquely determined from the input-output data under ideal conditions of noise-free observations and error-free model structure. The structural identifiability of the candidate models in this study is verified using DAISY software [84]. However, field measurement data always contain noise and error, which challenges the practical identifiability of the model. Therefore, the prediction performance and the physical plausibility of parameters are taken as the criteria for the model selection (see Section 3.2.3 for more details). Finally, for stochastic

models, a cumulative periodogram is used as an additional criterion to prove that the model is complex enough to capture the building dynamics.

3.2.3 Key performance indicators

Several key performance indicators (KPIs) are defined to evaluate the model performance. They can be divided into two categories: the physical plausibility of the identified parameters and the prediction performance of the model.

Physical plausibility means that the calibrated value of the model parameters should give a physically reasonable estimate of the thermal properties of the building. For conciseness in our study, it is not possible to report the value and variance of all the model parameters. However, the key parameters that are enough to support our conclusions are presented: the overall heat transfer coefficient (HTC) and the capacitances (C_i and C_e). In addition, one parameter modeling the influence of the solar radiation, the effective window area (A_i), will also be taken as KPI when the influence of the data pre-processing is discussed.

The overall heat transfer coefficient (HTC) is the total heat loss of the building in steady-state. Heat transfer by convection and long-wave radiative heat transfer is nonlinear. However, heat conduction is dominant and has good linear properties if the building is highly insulated and airtight. The combination of several resistances of the grey-box model forms the HTC, which is defined by Equation 3-7 for the 3R2C model. Therefore, only the value of the HTC is shown in the later discussion, not its variance.

$$HTC = \frac{1}{1/UA_{ie} + 1/UA_{ea}} + UA_{\text{inf}} \tag{3-7}$$

For the IDA-ICE experiment, the HTC has been estimated to be about 85 W/K (identified by applying a step function of the space-heating to the IDA ICE model). The C_e can be compared to the effective thermal capacitance C_{eff}. This one has been evaluated using one daily periodic excitation for the IDA ICE model according to the standard 13786:2017 [87] (see Paper 3) with a value of 3.9 kWh/K.

For the ZEB Living Lab, Clauβ et al. [88] evaluated the HTC value of the ZEB Living Lab to be 83 W/K, which is used as the reference value for the HTC. The C_{eff} range is taken from the recommended value based on Norwegian NS3031 standard [80], which gives the typical C_{eff} per square meter for lightweight Norwegian construction.

The long-term prediction performance is of the utmost importance if the main application of the grey-box model is being employed in an MPC. Equation 3-8 gives the method of calculating the normalized root mean squared error (NRMSE).

$$NRMSE = \frac{\| y_k - \hat{y}_k \|}{\| y_k - mean(y_k) \|} \tag{3-8}$$

The NRMSE fitting, defined in Equation 3-9, is used to evaluate prediction performance. It translates how well the response of the predicted model matches measurement data. If the fit is 100%, the model perfectly matches the measurement data, whereas a low or negative fit is a model of lower quality. The NRMSE fitting value is calculated based on simulation for the deterministic model and one-day ahead prediction for the stochastic model. In other words, for the stochastic model, the model selection is made using the one-step ahead prediction while the ability to perform MPC is evaluated using a one-day ahead prediction.

$$NRMSE_{fit} = (1 - NRMSE) \times 100\% \tag{3-9}$$

In addition to the NRMSE fitting value, the mean bias error (MBE) defined by Equation 3-10 is also used as a complementary index. Theoretically, an MBE value close to zero is best as this means that the residual of the model has a lower mean bias error.

$$MBE = \frac{1}{n}\sum_{i=1}^{n}(y_k - \hat{y}_k) \tag{3-10}$$

In practice, the results show that all our models have good MBE properties. Therefore, this index has been used but is not reported in the thesis.

3.3 MPC experiments setup

The MPC experiments are done with MATLAB and IDA ICE. The co-simulation of the virtual experiments uses the IDA ICE model in Section 3.1.2 as the emulator. The time step in the co-simulation is set to 15 min. At each step, IDA ICE first sends the calculated volume-averaged indoor temperature (T_i) of the building to MATLAB. The MPC controller then takes the prediction of the weather data and the internal heat gains into the MPC optimization. It generates the optimal control sequence (i.e., the optimal heating power, Q_h) over the prediction horizon. Only the first time step of the control sequence is sent to IDA ICE to be executed during one time step. After the first time step is completed, the new state of volume-averaged indoor temperature is sent back to MATLAB again and a new round starts. The process keeps iterating within the co-simulation framework until the predetermined simulation period is completed. A sketch of the co-simulation process is presented in Figure 3-8. Khatibi et al. [89] have used a similar co-simulation setup in IDA ICE in their study to investigate the flexibility of the air heating and ventilation system. IDA ICE requires an initialization period before the temperature difference between the zone to be realistic. Therefore, a PID control is taken at the beginning of the co-simulation before starting the MPC. The length of this initialization of the virtual experiment is set to be a half-day before switching to MPC.

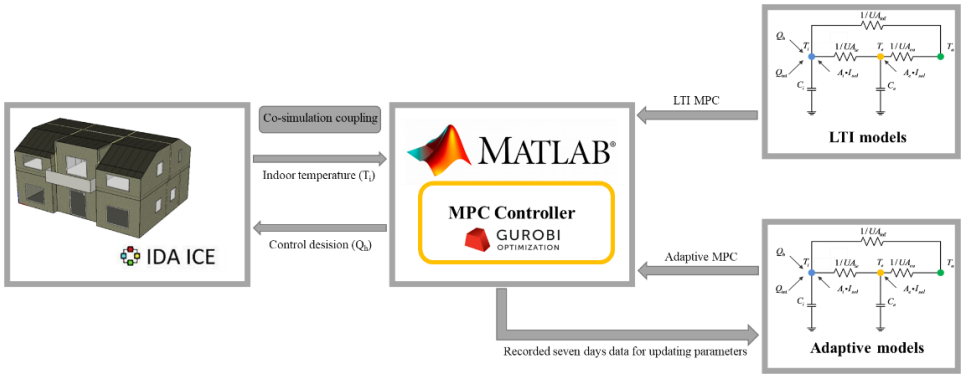

Figure 3-8: co-simulation experiment setup between IDA ICE and MATLAB.

In the MPC, the minimum indoor temperature limit is set to 20 °C and the maximum limit is set to 24 °C. There is a night setback for the minimum temperature limit decreasing from 20 °C to 16 °C from 11 PM to 7 AM. The room temperature bounds are defined as Equation (3-11). The indoor temperature limits are used as thermal comfort constraints for the MPC. For the sake of simplicity, the radiator in the IDA ICE model is assumed to be able to modulate its power by adjusting its part load ratio (PLR). The total heating power of all the radiators is 3220 W. Thus, the power constraint of the heating system is from 0 to 3220 W in the MPC.

$$T_{room} = \begin{Bmatrix} 16 \le T_{room} \le 24 \text{ if } t \in (23:00, 24:00) \\ 16 \le T_{room} \le 24 \text{ if } t \in (0:00, 7:00) \\ 20 \le T_{room} \le 24 \text{ if } t \in (7:00, 23:00) \end{Bmatrix} \quad (3\text{-}11)$$

3.3.1 Optimal Control Problem Formulation

The thesis investigates the performance of the MPC controllers with three different control objectives to make sure conclusions do not depend on the objective function.

1) Objective 1 (Energy Savings): Minimize the total electricity use of the heating system while limiting indoor thermal discomfort at the same time.
2) Objective 2 (Energy Cost Saving): Minimize the total electricity cost of the heating system while maintaining indoor thermal comfort. The electricity spot price from Nordpool and the historical weather data for 2019 are used.
3) Objective 3 (Energy Cost Saving with Peak Reduction): Minimize the total electricity cost and reduce the electricity use during the peak hour of the grid while limiting indoor thermal discomfort.

The second and third types of MPC are usually called economic model predictive control (EMPC) in other studies.

With these control objectives and the defined constraints, the optimal control problem can be formulated. As previously mentioned, the time step of each control decision is 15 minutes. The prediction horizon of the MPC controller is set to be 24 hours (96 slots, N = 96). The prediction length is a typical value in building MPC implementation [43,56,58]. The prediction length is also acceptable considering the computational cost. The equations of the optimization problem are given below.

Case 1: $$\min_{Q_h} \sum_{k=0}^{N-1} Q_h[k] + \varepsilon_1[k] L\varepsilon_1^{'}[k] + \varepsilon_2[k] L\varepsilon_2^{'}[k] \tag{3-12}$$

Case 2: $$\min_{Q_h} \sum_{k=0}^{N-1} c_h[k] Q_h[k] + \varepsilon_1[k] L\varepsilon_1^{'}[k] + \varepsilon_2[k] L\varepsilon_2^{'}[k] \tag{3-13}$$

Case 3: $$\min_{Q_h} \sum_{k=0}^{N-1} c_h[k] Q_h[k] + p_h[k] Q_h[k] + \varepsilon_1[k] L\varepsilon_1^{'}[k] + \varepsilon_2[k] L\varepsilon_2^{'}[k] \tag{3-14}$$

Subject to

$$x[k+1] = Fx[k] + Gu[k] + Ke[k], k \in N_0^{N-1} \tag{3-15}$$

$$T_{indoor}[k] = Cx[k], k \in N_0^{N-1} \tag{3-16}$$

$$T_{low}[k] - \varepsilon_1[k] \le T_{indoor}[k], k \in N_0^{N-1} \tag{3-17}$$

$$T_{indoor}[k] \le T_{up}[k] + \varepsilon_2[k], k \in N_0^{N-1} \tag{3-18}$$

$$0 \le Q_h[k] \le Q_{h,\max}[k], k \in N_0^{N-1} \tag{3-19}$$

$$0 \le \varepsilon_1[k]; 0 \le \varepsilon_2[k], k \in N_0^{N-1} \tag{3-20}$$

where $x[k]$ is the state vector in discrete-time, F, G and C are the discrete system matrices trained from the system identification process, $u[k]$ is the input vector in discrete-time and $y[k]$ is the output. K is the tuned steady Kalman gain of the model. $Q_h[k]$ is the calculated optimal heat power at each step in the prediction horizon, while $Q_{h,max}[k]$ is the max power of the heating system. $\varepsilon_1[k]$ and $\varepsilon_2[k]$ are the slack variables of the soft constraints on the thermal comfort band. L is the weighting factor that is set to penalize thermal discomfort in the objective function. The soft constraints enable the solver to avoid infeasible optimization problems by allowing thermal comfort bands to be violated. $ch[k]$ is the electricity price profile at each slot generated from the historical electricity price from Nordpool. $ph[k]$ is the penalty cost for using electricity during peak hours, which is a predefined arbitrary profile that has two levels.

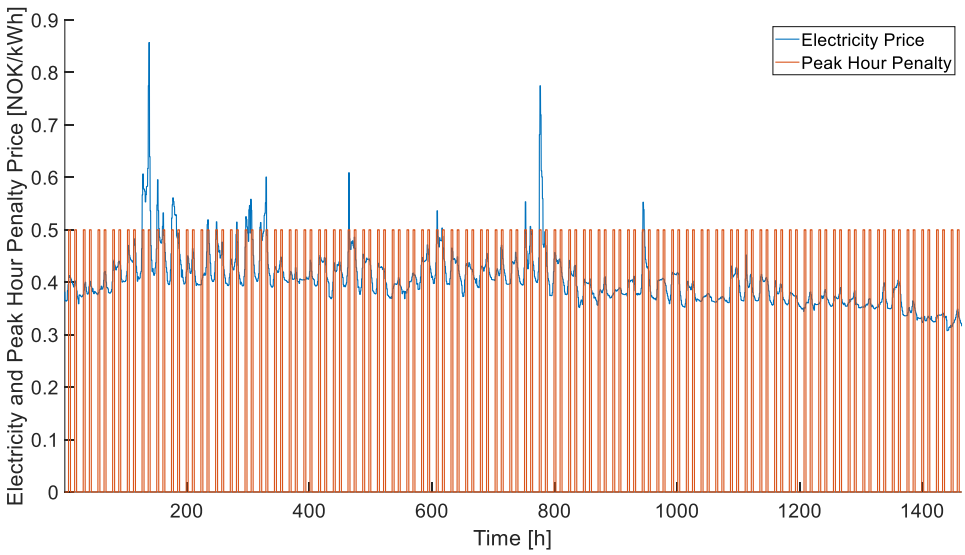

Figure 3-9: *Electricity and Peak Hour Penalty Cost Profile.*

The electricity price profile and the peak hour penalty cost profile are given in Figure 3-9 given in Norwegian Krone [NOK/kWh]. $T_{indoor}[k]$ is the predicted indoor temperature from the prediction model. $T_{low}[k]$ and $T_{up}[k]$ are the corresponding temperature boundaries inside the prediction horizon. The receding horizon is implemented in the MPC, so the above optimization problem is solved at each step (every 15 minutes) to get the optimal control decision. Then, the initial states of the control model and weather forecasts are updated with the receded prediction horizon. Thermal discomfort is not desirable. Thus, the penalty weight factor L of the slack variables is given with a large value. The baseline penalty weight factor L is set to 10^8 in this study, but L is also set at 10^6 in the sensitivity analysis. A solver that can solve quadratic programming optimization problems is needed due to the quadratic form of the slack variables ε_1 and ε_2. The toolbox YALMIP [90] in MATLAB is used for the optimization problem formulation, and Gurobi [91] is used to solve the optimization problem.

3.3.2 Conventional and Adaptive MPC

Two months of simulation are used to investigate the performance difference between the conventional and adaptive MPCs. The second-order 3R2C grey-box model has proven to be a suitable trade-off between model complexity and accuracy. Therefore, this thesis takes 3R2C as the prediction model structure, and details can be found in Paper 6. The conventional MPC is based on an LTI model and the parameter values are kept unchanged during simulation. The conventional MPC using three different LTI models is compared. The FullWinter model is trained with the entire winter season data where the building is heated using intermittent temperature setpoints. The two other LTI models are trained using the data from PRBS experiments of

November and December, respectively, called PRBSNOV and PRBSDEC. Two candidate adaptive MPC controllers are designed. The two adaptive MPCs take the FullWinter model as the initialization model. The Partially Adaptive MPC only updates the effective window area (A_i) parameter during the simulation. The effective window area is a model parameter which is the ratio between the solar gains injected in a node of the RC model and the total solar irradiation measured on a horizontal plane (I_{sol}). The main reason to focus on the effective window area is that solar gains are a dominant factor that influences the model accuracy. Due to cloud cover, changing altitude and zenith angles of the sun, the effective window area is expected to change significantly during the space-heating season, especially for high latitudes. The corresponding pseudo-code for updating the effective window area is presented in Algorithm 1. The Fully Adaptive MPC updates all seven parameters of the model during simulation. It gives more degrees of freedom as more parameters can be calibrated compared to the other adaptive MPC. However, the Fully Adaptive MPC theoretically takes more time to converge to update the model parameters. Furthermore, there is a risk of obtaining a set of unphysical parameters due to insufficient training data (meaning that the model is practically non-identifiable). The pseudo-code for the Fully Adaptive MPC is presented in Algorithm 2. The summary of the different cases is given in Table 3-5.

The sliding accumulated error (ErrorS) is used as the index to determine whether a parameter update is required. The sliding accumulated error is defined as the sum of absolute prediction error (i.e., the difference between the measurement and the model prediction at each time step) over the last 12 steps (i.e., 3 hours). The parameter updating routine is activated when ErrorS exceeds a predetermined threshold. The threshold is called ErrorIndex and is set to 5. A lower ErrorIndex means a lower tolerance for error, which can be tuned based on the application scenario.

Algorithm 1: *Pseudo-code for the partially adaptive MPC.*

Algorithm 1: Partially Adaptive MPC

Initialize: Set FullWinter as the prediction model for the Partially Adaptive MPC;

Input: ErrorS;

if ErrorS> ErrorIndex

  Update the parameter A_i.

else

  Keep A_i unchanged.

end

Algorithm 2: *Pseudo-code for the fully adaptive MPC.*

Algorithm 2: Fully Adaptive MPC

Initialize: Set FullWinter as the prediction model for the fully Adaptive MPC;

Input: ErrorS；

if ErrorS > ErrorIndex

  Update all parameters of the model.

else

  Keep parameters unchanged.

end

It is unreasonable to use short training period data to update the model parameters as it leads the parameters to be completely unphysical or have large uncertainty. On the other hand, taking a long period of historical data for retraining is also not optimal since the adaptive MPC should be able to adapt the parameters for changing operating conditions. Pushed to the extreme, a very long retraining period will make the adaptive model converge toward an LTI model. Therefore, the length of the retraining period for updating the parameters is set to seven days. Preliminary tests have shown that seven days of data using intermittent on-off heating leads to a model with physically plausible parameters and fair prediction performance. Given the duration of the retraining period, the adaptive MPC routines are not able to update parameters during the first seven days of co-simulation.

Table 3-5: *Cases summary of experiments.*

Case	Excitation	Training Period
FullWinter	Intermittent on–off	11/1/2019 - 3/31/2020
PRBSNOV	PRBS	11/23/2019 - 11/30/2019
PRBSDEC	PRBS	12/24/2019 - 12/31/2019
Partially Adaptive MPC	MPC operation	During operation
Fully Adaptive MPC	MPC operation	During operation

In the preliminary experimental operation, the deterministic model shows better prediction performance than the stochastic model when updating parameters with MPC operation data, which fits the conclusion from the previous study [92]. The physical plausible properties of the parameters are also monitored in this study, but the prediction performance of the model is of more importance for MPC

implementation. Therefore, the deterministic model is used to train the model parameters to obtain better MPC performance.

4 RESULTS AND DISCUSSION

This chapter presents the key results of the papers (from Paper 1 to Paper 7) and answers the corresponding research questions of this thesis. The results have three main parts, namely modeling (data collection), modeling (model identification) and control.

Section 4.1 presents the results regarding collecting data for modeling. Paper 1 to Paper 4 covers the content of this topic, which answers Question 1 to Question 3. Section 0 shows the results of the grey-box model identification. The content of Paper 1 to Paper 4 answers Question 4 to Question 6. Section 4.3 considers MPC virtual experiments of the residential building, which answers Question 7. The interconnections of all the listed papers are shown in Table 1-1 and Figure 1-2.

4.1 Modeling (data preparation)

Q 1: Which type, period and duration of the excitation signal are suitable for grey-box model identification of residential buildings?

In Paper 3, 20 different datasets have been generated using different excitation signals, duration of the experiment and weather data. Paper 3 is based on virtual experiments so that parametric runs can be performed only by varying the excitation signal and leaving the other inputs and boundary conditions unchanged. A description of the experiments and their abbreviation is given in Table 3-3. Results show that the intermittent heating with on-off control of the electric radiators is also a good excitation signal in addition to the PRBS signal. Furthermore, It enables normal occupancy of the building and the collection of long data series as well as contains both slow daily and fast dynamics. Results of 3R2C model are taken to answer this question and more details are illustrated in Paper 3.

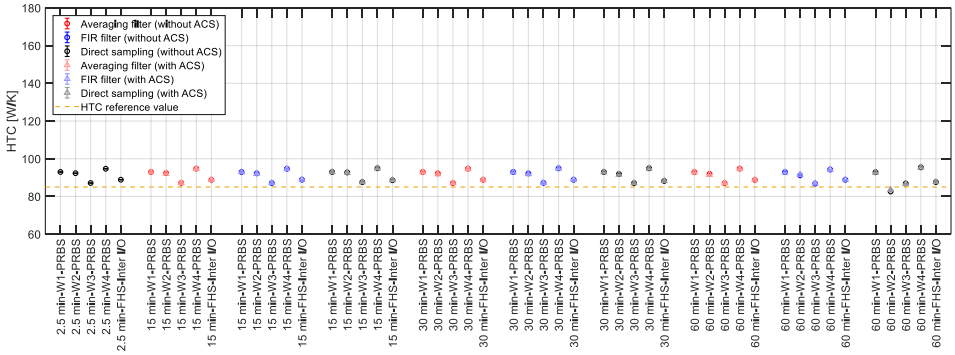

Figure 4-1: *Identified HTC of the 3R2C deterministic model for the cases 1,2,3,4 and 14, different sampling times and pre-filtering techniques; cases with ACS are shown by triangles in lighter colors.*

Figure 4-1 shows the value of HTC for the deterministic model, which is close to the

reference value of 85 W/K. The data pre-processing technique has no significant impact on HTC.

As shown in Figure 4-2, the period and type of excitation signal of the training dataset have the largest influence on C_e while data pre-processing has a limited impact. The value of C_e is similar between the four datasets using PRBS excitation (i.e., cases 1 to 4) and is plausible compared to the C_{eff} of 3.9 kWh/K determined using standards. However, it differs for case 14, corresponding to the intermittent on-off heating during the entire space-heating season that generates a higher value, well above 3.9 kWh/K. To further illustrate the influence of the dataset, the values of C_e identified using an intermittent on-off excitation during each month of the space-heating season are compared, i.e., cases 9 to 13, in Figure 4-3. Even though the excitation signal is generated from the same control (i.e., intermittent on-off control) and has the same duration of one month, the identified C_e strongly depends on the selected period used to train the model, meaning the specific month of the space-heating season.

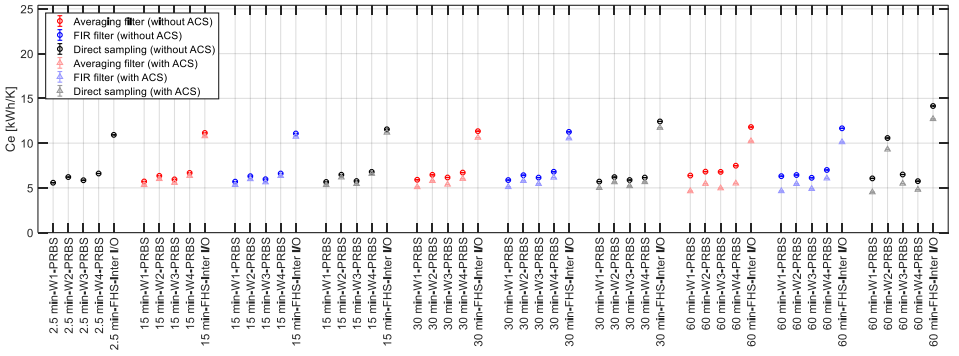

Figure 4-2: *Identified C_e of the 3R2C deterministic model for the cases 1,2,3,4 and 14, different sampling times and pre-filtering techniques; cases with ACS are shown by triangles in lighter colors.*

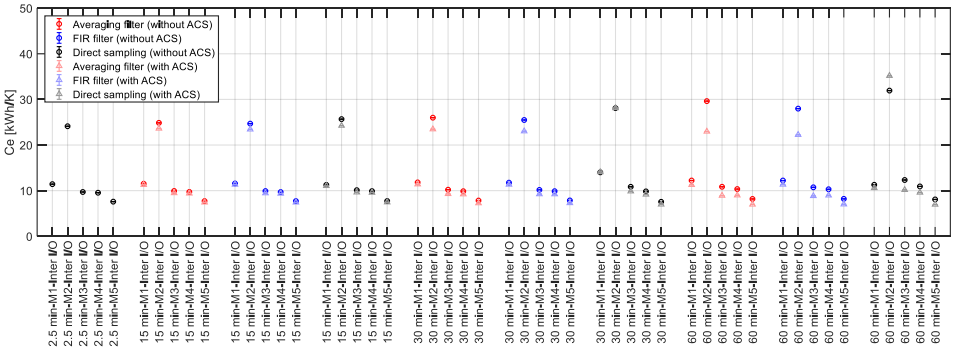

Figure 4-3: *Identified C_e of the 3R2C deterministic model for cases 9 to 13, different sampling times and pre-filtering techniques; cases with ACS are shown by triangles in lighter colors.*

The stochastic model is less dependent on the excitation signals. Figure 4-4 shows that as long as the sampling time is shorter than the system dynamics (i.e., T_s equal 2.5 min depicted by the first black points on the left), the value of C_e is independent of the training period and its variance is limited. The identified values are close to the C_{eff} of 3.9 kWh/K, the value of C_e is meaningful from a physical point of view. The same phenomenon is observed for the value and variance of C_i in Figure 4-5.

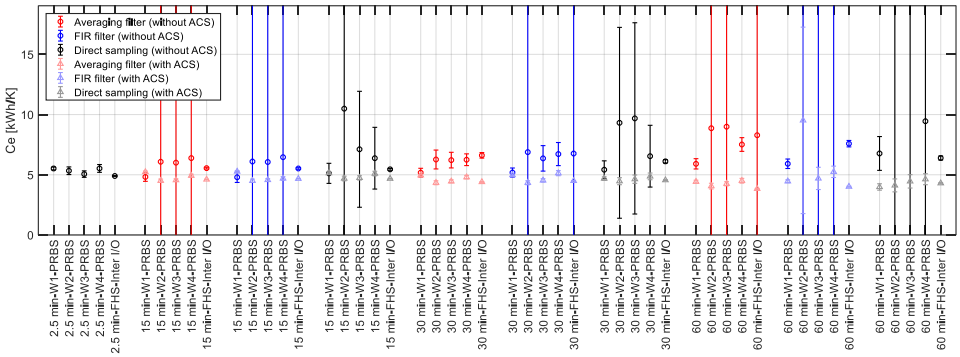

Figure 4-4: *Identified C_e of the 3R2C stochastic model for the cases 1,2,3,4 and 14, different sampling times and pre-filtering techniques; cases with ACS are shown by triangles in lighter colors.*

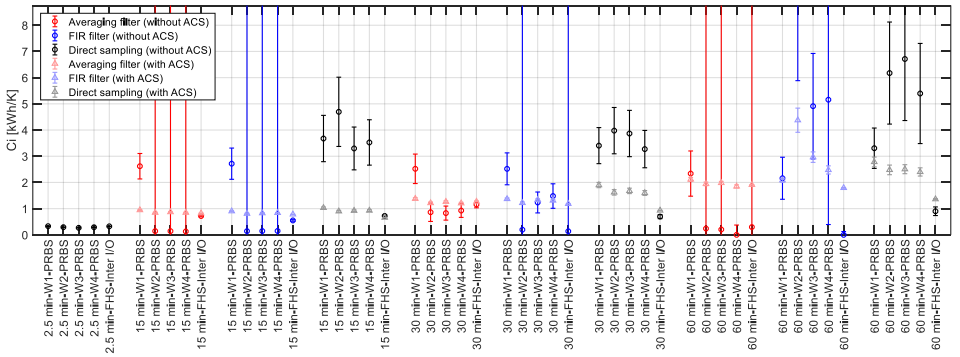

Figure 4-5: *Identified C_i of the 3R2C stochastic model for the cases 1,2,3,4 and 14, different sampling times and pre-filtering techniques; cases with ACS are shown by triangles in lighter colors.*

Even the parameters of the stochastic model are less dependent on the datasets. The parameters trained from different periods are not identical, which will cause the simulation performance from different sets of parameters will be different. This is also confirmed by the results from Paper 1 and Paper 4. The NRMSE fitting of the training dataset is always higher than the validation dataset. Thus, there is no period that is better than others for training the model parameters. It is impossible to use only one set of parameters for the grey-box model that can cover the full winter due to

large variations of complex weather conditions. This conclusion supports the need to investigate adaptive models (Q 7).

In conclusion, the identified parameters are strongly dependent on the types of excitation and the training period for deterministic models. Both the type of excitation (e.g., PRBS and intermittent on-off excitation) and the selected period during the space-heating season influence results. However, the identified parameters are less dependent on excitation signals for stochastic models.

Q 2: Influence of temperature sensor location and dynamics on the grey-box modeling results?

Paper 2 and Paper 4 present the results of the influence of temperature sensor location and dynamics on the grey-box modeling. All the datasets used and their corresponding abbreviations are given in Table 4-1.

Table 4-1: *Description of the datasets and their corresponding abbreviations from ZEB Living Lab.*

Case	Sensor	Sensor node in model	Dataset	Use
T1Exp2	Volume-averaged temperature (T1)	No	Experiment 2	Validation
T1Exp3	Volume-averaged temperature (T1)	No	Experiment 3	Validation
T1Exp4	Volume-averaged temperature (T1)	No	Experiment 4	Training
T2Exp4	Single temperature sensor in the air (T2)	No	Experiment 4	Training
T3Exp4	Single wall-mounted temperature sensor (T3)	No	Experiment 4	Training
T4Exp4	Single wall-mounted temperature sensor (T4)	Yes (τ)	Experiment 4	Training
T5Exp5	Single wall-mounted temperature sensor (T5)	No	Experiment 5	Training
T6Exp5	Single wall-mounted temperature sensor (T6)	Yes (τ)	Experiment 5	Training

Paper 2 is based on multi-zone virtual experiments in IDA ICE. It compares the model performance when the indoor temperature is taken as the volume-averaged air temperature or the exhaust ventilation air temperature. Simulation results from extracted air temperature show a slightly higher simulation NRMSE fitting value for the original training dataset. However, models trained with extracted air temperature show much worse simulation NRMSE fitting compared with volume-averaged temperature for the entire space-heating season data (FHS dataset). Thus, the volume-averaged air temperature is a more balanced choice of representative indoor temperature. In conclusion, even though this is a common choice in the literature, the exhaust air temperature is not always the best option to train the model and this conclusion could be even more severe if all the internal doors inside the building were closed. Then, large temperature differences can be created between the thermal zones

in the building and the exhaust ventilation air temperature may not be a good approximation of the average indoor temperature between the rooms.

Paper 4 identifies deterministic and stochastic models with data from ZEB Living Lab. Most of the results presented are based on the datasets with the electric heaters (i.e., Experiments 2 to 4) with the 3R2C model.

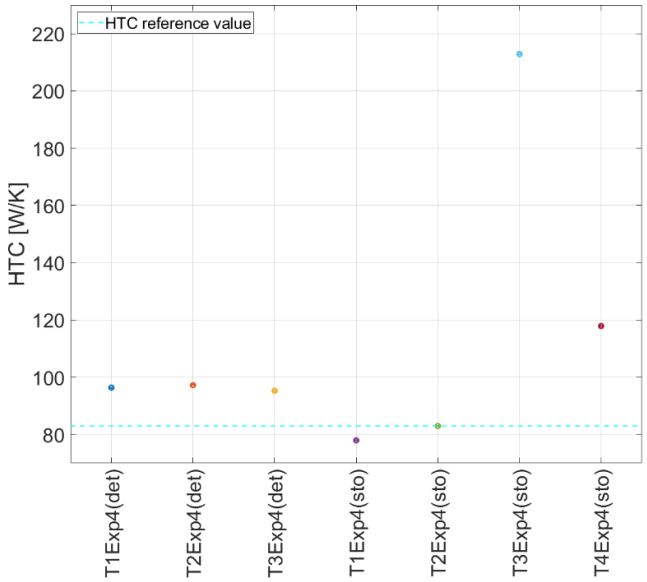

Figure 4-6: *Comparing the HTC of the 3R2C deterministic (det) and stochastic (sto) models using Experiment 4 and different types of temperature measurement (5min).*

In the description of experiments, it has been shown that the indoor temperature is dependent on the type of measurement, see Section 3.1.1. Consequently, Figure 4-6 and Figure 4-7 compare the identified value of two key indicators (HTC and C_e) for the different types of temperature measurement, still using a sampling time of 5 minutes. For the deterministic model, the difference in temperature measurements has a limited influence on the identified model parameters. However, for the stochastic model, the identified HTC value using the baseline 3R2C model and the single wall-mounted temperature sensor is much larger than the reference HTC value. Furthermore, the variance of C_e is also extremely large. Thus, the time constant of the wall-mounted sensor dynamics has a large impact on the stochastic 3R2C model. This conclusion is also confirmed by the cumulative periodogram of the residuals in Figure 4-8, which shows that the baseline 3R2C model with the wall-mounted sensor does not describe the system dynamics (between 0.4–1.4 × 10^{-3} Hz). As introduced in Section 3.4, an adapted model with a time constant for the sensor is added to the original 3R2C model. This adapted model improves the results since the parameters become physically plausible again. In addition, the cumulative periodogram of the residuals confirms this conclusion (see dataset T4Exp4). Furthermore, the one-day

ahead prediction comparison in Figure 4-9 also shows a significant improvement from the 3R2C adapted with a sensor time constant compared to the original baseline 3R2C model. The identified time constant (τ) has a value of 8.28 minutes, thus being larger than the sampling time.

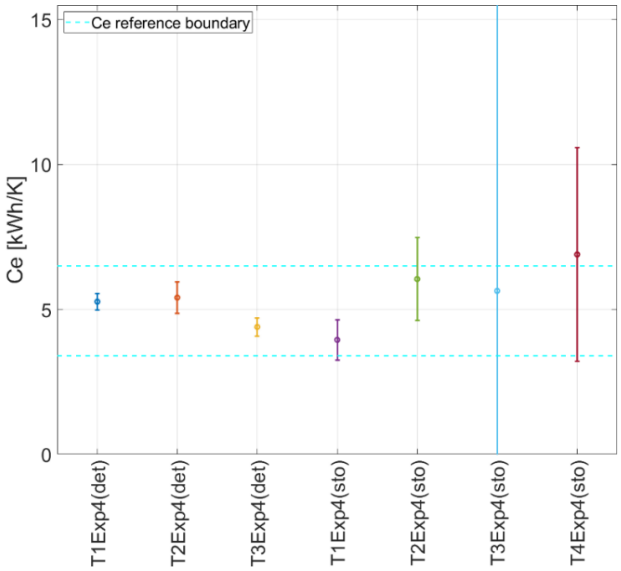

Figure 4-7: *Comparing the Ce of the 3R2C deterministic (det) and stochastic (sto) models using Experiment 4 and different types of temperature measurement (5 min).*

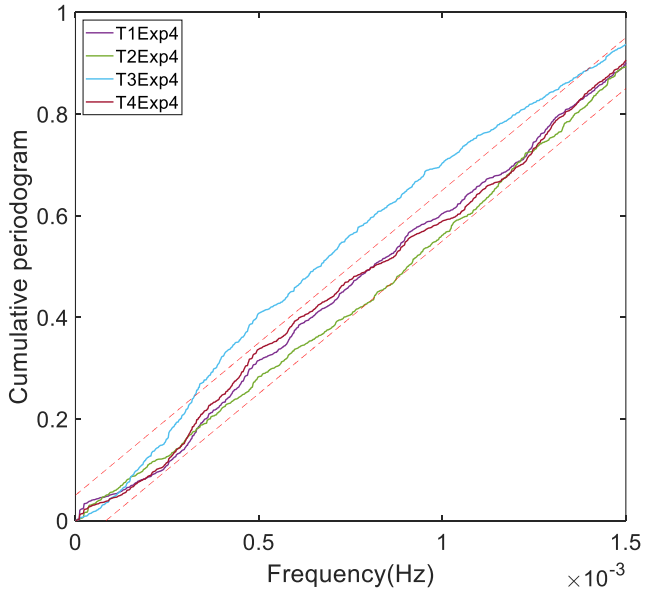

Figure 4-8: *Cumulative periodogram of the residuals of the model 3R2C for different types of indoor temperature measurement.*

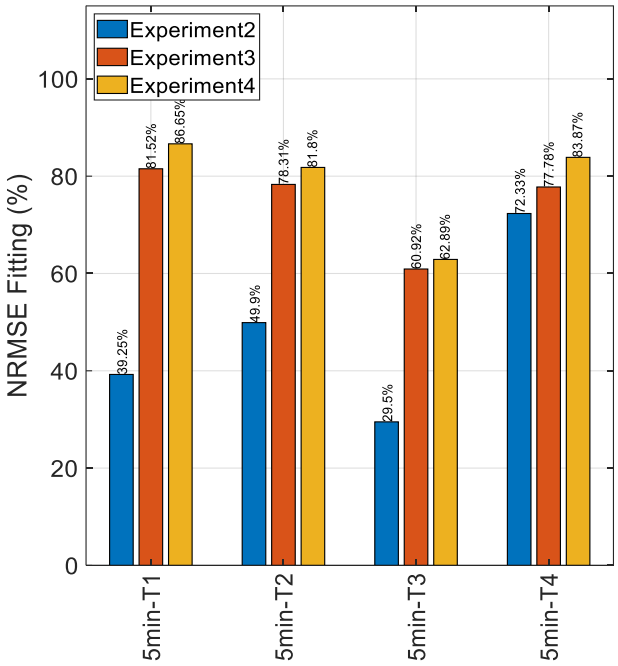

Figure 4-9: *Comparing the one-day ahead prediction of the 3R2C stochastic (sto) models with different types of temperature measurement, trained using Experiment 4 and validated using Experiments 2, 3.*

The air temperature was only measured using the wall-mounted sensors for the experiment using the hydronic radiator (i.e., Experiment 5). As it has been proven that the sensor node was necessary for the modeling, only the performance of the adapted model with the τ parameter is analyzed. Unlike the electric heater, the thermal dynamics of the hydronic radiator are significant. The analysis of the measured inlet and outlet temperatures of the hydronic radiator showed that its time constant is about 7 minutes. A priori, like the wall-sensor, it is expected that the hydronic radiator dynamics should influence the model performance, at least for a sampling time of 5 minutes (< 7 minutes). However, the wall-mounted temperature sensor has a time constant of about 8 minutes. Consequently, the dynamics of the hydronic radiator cannot be properly captured by a grey-box model since the time constant of the wall-mounted sensor is comparable (or slightly larger) than the time constant of the hydronic radiator. The analysis of the cumulative periodogram (not reported here for the sake of conciseness) shows that the adapted 3R2C can model the building heated using the hydronic radiator without the need to add a specific capacitance to model the hydronic radiator. In addition, preliminary results with an additional capacitance proved that the resulting model would be overfitted.

The experiments with the hydronic radiator and the electric heater have been performed in different years and different months of the heating season, leading to

different sun elevations between the experiments. The identified effective window area A_i is thus expected to be significantly different for Experiment 5 and Experiments 2 to 4. However, thermal properties that are intrinsic to the building fabric and less dependent on the outdoor conditions are used to analyze the model performance in Experiment 5, namely the HTC and C_e (Figure 4-10). The identified HTC is still close to the reference value. Unlike the experiments with the electric heater, there is no significant difference between the baseline and adapted 3R2C models.

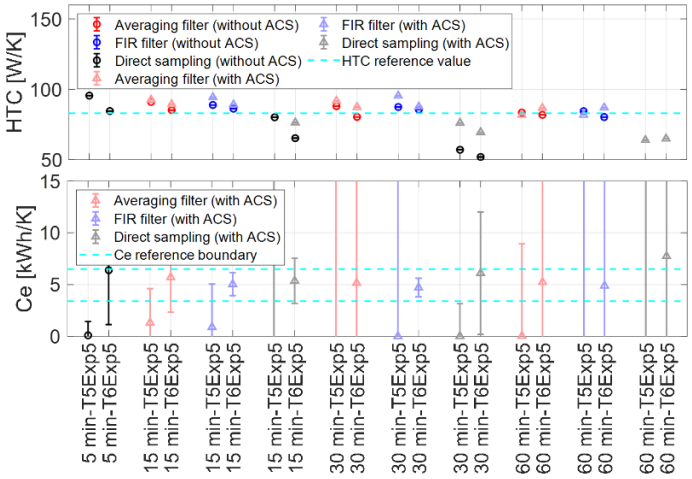

Figure 4-10: *HTC and C_e for the 3R2C stochastic model using Experiment 5 and different data pre-processing techniques.*

The improvement resulting from the adapted model and ACS is more visible when analyzing C_e. Again, the HTC translates into a steady-state performance while the capacitances are inherently related to the building dynamics. With the baseline 3R2C model, the estimated C_e is entirely non-physical. The results are noticeably improved with the adapted 3R2C model with a sensor node. The experiment with the hydronic radiator confirms the positive influence of the adapted model with τ. In conclusion, the thermal dynamics of the temperature should be modeled, but the dynamics of the hydronic radiator are due to its shorter time constant.

Q 3: Influence of data pre-processing on the grey-box modeling results?

Paper 3 and Paper 4 answer this question by applying a low-pass filter, resampling or a time shift of the input data, called anti-causal shift (ACS), with data from IDA ICE and the ZEB Living Lab, respectively.

The results of Paper 3 (Figure 4-1 to Figure 4-5) have proved that data pre-processing has limited influence on the deterministic model with virtual experimental data from IDA ICE. The results based on the data from ZEB Living Lab also confirm this conclusion (Paper 4). Figure 4-11 presents the identified parameters results for the

deterministic model using different types of temperature measurement and data pre-processing in the ZEB Living Lab.

The identified values of HTC show that no matter which type of temperature sensor is used for the identification, the HTC value is not significantly influenced by the pre-filtering method and ACS. The value is close to the reference value of ~83 W/K. The sampling time (T_s) does not have a noticeable impact on the HTC value.

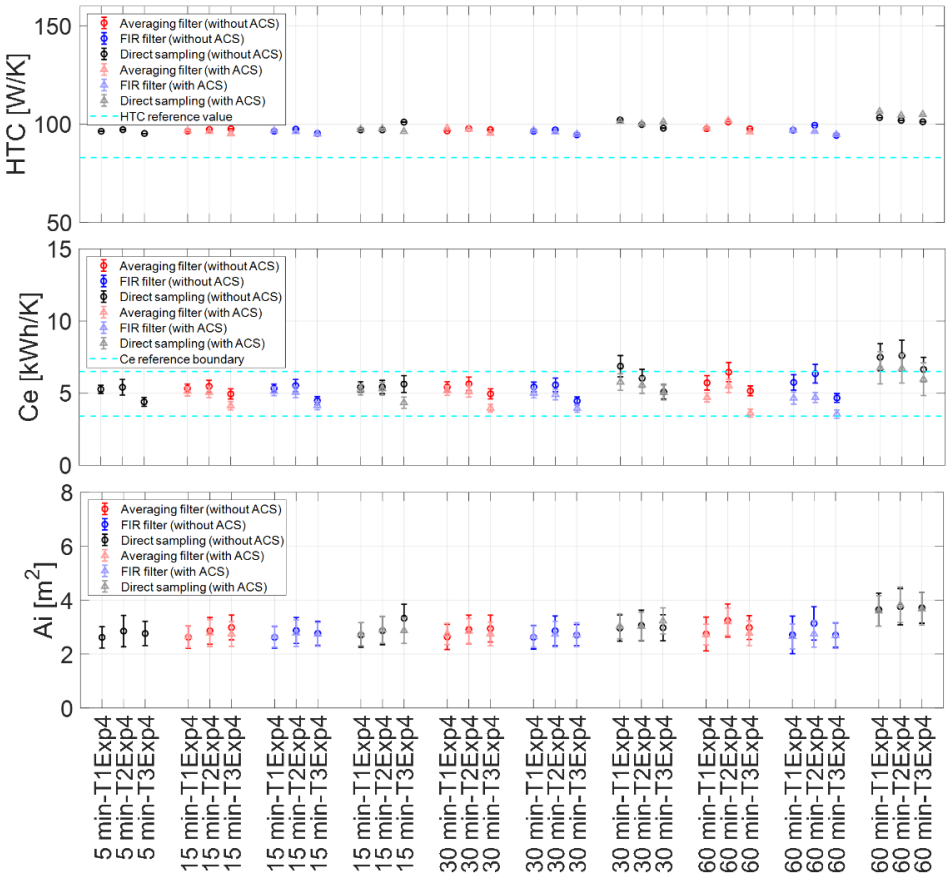

Figure 4-11: *Identified HTC, Ce and Ai of the 3R2C deterministic model for Experiment 4 with different types of temperature, data pre-processing techniques.*

The identified values of C_e give similar conclusions as the HTC value. The value of C_e is plausible for most of the cases since it is within the typical range (i.e., 3.4–6.5 kWh/K) given in standards [93]. The low-pass filtering and the ACS only have a slight impact on the results. With direct sampling, the C_e values are slightly outside the reference range when the sampling time is large (from 30 minutes). These conclusions are confirmed by the analysis of the effective window area A_i (related to the influence of solar radiation).

In conclusion, the pre-processing of data does not have a large influence on deterministic models. Neither the ACS, the pre-filtering technique nor the sampling time leads to a significant change in the parameter values. The only exception appears with very large T_s. Then, the pre-filtering can prevent the parameter value from becoming non-physical. The HTC characterizing the steady-state performance of the building has rather stable values while the other parameters characterizing the thermal dynamics of the building, here C_e and C_i, are more strongly impacted by the training dataset and the sampling time.

Data pre-processing has a more significant influence on the stochastic model. Based on Paper 3 and virtual experiments, the value for HTC for the 3R2C stochastic model in Figure 4-12 is similar to the deterministic model in Figure 4-1. As for the deterministic model, large sampling time can lead to a non-physical value of the HTC. While all the pre-filtering prevented the value from becoming non-physical for the deterministic model, only the moving-average filter and the ACS have the same effect for the stochastic model.

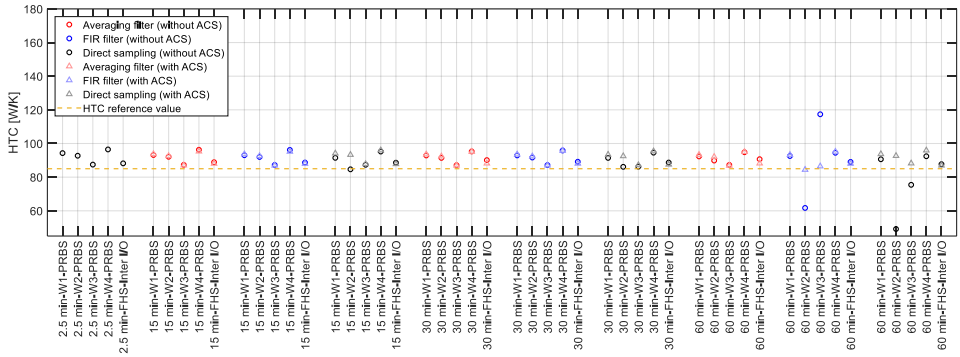

Figure 4-12: *Identified HTC of the 3R2C stochastic model for the cases 1,2,3,4 and 14, different sampling times and pre-filtering techniques; cases with ACS are shown by triangles in lighter colors.*

The value and variance of Ce from Paper 3 are shown in Figure 4-13. As long as the sampling time is shorter than the system dynamics (i.e., Ts equal 2.5 min), the value of Ce is independent of the training period and its variance is limited. Close to the C_{eff} of 3.9 kWh/K, the value of C_e is meaningful from a physical point of view. When the sampling time increases, the behavior should be distinguished with and without the application of an ACS. When the ACS is applied, the value and variance of C_e are regular even with large sampling time. The ACS has a strong positive effect on the physical plausibility of C_e. With ACS, pre-filtering has a limited influence on the results. Without ACS, the parameter value and variance become erratic with increasing T_s. Some values are so high that they fall outside the y-axis limit of the graph. In addition, no clear trend can be found on the influence of the pre-filtering and training period.

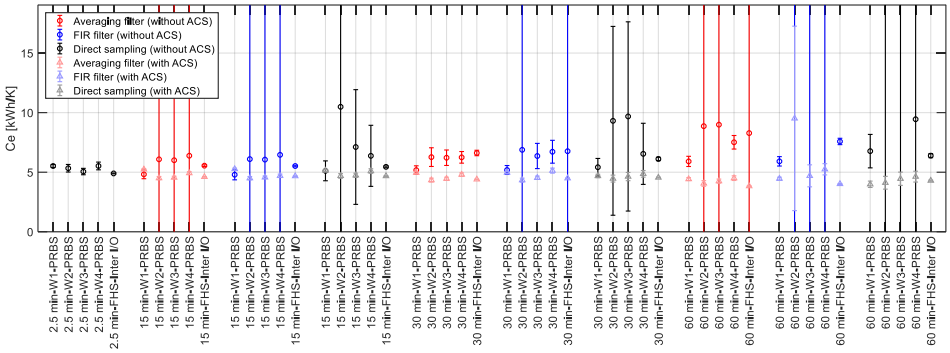

Figure 4-13: *Identified C_e of the 3R2C stochastic model for the cases 1,2,3,4 and 14, different sampling times and pre-filtering techniques; cases with ACS are shown by triangles in lighter colors.*

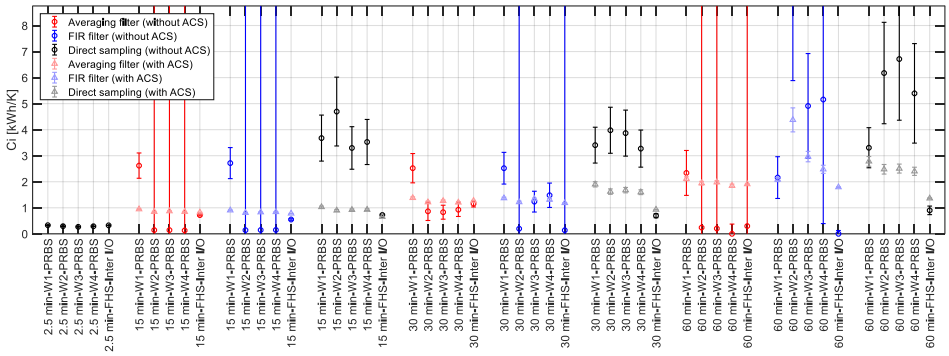

Figure 4-14: *Identified C_i of the 3R2C stochastic model for the cases 1,2,3,4 and 14, different sampling times and pre-filtering techniques; cases with ACS are shown by triangles in lighter colors.*

The same phenomenon is observed for the value and variance of C_i in Figure 4-14. Nonetheless, there is one aspect that differs from C_e. As for the deterministic model with ACS, the values of C_i with the corresponding stochastic version also tend to increase with the sampling time. However, C_i is related to the fast dynamics of the building with a time constant below one hour. Therefore, it is not surprising that C_i is influenced by the sampling time when it is changed from 5 minutes to one hour.

From all the results of the stochastic models, several conclusions can also be drawn. First, the identified parameters are strongly dependent on the sampling time. The identified parameters are always consistent if the T_s is taken small compared to the shortest time of the system T_{min} (influenced by the excitation). It is only when T_s gets equivalent or larger than the building dynamics that the parameters get non-physical without ACS, especially the thermal capacitances. The second conclusion is that ACS prevents the parameter value and variance from getting non-physical for large T_s. With ACS, the uncertainty of the parameters remains limited and their value remains

physically plausible. Pre-filtering only has limited influence with ACS while the pre-filtering influence without ACS does not show a clear trend, sometimes improving or degrading results. Finally, like the deterministic model, the steady-state characteristics HTC are less influenced by the dataset and pre-processing than the thermal capacitances. The conclusions are also validated by the field experiments of Paper 4.

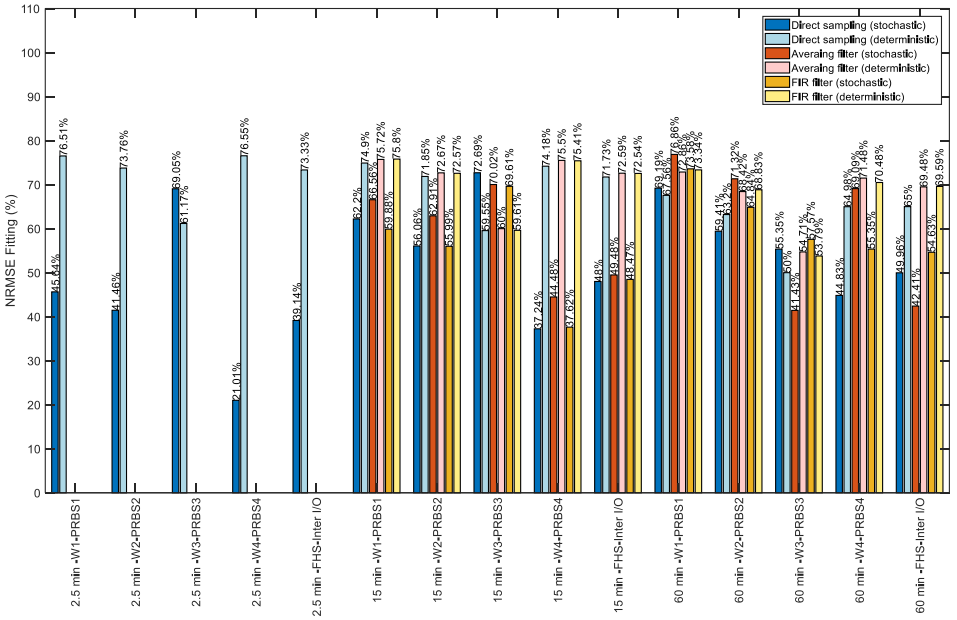

Figure 4-15: *Comparison of the simulation performance of the deterministic and stochastic 3R2C models trained on the dataset 14 without ACS and validated using the other datasets.*

The simulation performance of the grey-box models, analyzed here using the NRMSE fitting, is another important aspect of system identification. Figure 4-15 from Paper 3 compares the simulation performance of the deterministic and stochastic models without ACS. For different Ts and pre-filtering approaches, the deterministic model has a more constant simulation performance than the corresponding stochastic model. For the deterministic model, the NRMSE fitting tends to decrease slightly with increasing T_s while it tends to increase for the stochastic models (except for the PRBS3 case). The deterministic model generally has a better simulation performance than its corresponding model in stochastic form even though this difference tends to disappear for large T_s. This conclusion is noteworthy as for deterministic models the value of the parameters is significantly influenced by the training period and some of the values are not even physically plausible. In other words, identifying a model with parameters that have a more physical value does not necessarily lead to a model with better simulation performance. If one is not interested in the characterization of the thermal properties but rather the simulation performance (like in MPC), results

suggest that deterministic models can be more robust than stochastic models as they are less sensitive to the data pre-processing. As it will be shown in the answer of Q5 in Section 4.2, this also makes the resolution of the optimization problem to calibrate the model easier (as both local and global optimizers lead to the same parameters). In addition, it has been shown that pre-filtering techniques and T_s have a limited effect on model performance. This conclusion is important in the context of the design of MPC for small residential buildings where a control model should be identified at a low cost, potentially using a fully automated procedure.

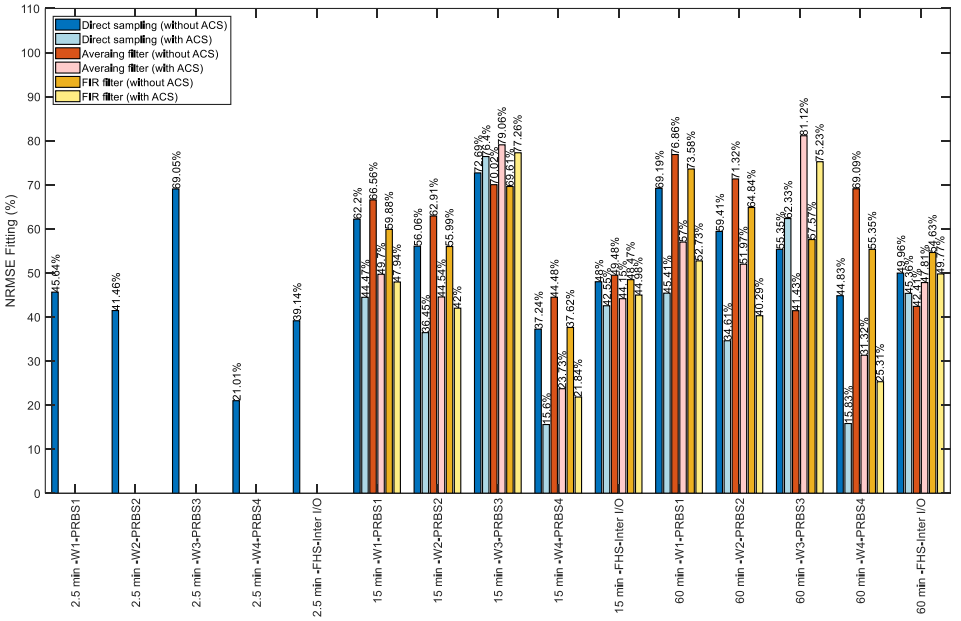

Figure 4-16: *Comparison of the simulation performance of the stochastic 3R2C model with and without ACS, trained with the dataset 14 and validated with datasets 1 to 4.*

Figure 4-16 of Paper 3 compares the simulation performance of the stochastic model with and without ACS. While the ACS tends to improve the physical plausibility of the model parameters and positively influence the optimization problem (as it will be shown in Section 4.2), the influence of ACS on prediction performance is not systematic for the stochastic model. It generally has a negative influence on the simulation performance of the model for the data from virtual experiments. As already mentioned, the NMRSE fitting generally increases with Ts for the stochastic models without ACS. This increase is less pronounced for the stochastic model with ACS even though the physical plausibility of the parameters has been improved. Two conclusions can be given. Firstly, it confirms that parameters that are more physically plausible do not necessarily lead to better simulation performance. Here, with large Ts and without ACS, the value of some parameters, such as Ce in Figure 4-13, is non-physical but it nonetheless leads to better simulation performance. Secondly, the ACS

showed to be a robust solution to characterize the thermal properties of the building and the resolution of the optimization problem. However, it appears from our investigations that the ACS comes at the price of lower simulation performance. Finally, none of the approaches investigated here manages to combine high physical plausibility and the highest simulation performance at large T_s. This is partly confirmed by the ZEB Living Lab field experiments in Paper 4, the ACS is beneficial to get physically-plausible parameters for large T_s but its influence on the prediction performance is not systematically negative unlike virtual experiments (i.e., sometimes positive or negative). The details of the results can be found in Paper 4.

4.2 Modeling (train parameters)

Q 4: What are the most suitable grey-box model structures for residential buildings?

The best trade-off between model accuracy and overfitting for a mono-zone model is second-order with the available data of our case study. This is in line with the conclusions from the literature review in Section 2.2. Even though the literature review also suggests that third-order models should also be appropriate.

Paper 1 and Paper 4 investigate the performance of grey-box models based on the knowledge of the building physics or using a generic model structure based on the standards EN 13790 and VDI 6007.

The discussion is first based on Paper 4 using experimental data from the ZEB Living Lab for both deterministic and stochastic grey-box models. Results are summarized in Table 4-2. The results show that the first-order 1R1C model is not enough to describe the heat dynamics of the building for neither the deterministic nor the stochastic models. This is confirmed by the cumulative periodogram of the residuals for the stochastic models in Figure 4-17. The cumulative periodogram falls largely outside the confidence interval, which indicates poor white noise properties of the residuals. The building thermal dynamics typically has two times constants for the fast (< 1h) and slow (> 24h) dynamics. A first-order model with a single time constant cannot reproduce both dynamics.

However, the second-order models, namely the 2R2C and 3R2C, show significant improvement in the NRMSE fitting compared to the first-order 1R1C model. The cumulative periodogram of the residuals also stays strictly within the confidence interval (see Figure 4-17). The difference between the 2R2C and 3R2C model lies in the thermal resistance U_{inf} that connects the interior node directly to the outdoor temperature (T_a). This resistance account for the heat transfer of envelope components with negligible thermal mass, such as doors and windows, and the ventilation losses. When using experimental data in the ZEB Living Lab, the ventilation losses were precomputed using measurement data and injected directly into the interior node. Therefore, ventilation losses do not contribute to U_{inf} in this

situation. In addition, the windows and doors of the highly-insulated ZEB Living Lab also have low conductance. Consequently, the value of U_{inf} remains relatively limited. This explains why 2R2C model is competitive for the ZEB Living Lab. However, this conclusion should be carefully generalized to other insulation levels of the building envelope or if ventilation losses are part of U_{inf}.

Although the third-order models (3R3C to 5R3C) sometimes present better NRMSE fitting with the deterministic model, the identified parameters are not physically plausible for the deterministic model. The capacitance of the interior node C_i has a larger value than the value of the internal walls node C_m, which does not translate the actual physics. Furthermore, for the 4R3C and 5R3C stochastic models, the UA_{ea} value is identified as close to 0, which also violates reality (as external walls are not perfectly insulated). Regarding the cumulative periodogram of the residuals, the 5R3C is outside the confidence interval while the 3R3C and 4R3C models remain within the confidence interval but do not perform better than the second-order models. The variance of the key parameter C_e also shows that the third-order models could lead to large values with deterministic models, which implies that the third-order models may be overfitting. Furthermore, the variance of C_e for the stochastic model also shows that the component UA_{inf} is necessary to be modeled. Finally, the objective function during the successive PSO iterations is plotted along with the parameter value in Paper 4. The scatter plots for parameters C_e and A_i for second-order and third-order models can also be found in the supplementary material of the paper. It is observed from the scatter plots that the optimum is flatter with third-order models, which corresponds to lower practical identifiability of the models. It can be concluded that the third-order models are (or are close to being) overfitted. The fitting of validation NRMSE fitting also confirms that the second-order model is the best trade-off between model complexity and accuracy.

The discussion is not extended with the results of Paper 1, also using the ZEB Living Lab but only considering deterministic models. Regarding grey-box models based on standards, the EN 13790 is a first-order model. The results show that the EN 13790 model is able to follow the general evolution of the indoor temperature and provides meaningful values of the parameters. However, the simulated temperature has significantly higher fluctuations directly corresponding to the start and stop cycles of the electric radiator. It is consistent with the previous conclusions that a first-order model is not able to capture the fast dynamics of the building. The VDI 6007 model is a second-order model but has six nodes and a relatively high number of parameters (i.e., resistance to connect the node and factors to distribute the internal, heating and solar gains between the nodes). It has a good prediction performance, but it generates parameter estimates that are physically not plausible. Consequently, the number of parameters of this model needs to be reduced to make the model identifiable.

On the one hand, Paper 4 demonstrated that a relevant model structure could be derived based on the knowledge of building physics without resorting to structures

defined in building energy simulation standards. On the other hand, Paper 1 showed that the model structure of two important standards, the EN 13790 and VDI 6007, should be adapted to give good performance. Based on these conclusions, it suggests that there is no need to resort to existing model structures from building energy simulation standards to identify good structures for grey-box models.

Table 4-2: *The values and the corresponding variance of* C_e.

Model	C_e Value [kWh/K]	C_e Variance [kWh/K]	NRMSE Fitting (simulation)	NRMSE Fitting (validation)	**Model**	C_e Value [kWh/K]	C_e Variance [kWh/K]	NRMSE Fitting (1-step ahead)	NRMSE Fitting (validation)
1R1Cdet	5.62	**0.754**	72.7%	55.1%	**1R1Csto**	4.78	0.437	99.0%	65.7%
2R2Cdet	6.11	0.369	93.0%	75.3%	**2R2Csto**	6.37	**1.77**	99.2%	79.2%
3R2Cdet	5.28	0.284	93.6%	79.7%	**3R2Csto**	4.22	0.748	99.2%	81.8%
4R2Cdet	5.40	0.430	93.5%	72.4%	**4R2Csto**	4.28	0.726	99.2%	81.5%
3R3Cdet	6.08	**0.689**	95.0%	78.6%	**3R3Csto**	11.9	**3.92**	99.2%	71.1%
4R3Cdet	3.94	**0.609**	95.3%	75.6%	**4R3Csto**	4.02	0.709	99.2%	82.7%
5R3Cdet	3.99	**0.613**	95.3%	76.0%	**5R3Csto**	5.73	0.718	99.2%	79.8%

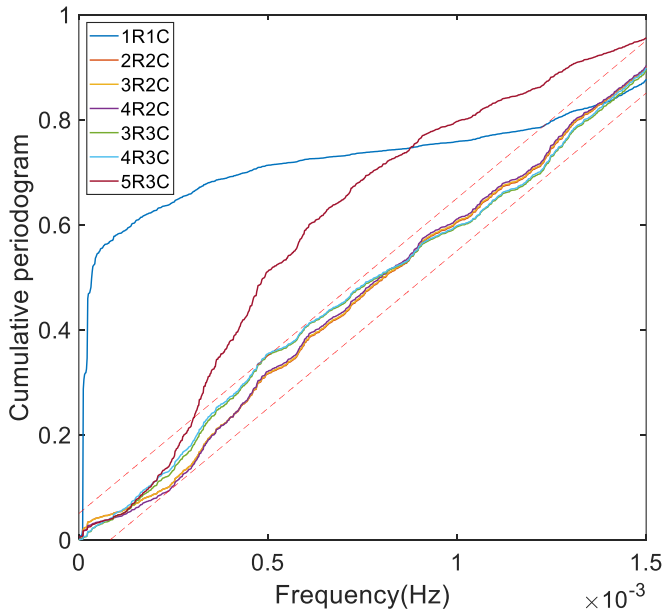

Figure 4-17: *Cumulative periodogram of the residuals for the stochastic models.*

In conclusion, second-order grey-box models are most suitable for our study as the prediction performance and the physical plausibility are good. In addition, the dominant physical processes are properly modeled as proven by the cumulative periodogram. The second-order models are selected in the thesis as they are accurate but not overfitted.

Q 5: Influence of the optimizer on the grey-box modeling results?

Paper 2 and Paper 3 mainly address this question by comparing the performance of grey-box models calibrated using the default gradient-based optimization and a global optimization routine. The question is discussed in detail in Paper 3 with low-order grey-box models. The performance of both optimizers defined is compared for a selected number of datasets (i.e., cases 1 to 4 and 14), with and without ACS, for both deterministic and stochastic models. Table 4-3 shows the optimizer that leads to the lowest prediction error for each test case. The symbol "D" represents the default *greyest* function, "G" represents the two-stage global optimization algorithm. The symbol "≈" is used when both optimizers lead to extremely close results in terms of prediction error and estimation of the model parameters. Only results for the sampling times of 2.5 and 30 min are presented in Table 4-3. However, the same conclusions are found for the other two sampling times (i.e., 15 and 60 minutes).

Table 4-3: *Optimizer leading to the lowest prediction error: each cell of the table has two symbols, one for the case without ACS (left) and the other with ACS (right); the symbol "D" means default greyest, "G" means global optimization and "≈" means equal performance.*

Time (Ts)	Case	1R1C *DS* *(det)*	1R1C MA *(det)*	1R1C *FIR* *(det)*	3R2C *DS* *(det)*	3R2C MA *(det)*	3R2C *FIR* *(det)*	1R1C *DS* *(sto)*	1R1C MA *(sto)*	1R1C *FIR* *(sto)*	3R2C *DS* *(sto)*	3R2C MA *(sto)*	3R2C MA *(sto)*
2.5min	**1**	≈/≈	-	-	≈/≈	-	-	G/≈	-	-	G/≈	-	-
	2	≈/≈	-	-	≈/≈	-	-	G/≈	-	-	G/≈	-	-
	3	≈/≈	-	-	≈/≈	-	-	G/≈	-	-	G/≈	-	-
	4	≈/≈	-	-	≈/≈	-	-	G/≈	-	-	G/≈	-	-
	14	≈/≈	-	-	≈/≈	-	-	G/≈	-	-	G/≈	-	-
30min	**1**	≈/≈	≈/≈	≈/≈	≈/≈	≈/≈	≈/≈	G/≈	G/≈	G/≈	G/≈	G/≈	G/≈
	2	≈/≈	≈/≈	≈/≈	≈/≈	≈/≈	≈/≈	G/≈	G/≈	G/≈	G/≈	G/≈	G/≈
	3	≈/≈	≈/≈	≈/≈	≈/≈	≈/≈	≈/≈	G/≈	G/≈	G/≈	G/≈	G/≈	G/≈
	4	≈/≈	≈/≈	≈/≈	≈/≈	≈/≈	≈/≈	G/≈	G/≈	G/≈	G/≈	G/≈	G/≈
	14	≈/≈	≈/≈	≈/≈	≈/≈	≈/≈	≈/≈	G/≈	G/≈	G/≈	G/≈	G/≈	G/≈

It is observed that the two optimizers have identical results for all the cases using a deterministic model, regardless an ACS is applied or not. However, global optimization generally performs better than the default *greyest* optimization for stochastic models without ACS, even if the model is first order. On the contrary, both optimizers have similar performance when ACS is applied. It means that ACS tends to preserve the physical plausibility of the model parameters when T_s is large, but it also positively influences the convexity of the optimization problem. In general, results confirm that it is better to use global optimization. Otherwise, the obtained sets of parameters are possibly located at a local minimum which mainly depends on the initial guess of the parameters.

Q 6: Prediction performance of grey-box compared to black-box models?

Some results of Paper 1 can give some indications to this question for deterministic models. The second-order subspace linear black-box model shows a good simulation performance equivalent to the second-order linear grey-box model. Nevertheless, with black-box models, the physical meaning of the states is unknown. However, the estimate of the overall heat transfer coefficient is similar between the second-order black-box and the best grey-box models. It is worth mentioning that these investigations were performed with high-quality input-output data. In addition, experiments corresponding to the validation data set took place a few days after the training period. The relative performance of black-box and grey-box models could be different if these experimental conditions were not fulfilled. The results nonetheless suggest that black-box models deserve to be investigated in detail to create a control-oriented model with limited knowledge of the building and a limited amount of time. In this respect, it is worth mentioning that Knudsen et al. [54]successfully tested an economic MPC in the ZEB Living Lab using a linear black-box model identified using the subspace method (n4sid in MATLAB).

4.3 Model Predictive Control

Q 7: What is the performance MPC using LTI and adaptive grey-box models and other types of data-driven models?

This question is mainly answered in Paper 5 and Paper 6 based on grey-box MPCs. Limited results in Paper 7 are given based on the comparison between different types of data-driven models for MPC.

4.3.1 MPC based LTI vs adaptive grey-box models

Paper 6 answers the question by comparing the performance of the different MPC controllers for the three different control objectives. Therefore, the co-simulation results are evaluated successively based on the control objectives. The co-simulation virtual experiment lasted for 61 days (from November 1st to December 31st). The trained parameter values of the three LTI models are shown in Table 4. As can be

seen, the HTC and A_i are significantly different for the LTI model identified using the FullWinter data than the two LTI models using the PRBS excitation signal.

Table 4-4: *Trained parameter values of the LTI models*

Case	HTC [W/K]	C_e [kWh/K]	C_i [kWh/K]	A_i [m^2]
FullWinter	81.42	4.03	0.33	6.09
PRBSNOV	96.43	4.81	0.42	16.96
PRBSDEC	94.25	4.93	0.41	15.94

Energy savings (ES)

Energy savings is the most basic control objective of this study. Figure 4-18 presents the indoor temperature profile under the operation of the different MPC controllers using the energy savings control objective. Figure 4-19 is a close-up section of Figure 4-18, for both $L = 10^8$ and $L = 10^6$ penalty factors. The total energy use and the thermal discomfort of those different MPC controllers with different penalty factors are calculated so that the MPC controller performance can be quantitatively compared in Table 4-5.

Table 4-5: *Summary of the MPC performance for the energy saving case*

Calculated Index	FullWinter MPC	PRBSNOV MPC	PRBSDEC MPC	Partially Adaptive MPC	Fully Adaptive MPC	Penalty Factor (*L*)
Energy Use [kWh]	800.15	829.26	853.42	799.14	864.22	10^6
Thermal Discomfort [Kh]	554.52	279.51	120..81	567.95	103.99	10^6
Consumed Energy [kWh]	803.73	855.18	875.60	804.06	893.62	10^8
Thermal Discomfort [Kh]	534.39	194.37	99.47	528.87	72.04	10^8

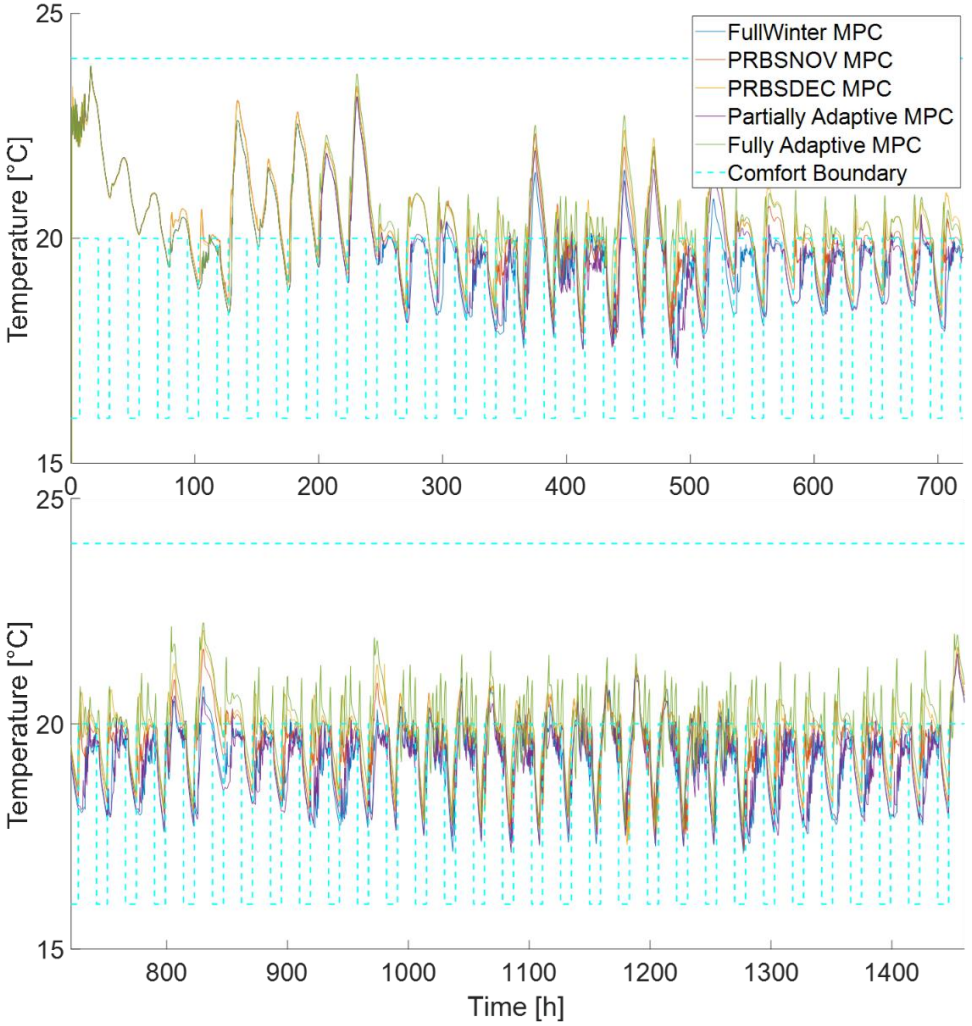

Figure 4-18: *Indoor temperature profile under the operation of different MPC controllers with energy saving objective ($L = 10^8$).*

Results show that the FullWinter model makes inaccurate indoor temperature predictions, which causes the thermal comfort constraint to be frequently violated. The Partially Adaptive MPC shows a similar inaccurate prediction compared to the FullWinter MPC. The thermal comfort constraint is still frequently violated. With the lower penalty factor 10^6, the thermal discomfort of Partially Adaptive MPC is even larger than the FullWinter MPC. These two models consume less energy compared to the other models (i.e., the Fully Adaptive MPC and the PRBS MPC) because they are less accurate, which causes the indoor temperature to drop below the minimum indoor temperature threshold. The heating system is switched on far too late in the morning, resulting in significant thermal discomfort. It indicates that the LTI grey-

box model trained using the data from the full space-heating season may not be suitable as the prediction model in MPC. Only updating the effective window area of the FullWinter model cannot correct the model to reach a satisfactory prediction.

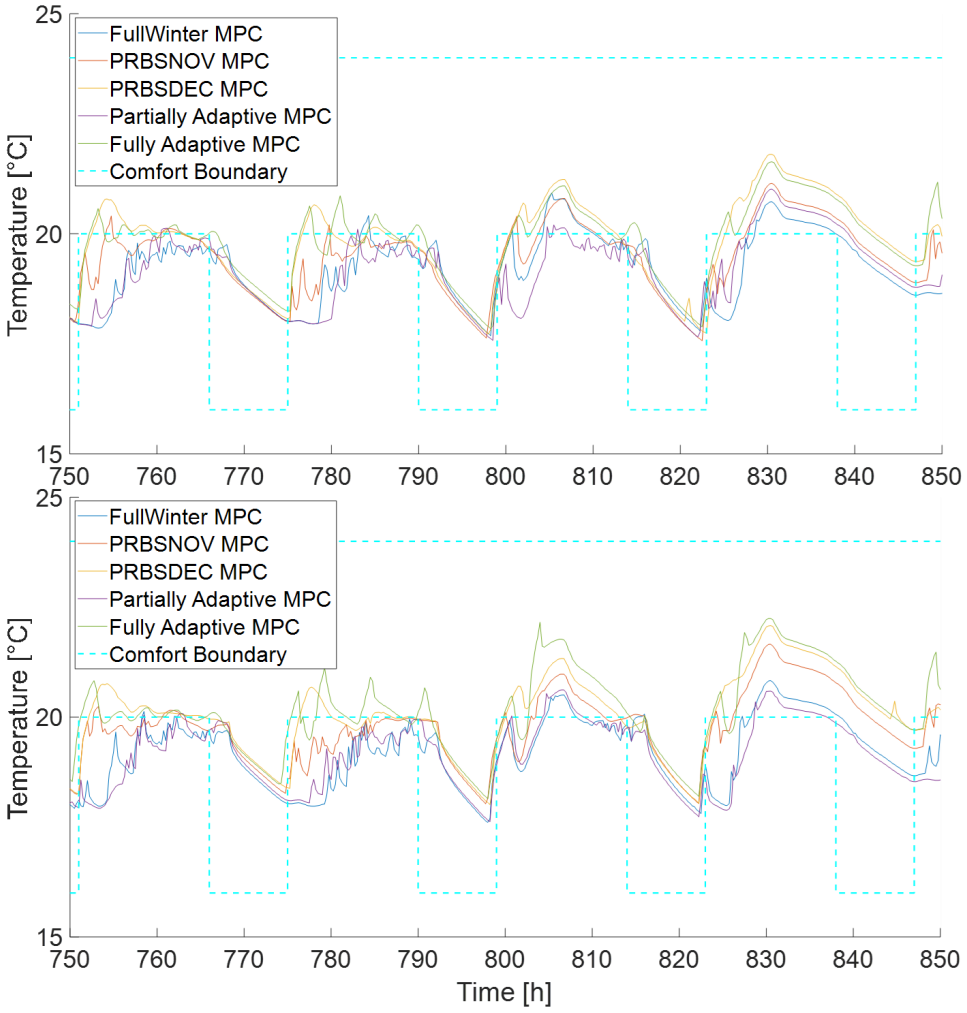

Figure 4-19: *Close-up of the indoor temperature profile under the operation of different MPC controllers with energy savings objective (Upper figure corresponding to 10^6, Lower figure corresponding to 10^8).*

PRBSNOV MPC and PRBSDEC MPC perform better than the FullWinter and Partially Adaptive MPC models in terms of avoiding thermal discomfort, which can be clearly seen in Figure 4-18 and Figure 4-19. PRBSDEC MPC performs slightly better than PRBSNOV MPC in terms of thermal comfort leading to slightly higher energy use. The influence of the penalty factor on PRBSNOV MPC is more evident than the PRBSDEC MPC. The better performance of PRBSNOV MPC and PRBSDEC MPC over the FullWinter MPC proves that it is important to use a model

that is trained with data generated from weather conditions similar to the period when the MPC will be operated.

The Fully Adaptive model performs the best among the MPCs in avoiding thermal discomfort, which can be clearly seen in Figure 4-19. The PRBSDEC MPC performs slightly better than the Fully Adaptive MPC with a lower penalty factor 10^6 mainly because the Fully Adaptive MPC operates with the FullWinter model in the first seven days. The Fully Adaptive MPC performs much better than the Partially Adaptive MPC due to more degrees of freedom to fit the model parameters.

Energy cost saving (EMPC)

An hourly electricity price profile is applied to the energy cost saving case. The total energy cost is the consumed energy at each time slot multiplied by the corresponding electricity price. Figure 4-20 shows the indoor temperature profile under the operation of different MPC controllers with the energy cost saving objective (with a penalty factor L = 10^8). Figure 4-21 is a close-up section of Figure 4-20 for the two penalty factors. The summary of the results of the total energy cost and the thermal discomfort for these different MPC controllers with different penalty factors is presented in Table 4-6.

Table 4-6: *Results summary of MPC controllers' performance for energy cost saving (EMPC) case*

Calculated Index	FullWinter MPC	PRBSNOV MPC	PRBSDEC MPC	Partially Adaptive MPC	Fully Adaptive MPC	Penalty Factor (*L*)
Energy Cost [NOK]	319.54	327.15	336.93	319.56	341.75	10^6
Thermal Discomfort [Kh]	453.93	216.76	96.84	462.61	79.74	10^6
Energy Cost [NOK]	328.56	334.77	342.51	326.32	353.89	10^8
Thermal Discomfort [Kh]	210.74	164.93	86.30	247.05	50.68	10^8

The results of the EMPC cases show that all the EMPCs can respond to the variable electricity price. The sharp drop in the indoor temperature during high electricity price periods (e.g., around 460 and 770 hours) reveals that the heating system is switched off to decrease the energy cost. However, the performance differs between the controllers due to different levels of prediction accuracy.

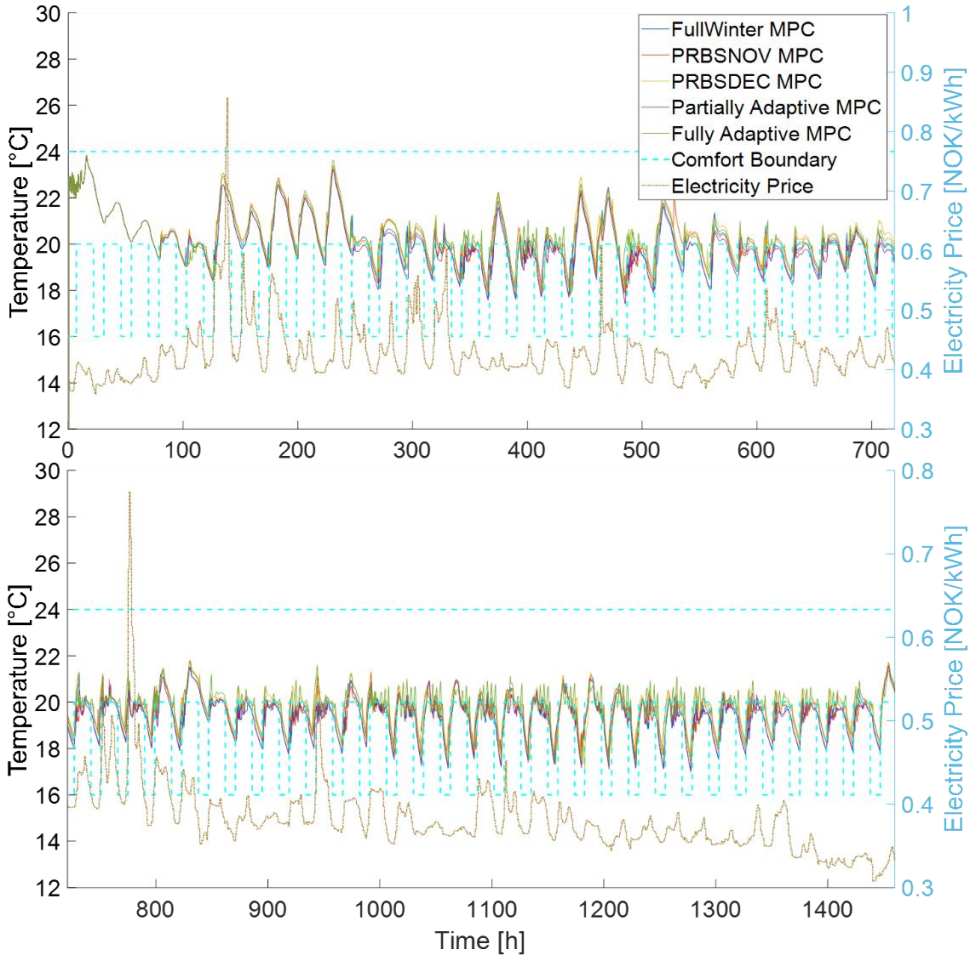

Figure 4-20: *Indoor temperature profile under the operation of different MPC controllers with energy cost saving objective ($L = 10^8$).*

Like the energy savings case, the FullWinter MPC and the Partially Adaptive MPC perform the worst. The thermal comfort constraint is frequently violated, which indicates that the prediction from the model is not accurate enough. It confirms that only updating the window area of the FullWinter model is not enough to reach good MPC performance. Although they have a relatively lower energy cost compared to the other models, this is a direct result of the large thermal discomfort of the two MPC controllers. Regarding the sensitivity to the penalty factor for these two cases, increasing L can decrease the discomfort of the two models, but it still remains at a comparatively high level. Furthermore, the Partially Adaptive MPC generally has a higher discomfort level than the FullWinter model, no matter whether a high or a low penalty factor is used. The reason is that the estimated effective area A_i of Partially Adaptive MPC is higher than the FullWinter MPC in most of the operation time, which leads to a higher heat gain from solar radiation. The HTC value of the

FullWinter MPC is lower than the reference true HTC value of the IDA ICE building is higher than the HTC value of the FullWinter model, causing an underestimated heating demand. However, the A_i value of the FullWinter MPC is also lower than the other LTI MPC, which corresponds to lower estimated solar heat gains. It neutralizes the effect of underestimated heating demand to a certain degree. Therefore, the correction of solar heat gain from Partially Adaptive MPC has a negative impact on thermal comfort for this case study. Partially Adaptive is not able to preheat the building enough because of the higher prediction of the solar gain compared to the FullWinter model, which causes a higher thermal discomfort level.

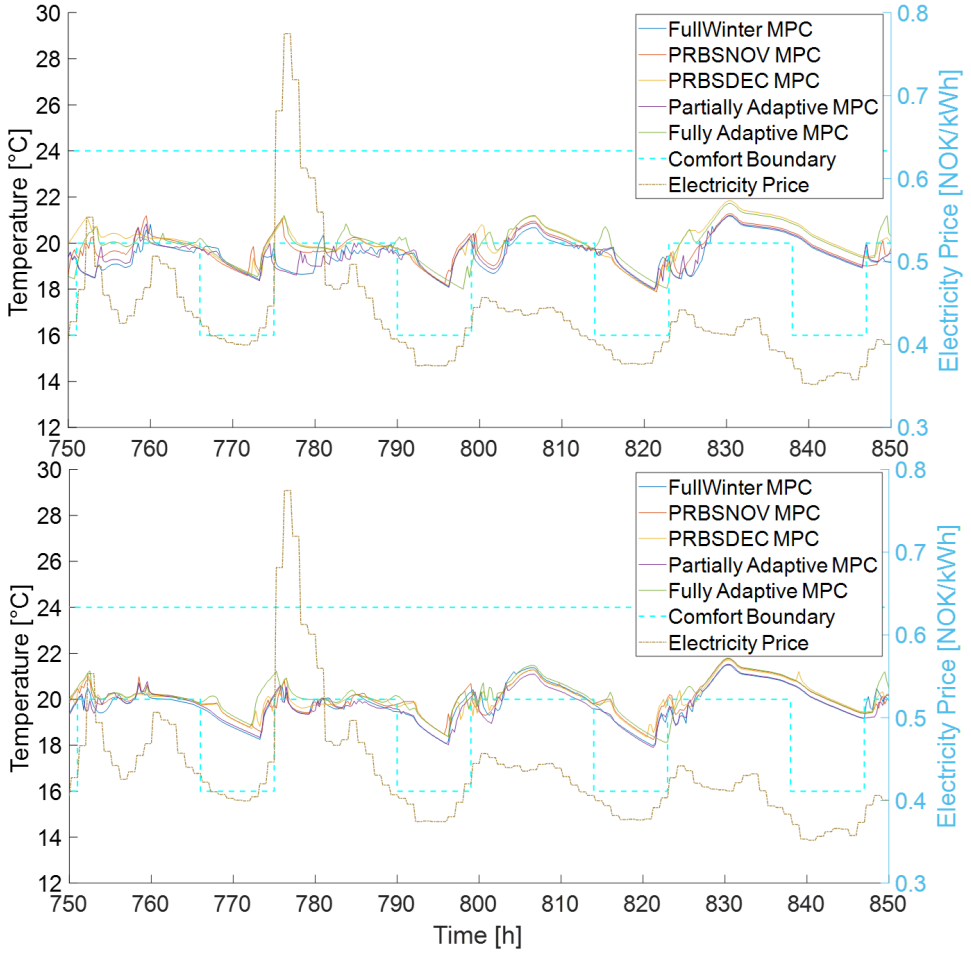

Figure 4-21: *Close-up of the indoor temperature profile under the operation of different MPC controllers with energy cost saving objective (Upper figure corresponding to 10^6, Lower figure corresponding to 10^8).*

The PRBSNOV MPC and PRBSDEC MPC models perform better than the previous two models in reducing thermal discomfort. The PRBSDEC MPC performs better

than PRBSNOV MPC for the EMPC case, which is similar to the energy savings case. The results of PRBSNOV MPC and PRBSDEC MPC confirm that it is preferable that use a model trained on data from similar weather conditions to the operation period.

The advantage of the Fully Adaptive model is more evident in the energy cost saving case. The thermal discomfort is lowest among the controllers, though it leads to a higher electricity cost. It can be clearly seen from Figure 4-20 and Figure 4-21 that the minimum indoor temperature constraint is less frequently violated. This proves that the Fully Adaptive MPC functions well for the control objectives of this case.

In general, the results of the energy cost saving case are very similar to the energy savings case. It is also not suitable to use the FullWinter model as the prediction model for EMPC, and only updating the effective window area of the model is not enough to correct the prediction model. The two PRBS models perform worse than the Fully Adaptive model due to less accurate prediction. In other words, the building is not preheated enough in the low electricity price period. The results of the Fully Adaptive MPC with $L = 10^6$ and the best LTI model (namely the PRBSDEC MPC) with $L = 10^8$ also confirm that if the energy cost is at the same level, the Fully Adaptive MPC has lower thermal discomfort. It proves the extra higher energy cost of the Fully Adaptive MPC is used for reducing thermal discomfort.

Energy cost saving with peak reduction (EMPCPR)

The energy cost saving with the peak reduction case is simply generated by adding a penalty for energy use during the peak hour to the EMPC case. Figure 4-22 shows the indoor temperature profile using the different MPC controllers with the energy cost saving and peak power reduction objective (with a penalty factor $L = 10^8$). The peak hour penalty is added to the hourly electricity price profile to reconstruct the new cost profile, which is also shown in Figure 4-23. The electricity energy cost is still the energy used at each time step multiplied by the corresponding electricity price. The total cost is the electric energy cost plus the peak hour penalty cost.

The MPC controllers are switched off in the heating system during high price periods (e.g., at about 460, 770 and 950 hours) to decrease the total cost, which can be seen from the decrease in the indoor temperature.

Table 4-7: *Results summary of MPC controllers' performance for energy cost saving (EMPCPR) case.*

Calculated Index	FullWinter MPC	PRBSNOV MPC	PRBSDEC MPC	Partially Adaptive MPC	Fully Adaptive MPC	Penalty Factor (*L*)
Energy Cost [NOK]	328.67	330.36	338.94	328.17	350.06	10^6
Total Cost [NOK]	405.38	384.13	403.31	408.80	379.77	10^6
Thermal Discomfort [Kh]	312.18	169.55	81.12	311.81	45.13	10^6
Peak Hour Energy [kWh]	38.36	26.89	32.19	40.31	14.86	10^6
Energy Cost [NOK]	327.53	345.13	348.70	325.81	355.80	10^8
Total Cost [NOK]	396.37	420.98	430.05	397.32	410.36	10^8
Thermal Discomfort [Kh]	200.11	96.51	44.98	220.24	30.51	10^8
Peak Hour Energy [kWh]	34.42	37.92	40.67	35.76	27.28	10^8

Results show that the FullWinter and the Partially Adaptive MPCs are still performing poorly in the case of EMPCPR. Large thermal discomfort is still occurring due to the inaccurate prediction of the model. It can be clearly seen in Figure 4-23 that the two MPC controllers choose to switch off the controller at the high price periods, even though the minimum indoor temperature constraint is violated. It consolidates the conclusion based on the previous two cases. An LTI model trained from full winter data is not appropriate to be used as the prediction model for MPC control. Only updating the effective window area of the FullWinter model leads to higher thermal discomfort, which is similar to the previous EMPC case. The explanation for this phenomenon is the same as the EMPC case. Increasing the penalty factor L can significantly reduce the thermal discomfort of these two MPCs.

Similar to the previous two cases, the PRBSDEC MPC performs slightly better than the PRBSNOV MPC in terms of thermal comfort. However, the PRBSDEC MPC causes an increased total cost and more peak hour electricity usage. In general, the two models generally have much better performance compared to the FullWinter and the Partially Adaptive MPCs. It proves again that it is necessary to have training data with similar weather conditions compared to the MPC operating period.

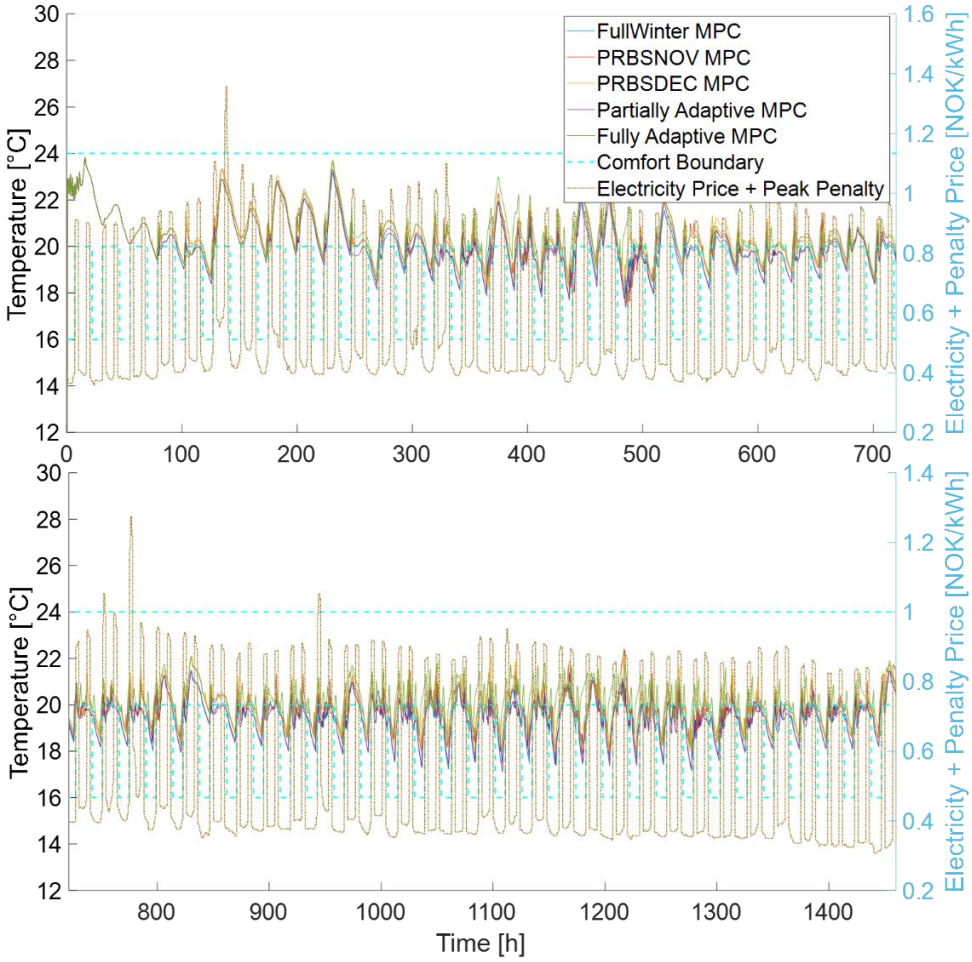

Figure 4-22: *Indoor temperature profile under the operation of different MPC controllers with energy cost saving and peak reduction ($L = 10^8$).*

The EMPCPR case clearly shows that the Fully Adaptive MPC outperforms the other MPCs. For the previous test cases, the best MPC based on LTI that could compete with the Fully Adaptive MPC was the PRBSDEC MPC. However, in the EMPCPR case, the Fully Adaptive MPC gives better performance for all the KPIs than the PRBSDEC. For both penalty factors: the thermal discomfort, the total cost and the energy use during peak hours are lower. By comparing the results of the Fully Adaptive MPC with $L = 10^6$ and the best LTI model (PRBSDEC MPC) with $L = 10^8$, it can be seen that the total cost of the Fully Adaptive MPC has a much lower value when the thermal discomfort level is almost identical.

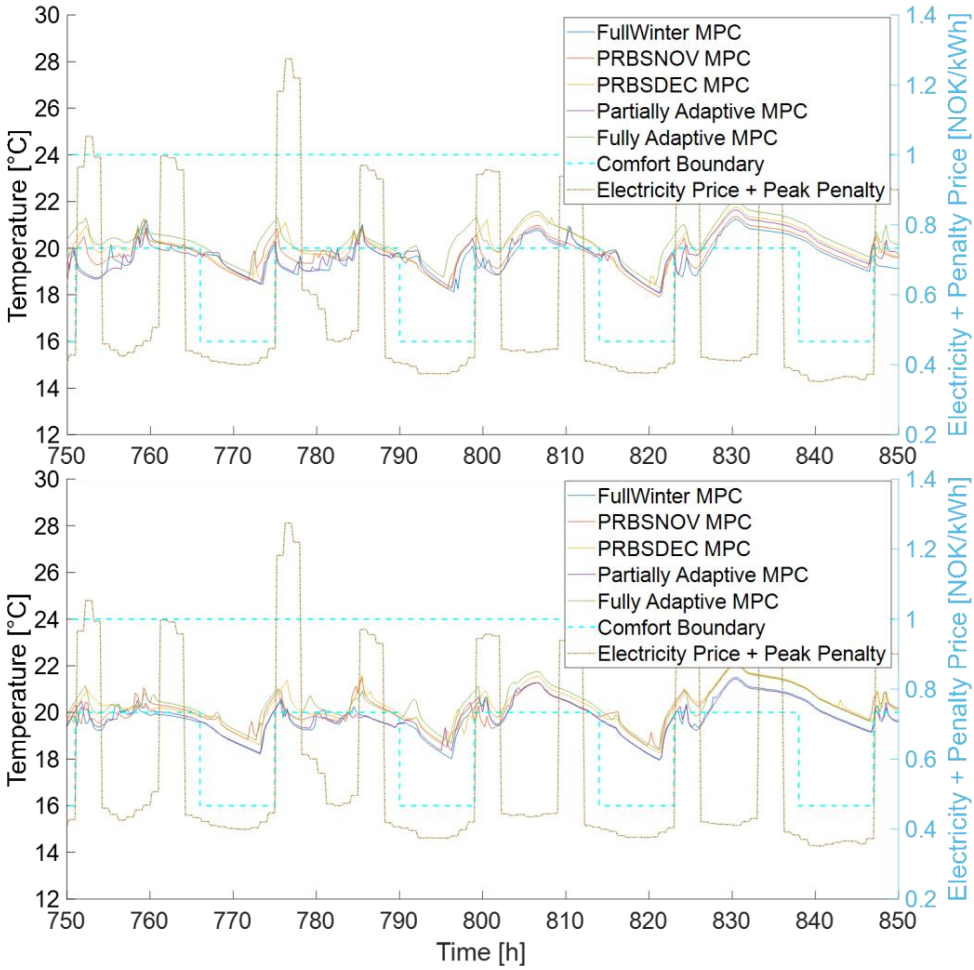

Figure 4-23: *Close-up of the indoor temperature profile under the operation of different MPC controllers with energy cost saving and peak reduction (Upper figure corresponding to 10^6, Lower figure corresponding to 10^8).*

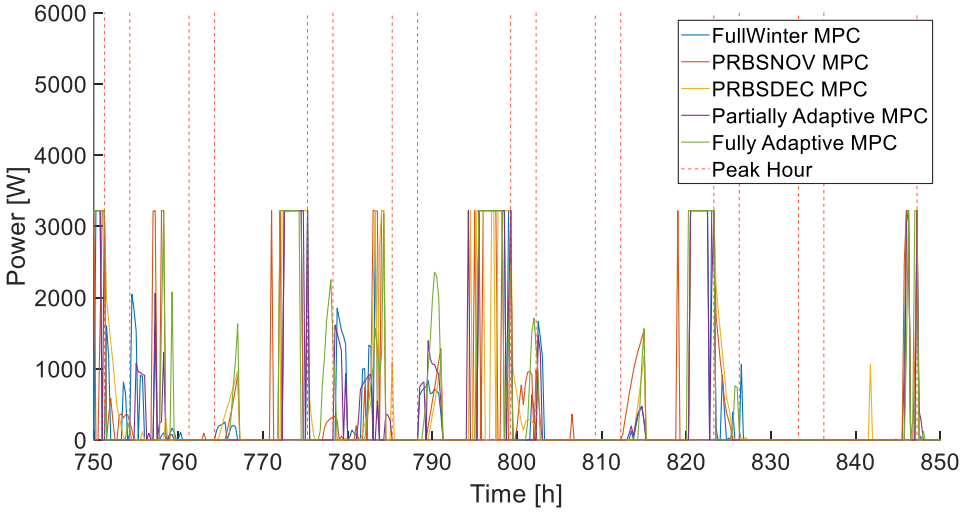

Figure 4-24: *Profile of the emitted power by the electric radiators for the different MPC controllers and the energy cost saving and peak reduction objective ($L = 10^8$).*

Figure 4-24 shows a close-up period of the emitted power profile with $L = 10^8$ for the different MPC controllers. It can be clearly seen that all the MPC controllers have shifted most of the energy use outside the peak period.

Time evolution of the parameters

This section presents the time evolution of the updated parameters with the high penalty value $L=10^8$. Figure 4-25 presents the history of the HTC value. The value of the FullWinter MPC and the Partially Adaptive MPC are overlapped due to the identical value. The results of the Fully Adaptive MPC have been distinguished with different line styles for the three different test cases. It can be seen that the Fully Adaptive MPC has two significant parameter updates during the simulation period, but the time when these updates occur is not identical. The obtained HTC values for the Fully Adaptive MPC are within the range to be physically plausible, the HTC difference being within 10%. The results indicate that the Fully Adaptive MPC can give satisfactory prediction performance with reasonable parameter values for a relatively long period and does not need to update the parameters frequently.

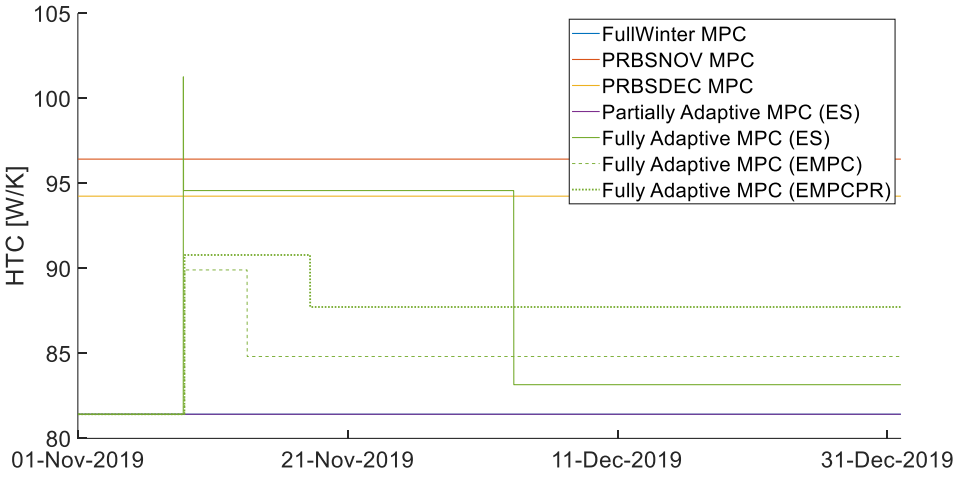

Figure 4-25: *History of the HTC value update.*

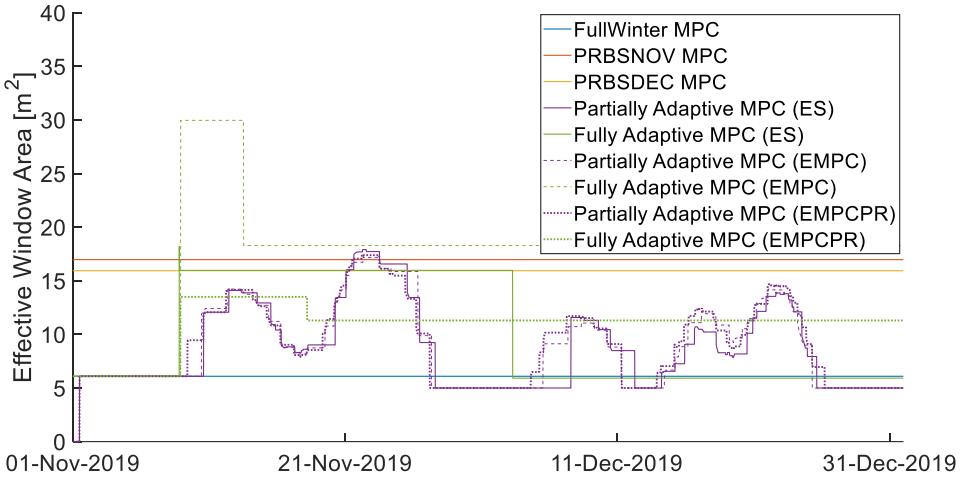

Figure 4-26: *History of the A_i value update.*

Figure 4-26 shows the history of parameter A_i. The results of the three cases are also distinguished with different line styles. The results show that the A_i updating history follows a similar trend to the Partially Adaptive MPC by first increasing in November and then decreasing in December. However, the updating history of A_i for the Fully Adaptive MPC is larger in amplitude compared to the Partially Adaptive MPC. Furthermore, parameter A_i is updated very frequently by the Partially Adaptive MPC, which indicates that the prediction error from the model is constantly large during the simulation. This confirms the previous conclusion regarding the FullWinter MPC and Partially Adaptive MPC: the FullWinter model cannot provide satisfactory prediction performance and the model cannot be corrected by only updating parameter A_i. The Fully Adaptive only updates A_i two times during simulation and the value is also

changing significantly. It indicates that parameter A_i may not play a dominant role in the prediction performance over a long timescale, though it has a significant influence on short-term temperature based on existing researches [45,52].

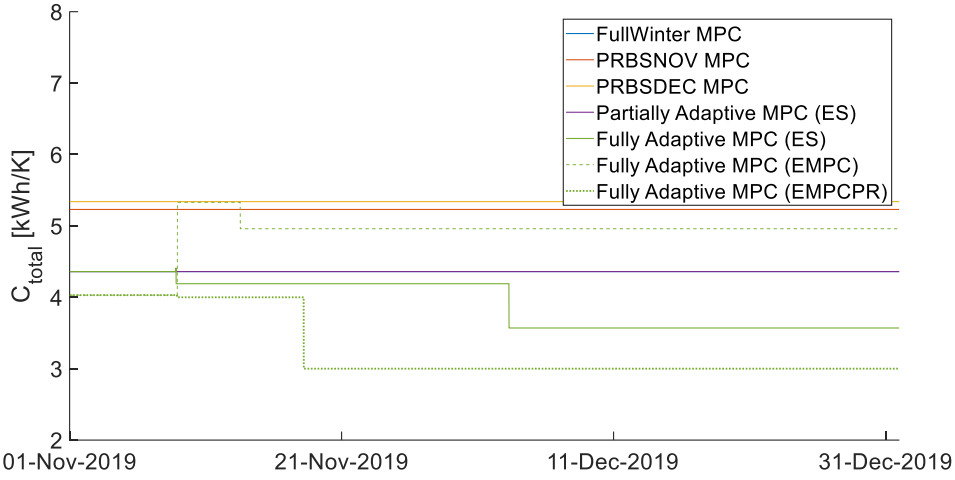

Figure 4-27: *History of the C_{total} value update.*

Figure 4-27 presents the updating history of the sum of capacitances C_e and C_i, named C_{total}. Results show that the values of the Fully Adaptive MPC are within the physical plausible range compared to the reference value C_{eff} of 3.9 kWh/K, although the values are different for the three cases. However, it is worth mentioning that the value of C_{total} is also correlated with the value of the HTC and A_i. Considering the fact that the model only takes seven days of data under normal operation to update the parameters, it is reasonable that the obtained value of HTC and C_{eff} has some variations in the value as long as it can deliver decent prediction performance.

4.3.2 Other types of data-driven models for MPC

Paper 7 is a cooperative paper in the framework of the IEA EBC Annex 71 entitled: "Building energy performance assessment based on in situ measurements". Some of its results can give complementary information to Q7. The building model has been modeled using the Modelica language in Dymola software and the OpenIDEAS library. This simulation model in Dymola serves as the emulator in this study. The case building is one of the test cases of Annex 71 project and is a two-storey experimental dwelling located in Holzkirchen, Germany. Various data-driven models for the investigated building have been developed in this study. An MPC setup has been developed in which the performance of the predictive models could be evaluated and compared. The MPC aims to optimize two objectives, namely thermal discomfort and electricity costs. The controller has been developed in SIMULINK. Hence, a way of communication is required to make the co-simulation between the SIMULINK and

Dymola. An interface is applied to tackle this issue, which facilitates the connection between Dymola and Matlab, which is called Functional Mock-up Interface (FMI).

Paper 7 compares the performance of different types of linear MPCs in addition to grey-box models in an MPC experiment. These models range from single-state grey-box models, state-space models to more advanced artificial intelligence models Artificial Neural Networks (ANN) and Support Vector Machine (SVM).

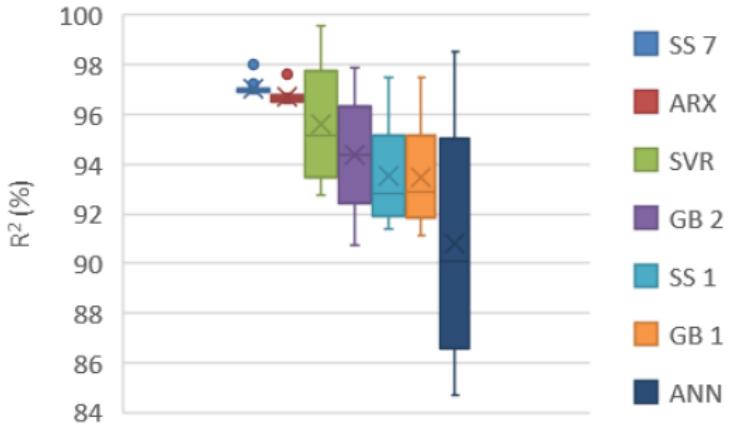

Figure 4-28: *R^2(%) of models against test dataset.*

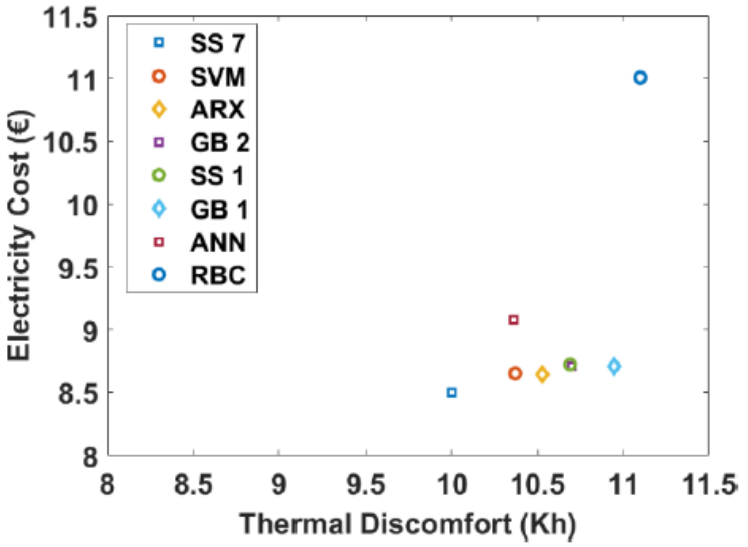

Figure 4-29: *KPIs deploying different predictive models.*

Figure 4-28 provides the boxplot accuracy of different modeling techniques used in this study. The maximum in each box corresponds to the one-step ahead prediction accuracy while the minimum corresponds to N (Control horizon) steps ahead prediction accuracy. As it can be seen in Figure 4-28, NARX model and the SVR are

the best performing models in terms of one-step ahead prediction accuracy. Nevertheless, these two models are not the best performing models in the MPC framework. This statement is especially more significant in the case of the NARX model since it leads to the highest electricity cost compared to the other models. Looking at Multi-Step ahead prediction error (MSPE), one can easily realize that, although the NARX model has the second-highest one-step ahead R^2, its multi-step ahead prediction performance is the poorest amongst all the models. The reason for this observation is explained by the fact that ANNs easily become over-fit to training data if no regularization of some sort is used [94]. This issue should be tackled when using ANNs as predictive models otherwise one might end up with an ANN model, which is highly accurate for one-step ahead prediction but provides poor forecasts for multi-step ahead prediction.

Analyzing the results as illustrated in Figure 4-29, it could be concluded that the best performing MPC (namely the state-space model with seven states) reduces electricity cost from 11€ to 8.5 € compared to RBC, which corresponds to 22.7%. Comparing different MPCs we can deduce that the difference between electricity costs resulting from using different predictive models in the MPC is 7%: electricity cost of 8.5 € in the SS7 model compared to 9.1 € achieved by using the NARX model. Considering the 22.7% as the highest potential of MPC achieved by our models for this case study, it could be inferred that the models used here vary by 24% in terms of activating the potential energy savings achieved by MPC, which demonstrates the importance of using models with high multi-step ahead prediction accuracy in the MPC.

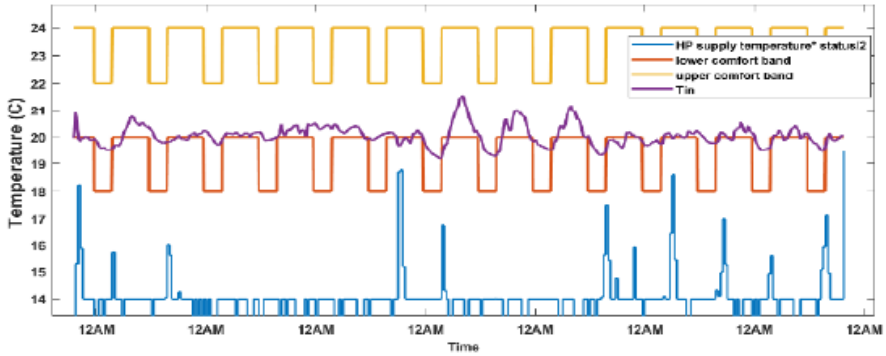

Figure 4-30: *Building's temperature profile due to MPC.*

Results obtained by applying state-space model with seven states are presented in Figure 4-30 and Figure 4-31. It is illustrated in Figure 4-30, the controller is able to maintain the temperature within the thermal comfort band, although there are some minor violations. These violations could have two main causes. First, the magnitude of weight (L) scalar in the objective function, which allows thermal discomfort to some extent, especially when the electricity cost is relatively high. The second reason behind the minor thermal discomfort could be the mismatch between the predictive

model and the emulator. The electricity price shown in Figure 4-31 is based on the time of use pricing structure from a supplier in Belgium. As seen in Figure 4-31, the load profile does not completely correspond with the time-of-use price. This observation is expected since the MPC does not optimize the building's behavior only for one time-step but for the whole control horizon.

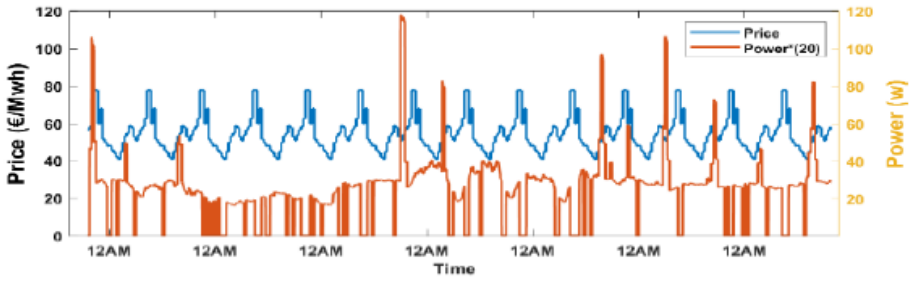

Figure 4-31: *Electricity use against electricity price.*

5 CONCLUSIONS AND FUTURE RESEARCH

This chapter summarizes the main findings of the PhD thesis. Key conclusions of each part are presented in Section 5.1. Section 5.2 lists the limitations of the studies while Section 5.3 gives recommendations for future research.

5.1 Concluding remarks

This thesis investigates the model-based control to unlock the energy flexibility of residential buildings so that more renewable energy resources can be integrated into the current energy system. The research mainly focuses on grey-box modeling and MPC. The most important conclusions are as follows:

On the modeling side

This study is based on both virtual and field experiments. The field experiment includes two experimental setups of the ZEB Living Lab using two different space-heating emission systems, namely an electric heater and a hydronic radiator.

The pre-processing techniques include low-pass filtering (using MA or FIR), the sampling time (T_s) and the application of *anti-causal shift* (ACS). Three different types of temperature measurements are analyzed to investigate the influence of the sensor location and dynamics (i.e., volume-averaged air temperature, single temperature sensor without casing and single wall-mounted sensor with casing).

Different excitation signals have been considered to generate input-output data in this thesis. Regarding the excitation signal, results showed that intermittent heating with on-off control of the electric radiators is a good excitation signal. It enables normal occupancy of the building and the collection of long data series as well as excites the slow daily and fast building dynamics.

The research confirmed the conclusion of the literature review that second-order is a good trade-off between modeling accuracy and overfitting. Based on this conclusion, the subsequent analyses of the thesis are done mainly based on a second-order grey-box model. The other conclusions regarding the modeling are presented separately between deterministic and stochastic models.

Deterministic model:

- For the deterministic model, the identification results from the default gradient-based and global optimization routines are almost identical (with and without ACS).
- The data pre-processing has a limited influence on the model performance based on virtual experiment results. This is confirmed using field experiments. In addition, the sensor thermal dynamics also have a limited influence on the deterministic model performance.

Stochastic model:

- For the stochastic model, the two-stage global optimization leads to lower NRMSE than the default gradient-based optimizer and the resulting parameters have significantly different values.
- It is always recommended to sample the measurement data at a higher frequency than the fastest dynamics of the system to be modeled (T_{min}). The parameters became non-physical without ACS for large sampling time (T_s). However, large sampling times did not alter the simulation performance significantly. Although the ACS tends to improve the physical plausibility of the model parameters with T_s, it had in general a negative influence on the simulation performance of the model.
- Large T_s can cause the parameters to become non-physical without ACS. ACS is excessively beneficial in guaranteeing the physical plausibility of parameters, making the identified parameters insensitive to the sampling time. This conclusion is valid for both our virtual and field experiments. However, the influence of ACS on prediction performance is different for virtual and field experiments. ACS has in general a negative influence on the simulation performance in the virtual experiment. In the field experiment, large T_s has a limited effect on the prediction performance for the temperature sensors without casing. However, for the wall-mounted sensor, pre-filtering and sometimes ACS should be used to converse the prediction performance at large T_s. Pre-filtering also has a beneficial influence on the model prediction performance for field experiments, but not in a dominant way. Unlike the results based on virtual experiments, the influence of ACS on prediction performance is most often beneficial in our study. At this stage, it can be concluded that the influence of the sampling time and ACS on the prediction performance is not systematic (i.e., sometimes positive or negative).
- The results for stochastic models depend on the type of indoor temperature sensor. Firstly, the cases with temperature sensors with negligible thermal dynamics (i.e., free-standing air temperature sensors without casing) are analyzed. Even though the vertical thermal stratification is significant, there is only a slight reduction in the model performance when moving from a volume-averaged measurement to a single sensor located at mid-height in the room. Secondly, when the temperature sensor is the wall-mounted temperature sensor, an adapted model with time constant dynamics for the sensor is needed to obtain a physically plausible estimation of the parameters. This is an important conclusion as most buildings are equipped with wall-mounted temperature sensors. To limit the investment, the number of sensors should also be limited, making a volume-averaged measurement expensive.

- The dynamics of the hydronic radiator (with significant thermal mass) are not necessary to be modeled if the time constant of the measurement device is larger than that of the hydronic radiator.

On the control side

In this study, the MPC uses the thermal mass of the building as short-term thermal storage to perform DR.

The performance of different MPC controllers based on a linear grey-box model of the thermal dynamics of the building is first compared for three different control objectives. The model performance is assessed from the degree of completion to fulfill the defined objectives and the avoidance of thermal discomfort. This study uses a highly-insulated detached house simulated using the BPS software IDA ICE as the emulator. The IDA ICE model is coupled with MATLAB in a co-simulation setup. The control signal is calculated by the MPC controller implemented in MATLAB and sent to the heating system so that the indoor temperature of the building in IDA ICE can be controlled.

Results show that an LTI model trained using the data from the entire space-heating season (FullWinter model) is not suitable to be used as the prediction model for a long period of operation in MPC. It shows that a longer training period is not always a synonym for better model performance. Only updating the window area of the model (Partially Adaptive MPC) is not enough to correct this LTI model and it sometimes even has negative effects on the results. The MPC based on two LTI models training using two short periods of data using a PRBS excitation (PPRBSNOV MPC and PRBSDEC MPC) generally performs better than the FullWinter and Partially Adaptive MPCs. This confirms that if an LTI grey-box model is used in MPC, it should be trained with data generated during similar weather conditions to the period when the MPC will be operated. The Fully Adaptive MPC outperforms the two PRBS LTI MPCs. It demonstrates the need to update all the model parameters if this model is to be used during the entire space-heating season. The Fully Adaptive model gives a more accurate prediction, which causes the thermal discomfort to be significantly reduced. It is worth mentioning that the number of parameter updates in the Fully Adaptive MPC is limited (i.e., two to three for the two months of MPC operation).

This thesis also implemented a parametric investigation of MPC performance based on other types of data-driven models than grey-box models. Comparing the performance of MPCs using different models shows that model trained based on MSPE criteria reflects the better suitability of predictive performance compared to models trained based on one-step ahead prediction. On the one hand, it has also been shown that models with similar one-step ahead accuracy could lead to 24% difference in terms of activating the potential cost savings achieved by MPC. On the other hand, ANN-based NARX model yielded the highest electricity cost, which is due to its poor

multi-step ahead prediction performance. Furthermore, MPC is compared to a well-tuned Rule Based Controller (RBC). Best performing MPC (using state space model with 7 states) yielded 22.7% decrease in energy cost compared to the RBC.

5.2 Limitations

On the modeling side

Many findings from the field experiments are based on a single test case, and these findings provide practical guidelines for identifying the thermal dynamics of buildings using grey-box models and field measurement data. Therefore, additional research on real buildings is needed to generalize the conclusions. The occupants' behavior based on a fixed schedule in the experiment is also very artificial with are not close enough to real conditions. Our virtual experiment does not reflect the stochasticity of the user behavior sufficiently, which may also need field tests to validate the findings. The conclusion might change if the data is collected from a building with (real) people living inside.

The thesis only considers mono-zone grey-box models. This is acceptable for the two test cases considered in the thesis. These cases are highly-insulated with balanced mechanical ventilation and a heat recovery which limits the temperature difference between the rooms. In addition, the internals was open in most of the scenarios. Most of the existing buildings in the Norwegian building stock are not well insulated. Many Norwegian actually prefer colder bedrooms (with lower temperature setpoints for bedrooms). In this case, residential buildings are inherently multi-zone, which requires a multi-zone model for MPC. If the windows of bedrooms are open at night, the natural ventilation should also be considered based on the multi-zone model. However, this limitation does not significantly impact the conclusions of the thesis. For example, the literature review has shown that second-order grey-box models are typically selected as the basic element to model one zone in a multi-zone model.

It should be remembered that the pre-filtering and resampling performed on the data from the two test cases are applied to all the variables (meaning the input data and output data). Therefore, this does not introduce any delay between these variables. This assumption is acceptable when the data preprocessing is a deliberate choice of the modeler. However, some of the data pre-processing can be implicit and performed by the sensor or hardware without the modeler's knowledge. Then, the exact data pre-treatment is not known and can be different for the different variables measured. Then a more detailed analysis of the delays between the variables should be performed.

The analysis is based on the MATLAB system identification toolbox, where the stochastic equations are written in innovation form. For generalization, results should be reproduced in other system identification tools and formulations, such as CTSM-R [95].

On the control side

The virtual experiment length of this thesis is set to two months due to the limitation of the co-simulation framework. The co-simulation was operated on a workstation with an Intel Xeon E5-2697 18-core CPU clocked at 2.30 GHz, 2301 Mhz, 64 GB RAM running a 64-bit version of Windows 10 Enterprise. The co-simulation of two months takes approximately 20 hours on average to finish. The EMPC case of the Fully Adaptive MPC is taken as an example, and it takes 1130.4 minutes to complete. The co-simulation for the Partially Adaptive MPC can take a much longer time due to frequent updates of the parameters. It is interesting to see the testing be done in a longer simulation period and different years so that the results can be more generalized.

Due to the inherent modeling simplifications in BPS, the conclusion might be different for real field experiments. The test building in our study is highly-insulated so that solar gains contribute significantly to the space heating and the air infiltrations are limited. With an older building, the situation would be the opposite (i.e., the insulation level would be lower and air infiltrations higher), which would give a different dependence on the variations in the weather conditions during the space-heating season. This may impact the conclusions on the MPC based on adaptive grey-box models that were derived for a highly-insulated building.

5.3 Future research

This thesis investigates the topic of model predictive control to activate the building energy flexibility mainly based on grey-box modeling techniques. With all the findings of this thesis and the limitations, the potential future research is outlined below.

- For generalization purposes, results should be reproduced in other simulation platforms or on a real experiment performed over a long period of time. Many MPC studies using field measurements are based on a short experimental period, see e.g., [54].
- The analysis can also be repeated for other building types or levels of thermal performance of the building envelope. For instance, older buildings are typically naturally ventilated and this phenomenon is intrinsically more non-linear. The modeling of the air handling unit (AHU) with fixed effectiveness in IDA ICE can also be improved.
- It will be interesting to do more testing with black-box modeling techniques. It can significantly reduce the expertise in building physics of the modeler if the black-box models can give robust predictions and avoid overfitting problems.
- It is also interesting to make the adaptive control MPC test in a residential building with human occupants to see if the control algorithm is still valid. In

addition, a multi-zone version of the adaptive MPC should be developed in the future for more advanced and precise control purposes of the building.

- This study mainly takes the spot prices of electricity into consideration for the objective function design of the MPC. However, $CO_{2eq.}$ intensities of the electricity mix or $CO_{2eq.}$ intensities coupled with electricity prices could also be considered as the index for the objective function design of the MPC.
- The model identification and the analysis of the data pretreatment have been made manually in this thesis. In other words, parametric runs have been used, but results have been mostly analyzed directly by the modeler. It should ideally be automated to make the procedure less time-consuming and more cost-efficient for market penetration, especially for small residential buildings. As previously mentioned in the limitations, the data pretreatment is here applied for all input and output variables. In future work, the effect of distinct data pre-treatment on the different variables should be considered, which, for instance, requires analyzing the delays (lag) between the variables.

BIBLIOGRAPHY

[1] Stinner S, Huchtemann K, Müller D. Quantifying the operational flexibility of building energy systems with thermal energy storages. Appl Energy 2016;181:140–54. https://doi.org/10.1016/j.apenergy.2016.08.055.

[2] Pérez-Lombard L, Ortiz J, Pout C. A review on buildings energy consumption information. Energy Build 2008;40:394–8. https://doi.org/10.1016/j.enbuild.2007.03.007.

[3] OECD/IEA. ENERGY POLICIES OF IEA COUNTRIES Norway 2017 Review. 2017.

[4] Steindl G, Kastner W, Stangl V. Comparison of Data-Driven Thermal Building Models for Model Predictive Control. J Sustain Dev Energy, Water Environ Syst 2019;7:730–42. https://doi.org/10.13044/j.sdewes.d7.0286.

[5] Siano P. Demand response and smart grids — A survey. Renew Sustain Energy Rev 2014;30:461–78. https://doi.org/10.1016/j.rser.2013.10.022.

[6] Jensen SØ, Marszal-Pomianowska A, Lollini R, Pasut W, Knotzer A, Engelmann P, et al. IEA EBC Annex 67 Energy Flexible Buildings. Energy Build 2017;155:25–34. https://doi.org/10.1016/j.enbuild.2017.08.044.

[7] Losi A, Mancarella P, Vicino A. Integration of demand response into the electricity chain: challenges, opportunities, and Smart Grid solutions. John Wiley & Sons; 2015.

[8] Le Dréau J, Heiselberg P. Energy flexibility of residential buildings using short term heat storage in the thermal mass. Energy 2016;111:991–1002. https://doi.org/10.1016/j.energy.2016.05.076.

[9] Reynders G. Quantifying the impact of building design on the potential of structural strorage for active demand response in residential buildings. 2015. https://doi.org/10.13140/RG.2.1.3630.2805.

[10] Zong Y, Böning GM, Santos RM, You S, Hu J, Han X. Challenges of implementing economic model predictive control strategy for buildings interacting with smart energy systems. Appl Therm Eng 2017;114:1476–86. https://doi.org/10.1016/j.applthermaleng.2016.11.141.

[11] Advanced Metering System (AMS) Status and plans for installation per Q2 2016. 2016.

[12] Vortanz K, Zayer P. How energy providers can prepare for the rollout: Roadmap for the way into the future | Wie sich Energieversorger auf den Rollout vorbereiten können: Fahrplan für den Weg in die Zukunft. BWK-Energie-Fachmagazin 2015;67:30–1.

[13] De Coninck R, Magnusson F, Åkesson J, Helsen L. Toolbox for development and validation of grey-box building models for forecasting and control. J Build Perform Simul 2016;9:288–303.

https://doi.org/10.1080/19401493.2015.1046933.

[14] Killian M, Kozek M. Ten questions concerning model predictive control for energy efficient buildings. Build Environ 2016;105:403–12. https://doi.org/10.1016/j.buildenv.2016.05.034.

[15] Atam E, Helsen L. Control-Oriented Thermal Modeling of Multizone Buildings: Methods and Issues: Intelligent Control of a Building System. IEEE Control Syst 2016;36:86–111. https://doi.org/10.1109/MCS.2016.2535913.

[16] Wetter M, Zuo W, Nouidui TS. Recent Developments of the Modelica" Buildings" Library for Building Energy and Control Systems. Lawrence Berkeley National Lab.(LBNL), Berkeley, CA (United States); 2011.

[17] Pang X, Wetter M, Bhattacharya P, Haves P. A framework for simulation-based real-time whole building performance assessment. Build Environ 2012;54:100–8.

[18] Hilliaho K, Lahdensivu J, Vinha J. Glazed space thermal simulation with IDA-ICE 4.61 software—Suitability analysis with case study. Energy Build 2015;89:132–41.

[19] Harb H, Boyanov N, Hernandez L, Streblow R, Müller D. Development and validation of grey-box models for forecasting the thermal response of occupied buildings. Energy Build 2016;117:199–207. https://doi.org/10.1016/j.enbuild.2016.02.021.

[20] Wolisz H, Harb H, Matthes P, Streblow R, Müller D. Dynamic simulation of thermal capacity and charging/discharging performance for sensible heat storage in building wall mass. Proc. Build. Simul. Conf., 2013.

[21] Ruano AE, Crispim EM, Conceição EZE, Lúcio MMJR. Prediction of building's temperature using neural networks models. Energy Build 2006;38:682–94. https://doi.org/10.1016/j.enbuild.2005.09.007.

[22] Crabb JA, Murdoch N, Penman JM. A simplified thermal response model. Build Serv Eng Res Technol 1987;8:13–9.

[23] Laret L. Use of general models with a small number of parameters, Part 1: Theoretical analysis. Proc. Conf. Clima, 2000, p. 263–76.

[24] Afram A, Janabi-Sharifi F. Review of modeling methods for HVAC systems. Appl Therm Eng 2014;67:507–19. https://doi.org/10.1016/j.applthermaleng.2014.03.055.

[25] Li Y, O'Neill Z, Zhang L, Chen J, Im P, DeGraw J. Grey-box modeling and application for building energy simulations - A critical review. Renew Sustain Energy Rev 2021;146:111174. https://doi.org/10.1016/j.rser.2021.111174.

[26] Yao Y, Shekhar DK. State of the art review on model predictive control (MPC) in Heating Ventilation and Air-conditioning (HVAC) field. Build

Environ 2021;200:107952. https://doi.org/10.1016/j.buildenv.2021.107952.

[27] Madsen H, Bacher P, Bauwens G, Deconinck A-H, Reynders G, Roels S, et al. IEA EBC Annex 58-Reliable building energy performance characterisation based on full scale dynamic measurements. Report of subtask 3, part 2: Thermal performance characterisation using time series data-statistical guidelines 2016.

[28] Hedegaard RE, Pedersen TH, Knudsen MD, Petersen S. Towards practical model predictive control of residential space heating: Eliminating the need for weather measurements. Energy Build 2018;170:206–16. https://doi.org/10.1016/j.enbuild.2018.04.014.

[29] Freund S, Schmitz G. Implementation of model predictive control in a large-sized, low-energy office building. Build Environ 2021;197:107830. https://doi.org/10.1016/j.buildenv.2021.107830.

[30] Wang J, Li S, Chen H, Yuan Y, Huang Y. Data-driven model predictive control for building climate control: Three case studies on different buildings. Build Environ 2019;160:106204. https://doi.org/10.1016/j.buildenv.2019.106204.

[31] Halvgaard R, Poulsen NK, Madsen H, Jørgensen JB. Economic model predictive control for building climate control in a smart grid. 2012 IEEE PES Innov. smart grid Technol., IEEE; 2012, p. 1–6.

[32] Knudsen MD, Hedegaard RE, Pedersen TH, Petersen S. System identification of thermal building models for demand response–A practical approach. Energy Procedia 2017;122:937–42.

[33] Awadelrahman MAA, Zong Y, Li H, Agert C. Economic model predictive control for hot water based heating systems in smart buildings. Energy Power Eng 2017;9:112–9.

[34] Merema B, Saelens D, Breesch H. Demonstration of an MPC framework for all-air systems in non-residential buildings. Build Environ 2022;217:109053. https://doi.org/10.1016/j.buildenv.2022.109053.

[35] Coninck R De. Grey-Box Based Optimal Control for Thermal Systems in Buildings Unlocking Energy Efficiency and Flexibility 2015. https://doi.org/10.13140/RG.2.1.4761.6166.

[36] Hazyuk I, Ghiaus C, Penhouet D. Model Predictive Control of thermal comfort as a benchmark for controller performance. Autom Constr 2014;43:98–109. https://doi.org/10.1016/j.autcon.2014.03.016.

[37] Hedegaard RE, Kristensen MH, Pedersen TH, Brun A, Petersen S. Bottom-up modelling methodology for urban-scale analysis of residential space heating demand response. Appl Energy 2019;242:181–204. https://doi.org/10.1016/j.apenergy.2019.03.063.

[38] Hu M, Xiao F, Wang L. Investigation of demand response potentials of

residential air conditioners in smart grids using grey-box room thermal model. Appl Energy 2017;207:324–35. https://doi.org/10.1016/j.apenergy.2017.05.099.

[39] Van Impe JF, Vanrolleghem PA, Iserentant DM. Advanced instrumentation, data interpretation, and control of biotechnological processes. Springer Science & Business Media; 2013.

[40] Ljung L, Wills A. Issues in sampling and estimating continuous-time models with stochastic disturbances. Automatica 2010;46:925–31. https://doi.org/10.1016/j.automatica.2010.02.011.

[41] Arendt K, Jradi M, Wetter M, Veje CT. ModestPy: An Open-Source Python Tool for Parameter Estimation in Functional Mock-up Units. Proc. Am. Model. Conf. 2018, Oct. 9-10, Somb. Conf. Center, Cambridge MA, USA, vol. 154, 2019, p. 121–30. https://doi.org/10.3384/ecp18154121.

[42] Prívara S, Cigler J, Váňa Z, Oldewurtel F, Sagerschnig C, Žáčeková E. Building modeling as a crucial part for building predictive control. Energy Build 2013;56:8–22. https://doi.org/10.1016/j.enbuild.2012.10.024.

[43] Knudsen MD, Petersen S. Economic model predictive control of space heating and dynamic solar shading. Energy Build 2020;209. https://doi.org/10.1016/j.enbuild.2019.109661.

[44] Knudsen MD, Petersen S. Model predictive control for demand response of domestic hot water preparation in ultra-low temperature district heating systems. Energy Build 2017;146:55–64. https://doi.org/10.1016/j.enbuild.2017.04.023.

[45] Bacher P, Madsen H. Identifying suitable models for the heat dynamics of buildings. Energy Build 2011;43:1511–22. https://doi.org/10.1016/j.enbuild.2011.02.005.

[46] Vogler-Finck PJC, Clauß J, Georges L, Sartori I, Wisniewski R. Inverse Model Identification of the Thermal Dynamics of a Norwegian Zero Emission House. Cold Clim. HVAC Conf., Springer; 2018, p. 533–43.

[47] Yang S, Wan MP, Chen W, Ng BF, Zhai D. An adaptive robust model predictive control for indoor climate optimization and uncertainties handling in buildings. Build Environ 2019;163:106326. https://doi.org/10.1016/j.buildenv.2019.106326.

[48] Yang S, Wan MP, Chen W, Ng BF, Dubey S. Model predictive control with adaptive machine-learning-based model for building energy efficiency and comfort optimization. Appl Energy 2020;271:115147. https://doi.org/10.1016/j.apenergy.2020.115147.

[49] Fux SF, Ashouri A, Benz MJ, Guzzella L, Artiges N, Nassiopoulos A, et al. EKF based self-adaptive thermal model for a passive house. Energy Build 2014;68:811–7. https://doi.org/10.1016/j.enbuild.2012.06.016.

[50] Choi YJ, Park BR, Hyun JY, Moon JW. Development of an adaptive artificial neural network model and optimal control algorithm for a data center cyber – physical system. Build Environ 2022;210:108704. https://doi.org/10.1016/j.buildenv.2021.108704.

[51] Maree JP, Gros S, Walnum HT. Adaptive control and identification for heating demand-response in buildings. 2021 Eur. Control Conf. ECC 2021, EUCA; 2021, p. 1931–6. https://doi.org/10.23919/ECC54610.2021.9655010.

[52] Zhang X, Rasmussen C, Saelens D, Roels S. Time-dependent solar aperture estimation of a building : Comparing grey-box and white-box approaches. Renew Sustain Energy Rev 2022;161:112337. https://doi.org/10.1016/j.rser.2022.112337.

[53] Wolisz H, Kull TM, Müller D, Kurnitski J, Yang S, Pun M, et al. Self-learning model predictive control for dynamic activation of structural thermal mass in residential buildings. Energy Build 2020;207:109542. https://doi.org/10.1016/j.enbuild.2019.109542.

[54] Knudsen MD, Georges L, Skeie KS, Petersen S. Experimental test of a black-box economic model predictive control for residential space heating. Appl Energy 2021;298:117227. https://doi.org/10.1016/j.apenergy.2021.117227.

[55] Hedegaard RE, Pedersen TH, Petersen S. Multi-market demand response using economic model predictive control of space heating in residential buildings. Energy Build 2017;150:253–61. https://doi.org/10.1016/j.enbuild.2017.05.059.

[56] De Coninck R, Helsen L. Practical implementation and evaluation of model predictive control for an office building in Brussels. Energy Build 2016;111:290–8. https://doi.org/10.1016/j.enbuild.2015.11.014.

[57] Prívara S, Široký J, Ferkl L, Cigler J. Model predictive control of a building heating system: The first experience. Energy Build 2011;43:564–72. https://doi.org/10.1016/j.enbuild.2010.10.022.

[58] Pedersen TH, Petersen S. Investigating the performance of scenario-based model predictive control of space heating in residential buildings. J Build Perform Simul 2017;1493:1–14. https://doi.org/10.1080/19401493.2017.1397196.

[59] Favero M, Sartori I, Carlucci S. Human thermal comfort under dynamic conditions: An experimental study. Build Environ 2021;204:108144. https://doi.org/10.1016/j.buildenv.2021.108144.

[60] Freund S, Schmitz G. Development of a Framework for Model Predictive Control (MPC) in a Large-Sized Low-Energy Office Building Using Modelica Grey-Box Models. Build. Simul. 2019 16th Conf. IBPSA, Rome, Italy, 2019, p. 2864–71.

[61] Berechnung D, Fensterrahmen A. VDI 6007 Blatt 1 Änderungsblatt 1 zur

Ausgabe Juni 2015 2016.

[62] DIN E. 6946: 2008-04: Bauteile—Wärmedurchlasswiderstand und Wärmedurchgangskoeffizient—Berechnungsverfahren (ISO 6946: 2007). Dtsch Fassung EN ISO 2007;6946.

[63] Georges E, Cornélusse B, Ernst D, Lemort V, Mathieu S. Residential heat pump as flexible load for direct control service with parametrized duration and rebound effect. Appl Energy 2017;187:140–53. https://doi.org/10.1016/j.apenergy.2016.11.012.

[64] International Organization for Standardization. Energy performance of buildings e calculation of energy use for space heating and cooling (ISO 13790:2008). Geneva: 2008.

[65] Hedegaard RE, Pedersen T, Knudsen MD, Petersen S. Identifying a comfortable excitation signal for generating building models for model predictive control: a simulation study. CLIMA2016 12th REHVA World Congr. World Congr., Aalborg Universitet; 2016. https://doi.org/https://doi.org10.3384/ecp18154121.

[66] Hedegaard RE, Petersen S. Evaluation of Grey-Box Model Parameter Estimates Intended for Thermal Characterization of Buildings. Energy Procedia, vol. 132, Elsevier B.V.; 2017, p. 982–7. https://doi.org/10.1016/j.egypro.2017.09.692.

[67] Reynders G, Diriken J, Saelens D. Quality of grey-box models and identified parameters as function of the accuracy of input and observation signals. Energy Build 2014;82:263–74. https://doi.org/10.1016/j.enbuild.2014.07.025.

[68] Blum DH, Arendt K, Rivalin L, Piette MA, Wetter M, Veje CT. Practical factors of envelope model setup and their effects on the performance of model predictive control for building heating, ventilating, and air conditioning systems. Appl Energy 2019;236:410–25. https://doi.org/10.1016/j.apenergy.2018.11.093.

[69] Berthou T, Stabat P, Salvazet R, Marchio D. Development and validation of a gray box model to predict thermal behavior of occupied office buildings. Energy Build 2014;74:91–100. https://doi.org/10.1016/j.enbuild.2014.01.038.

[70] Kasten F, Czeplak G. Solar and terrestrial radiation dependent on the amount and type of cloud. Sol Energy 1980;24:177–89.

[71] Brastein OM, Perera DWU, Pfeifer C, Skeie NO. Parameter estimation for grey-box models of building thermal behaviour. Energy Build 2018;169:58–68. https://doi.org/10.1016/j.enbuild.2018.03.057.

[72] Arroyo J, Spiessens F, Helsen L. Identification of multi-zone grey-box building models for use in model predictive control. J Build Perform Simul

2020;13:472–86. https://doi.org/10.1080/19401493.2020.1770861.

[73] Agbi C, Song Z, Krogh B. Parameter identifiability for multi-zone building models. Proc IEEE Conf Decis Control 2012:6951–6. https://doi.org/10.1109/CDC.2012.6425995.

[74] Kim D, Cai J, Braun JE, Ariyur KB. System identification for building thermal systems under the presence of unmeasured disturbances in closed loop operation: Theoretical analysis and application. Energy Build 2018;167:359–69. https://doi.org/10.1016/j.enbuild.2017.12.007.

[75] Wang Z, Chen Y, Li Y. Development of RC model for thermal dynamic analysis of buildings through model structure simplification. Energy Build 2019;195:51–67. https://doi.org/10.1016/j.enbuild.2019.04.042.

[76] Vogler-Finck P, Clauß J, Georges L. A dataset to support dynamical modelling of the thermal dynamics of a super-insulated building 2017. https://doi.org/10.5281/ZENODO.1034820.

[77] Norge S. NS 3700: 2013 Criteria for passive houses and low energy buildings-Residential buildings 2013.

[78] Johnsen T, Taksdal K, Clauß J, Yu X, Georges L. Influence of thermal zoning and electric radiator control on the energy flexibility potential of Norwegian detached houses. E3S Web Conf 2019;111:06030. https://doi.org/10.1051/e3sconf/201911106030.

[79] Bøeng AC, Halvorsen B, Larsen BM. Kartlegging av oppvarmingsutstyr i husholdningene. Rapp 2014/45 2014.

[80] Norge S. SN/TS 3031: 2016 Energy performance of buildings. Calc Energy Needs Energy Supply 2016.

[81] Åström KJ. Introduction to stochastic control theory. Courier Corporation; 2012.

[82] Kennedy J, Eberhart R. Particle swarm optimization. Proc. ICNN'95-International Conf. Neural Networks, vol. 4, IEEE; 1995, p. 1942–8.

[83] Particle Swarm Optimization Algorithm - MATLAB & Simulink - MathWorks n.d. https://se.mathworks.com/help/gads/particle-swarm-optimization-algorithm.html#mw_522b9230-864b-47d1-a0db-1bf6c882d862.

[84] Bellu G, Saccomani MP, Audoly S, D'Angiò L. DAISY: A new software tool to test global identifiability of biological and physiological systems. Comput Methods Programs Biomed 2007;88:52–61. https://doi.org/10.1016/j.cmpb.2007.07.002.

[85] Saccomani MP, Audoly S, Bellu G, D'Angiò L. Examples of testing global identifiability of biological and biomedical models with the DAISY software. Comput Biol Med 2010;40:402–7.

https://doi.org/10.1016/j.compbiomed.2010.02.004.

[86] Villaverde AF, Barreiro A, Papachristodoulou A. Structural identifiability of dynamic systems biology models. PLoS Comput Biol 2016;12:e1005153.

[87] European Comittee for Standardization. ISO 13786:2017 - Thermal performance of building components - Dynamic thermal characteristics - Calculation methods 2017.

[88] Clauß J, Vogler-Finck P, Georges L. Calibration of a high-resolution dynamic model for detailed investigation of the energy flexibility of a zero emission residential building. Cold Clim. HVAC Conf., Springer; 2018, p. 725–36.

[89] Khatibi M, Rahnama S, Vogler-Finck P, Bendtsen JD, Afshari A. Investigating the flexibility of a novel multi-zone air heating and ventilation system using model predictive control. J Build Eng 2022;49:104100. https://doi.org/10.1016/j.jobe.2022.104100.

[90] Lofberg J. YALMIP: A toolbox for modeling and optimization in MATLAB. 2004 IEEE Int. Conf. Robot. Autom. (IEEE Cat. No. 04CH37508), IEEE; 2004, p. 284–9.

[91] Lofberg J, Gurobi Optimization LLC. Gurobi optimizer reference manual. 2004 IEEE Int. Conf. Robot. Autom. (IEEE Cat. No. 04CH37508), IEEE; 2004, p. 284–9.

[92] Yu X, Georges L, Imsland L. Data pre-processing and optimization techniques for stochastic and deterministic low-order grey-box models of residential buildings. Energy Build 2021;236:110775. https://doi.org/10.1016/j.enbuild.2021.110775.

[93] Standard Norge. NS 3031 Energy Performance of Buildings: Calculation of Energy Needs and Energy Supply 2016.

[94] Afroz Z, Shafiullah GM, Urmee T, Higgins G. Modeling techniques used in building HVAC control systems: A review. Renew Sustain Energy Rev 2018;83:64–84. https://doi.org/10.1016/j.rser.2017.10.044.

[95] Juhl R, Møller JK, Madsen H. ctsmr-Continuous time stochastic modeling in R. ArXiv Prepr ArXiv160600242 2016.

RESEARCH PUBLICATIONS

This section contains the publications that make up the thesis.

PAPER 1

Yu X, Georges L, Knudsen MD, Sartori I, Imsland L. Investigation of the Model Structure for Low-Order Grey-Box Modelling of Residential Buildings. *Proceedings of Building Simulation 2019 16th Conference IBPSA*, International Building Performance Simulation Association (IBPSA), 2nd-4th September 2019, Rome, Italy.

Investigation of the Model Structure for Low-Order Grey-Box Modelling of Residential Buildings

Xingji Yu[1*], Laurent Georges[1], Michael Dahl Knudsen[2], Igor Sartori[3], Lars Imsland[4]
[1]NTNU, Dept. of Energy and Process Engineering, Trondheim, Norway
[2]AU, Dept. of Indoor Climate and Energy, Aarhus, Denmark
[3]SINTEF Building and Infrastructure AS, Oslo, Norway
[4]NTNU, Dept. of Engineering Cybernetics, Trondheim, Norway
* *corresponding author: xingji.yu@ntnu.no*

Abstract

Model Predictive Control (MPC) is a key technology to activate the building energy flexibility. A reliable control-based model should be developed for each specific building. The structure of grey-box models is usually based on the physical knowledge of the building. Firstly, it is not certain that this information will be available for all buildings, especially for small residential buildings. Secondly, developing a specific model structure for each building is most probably not affordable. Therefore, the paper investigates the dependency on the model structure to create reliable control-oriented model for the thermal mass of residential buildings. Using a test case, the performance of grey-box models based on the physical knowledge of the building are compared to grey-box models based on a generic structure taken from building standards (EN 13790 and VDI 6007) as well as black-box models where no knowledge of the building is required.

Introduction

Renewable energy plays an increasingly important role in economy growth and to limit CO_2 emissions. However, the increasing penetration of renewables in the grid poses a challenge for balancing the demand and supply of electricity. Electricity generated from renewables may not be consumed optimally and this mismatch can also cause challenges in the power system. Thus, multiple types of flexibility are needed in the energy sectors for smart grid integration (You, Jin, Hu, Zong, & Bindner, 2015). Buildings accounts for more than one-third of the total final energy consumption worldwide (*Transition to Sustainable Buildings*, 2013). A considerable portion of the energy consumed by buildings is used for heating, especially in Nordic countries where the space-heating season is long and cold. It has been shown that the thermal mass of buildings can be a significant heat storage (Le Dréau & Heiselberg, 2016; Glenn Reynders, 2015; Zong et al., 2017) to perform demand response (DR). Model predictive control (MPC) is often considered to be a key technology to activate the thermal energy flexibility. The control will take the predictions of future disturbances and system constraints into the optimization so that an optimal control decision could be made at each time step to perform DR. The typical disturbances taken into account are the ambient temperature, solar radiation and internal heat sources. The objective of the optimization using MPC is usually to minimize energy use, power, energy costs or CO_2 emissions while subjected to thermal comfort constraints (Dahl Knudsen & Petersen, 2016).

An effective implementation of a MPC requires a specific control model of the thermal dynamics of the building. Methods are typically divided into white-, black- and grey-box models. White-box models are almost entirely based on physical laws. Therefore, they require detailed knowledge of the system to be modelled and its parameters (such as the geometry). It is often difficult and very time-consuming to obtain this information in practice. Some parameters may also change during operation and deviate from the original design. In addition, the mathematical complexity of white-box models makes them unsuited for MPC due to the computational cost to optimize a large non-linear system of equations in real time. Model reduction techniques can nonetheless be applied to white-box models. Black-box modelling is a data-driven method only considering system inputs and outputs. It can be applied even if a limited physical knowledge of the system is available. Since the data is the only information for the modelling process, the quality and amount of data will significantly influence the precision of black-box models. Their ability to predict the system dynamics outside operating conditions considered during the model training is also critical. Grey-box modelling is a combination of the previous two approaches. The physical knowledge of the system is used to determine a general model structure (a low-order model) and the model parameters are identified using experimental data. Due to the model structure based on physical grounds, grey-box models require less experimental data than black-box models and are less sensitive to the data quality. In addition, they should be more robust to extrapolate outside the operating conditions used during the period of the model training.

A single residential building will not provide a large amount of energy flexibility to the grid. In the context of smart grids, a large number of residential buildings needs to be considered. However, the thermal dynamics is different for each single building. Creating a suitable control-oriented model is also acknowledged as the most time-consuming part of the MPC implementation (Atam & Helsen, 2016), especially when physical knowledge specific to the building is required (such as in grey-box models). For grey-box models, the typical approach is to progressively increase the complexity of the model structure and to perform a forward selection process to identify the optimal configuration.

https://doi.org/10.26868/25222708.2019.211209

Some research work has been recently done to develop a tool that can automatically identify the grey-box models based on a BIM (Andriamamonjy, Klein, & Saelens, 2019). However, it is still worth investigating if generic model structures can be an acceptable option to lower the cost of modelling in MPC. For this purpose, three modelling approaches are compared on a test case. It is here assumed that model should be identified using indoor temperature measurements only. Firstly, a traditional grey-box modelling approach is used where models of increasing complexity are created based on the physical knowledge of the building (i.e. forward approach). Secondly, the model structures of building standards EN 13790 and VDI 6007 are considered. These models are low-order white-box models that are able to successfully predict space-heating needs for various building types. For instance, some studies have also been done to compare the simulation results of the two standard white-box models with TRNSYS simulation (Bruno, Pizzuti, & Arcuri, 2016; Vivian, Zarrella, Emmi, & De Carli, 2017). Their structures, even not optimal for a specific building, may nonetheless be a good candidate for a generic structure of grey-box models. Finally, these two methods to create grey-box models are compared to black-box models identified using a subspace method and then refined using numerical minimization of simulation errors. The long-term predictions (i.e. simulation without a disturbance model) of these models are evaluated as well as their estimates of some major building thermal characteristics (such as overall heat loss coefficient and thermal capacities).

Dataset and platform description

The ZEB Living Lab is a zero-emission single-family house located in the campus of the Norwegian University of Science and Technology (NTNU) in Trondheim. The total floor area of the building is about 100 m^2. The envelope is a wooden frame insulated with 35-40 cm mineral wool and with a glazing ratio of 0.2. Photovoltaic panels installed on the roof has been designed to provide enough onsite renewable energy production to reach a zero CO_{2eq} emission balance over the building lifetime. The water-based heating system consists of a ground source heat pump. The space-heating can be either performed by floor heating, a central radiator or the ventilation air. However, the current study is based on measurement data from a previous experiment where space heating was performed using an electrical heater (P. Vogler-Finck, Clauß, & Georges, 2017; P. J. C. Vogler-Finck, Clauß, Georges, Sartori, & Wisniewski, 2018). The electric heater was located in the middle of the building while a Pseudo-Random Binary Signal (PRBS) was used to excite the thermal dynamic of the building in a large spectrum of frequencies. The floor plan of the building is shown in Figure 1 along with the location of the electric radiator and the temperature sensors.

The dataset contains three successful experiments, which are named experiment 2, 3 and 4 (experiment 1 being omitted). The data includes measurements every 5 minutes of the ambient temperature, indoor air operative temperatures as well as the global solar radiation on a horizontal plane and the electricity consumption. In this study, the ventilation losses are not identified but directly introduced in the model as heat losses. These losses have been evaluated using the measured temperature difference between the supply and exhaust ventilation air combined with the measured airflow rate (constant during experiments). This research focuses on data from experiments 2 and 4 since both experiments were conducted with the building unoccupied and internal doors opened. This leads to an almost uniform spatial distribution of the air temperature inside the building. However, there is some temperature stratification and all air temperature sensors are therefore volume-averaged to represent the mean indoor air temperature T_i. Experiment 2 is used to train the model while experiment 4 is used for validation.

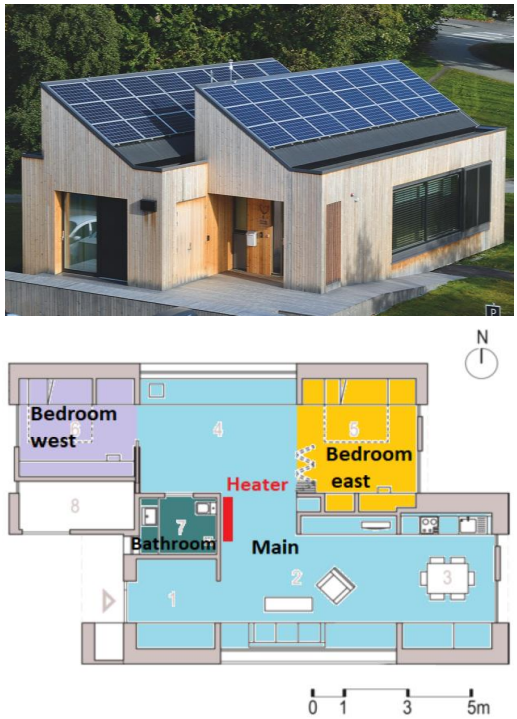

Figure 1: Picture and Floor plan of the ZEB Living Lab (P. J. C. Vogler-Finck et al., 2018)

Grey-box models

As mentioned in the introduction section, grey-box modelling is a combination of measurement data and physical knowledge. The thermal dynamics of the ZEB Living Lab is assumed to be linear and time invariant which is a common approximation for building envelopes. It can then be approximated by low-order resistance-capacitance (RC) networks. The model order is defined by the number of heat capacitances included in the model. This paper considers two categories of structure for the grey-box model: seven structures derived from our prior knowledge of the Living Lab and two

generic structures derived from standards for energy calculations (EN 13790) and (VDI 6007).

Knowledge-based models

The simplest model structure is a 1st order model. The other models are created by progressively adding more components, the most complex structure being a 3rd order model. Only the most complicated 3rd order model is presented in Figure 2 since the other models are simplifications of this structure as described in Table 1.

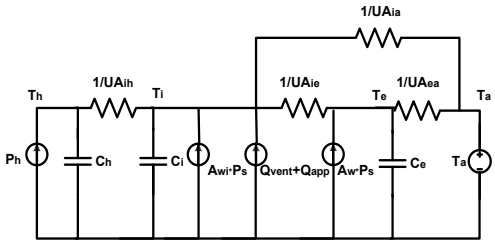

Figure 2: Most complex model structure (3C).

The 1st order model has one heat capacitance (C_i), the 2nd order model has two heat capacitances (C_i and C_e) while the 3rd order model has three heat capacitances (C_i, C_e and C_h). The physical meaning of these components is described here below.

Table 1: Structure of the different knowledge-based grey-box models.

MODEL	1C	2Cs	2C	3Cs	3C	3Csd	3Cd
R_{ih}	×	×	×	✓	✓	✓	✓
R_{ie}	×	✓	✓	✓	✓	✓	✓
R_{ea}	×	✓	✓	✓	✓	✓	✓
R_{ia}	✓	×	✓	×	✓	×	✓
C_e	×	✓	✓	✓	✓	✓	✓
C_i	✓	✓	✓	✓	✓	✓	✓
C_h	×	×	×	✓	✓	✓	✓
A_{wi}	✓	✓	✓	✓	✓	✓	✓
A_{we}	×	✓	✓	✓	✓	×	×

T_i Temperature of interior heat capacity [°C].

T_e Temperature of the building envelope [°C].

T_h Temperature of the electric heater [°C].

T_a The outdoor/ambient temperature [°C].

C_i Heat capacity of the interior which is assumed to be the combination of the thermal mass of the air, the furniture, internal walls and the first centimeters of the internal surface of external walls [kWh/K].

C_e Heat capacity of the building envelope, (external walls and windows) [kWh/K].

C_h Heat capacity of the heater which is assumed to the combination of its thermal mass and some air around the heater [kWh/K].

R_{ie} ($1/UA_{ie}$) Heat resistance between the building envelope and the interior of the building [K/kW].

R_{ea} ($1/UA_{ea}$) Heat resistance between the ambient and the building envelope [K/kW].

R_{ia} ($1/UA_{ia}$) Heat resistance between the ambient and the interior of the building [K/kW].

P_h Heat gain from the electric heater [kW].

P_s Global solar irradiation on a horizontal plane [kW].

Q_{app} Heat gain from internal loads (appliances) [kW].

Q_{vent} Heat gains from the ventilation [kW].

A_{wi} Effective window area for the solar gain that enters directly the interior node [m^2].

A_{we} Effective wall area for the solar gain directly applied to the envelope of the building [m^2].

Standard models

The structure of the two RC-models is taken from the standards EN 13790 and VDI 6007 (Vivian et al., 2017) The EN 13790 model has originally five resistances and one capacitance, as shown in Figure 3. The heat capacitance represents the heat capacity of the building envelope. Since the ventilation heat loss is directly injected as a heat gain in our model, the specific resistance of EN 13790 related to ventilation is removed. The resulting grey-box model has therefore four resistances. Detailed physical explanation of the RC components in EN 13790 are described below.

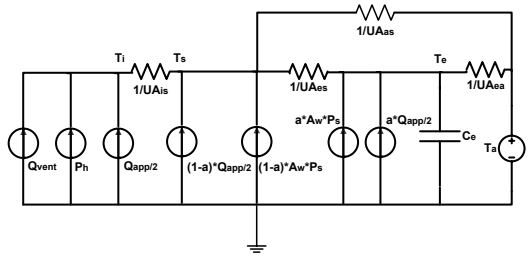

Figure 3: Model structure of EN 13790.

T_i Interior temperature (as previously defined) [°C].

T_e Temperature of the building envelope [°C].

T_s The temperature of the internal surface of the building envelope [°C].

T_a The outdoor/ambient temperature [°C].

C_e Heat capacity of the building envelope [kWh/K].

R_{es} ($1/UA_{es}$) Heat resistance between the building envelope and the internal surface of the building envelope [K/kW].

R_{ea} ($1/UA_{ea}$) Heat resistance between the ambient and the building envelope [K/kW].

R_{as} ($1/UA_{as}$) Heat resistance between the ambient and the internal surface of the building envelope [K/kW].

R_{is} ($1/UA_{is}$) Heat resistance between the internal surface of the building envelope and the internal node [K/kW].

P_h Heat gain from the electric heater [kW].

P_s Global solar irradiation on a horizontal plane [kW].

Q_{app} Heat gain from internal loads (appliances) [kW].

Q_{vent} Heat gains from the ventilation [kW].

A_w Effective window area for the solar gain [m^2].

According to EN 13790, half of the internal gains Q_{app} is directly entering the internal node (T_i) while the heat emitted by the radiator is fully entering this node. Thus, a coefficient of 1/2 is applied to Q_{app} and a coefficient of 1 to the space-heating power P_h. In EN 13790, the fraction of internal and solar gains entering the internal surface (T_s) and the envelope nodes (T_e) should be evaluated using the detailed geometry of the building. Therefore, one model parameter (a) is added and should be identified. In order to guarantee energy conservation, the sum of the two fractions of Q_{app} applied respectively to nodes T_s and T_e is constrained to 1/2. Solar radiation only enters at nodes T_s and T_e, so the sum of the two fractions of solar gains at T_s and T_e is constrained to 1.

The VDI 6007 model originally has seven resistances and two capacitances. Like EN 13790, the heat resistance related to the ventilation heat losses is substituted by the measured ventilation heat gains. Detailed physical explanations of the RC components of VDI 6007 are shown below.

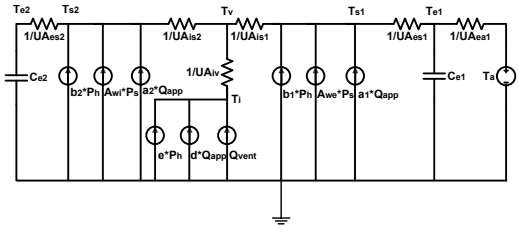

Figure 4: Model structure of VDI 6007.

T_i Interior air and furniture temperature [°C].

T_v Interior "star" node [°C].

T_{s1} The internal surface temperature of building envelope (meaning external walls and windows) [°C].

T_{s2} The internal surface temperature of internal walls [°C].

T_{e1} Temperature of the building envelope [°C].

T_{e2} Temperature of internal walls [°C].

T_a The outdoor/ambient temperature [°C].

C_{e1} Heat capacitance of the building envelope [kWh/K].

C_{e2} Heat capacitance of internal walls [kWh/K].

R_{es1} ($1/UA_{es1}$) Resistance between the building envelope and the internal surface of the envelope [K/kW].

R_{es2} ($1/UA_{es2}$) Resistance between the internal walls and their surface [K/kW].

R_{is1} ($1/UA_{is1}$) Heat resistance between the internal surface of the envelope and the star node [K/kW].

R_{is2} ($1/UA_{ea1}$) Heat resistance between the ambient and the building envelope [K/kW].

R_{ea1} ($1/UA_{ea1}$) Heat resistance between the ambient and the building envelope [K/kW].

R_{iv} ($1/UA_{ea1}$) Heat resistance between the star node and the indoor air and furniture node [K/kW].

P_h Emitted heat from the electric heater [kW].

P_s Global solar irradiation on a horizontal plane [kW].

Q_{app} Heat gain from internal loads (appliances) [kW].

Q_{vent} Heat gains from the ventilation [kW].

A_w Effective window area for the solar gain [m^2].

The coefficient for internal heat gains (Q_{app}) and the emitted power by the radiator (P_h) are estimated by the grey-box modelling approach. It results in six parameters a_1, a_2, b_1, b_2, d and e. To guarantee the conservation of energy, additional constraints for these variables are applied: the sum of the coefficients of a_1, a_2 and d and the sum of coefficients of b_1, b_2 and e are set to 1.

Black-box models

In black-box modelling, data is used to train mathematical models with parameters that cannot be given an immediate physical interpretation. In this study linear time-invariant state-space models with model orders from one to three are examined:

$$x^{k+1} = \mathbf{A}\, x^k + \mathbf{B}\, u^k \quad (1)$$

$$y^k = \mathbf{C}\, x^k \quad (2)$$

where x is the state vector and $\boldsymbol{A}$, $\boldsymbol{B}$ and $\boldsymbol{C}$ are system matrices. u is the input (outdoor temperature, solar radiation and heat gains) and y is the output (indoor temperature). Note that no disturbance term $\boldsymbol{K}$ (Kalman gain) is included because we focus on long-term predictions. All coefficients in the system matrices are free and unconstrained which gives the optimizer maximum freedom (for a given model order) to adjust the coefficients to fit to the training data. The downfall is that the model cannot be guaranteed to always comply with physical laws (i.e. conservation of energy). In case of poor training data, the model might have a very poor performance on new data.

This study has trained the black-box models in two steps. Firstly, subspace system identification estimates an initial model using the *n4sid* function in MATLAB (Ljung, 2011). Secondly, the model is refined through numerical simulation-error minimization using the *pem* function of MATLAB.

It should be noted that, even though the black-box parameters do not have an immediate physical meaning, it is in fact possible to extract some insight on the thermal characteristics of the building. For instance, the overall heat loss coefficient can be estimated as the inverse of the steady-state output (i.e. the room temperature) for a step response of the heat input. This value is also shown in Tables 2 and 3 for the 2nd order black box model (2B).

Results

Tables 2 and 3 show some of the most important physical parameters identified and the simulation results for all models, respectively for the original sampling time of 5 minutes and a data subset based on 15-minutes averaging. Since this paper mainly focuses on the long-term stable prediction of the model, no disturbance model is included to correct the current state based on prediction errors. Other studies on grey-box modelling often focus on the one-step ahead predictions (Bacher & Madsen, 2011), but for MPC implementation it is important to have good performance for a longer prediction horizon. Since there is no human occupancy during experiments and since energy consumption and the indoor temperature are accurately measured, the data quality is considered to be relatively high compared to what can be expected in real building operation: the signal-to-noise ratio (SNR) is expected to be high. The model performance is evaluated using the NRMSE (fitting), RMSE and the range of magnitude taken by the physical parameters (which should be related to the building physics to a reasonable degree). AIC (Akaike information criterion) and BIC (Bayesian information criterion) are used as complementary performance criteria to judge if the model is over-fitting.

Knowledge-based models are first analysed. The fitting of the 1st order model is relatively low: the NRMSE fitting is 58% for the training dataset while the fitting decreases to only 23% for the validation dataset. This implies that only one state is not enough to describe the thermal dynamics of this building. The 2nd order model has a new state related to the building envelope which can significantly improve the model prediction performance compared to the 1st order model. This is confirmed by the results reported in Table 2. The fitting of the 2nd order model 2Cs increases significantly to 81% for the training dataset and 79% for the validation dataset, RMSE values confirms this trend with decreasing values (from 0.5502 to 0.2489 in the training dataset). The 2nd order model 2C has one additional resistance (R_{ia}) compared to the model 2Cs. R_{ia} represents the heat losses from infiltrations and heat conduction through components of the building envelope with negligible thermal mass (such as windows or external doors of the building). However, results show that the value of $1/R_{ia}$ is zero so that the model collapses into the 2Cs models (with parameters being exactly the same). The AIC and BIC values of 2C are slightly higher than the 2Cs. The ZEB Living Lab is a super-insulated building envelope with limited infiltrations. It was therefore anticipated that the contribution of infiltrations should be negligible. However, the building has a large amount of glazing. An infinite R_{ia} was therefore unexpected based on prior physical knowledge. In conclusion, for this test case, the resistance R_{ia} is not necessary for the 2nd order model. Based on the simulation performance and the value of the parameters, the model 2Cs could be a reliable control model for the ZEB Living Lab. Comparing the 2Cs model for 5- and 15-minutes time intervals, it shows very similar physical parameters and simulation performance. The 2nd order black-box model 2B has an 83% fit on training data and 88% on validation data. It is thus the best performing 2nd order model.

In order to investigate whether the 2nd order model could be further improved, a new state corresponding to the heater is introduced in the grey-box model. The physical reason for adding this additional state is to compensate for the potential time delay related to the thermal dynamics of the electric heater. Four 3rd order models are tested in this paper. Model 3Cs shows a good fitting of 81% for the training dataset (with a RMSE value of 0.248) while the AIC and BIC values are lower than for the 2Cs model. However, the heat capacity of the interior (C_i) is extremely low while the heat capacity of the heater (C_h) is estimated to be 1.496 kWh/K, which is too high for an electric radiator. As the value of these parameters has limited physical meaning, the model 3Cs is discarded. The fitting of model 3C is low compared to the others. Its AIC and BIC values are also much higher so that this model is also discarded. As for 3Cs, model 3Csd has a relatively good fitting of 79% on the training dataset but the values for the parameters related to the building envelope and heater are far from reasonable. This model is also rejected. Model 3Cd has a fit of 81% and an RMSE value of 0.253 on the training data. However, the fit for the validation dataset is 70%, which is not as good as the 2nd order model 2Cs. The parameter values of model 3Cd are within a reasonable range. However, the value of the AIC and BIC criteria increases noticeably. Therefore, the model 3Cd could also be kept for further investigations. Nevertheless, when analyzing results for the 15-minutes time interval, the values of the heat capacitances completely change. The parameters of model 3Cd vary significantly with the time step which can be considered as a lack of reliability. The overall conclusion regarding 3rd order models is that none of them are completely satisfactory. Two possible reasons are that the heat capacitance (C_h) was probably not required for the electric radiator and the increasing the number of parameters leads the model to be over-fitting. The 3rd order black-box model has a fit of 88% on the validation data which is equivalent to the 2nd order model (2B). The 2B model is therefore the appropriate order for a linear model of this building based on the current dataset.

Secondly, the performance of the two standard models is investigated. The 1st order EN 13790 model has much better fit compared to the knowledge-based 1st order model: the NRMSE fitting can reach 71% for the training dataset but the fitting drops to 37% for the validation dataset. Accordingly, the RMSE value increases drastically to 1.509 for the validation dataset. This

confirms the previous conclusion that one state is not enough to describe the thermal dynamics of this building. From the Figure 5, it is very clear that the EN 13790 model can predict the general trend of the indoor air temperature. However, there are obvious excessive fluctuations in the indoor temperature prediction. This can be easily explained. In the EN 13790 model, the heat emitted by the radiator (P_h) is directly injected in the node T_i while no capacitance is allocated to this node. Therefore, the indoor air will immediately respond to the heat injection of the electric heater (P_h), without delay. It again proves that only one capacitance is not enough for capturing all the dynamics of the building. The conclusion regarding EN 13790 is that it could be a good candidate for a generic model but it needs to be adapted to capture the faster thermal dynamics of the air, furniture and the first centimeters of the walls. For instance, an extension of the EN13790 model to a 5R2C model has been recently proposed (Hedegaard, Kristensen, Pedersen, Brun, & Petersen, 2019) showing much better prediction performance compared to original EN13790.

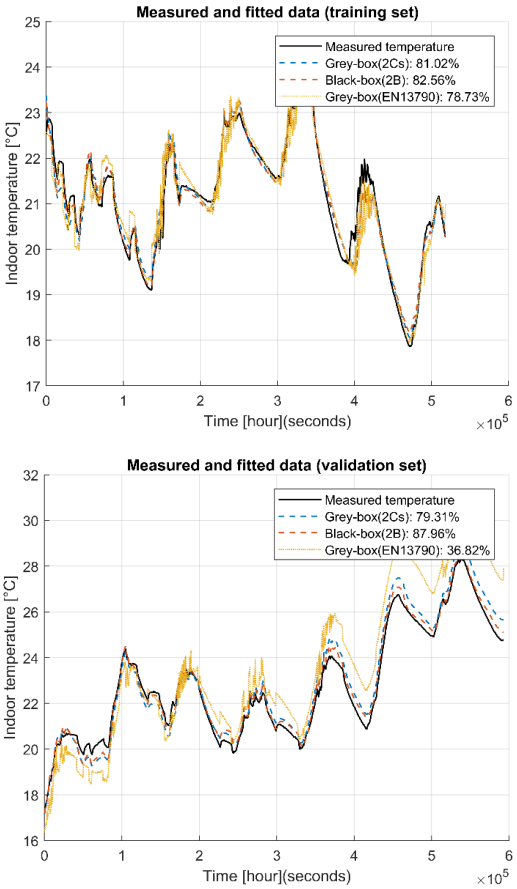

Figure 5: Comparison of the simulation performance of the most representative models

The 2nd order model VDI 6007 has decent fitting results (i.e. 71% for training and 81% for validation). Nevertheless, the values of the two heat capacitances and the overall UA-values are extremely small. These parameters do not have physical meaning. In conclusion, the VDI 6007 structure contains many physical phenomena but is too complicated to be correctly identified only using indoor air temperature measurements. This is confirmed by the high AIC and BIC values evaluated for this model. To be a potential candidate for a generic model structure, the number of parameters needs to be decreased to increase the identifiability of the model (Hedegaard & Petersen, 2017). Alternatively, additional measurements could be made inside the building in order to make the model identifiable (such as wall surface temperature and/or heat flux) (G. Reynders, Diriken, & Saelens, 2014). However, it is here assumed that these measurements will not be made available for all existing residential buildings.

Conclusion and future work

This paper investigates the performance of grey-box models based on a physical knowledge of the building to grey-box models using a generic model structure (based on the building standards EN 13790 and VDI 6007) as well as black-box models. Their performance is evaluated on the long-term prediction of the thermal dynamics, here using a single-family house as a test case (the ZEB Living Lab). The model identification is based on the measurement of the indoor air temperature resulting from the space heating using an electric radiator controlled by a PRBS. The building was unoccupied during experiments.

For knowledge-based grey-box models, results show that the 2nd order model has reasonable parameter estimates and the prediction error is small (within the range of +/- 1°C). The prediction performance varies significantly between the investigated 3rd order models. However, in all cases, the estimated parameters do not have reasonable values. In addition, none of the 3rd order models investigated were able to significantly improve the prediction performance of the 2nd order model. Therefore, the 2nd order model is considered as a good candidate for this test case.

Regarding grey-box models based on standards, results show that the 1st order EN 13790 model is able to follow the general evolution of the indoor temperature and provides meaningful values of the parameters. However, the simulated temperature has significantly higher fluctuations directly corresponding to the start and stop cycles of the electric radiator. As recently proposed by Hedegaard et al., the EN 13790 is a potential candidate for a generic model structure but it should be adapted by adding a state corresponding to the fast dynamics of the building (< 1h). The 2nd order grey-box model based on VDI 6007 has good prediction performance, but it generates parameter estimates that cannot be explained from a physical point of view. The number of parameters of this model needs to be reduced to make it identifiable. In future work, it should be investigated whether this

simplification can be done without impairing significantly the model universality.

The 2nd order black-box model shows a good performance equivalent to the 2nd order grey-box model. Nevertheless, with black-box models, the physical meaning of the states is unknown. However, the estimate of the overall heat transfer coefficient is similar between the 2nd order black-box and the best grey-box models. It is worth mentioning that these investigations were performed with high-quality input-output data. In addition, experiments corresponding to the validation data set took place a few days after the training period. The relative performance of black-box and grey-box models could be different if these experimental conditions were not fulfilled. This research nonetheless suggests that black-box models deserve to be investigated in detail to create control-oriented model with a limited knowledge of the building and limited amount of time.

Acknowledgement

The authors would like to acknowledge the valuable input from Pierre Vogler-Finck and John Clauß. They also would like to thank the Norwegian Research Centre on Zero Emission Neighbourhoods in Smart Cities (ZEN) and its industry partners.

References

Andriamamonjy, A., Klein, R., & Saelens, D. (2019). Energy & Buildings Automated grey box model implementation using BIM and Modelica. *Energy & Buildings*, *188–189*, 209–225. https://doi.org/10.1016/j.enbuild.2019.01.046

Atam, E., & Helsen, L. (2016). Control-Oriented Thermal Modeling of Multizone Buildings: Methods and Issues: Intelligent Control of a Building System. *IEEE Control Systems*, *36*(3), 86–111. https://doi.org/10.1109/MCS.2016.2535913

Bacher, P., & Madsen, H. (2011). Identifying suitable models for the heat dynamics of buildings. *Energy and Buildings*, *43*(7), 1511–1522. https://doi.org/10.1016/j.enbuild.2011.02.005

Bruno, R., Pizzuti, G., & Arcuri, N. (2016). The prediction of thermal loads in building by means of the EN ISO 13790 dynamic model: A comparison with TRNSYS. *Energy Procedia*, *101*, 192–199.

Dahl Knudsen, M., & Petersen, S. (2016). Demand response potential of model predictive control of space heating based on price and carbon dioxide intensity signals. *Energy and Buildings*, *125*, 196–204. https://doi.org/10.1016/j.enbuild.2016.04.053

Hedegaard, R. E., Kristensen, M. H., Pedersen, T. H., Brun, A., & Petersen, S. (2019). Bottom-up modelling methodology for urban-scale analysis of residential space heating demand response. *Applied Energy*, *242*, 181–204.

Hedegaard, R. E., & Petersen, S. (2017). ScienceDirect ScienceDirect ScienceDirect Evaluation of Grey-Box Model Parameter Estimates Intended for The 15th International Symposium on District Heating and Cooling Thermal Characterization of Buildings Assessing the feasibility of using the heat temperature function for a long-term district heat demand forecast. *Energy Procedia*, *132*, 982–987. https://doi.org/10.1016/j.egypro.2017.09.692

Le Dréau, J., & Heiselberg, P. (2016). Energy flexibility of residential buildings using short term heat storage in the thermal mass. *Energy*, *111*, 991–1002. https://doi.org/10.1016/j.energy.2016.05.076

Ljung, L. (2011). System identification toolbox. *The Matlab User's Guide*, *1*, 237.

Reynders, G. (2015). Quantifying the impact of building design on the potential of structural strorage for active demand response in residential buildings, (September), 266. https://doi.org/10.13140/RG.2.1.3630.2805

Reynders, G., Diriken, J., & Saelens, D. (2014). Quality of grey-box models and identified parameters as function of the accuracy of input and observation signals. *Energy and Buildings*, *82*. https://doi.org/10.1016/j.enbuild.2014.07.025

Transition to Sustainable Buildings. (2013). https://doi.org/10.1787/9789264202955-en

Vivian, J., Zarrella, A., Emmi, G., & De Carli, M. (2017). An evaluation of the suitability of lumped-capacitance models in calculating energy needs and thermal behaviour of buildings. *Energy and Buildings*, *150*, 447–465. https://doi.org/10.1016/j.enbuild.2017.06.021

Vogler-Finck, P., Clauß, J., & Georges, L. (2017, October). A dataset to support dynamical modelling of the thermal dynamics of a super-insulated building. https://doi.org/10.5281/ZENODO.1034820

Vogler-Finck, P. J. C., Clauß, J., Georges, L., Sartori, I., & Wisniewski, R. (2018). Inverse Model Identification of the Thermal Dynamics of a Norwegian Zero Emission House. In *Cold Climate HVAC Conference* (pp. 533–543). Springer.

You, S., Jin, L., Hu, J., Zong, Y., & Bindner, H. W. (2015). The Danish perspective of energy internet: From service-oriented flexibility trading to integrated design, planning and operation of multiple cross-sectoral energy systems. *Zhongguo Dianji Gongcheng Xuebao*, *35*(14), 3470–3481.

Zong, Y., Böning, G. M., Santos, R. M., You, S., Hu, J., & Han, X. (2017). Challenges of implementing economic model predictive control strategy for buildings interacting with smart energy systems. *Applied Thermal Engineering*, *114*, 1476–1486. https://doi.org/10.1016/j.applthermaleng.2016.11.141

Table 2: Results of the grey- and black-box identification using 5 minutes time interval.

Model	1C	2Cs	2C	3Cs	3C	3Csd	3Cd	EN13790	VDI6007	2B
C_e	-	8.032	8.032	8.224	0.303	10.000	7.638	8.451	-	-
C_i	7.115	1.366	1.366	$1.24*10^{-7}$	$1.48*10^{-7}$	1.781	2.158	-	-	-
C_h	-	-	-	1.496	6.445	4.822	0.028	-	-	-
C_{e1}	-	-	-	-	-	-	-	-	$1.77*10^{-5}$	-
C_{e2}	-	-	-	-	-	-	-	-	$3.49*10^{-5}$	-
A_{we}	-	3.158	3.158	3.185	3.815	11.806	-	-	1.928	-
A_{wi}	8.375	4.163	4.163	4.071	5.955	0.186	4.923	9.152	1.656	-
UA_{tot}	0.125	0.115	0.115	0.114	0.117	0.186	0.102	0.125	$5.17*10^{-7}$	0.114
$RMSE_t$	0.55	0.25	0.25	0.25	0.40	0.27	0.25	0.36	0.28	0.23
$RMSE_v$	1.84	0.49	0.49	0.40	1.33	1.07	0.70	1.51	0.47	0.29
$NRMSE_t$	58%	81%	81%	81%	69%	79%	81%	73%	79%	83%
$NRMSE_v$	23%	79%	79%	83%	44%	55%	71%	37%	81%	88%
AIC	$2.847*10^3$	113.4166	115.4166	102.8692	$1.775*10^3$	450.2877	177.9489	$1.371*10^3$	522.9770	-
BIC	$2.869*10^3$	157.0543	164.5091	162.8711	$1.841*10^3$	504.8349	237.9508	$1.414*10^3$	599.3430	-

t: training data
v: validation data

Table 3: Results of the grey- and black-box identification using 15 minutes time interval.

Model	1C	2Cs	2C	3Cs	3C	3Csd	3Cd	EN13790	VDI6007	2B
C_e	-	8.038	8.038	8.154	3.481	10.000	7.802	8.339	-	-
C_i	7.122	1.346	1.346	$2.87*10^{-5}$	$4.88*10^{-8}$	1.764	$2.04*10^{-7}$	-	-	-
C_h	-	-	-	1.5978	5.1958	4.8375	2.2863	-	-	-
C_{e1}	-	-	-	-	-	-	-	-	$1.55*10^{-5}$	-
C_{e2}	-	-	-	-	-	-	-	-	$2.38*10^{-5}$	-
A_{we}	-	3.213	3.213	2.776	14.380	-	-	-	2.042	-
A_{wi}	8.394	4.152	4.152	4.197	1.617	11.780	4.893	8.872	1.511	-
UA_{tot}	0.125	0.115	0.115	0.113	0.108	0.186	0.102	0.124	$3.99*10^{-7}$	0.114
$RMSE_t$	0.55	0.25	0.25	0.24	0.37	0.27	0.25	0.39	0.28	0.23
$RMSE_v$	1.84	0.51	0.51	0.31	0.79	1.06	0.73	1.45	0.43	0.29
$NRMSE_t$	58%	81%	81%	81%	72%	79%	81%	70%	79%	83%
$NRMSE_v$	23%	79%	79%	87%	67%	56%	70%	39%	82%	88%
AIC	953.9709	51.3763	53.3763	34.8207	519.5818	163.0977	41.9178	598.7925	201.7279	-
BIC	971.3953	86.2252	92.5813	82.7379	571.8551	206.6588	93.8350	633.6413	262.7134	-

t: training data
v: validation data

PAPER 2

Yu X, Georges L. Influence of Data Pre-Processing Techniques and Data Quality for Low-Order Stochastic Grey-Box Models of Residential Buildings. *International Conference Organised by IBPSA-Nordic*, 13th–14th October 2020, Oslo, Norway. BuildSIM-Nordic 2020 (BSN2020). Selected papers. SINTEF Academic Press.

RESEARCH PUBLICATIONS

SINTEF
PROCEEDINGS
5

International Conference Organised by IBPSA-Nordic, 13th–14th October 2020, OsloMet

BuildSIM-Nordic 2020

Selected papers

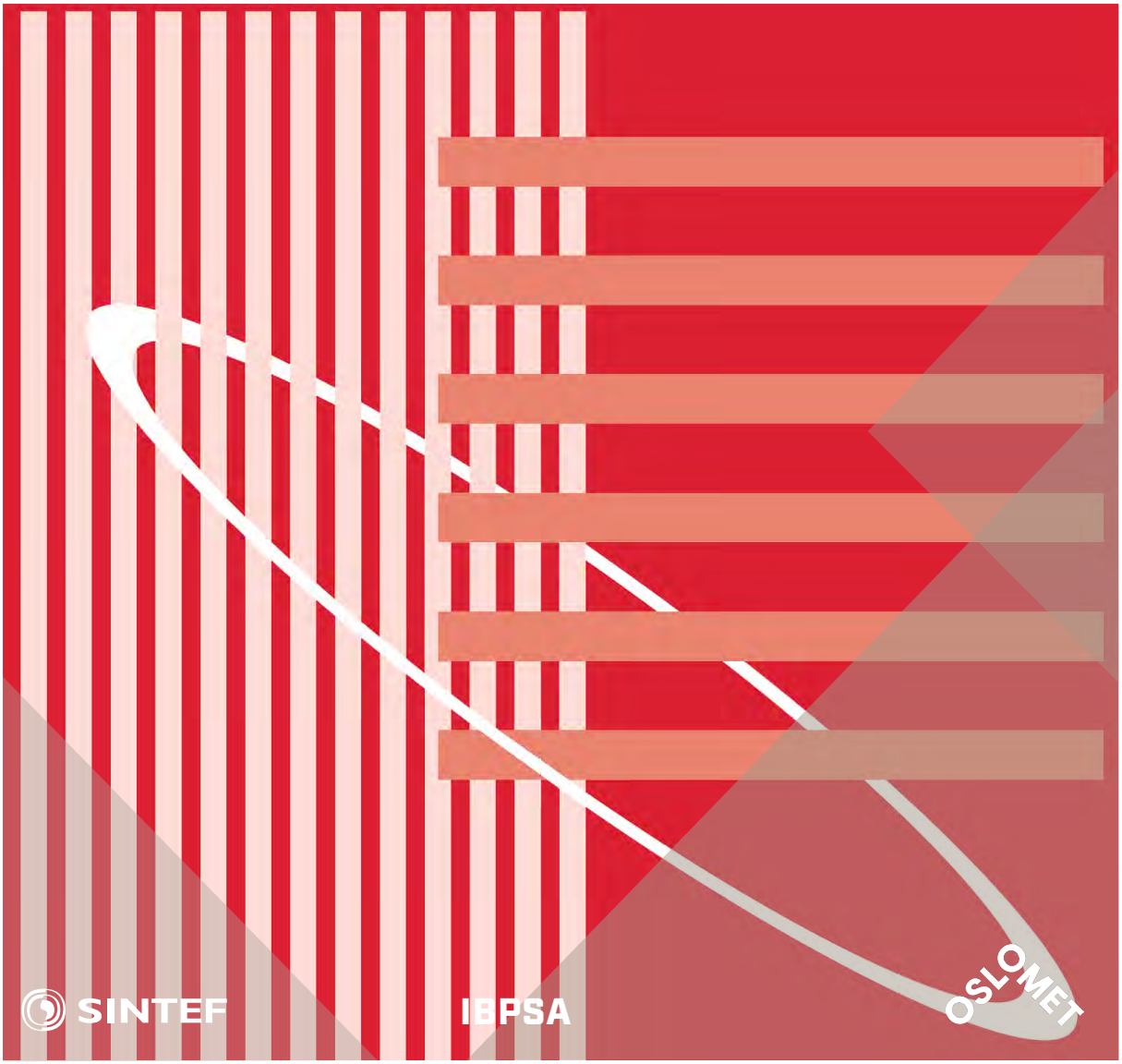

SINTEF Proceedings

Editors:
Laurent Georges, Matthias Haase, Vojislav Novakovic and Peter G. Schild

BuildSIM-Nordic 2020

Selected papers

International Conference Organised by IBPSA-Nordic,
13th–14th October 2020, OsloMet

SINTEF Academic Press

SINTEF Proceedings no 5
Editors:
Laurent Georges, Matthias Haase, Vojislav Novakovic and Peter G. Schild
BuildSIM-Nordic 2020
Selected papers
International Conference Organised by IBPSA-Nordic,
13th–14th October 2020, OsloMet

Keywords:
Building acoustics, Building Information Modelling (BIM), Building physics, CFD and air flow, Commissioning and control, Daylighting and lighting, Developments in simulation, Education in building performance simulation, Energy storage, Heating, Ventilation and Air Conditioning (HVAC), Human behavior in simulation, Indoor Environmental Quality (IEQ), New software developments, Optimization, Simulation at urban scale, Simulation to support regulations, Simulation vs reality, Solar energy systems, Validation, calibration and uncertainty, Weather data & Climate adaptation, Fenestration (windows & shading), Zero Energy Buildings (ZEB), Emissions and Life Cycle Analysis

Cover illustration: IBPSA-logo

ISSN 2387-4295 (online)
ISBN 978-82-536-1679-7 (pdf)

SINTEF Academic Press
Address: Børrestuveien 3
PO Box 124 Blindern
N-0314 OSLO
Tel: +47 40 00 51 00

www.sintef.no/community
www.sintefbok.no

SINTEF Proceedings
SINTEF Proceedings is a serial publication for peer-reviewed conference proceedings on a variety of scientific topics.
The processes of peer-reviewing of papers published in SINTEF Proceedings are administered by the conference organizers and proceedings editors. Detailed procedures will vary according to custom and practice in each scientific community.

Influence of Data Pre-Processing Techniques and Data Quality for Low-Order Stochastic Grey-Box Models of Residential Buildings

Xingji Yu[1]*, Laurent Georges[1]
[1]Department of Energy and Process Engineering, Faculty of Engineering, NTNU - Norwegian University of Science and Technology, Kolbjørn Hejes vei 1a, 7034 Trondheim, Norway
corresponding author: xingji.yu@ntnu.no

Abstract

Model Predictive Control (MPC) has proved to be a key technology to activate the energy flexibility of buildings. A reliable control-based model should be developed to implement an efficient optimal control. Grey-box models, as a combination of physical knowledge and experiment data, have been widely used in the literature. However, in the identification process of grey-box models, many factors affect the results. This paper uses data from virtual experiments in IDA-ICE to investigate the influence of the optimization methods, the filtering methods, the training dataset and the sampling time interval on stochastic grey-box models. It shows that global optimization increases the chance to avoid a local minimum. Pre-filtering methods have a small influence on the model quality. Larger data sampling time will cause the identified parameters to become non-physical. However, the simulation performance of the model is kept almost unchanged.

Introduction

The share of Renewable Energy Sources (RES) is increasing constantly in today's energy system. The volatile property of RES generation has brought notable challenges to the grid. Thus, flexible loads become a requirement to further increase the penetration of RES. Demand response (DR) is considered to be one of the key components to provide flexibility in smart grid [1]. DR can be described as the interaction and responsiveness of the end-use customer to a penalty signal (e.g. price signal, CO_2 intensity factor for electricity) [2]. In addition, due to the continuous increase of the electric consumption of households and the introduction of electric vehicles, DR can be used for peak-shaving in order to avoid congestion in the distribution grid [3]. Consequently, peak-shaving would enable to minimize or postpone the reinforcement of these grids.

About 25% of the final energy consumption is consumed by buildings and more than 65% of this energy is used for heating and cooling demand in European households, which makes HVAC systems a promising candidate for demand response [4]. In Nordic countries, the space-heating season is long and cold, the energy consumption is mainly related to space-heating. The thermal mass of buildings can be a significant heat storage [5,6]. When using the thermal mass to perform DR, the heating demand will be shifted optimally, while the thermal comfort constraints can still be respected [7]. The targets of DR in buildings are usually the reduction of peak load, lower CO_2 emissions, maximize the use of RES or minimize energy cost [8]. Model predictive control (MPC) is often considered as an important technique to perform demand response (DR) using the thermal mass of the building. The logic of MPC in a building is that the control agent (computers, built-in intelligent devices, etc.) takes the predictions of future disturbances (weather data, power generation from RES, etc.) and the system constraints into an optimization problem and generate an optimal control decision at each control time step. Thus, it is important that the dynamic model embedded in the MPC controller has decent prediction accuracy. A poor-quality model could lead to suboptimal performance, such as increased energy costs, violation of the thermal comfort or even be counterproductive for the electricity grid. In addition, the model identification should also be low-cost to make the investment costs of MPC sufficiently low.

Control models for MPC controller can be divided into three main categories, namely white-, black- and grey-box models. White-box models are based on physical laws, which require detailed knowledge of the system, the underlying physical process and parameters. In practice, it is too complicated and time-consuming to access all the information and to keep it updated during the building's operational lifetime. This type of model usually has higher accuracy but is mathematically more complex, which may cause challenges for the MPC optimizer. This fact makes this kind of model sometimes too complex for MPC [4]. Black-box models are pure data-driven methods considering only measured inputs and outputs from the system. The physical knowledge of the system is not needed. However, this method requires a larger amount of data for training and the precision of black-box models is significantly influenced by the data quality. Black-box models are known to have lower generalization (extrapolation) properties. Grey-box modelling is a combination of physical knowledge and statistical methods. Since the grey-box models have a model structure based on physical knowledge, grey-box models usually require less experimental data compared to black-box models and are hopefully less sensitive to data quality [9].

A common way to create Linear Time Invariant (LTI) grey-box models for buildings is to use lumped capacitance models (RC models). The thermal conditions of the building are expressed with an electrical circuit analogy [10]. This paper mainly focuses on five specific

factors influencing the grey-box modelling of the building thermal dynamics. The first aspect (Q1) is data preprocessing. Few publications are addressing the importance of data preprocessing for building thermal dynamics. The topic is discussed in other disciplines, like [11] in process engineering, but not in building science. The second aspect (Q2) is the convexity of the optimization problem. Except for models with an extremely simple structure like first-order models, the optimization problem for identifying parameters of the grey-box models is not convex. Therefore, grey-box models are very sensitive to initial guess and the search method (i.e. the optimizer). For instance, Generic Algorithm (GA) combined with gradient-based optimization is used in the paper [12] to avoid the identification results ending up in a local minimum. The selection of the optimization algorithm to avoid the local minimum will be discussed in this paper. The third aspect (Q3) is how data quality (e.g. level of excitation signal and amount of data) influences the identification results. It is often said that the temperature of the ventilation extract air is a good image of the average building temperature and is reliable to identify a grey-box model, see e.g. [13]. Thus, the fourth aspect (Q4) is about the selection of the representative indoor temperature for system identification. The last aspect (Q5) considers the sensitivity of the grey-box parameters to the selection of the data sampling time (Ts). The theoretical analysis of Ljung showed that the continuous grey-box models are sensitive to the selection of the sampling time that should be taken lower than the shortest time of the system to be investigated [14]. This analysis needs to be repeated for building applications. All the research in this paper is performed using stochastic grey-box models in innovation form using the disturbance matrix K and the MATLAB identification toolbox.

Methodology

Dataset and virtual experiments

IDA ICE is a detailed dynamic simulation tool for studying thermal indoor climate as well as the energy consumption of buildings. A two-storey detached house with a heated floor area of 160 m² is used as virtual experiment for our case study. The three-dimensional geometry of the building from IDA ICE is shown in Fig. 1. The building is constructed in wood (i.e. lightweight construction) and complies with the requirement of the Norwegian passive house standard, NS 3700 [15]. The detailed description of the building construction can be found in [16]. The building is equipped with balanced mechanical ventilation with a heat recovery unit. The heat exchanger is here modelled using a constant effectiveness of 85% without bypass, like a plate heat exchanger.

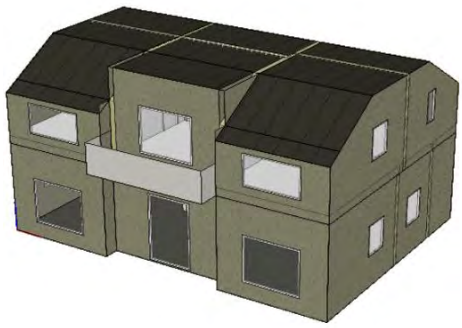

Figure 1: 3D geometry of the building model in IDA ICE (showing the southwest façade).

The building is simulated with a multi-zone model with open internal doors. IDA ICE has an embedded ventilation network model which accounts for the large bidirectional airflow through open doorways. This large convective heat transfer leads to relatively uniform air temperatures in the entire building. However, bathrooms are kept separated with closed doors. Following the cascade ventilation principle, ventilation air is supplied in living areas and bedrooms and mostly extracted in wet rooms (i.e. bathrooms and the laundry). The space-heating was performed using an electrical heater in this case study. Direct electricity is a most common way to heat small residential buildings in Norway [17] . The hourly profiles of internal heat gains for artificial lighting, electric appliances and occupancy is taken from a Norwegian standard [18].

Two types of excitation signals are used to activate the thermal mass of the building in order to collect data for system identification. The first signal is called Pseudo-Random Binary Signal (PRBS) with a minimum and maximum step of 10 and 80 min, respectively. The reason for choosing a PRBS signal is that it approximates white noise, which can activate the dynamic system in a large spectrum of frequencies [19,20]. The other excitation signal is an intermittent set-point, which means that the temperature set-point changes between daytime and night-time (i.e. night setback). In this case, an on-off control is implemented in IDA ICE to track the temperature set-point, like in real direct electric radiators. Both excitation signals are applied to an electric radiator placed in each zone, except for bathrooms as these rooms are relatively small and typically heated by floor heating (with significant thermal inertia). Five different periods with specific weather conditions are implemented in the virtual experiments, as described in the table below.

IDA ICE uses a time-varying time-step so that the data is not generated at constant time intervals. The data output from IDA ICE is therefore interpolated on a uniform time discretization of 2.5 min (thus well shorter than the 10 min time interval of the PRBS).

Table 1: Weather condition of four PRBS experiments.

Type	Outdoor Temperature	Sky	Date	Duration
Very Cold	-10 °C	Clear sky	12/13 /2019	One week
Cold	0 °C	Overcast	12/24 /2019	One week
Cold	0 °C	Clear sky	3/23/ 2019	One week
Mild	5 °C	Overcast	11/23 /2019	One week

Grey-box model structure and identification

The main purpose of this paper is not to investigate the grey-box model structure. This topic is already discussed in previous works [21–23]. Only first-order (1R1C) and second-order (3R2C) grey-box models are considered in this paper with a single temperature node inside the building (i.e. mono-zone model). Preliminary tests have shown that a third-order model would be over-fitted for this test case. Higher-order models can cause over-parameterization more easily, which has been shown in the papers [23,24]. The structure of the two grey-box models follows a RC-formalism. The lumped resistance and capacitance as well as the physical interpretation of these parameters can be found in Figures 2 and 3 below. The free parameters of these grey-box models are calibrated using the IDA ICE data. The ventilation exhaust air temperature or the volume-averaged temperature can be selected to represent the measured interior node Ti and their respective model performance will be compared.

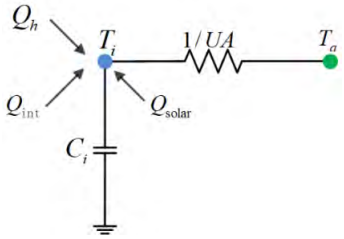

Figure 2: First-order model (1R1C)

T_i Temperature of interior heat capacity [°C].

T_a The outdoor (or ambient) temperature [°C].

C_i Heat capacity of the building [kWh/K].

R ($1/UA$) Overall heat resistance between the building and the ambient, including ventilation [K/kW].

Q_{int} Internal heat gain from artificial lighting, people and electric appliances [kW].

Q_{solar} Heat gain from solar radiation [kW].

Q_h Heat gain from the electric heater [kW].

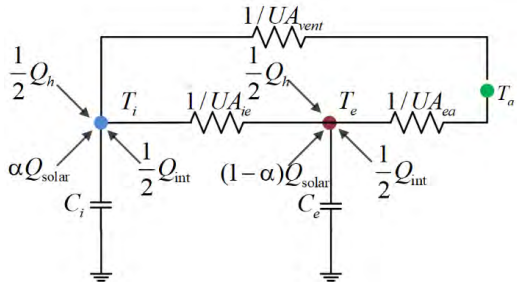

Figure 3: Second-order model (3R2C)

T_e Temperature of the building envelope [°C].

T_a The outdoor temperature [°C].

C_i Heat capacity of the building combining the thermal mass of the air, the furniture, internal walls and, potentially, the first centimetres of external walls [kWh/K].

C_e Heat capacity of the node Te [kWh/K].

R_{ie} ($1/UA_{ie}$) Heat resistance between the building envelope and the interior [K/kW].

R_{ea} ($1/UA_{ea}$) Heat resistance between the ambient and the building envelope [K/kW].

R_{vent} ($1/UA_{vent}$) Heat resistance between the ambient and the interior [K/kW].

α Fraction of solar gains to air node.

The internal gains and solar gains are computed exactly by IDA ICE. In this work, they are not identified and are introduced directly in the grey-box model. Consequently, in the 3R2C model, only the coefficient α to distribute the solar gains between the two temperature nodes needs to be identified regarding gains. In real application, gains are not known exactly. However, simplifying the problem enables to emphasize the specific research questions of the article.

The MATLAB identification toolbox is used for model identification. In grey-box models, the continuous time model is first discretized in order to identify the model parameters using discrete measurement data. The discretization assumes the input data to be piecewise constant during each time interval (i.e. zero-order hold). Regarding the optimization problem, the initialization value of the model parameters and their corresponding range (i.e. minimum and maximum values) should be defined. The optimizer will then iterate to find the parameters that minimize the Normalized Root Mean Square Error (NRMSE) of the one-step ahead prediction. Then, the toolbox covert the discrete time model back to continuous time:

$$\dot{x}(t) = \mathbf{A}\, x(t) + \mathbf{B}\, u(t) + \mathbf{K}\, e(t) \quad (1)$$

$$\dot{y}(t) = \mathbf{C}\, x(t) + e(t) \quad (2)$$

where x is the state vector and A, B and C are the system matrices. u is the input vector (T_a, Q_{solar}, Q_{int}, Q_h) and y is the output (indoor temperature, T_i). K is the disturbance

matrix of the innovation form (Kalman gain). It is a transformed representation from the general process [25].

Influence of the optimizer

In MATLAB, the function *greyest* identifying the model parameters has four different gradient-based iterative search methods, used in sequence. However, preliminary tests using the 3R2C model show a quick converge to a local minimum close to the initial estimate of the parameters. A similar behavior is also reported in the paper [12]. The authors used GA combined with gradient-based optimization to overcome the non-convexity of the optimization problem. Consequently, a global optimization algorithm has been implemented in this paper. Instead of the GA method, the first stage optimization uses particle swarm optimization (PSO) while the second stage uses the default *greyest* function to further polish the results. Each optimization method is able to identify the parameters' value and their corresponding variance. For each case, the optimizer giving the lowest NMRSE for the one-step ahead prediction is selected and provides the selected model parameters.

Pre-filtering methods

In real-life applications, it is difficult to guarantee that the measurement data will be sampled at a higher frequency (Ts) than the highest frequency of the system (here 10 min, imposed by the PRBS). For instance, the Advanced Metering System (AMS) in Norway has a typical time interval of 15 min [26]. It is important to investigate the influence of data pre-processing by low-level digital measurement devices before they log the data at an appropriate time interval. Temperature sensors can register data at a very high frequency (here 2.5 min). This data can be pre-processed before being sampled and logged at a longer time interval (Ts > 2.5 min). A low-pass discrete filter can first be applied, such as a moving average (MA) or a finite impulse response (FIR). Without this low-pass filter (i.e. direct sampling), the aliasing error may be high. With MA, the aliasing error is smaller but still present while the FIR (applied with a sufficient order) would lead to negligible aliasing. By comparing the performance of (MA + sampling), (FIR + sampling) and the direct sampling on the parameter identification, it is possible to understand the influence of aliasing. The low-pass filter is applied to all the input and output variables of the model. If the filter introduces a time delay (like MA), this delay is the same for all variables and will thus not affect the model. The situation would be more complex if the low-pass filter is only applied to a subset of the input or output variables.

Results

Influence of the optimizer (Q2)

Five datasets using the four PRBS signals and the intermittent on-off heating during the full heating season (FHS) are used to investigate the influence of the optimizer. The two optimization methods do not show much difference for the 1R1C model. In most cases, the two optimization methods converge to the same parameter values. However, the identified parameters from *greyest* function are not identical for the 3R2C model. This implies that the optimization is already non-convex from the second-order model, this conclusion is also confirmed in Arendt et al. [12]. The best optimizer leading to lowest NRMSE for the second-order model can be found in Table 2 (with different time intervals, excitation signals and filters). The figure shows that global optimization is selected for all cases no matter the time interval or filtering method.

Table 2: Best optimizer for the four PRBS and FHS experiments.

Sampling time	Type	Direct sampling	Averaging filter	FIR filter
2.5min	**PRBS1**	Global	Global	Global
	PRBS2	Global	Global	Global
	PRBS3	Global	Global	Global
	PRBS4	Global	Global	Global
	FHS	Global	Global	Global
15min	**PRBS1**	Global	Global	Global
	PRBS2	Global	Global	Global
	PRBS3	Global	Global	Global
	PRBS4	Global	Global	Global
	FHS	Global	Global	Global
30min	**PRBS1**	Global	Global	Global
	PRBS2	Global	Global	Global
	PRBS3	Global	Global	Global
	PRBS4	Global	Global	Global
	FHS	Global	Global	Global
60min	**PRBS1**	Global	Global	Global
	PRBS2	Global	Global	Global
	PRBS3	Global	Global	Global
	PRBS4	Global	Global	Global
	FHS	Global	Global	Global

Since the datasets contain different excitation signals and weather conditions, it is a strong proof that global optimization can give more robust and higher-quality results when the optimization problem is not convex. In other words, the global optimization algorithm can increase the chance to avoid a local minimum in the grey-box identification process.

Influence of the selection of input (Q4)

While the one-step prediction is used to train the models, the simulation performance is more relevant for MPC applications. Therefore, the simulation NRMSE fitting is mainly used as the performance index in this subsection. Table 3 and Table 4 compare the cross-validation simulation performance using the volume-averaged air temperature and the extracted air as representative indoor temperature respectively. Only datasets trained with the original 2.5 min sampling time is used to avoid the influence of other factors (e.g. dataset, discretization error and pre-filtering method).

Table 3:Simulation NRMSE fitting using the volume-averaged air temperature (Ts = 2.5min)

Training dataset	Validation dataset and simulation NRMSE fitting				
	PRBS1	PRBS2	PRBS3	PRBS4	FHS
PRBS1	84.25%	74.96%	0.53%	72.34%	-17.72%
PRBS2	77.10%	74.16%	24.25%	60.58%	9.49%
PRBS3	39.36%	34.03%	64.20%	14.41%	33.24%
PRBS4	82.19%	69.36%	-17.69%	78.45%	-42.34%
FHS	45.95%	41.11%	69.06%	20.59%	39.17%

Table 4:Simulation NRMSE fitting using the extracted ventilation air temperature (Ts = 2.5 min)

Training dataset	Validation dataset and simulation NRMSE fitting				
	PRBS1	PRBS2	PRBS3	PRBS4	FHS
PRBS1	90.21%	70.83%	16.97%	79.05%	-94.10%
PRBS2	73.51%	81.86%	29.88%	71.77%	-74.10%
PRBS3	30.44%	43.28%	68.02%	25.09%	-15.82%
PRBS4	78.70%	73.55%	-10.68%	83.63%	-155.32%
FHS	78.11%	71.50%	52.43%	64.46%	25.33%

In general, simulation performance with the two different representative temperatures are following the same trend. The simulation NRMSE fitting is higher for the original training dataset and lower for the validation datasets. The model identified from the intermittent set-point and on-off control dataset during the FHS presents higher performance on the validation datasets: the validation fitting is acceptable at each period never completely collapsing. Models trained from the PRBS excitation signals of one week have a good simulation NRMSE fitting on their own training data but largely fail in some cross-validation datasets. Simulation results from extracted air temperature show a slightly higher simulation NRMSE fitting value for the original training dataset. However, models trained with extracted air temperature show worse simulation NRMSE fitting compared with volume-averaged temperature when they are trained and validated with the FHS dataset (values in red in Table 3. Thus, the volume-averaged air temperature is a more balanced choice of representative indoor temperature. The exhaust air temperature is not always the best option to train the model and this conclusion could be even more severe if all the internal doors inside the building were closed.

Influence of pre-filtering methods and data-quality (Q1, Q3 and Q5)

Figures 4 to 6 show three key identified parameters for the second-order model. For the value of the total heat transfer coefficient in Figure 4, the estimated value from a step-response of the heating power applied in IDA-ICE is about 85 W/K. Figure 4 shows that most of the results are close to the estimation from IDA-ICE. When the Ts is increased to 60 min, some values using the FIR filter or

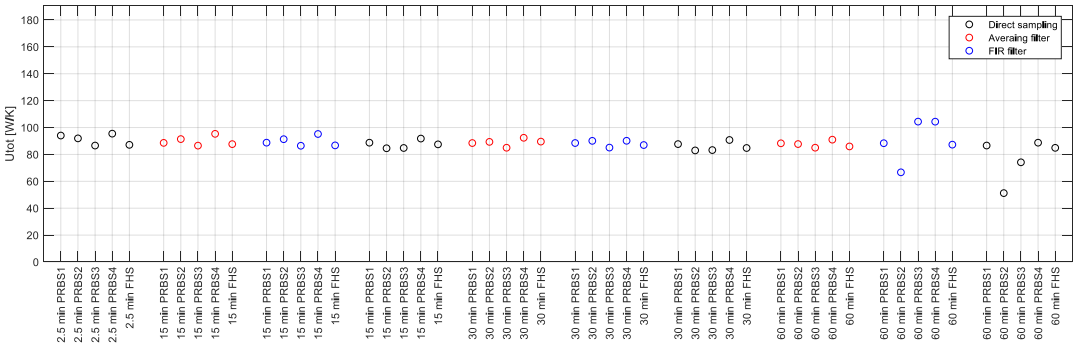

Figure 4: Identified Utot of the 3R2C model (variance is not given as Utot combines the 3R)

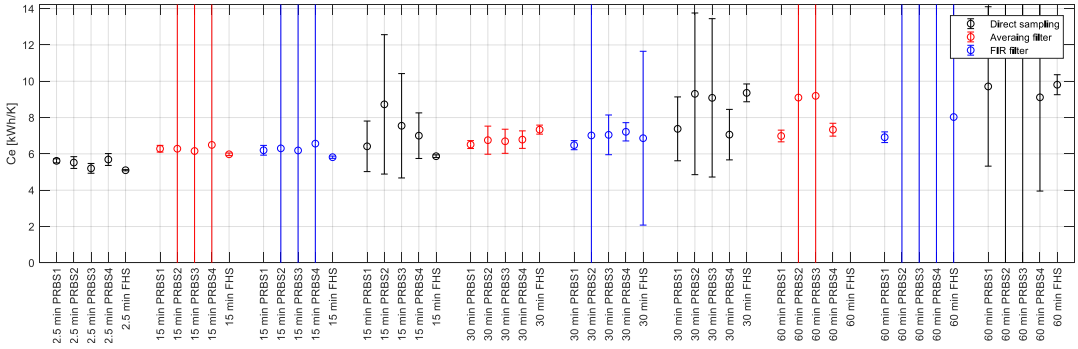

Figure 5: Identified Ce of the 3R2C model

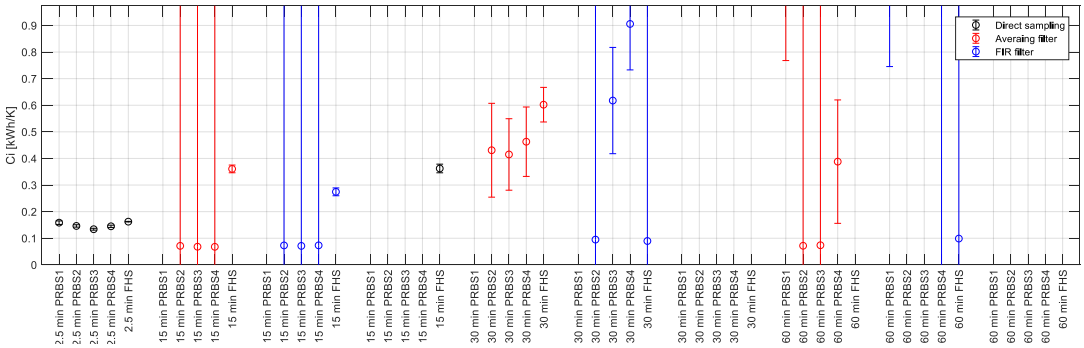

Figure 6: Identified Ci of the 3R2C model

direct sampling starts to depart from the estimated value. Figure 5 shows the value and variance of the heat capacitance of the external wall C_e. Regarding the value of C_e, direct sampling has the tendency to generate a larger capacitance value with increasing sampling time. Some values are not visible because completely outside the y-axis limits of the graph. The same problem is even more pronounced for the value of the heat capacitance C_i in Figure 6. The value of C_i diverges quickly when Ts is increased for every pre-filtering method. Although it shows that the low-pass filter, especially the moving-average, can improve the results of identified value for these key parameters. Regarding the variance of the parameters, it is very limited for the sampling time of 2.5 min. Like the parameter value, the parameter variance increases with the sampling time. However, this increase of the variance is less systematic and regular than for the parameter value.

Regarding the influence of filters, FIR does not show a significant advantage over the moving-average for the identification even though the FIR filter is theoretically better. On the contrary, FIR filter sometimes has worse results than the moving-average filter when Ts is large.

Another important conclusion can be found. The FHS dataset has more stable identified parameters (both values and variance) than the PRBS datasets. This shows that a dataset generated from a normal building operation over a long time period with comfortable indoor temperatures (and thus possible occupancy) can give equivalent or even better parameter identification than a short training period using a better excitation signal (here PRBS) but leading to uncomfortable indoor temperatures, probably preventing occupancy.

The simulation performance is shown in Figure 7 taking the FHS period to train the model. For the sake of the conciseness, the other cases using the other training

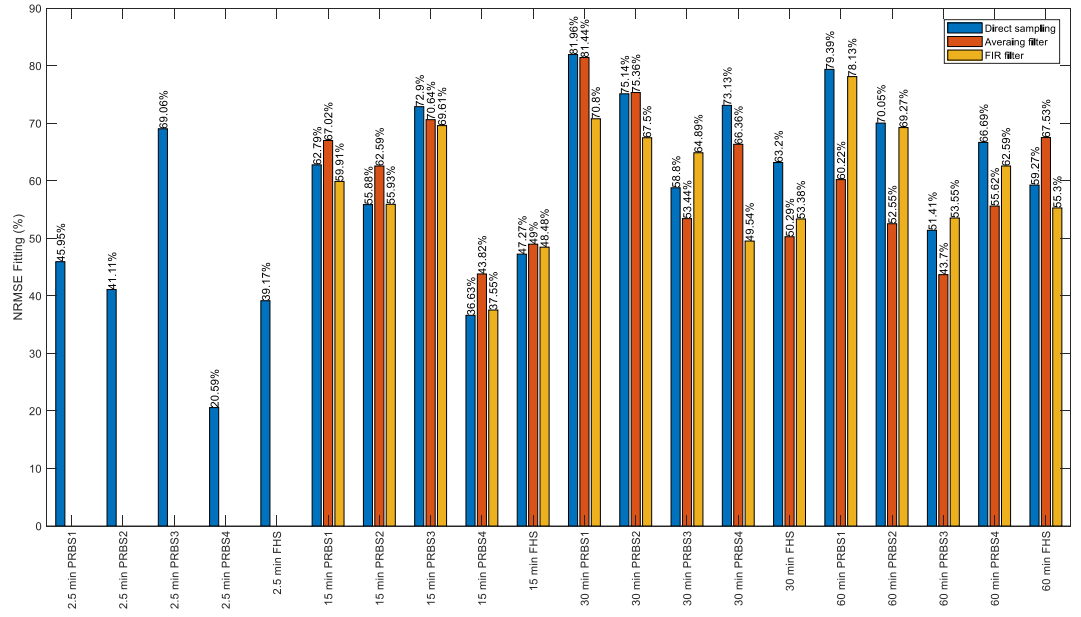

Figure 7: Simulation performance of the models trained using the FHS dataset.

periods are not reported but they give similar conclusions. Unlike, the parameter value and variance, it is clear that the increase of the sampling time (Ts) does not degrade the simulation performance. In some cases, even though the identified parameters have non-physical value or variance, this does not alter the simulation performance. The simulation performance is the main property of interest for the application of MPC. This demonstrates that training of a model for MPC application or characterization of the building thermal properties does not require the same quality of the input data. For instance, the pre-filtering methods (MA, FIR or direct sampling) do not affect much the simulation performance as well. It is difficult to rank the three pre-filtering methods as their relative performance changes between the validation cases.

Conclusions

The sampling time (Ts) of data should be limited to guarantee the physical meaning of the parameter value and variance. Larger Ts can result in non-physical parameter values and variance (Q5). If a small Ts is not applicable, the data should be low-pass filtered before being sampled even though this measure alone does not guarantee that the parameters will be physical for all Ts. This answers the first question in the introduction (Q1). More than the data pre-filtering, the selection of the right sampling time is the dominating factor to guarantee the physical meaning of the parameters. Nevertheless, sampling time and pre-filtering do not seem to affect the simulation performance of the identified models, which is a positive conclusion for MPC applications.

Even if a grey-box model has good simulation performance, having meaningful physical parameters in the model remains interesting. Firstly, it increases the physical understanding of the system, it enables to create benchmark values for other buildings of the same category. Secondly, if the parameters have not physical meaning, the model may have no additional value compared to a pure black-box model. However, to conclude this, the simulation performance of black-box models should be compared as well.

Regarding the selection of the optimizer (Q2), the results show that only the oversimple structure of the first-order model shows convexity property. Significant non-convexity already emerged from the second-order grey-box model. When applying the four different gradient-based iterative optimizers, the trained second-order grey-box model has lower NRMSE for the one-step ahead prediction compared to the model from global optimization. Therefore, it is better to use global optimization to increase the chance of avoiding a local minimum.

It is hard to say whether PRBS or FHS is a better option from the results that we observe. Since it also depends on the target period of the model (better fitting on a certain period or longer period of the FHS). However, it is clear that with a larger amount of data (longer observation period or more samples with smaller sampling time), the chance to identify a model with higher fitting and more physical parameters can be increased. This answers the third question (Q3) of the introduction. The data quality does influence the identified results of the grey-box model. Nevertheless, it is not always realistic to use the PRBS signal to excite the building's thermal mass with normal occupancy in the residential building. Data from normal operation (here intermittent on-off heating) over long periods seems more accessible. The results of this paper also show that an acceptable model can be obtained with normal building operations if large amount of data is accessible.

The selection of the correct input and output is also important for system identification (Q4). In the case study, the identified results from volume-averaged temperatures are better than those from the extracted air temperature. This proves that the correct selection of the representative indoor temperature of the building can increase the model quality and that choosing the extracted air temperature does not systematically give the best performance.

This work has answered some questions for the identification of stochastic grey-box models. However, the data in this paper is based on the results of virtual experiments without measurement noise. For future work, it will be worth investigating the influence of the measurement noise on the identification results. In addition, complementary pre-processing methods to increase the chance to identify parameters with a physical value is also an interesting topic.

Acknowledgement

The authors would like to thank the Norwegian Research Council and industry partners as this work was done in the framework of the Norwegian Research Centre on Zero Emission Neighbourhoods in Smart Cities (ZEN).

References

[1] A. Losi, P. Mancarella, A. Vicino, Integration of demand response into the electricity chain: challenges, opportunities, and Smart Grid solutions, John Wiley & Sons, 2015.

[2] P. Siano, Demand response and smart grids — A survey, Renew. Sustain. Energy Rev. 30 (2014) 461–478. https://doi.org/10.1016/j.rser.2013.10.022.

[3] J. Hu, H. Morais, T. Sousa, M. Lind, Electric vehicle fleet management in smart grids: A review of services, optimization and control aspects, Renew. Sustain. Energy Rev. 56 (2016) 1207–1226. https://doi.org/10.1016/j.rser.2015.12.014.

[4] G. Steindl, W. Kastner, V. Stangl, Comparison of Data-Driven Thermal Building Models for Model Predictive Control, J. Sustain. Dev. Energy, Water Environ. Syst. 7 (2019) 730–742. https://doi.org/10.13044/j.sdewes.d7.0286.

[5] J. Le Dréau, P. Heiselberg, Energy flexibility of residential buildings using short term heat storage in the thermal mass, Energy. 111 (2016) 991–1002. https://doi.org/10.1016/j.energy.2016.05.076.

[6] G. Reynders, Quantifying the impact of building design on the potential of structural strorage for active demand response in residential buildings, 2015. https://doi.org/10.13140/RG.2.1.3630.2805.

[7] M. Dahl Knudsen, S. Petersen, Demand response potential of model predictive control of space heating based on price and carbon dioxide intensity signals, Energy Build. 125 (2016) 196–204. https://doi.org/10.1016/j.enbuild.2016.04.053.

[8] B.P. Esther, K.S. Kumar, A survey on residential Demand Side Management architecture , approaches , optimization models and methods, Renew. Sustain. Energy Rev. 59 (2016) 342–351. https://doi.org/10.1016/j.rser.2015.12.282.

[9] T.P. Bohlin, Practical Grey-box Process Identification, Springer London, 2006. https://doi.org/10.1007/1-84628-403-1.

[10] J.A. Crabb, N. Murdoch, J.M. Penman, A simplified thermal response model, Build. Serv. Eng. Res. Technol. 8 (1987) 13–19.

[11] J.F. van Impe, P.A. Vanrolleghem, D.M. Iserentant, Advanced instrumentation, data interpretation, and control of biotechnological processes, Springer Science & Business Media, 2013.

[12] K. Arendt, M. Jradi, M. Wetter, C.T. Veje, ModestPy: An Open-Source Python Tool for Parameter Estimation in Functional Mock-up Units, in: Proc. Am. Model. Conf. 2018, Oct. 9-10, Somb. Conf. Center, Cambridge MA, USA, 2019: pp. 121–130. https://doi.org/10.3384/ecp18154121.

[13] A. Afram, A.S. Fung, F. Janabi-Sharifi, K. Raahemifar, Development and performance comparison of low-order black-box models for a residential HVAC system, J. Build. Eng. 15 (2018) 137–155. https://doi.org/10.1016/j.jobe.2017.11.021.

[14] L. Ljung, A.G. Wills, Issues in sampling and estimating continuous-time models with stochastic disturbances, in: IFAC Proc. Vol., 2008. https://doi.org/10.3182/20080706-5-KR-1001.0271.

[15] S. Norge, NS 3700: 2013 Criteria for passive houses and low energy buildings-Residential buildings, (2013).

[16] T. Johnsen, K. Taksdal, J. Clauß, X. Yu, L. Georges, Influence of thermal zoning and electric radiator control on the energy flexibility potential of Norwegian detached houses, E3S Web Conf. 111 (2019) 06030. https://doi.org/10.1051/e3sconf/201911106030.

[17] A.C. Bøeng, B. Halvorsen, B.M. Larsen, Kartlegging av oppvarmingsutstyr i husholdningene, Rapp. 2014/45. (2014). https://www.ssb.no/energi-og-industri/artikler-og-publikasjoner/kartlegging-av-oppvarmingsutstyr-i-husholdningene.

[18] S. Norge, SN/TS 3031: 2016 Energy performance of buildings, Calc. Energy Needs Energy Supply. (2016).

[19] P. Bacher, H. Madsen, Identifying suitable models for the heat dynamics of buildings, Energy Build. 43 (2011) 1511–1522. https://doi.org/10.1016/j.enbuild.2011.02.005.

[20] N.R. Kristensen, H. Madsen, S.B. Jørgensen, Parameter estimation in stochastic grey-box models, Automatica. 40 (2004) 225–237. https://doi.org/10.1016/j.automatica.2003.10.00.

[21] R.E. Hedegaard, T.H. Pedersen, M.D. Knudsen, S. Petersen, Towards practical model predictive control of residential space heating: Eliminating the need for weather measurements, Energy Build. 170 (2018) 206–216. https://doi.org/10.1016/j.enbuild.2018.04.014.

[22] R.E. Hedegaard, T. Pedersen, M.D. Knudsen, S. Petersen, Identifying a comfortable excitation signal for generating building models for model predictive control: a simulation study, in: CLIMA2016 12th REHVA World Congr. World Congr., Aalborg Universitet, 2016. https://doi.org/https://doi.org10.3384/ecp18154121.

[23] X. Yu, L. Georges, M.D. Knudsen, I. Sartori, L. Imsland, Investigation of the Model Structure for Low-Order Grey-Box Modelling of Residential Buildings, in: Proc. Build. Simul. 2019 16th Conf. IBPSA, International Building Performance Simulation Association (IBPSA), 2019. https://doi.org/10.26868/25222708.2019.211209.

[24] O.M. Brastein, D.W.U. Perera, C. Pfeifer, N.O. Skeie, Parameter estimation for grey-box models of building thermal behaviour, Energy Build. 169 (2018) 58–68. https://doi.org/10.1016/j.enbuild.2018.03.057.

[25] K.J. Åström, Introduction to stochastic control theory, Courier Corporation, 2012.

[26] Advanced Metering System (AMS) Status and plans for installation per Q2 2016, 2016. https://www.nve.no/energy-market-and-regulation/retail-market/smart-metering-ams/.

RESEARCH PUBLICATIONS

PAPER 3

Yu X, Georges L, Imsland L. Data pre-processing and optimization techniques for stochastic and deterministic low-order grey-box models of residential buildings. *Energy and Buildings*. 2021; 236: 110775.

RESEARCH PUBLICATIONS

Energy & Buildings 236 (2021) 110775

Contents lists available at ScienceDirect

Energy & Buildings

journal homepage: www.elsevier.com/locate/enb

Data pre-processing and optimization techniques for stochastic and deterministic low-order grey-box models of residential buildings

Xingji Yu [a,*], Laurent Georges [a], Lars Imsland [b]

[a] Department of Energy and Process Engineering, Faculty of Engineering, NTNU – Norwegian University of Science and Technology, Kolbjørn Hejes vei 1a, 7034 Trondheim, Norway
[b] Department of Engineering Cybernetics, Faculty of Engineering, NTNU – Norwegian University of Science and Technology, O. S. Bragstads Plass 2, 7034 Trondheim, Norway

ARTICLE INFO

Article history:
Received 12 July 2020
Revised 15 January 2021
Accepted 24 January 2021
Available online 1 February 2021

Keywords:
Data pre-processing
Grey-box modelling
Building thermal mass

ABSTRACT

Grey-box models are data-driven models where the structure is defined by the physics while the parameters are calibrated using data. Low-order grey-box models of the building envelope are typically used for two main applications. Firstly, they are used as a control model in Model Predictive Control (MPC) where the thermal mass of the building is activated as storage (for instance in demand response). Secondly, they are used to characterize the thermal properties of the building envelope using on-site measurements. The influence of the data pre-treatment on the performance of grey-box models is hardly discussed in the literature. However, in real applications, information about data pre-processing by sensors or data acquisition systems is expected to be limited. Therefore, the influence of the sampling time, low-pass filters and *anti-causal shift* (also called data labeling) are analyzed for grey-box models in deterministic and stochastic innovation form. The influence on the optimizer performance is also investigated. The datasets are generated from virtual experiments using multi-zone building performance simulations of a residential building (in lightweight wooden construction) heated using different types of excitation signals. Results show that the parameters of deterministic grey-box models are significantly influenced by the training data while the data pre-treatment has a limited impact on the model and optimizer performance. Depending on the training data, the value taken by some parameters is not physically plausible. On the contrary, stochastic models are significantly influenced by the data pre-treatment, especially the sampling time, and less by the training data. The parameters can become non-physical for large sampling times. However, the *anti-causal shift* proves to be efficient to keep the parameters almost constant with increasing sampling times. Even though the parameter values of the deterministic model are less physically plausible, the simulation performance of deterministic models is higher than using the equivalent stochastic models. These results suggest that deterministic models seem better suited for MPC while stochastic models are better suited for the characterization of thermal properties (if suitable data pre-treatment is applied).

1. Introduction

The share of Renewable Energy Sources (RES) is increasing constantly in today's energy system. Power generation from RES is often decentralized and intermittent, such as solar and wind energy, which brings considerable volatility to the electric grid. The supply and demand sides in the power system have to be balanced at each time step. Any power imbalance can cause severe consequences for power quality and reliability (e.g. voltage fluctuations and power outage) [1,2]. Therefore, more flexible loads are needed to further increase the share of intermittent RES. Demand response (DR) is the interaction and responsiveness of the end-use customer to a specific penalty signal (e.g. price signal, CO_2 intensity factor for electricity signal) [3,4]. It is considered to be an important component to provide flexibility for smart grids [5]. In addition, DR can also be used for peak-shaving to avoid congestion [6,7] in the distribution grid so that the reinforcement of these grids can be postponed.

The share of the total final energy consumed by buildings is 20–40% and this is increasing at the rate of 0.5–5% per year in developed countries [8]. In Nordic countries, the building energy consumption is dominated by space-heating due to the long and cold heating season. Building thermal mass can be considered as short-term heat storage and be used to perform DR [9–11], which can contribute to providing flexibility to the smart grid. Model

* Corresponding author.
E-mail address: xingji.yu@ntnu.no (X. Yu).

https://doi.org/10.1016/j.enbuild.2021.110775
0378-7788/

Nomenclature

DR	Demand Response
MPC	Model Predictive Control
BPS	Building Performance Simulation
AMS	Advanced Metering System
RC	Resistance and Capacitance
PRBS	Pseudo-Random Binary Signal
PI	Proportional Integral
NRMSE	Normalized Root Mean Squared Error
FHS	Full Heating Season
GA	Genetic Algorithm
PSO	Particle Swarm Optimization
ACS	Anti-Causal Shift
DS	Direct Sampling
MA	Moving Average
FIR	Finite Impulse Response
det	Deterministic Model
sto	Stochastic Model
HTC	Heat Transfer Coefficient

Predictive Control (MPC) is considered a promising technique to apply DR. In an MPC, a dynamic model is used to predict the response of the building to future boundary conditions (e.g. forecast of weather conditions, and production of the energy system). The MPC control agent (computers, built-in intelligent devices, etc.) will take the optimal control decisions based on the predictions of the model and system constraints. In buildings, the constraints for the MPC are usually the power limitation of the SH system, and thermal comfort. The performance of the MPC controller thus strongly relies on the quality of the dynamic model of the system to be controlled. Poor quality models could result in undesired control outcomes (e.g. increased energy cost, violation of thermal comfort, or even be counterproductive for the grid). In practice, MPC is currently applicable for only a small fraction of existing buildings due to cost criteria [12]. However, the ongoing implementation of smart meters, like the Advanced Metering System (AMS) in Norway [13] and "Key principles for the package of ordinances governing smart grids" in Germany [14], will make the MPC control concept more accessible in the future. The recent emergence of small, low-cost and wireless sensors with a data collection function [15] will also contribute to accelerate the implementation of MPC in buildings. Finally, creating a suitable model is acknowledged to be the most time-consuming part of MPC implementation [16]. Therefore, the cost related to the identification of the control model should also be limited to reduce the total investment cost of the MPC controller. The need to identify a control model at a low cost is even more severe for small residential buildings.

The modelling methods for MPC can be divided into three main categories, namely white-, black- and grey-box models. White-box models are based on physical laws. They require exhaustive information about the building including underlying physical processes, and parameters. This type of model is usually mathematically complex but has high accuracy. This approach is often used in Building Performance Simulation (BPS) software like Modelica [14], EnergyPlus [14] and IDA [17]. However, white-box models are time-consuming to calibrate as a lot of input parameters have to be defined and they need to be updated during the operational lifetime of the building. Moreover, the mathematical complexity requires extensive computational power [9] or the white-box model has to be simplified using linearization and model reduction techniques [18]. All these factors challenge the feasibility of white-box models for the MPC of the existing building. Black-box models are pure data-driven methods based on the measured input and output time-series data from the system. Statistical regression and Artificial Neural Network (ANN) are common mathematical techniques for black-box models [19]. However, this method requires sufficient data for training to guarantee the accuracy of the model [20]. The precision of black-box models is also significantly influenced by data quality. Grey-box modelling is an intermediate strategy between white- and black-box models. It exploits the dominant physical properties of the system to construct the model structure and uses measurement data to estimate the model parameters. Grey-box models have better generalization (extrapolation) properties [21] and usually require less experimental data compared to black-box models [22]. Lumped resistance and capacitance models (i.e. RC models) are a common approach to create grey-box models, which means the thermal conditions of the building are expressed with an electric circuit analogy [23]. Existing work has already applied grey-box models for MPC in buildings. For instance, Coninck et al. [24] made use of a grey-box model identified by monitoring data to implement MPC. Zong et al. [25] used an economic MPC with a multi-zone grey-box model to control the power of heating radiators in a three-story Danish residential house.

This study mainly focuses on the grey-box modelling of the building thermal dynamics. A significant amount of research has already addressed the question of the structure of grey-box models. Viot et al. [26] gave a detailed list of research papers using RC models for the MPC In the study by Fux et al. [27], a one-capacitance model was used to forecast the indoor temperature of a residential building and it gave satisfactory results. Bacher and Madsen [28] used the data collected from an unoccupied office building to identify a suitable model. Models of different orders were evaluated based on likelihood ratio tests. These showed that from third-order, increasing the model order cannot lead to significant improvements in the results. Palomo Del Barrio et al. [29] concluded that a second-order model is sufficient for forecasting results for both indoor temperature and heating power. The study of Reynders et al. [30] also confirmed that the second-order model is enough to deliver decent prediction performance. Moreover, Reynders et al. concluded that heat flux measurements were needed to guarantee observability for higher-order models (i.e. fourth and fifth-order models) since overfitting and convergence problems occurred. Yu et al. [31] compared two grey-box model structures generated from VDI 6007 [32] and ISO 13,790 [33]. The results revealed that with limited measurements and a large number of unknown parameters, the parameters of the identified model can easily become non-physical. Brastein et al. [34] showed that deterministic grey-box models at second-order can already face the problem of practical identifiability. Based on these previous findings, our paper only uses first- and second-order grey-box models to address the research questions so that the challenges related to overfitting can be eliminated from the study. When space-heating power is used as input and the indoor temperature is used as an output, previous works showed that second-order models are a good trade-off between accuracy and identifiability. Therefore, our paper only resorts to first- and (simple) second-order grey-box models to eliminate challenges related to overfitting from the study.

Data pre-processing (or data pre-treatment) is acknowledged to have a key influence on the model identification results [35]. However, this topic has hardly been addressed in the field of grey-box models for buildings. Ljung and Wills [36] revealed several issues when applying a long sampling time to estimate continuous-time models with stochastic disturbances. However, the analysis of Ljung and Wills is illustrated using a theoretical example. Therefore, our paper investigates the influence of long sampling times in building applications. The time-series data is generated using virtual experiments using the BPS software IDA ICE. In addition to the sampling time, the influence of the data pre-processing using a low-pass filter is investigated as well as the influence of shifting the input data in time, called *anti-causal shift* (ACS). In this context, the performance of grey-box models in the deterministic and stochastic innovation forms is compared using the MATLAB identification toolbox [37]. To analyze the model performance, the ability to characterize the thermal properties of the building envelope and the simulation performance are clearly distinguished. The simulation performance is a good indicator of the model accuracy for MPC applications. Finally, these research questions are important as data can be processed (or altered) by sensors, the data acquisition system or by the building modeler prior to the model identification.

The remainder of the paper is structured as follows. Section 2 provides information on the virtual experiment using BPS software, which includes detailed information about the virtual building, the excitation signals and the boundary conditions. Section 3 describes the grey-box model structure used for this study. The model identification tool and method are also outlined, followed by the data pre-processing method. Section 4 shows results split into three aspects. The model performance to characterize the building thermal properties is first discussed. Then, the analysis of the optimizer performance and the simulation performance is analyzed. Section 5 gives some complementary discussions based on the results. Conclusions are presented in Section 6.

2. Virtual experiments

2.1. Detailed multi-zone dynamic simulations

IDA ICE is a detailed dynamic simulation tool to study the indoor environment and the energy consumption of buildings. In this study, an IDA ICE building model is used as a virtual experiment to generate data for system identification. It is a two-story detached house located in Oslo with a heated floor area of 160 m^2. The building is constructed in wood, meaning a lightweight construction, and complies with the requirement of the Norwegian passive house standard, NS 3700 [38]. The three-dimensional geometry of the building is shown in Fig. 1. The building is equipped with balanced mechanical ventilation with a heat recovery unit. A cascade ventilation strategy is applied. This heat exchanger is modelled using constant effectiveness of 85% without bypass (like a plate heat exchanger) to promote the linearity of the model. This is done because the research focuses on the thermal dynamics of the building envelope and does not aim at modelling the air handling unit (AHU) in detail. Other detailed information regarding the BPS software model can be found in [39].

The detailed building model is multizone and the zoning follows the floor plan presented in Fig. 2. For the sake of simplicity, the grey-model models considered in our study are mono zone: it is not necessary to use multi-zone grey-box models to address our research questions. Consequently, the indoor temperature in our virtual experiments should be as uniform as possible. This is done by opening all the internal doors inside the building. IDA ICE has an embedded ventilation network model which accounts for the large bidirectional airflow through open doorways. Thus, the air temperature inside the building computed by IDA ICE is relatively uniform due to the large convective heat transfer between rooms. The volume-averaged temperature is selected to represent the measured indoor air temperature. The mean air temperature of the extract ventilation air is also a common choice. However, based on preliminary investigations, the volume-averaged temperature proved to give better grey-box models for this test case. The building is heated using electric radiators as these are the most common space-heating systems for residential buildings in Norway [40]. This heating system has smaller thermal inertia than the building envelope so that the dynamics of the radiators are expected to play a limited role. Hourly profiles for internal gains generated by artificial lighting, electric appliances and occupancy are taken from the Norwegian technical standard TS3031:2016 [41]. The typical meteorological year (TMY) of Oslo with a resolution of one hour is used for the IDA ICE simulations. Like internal gains, solar gains have thus a resolution of one hour.

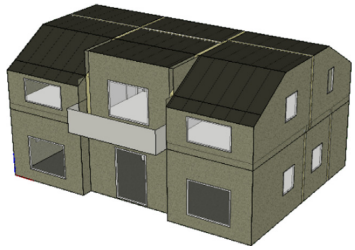

Fig. 1. 3D geometry of the building model in IDA ICE (showing the southwest facade).

2.2. Excitation signals of the building thermal dynamics

The system needs to be perturbed to obtain data for model identification. It is often recommended to use excitations having no correlation with the other inputs [28]. The Pseudo-Random Binary Signal (PRBS) is a periodic and deterministic signal which approximates white noise properties [42]. The PRBS signal can activate the dynamic system in a large spectrum of frequencies with a high signal-to-noise ratio (SNR) [28,43,44]. In this study, the excitation signal is simultaneously applied to all the electric radiators in the BPS model. Following the guidelines of the IEA EBC Annex 58 [45], the excitation signal is in fact the combination of the two PRBS signals, see Fig. 3. One sequence to identify the short-time dynamics with a period (T) of 10 min and with an order (n) of 8. The second sequence aims at identifying the long time constant of the building with a period (T) of 3.5 h and n equals to 5. The resulting time profiles for the space-heating are shown in Fig. 2. The PRBS signal can be applied to four different weeks in the space-heating season. These weeks are characterized by different weather conditions, as described in Table 1.

However, it is not always desirable to apply a PRBS signal to the space-heating system as large variations of the indoor temperature may occur and lead to thermal discomfort for the occupants. Therefore, conventional controls of heating systems are also investigated. Intermittent heating with a temperature setpoint changing between daytime and night-time is considered (i.e. a night setback). Two different local controllers are tested to track the setpoint temperature in each room: a Proportional-Integral (PI) control and an on–off control (with a differential of 1 K). The last one is the most common control strategy for electric radiators in buildings. When a PRBS signal is applied over a long period of time

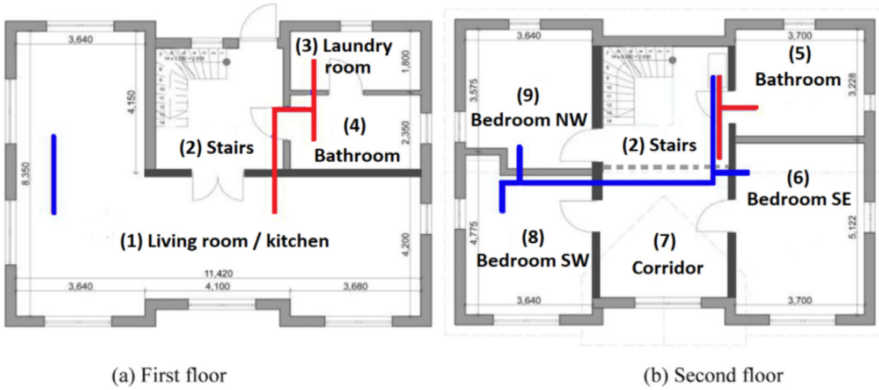

Fig. 2. Floor plan of the test building (ducts for the supply air are in blue and in red for extraction). (For interpretation of the references to color in this figure legend, the reader is referred to the web version of this article.)

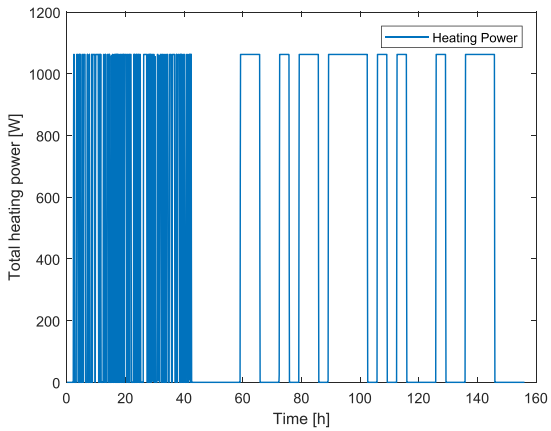

Fig. 3. Time profile of the PRBS signal applied to electric radiators.

(i.e. longer than one week), it is difficult to design the signal so that the indoor temperature is kept within comfortable temperature limits for the occupants. By definition, conventional heating controls enable to have normal occupancy of the building during the experiments used to collect data for model identification. It is thus possible to collect data over a longer period of time than one week without impacting the thermal comfort of building users. The full space-heating season (FHS) starting in November and finishing at the end of March can be used to train the model. However, it is also interesting to test whether a shorter training period of one month would be sufficient to train the grey-box models. It is also interesting to check whether specific months are more suited for this task. Therefore, the model parameters are also identified using each of five different months of the space-heating season (i.e. Month 1 to 5).

To investigate the influence of data pre-processing techniques and the grey-box modelling approaches, 20 different datasets have been generated using different excitation signals, duration of the experiment and weather data. The detailed description of each case can be found in Table 2 below. IDA ICE assumes that variables are piecewise linear during one-time step. The model equations are integrated numerically using a variable time-step so that data is not generated at constant time intervals. Consequently, conservative interpolation has been used to interpolate IDA ICE data on a uniform grid of 2.5 min. This time step is significantly smaller than the shortest period of the PRBS (i.e. 10 min).

3. Methodology for grey-box modelling

3.1. Grey-box model structure

Based on the literature review (see the introduction section), only first-order and second-order grey-box models are considered in this paper. Preliminary tests using our virtual experiments confirmed that a third-order model would be overfitted. The structure of the grey-box model expresses the conservation of energy. As mono zone grey-box models are considered (with a single node related to the indoor air temperature), the dominant process to be integrated is the heat transfer between the building and its outdoor environment. The influence of solar radiation and internal gains are also included in the grey-box models. Two model structures are studied: a one-resistance, one-capacitance (1R1C) in Fig. 4, and a three-resistance, two-capacitance (3R2C) model in Fig. 5. The physical interpretation of their respective parameters can be found in Table 3.

The internal and solar gains can be computed accurately by BPS. For the sake of simplicity, these gains have been introduced directly in the grey-box models rather than identified. For the

Table 1
Weather conditions in four PRBS experiments.

Type	Outdoor Temperature	Sky	Date	Duration
Very Cold	-10 ℃	Clear sky	12/13/2019	One week
Cold	0 ℃	Overcast	12/24/2019	One week
Cold	0 ℃	Clear sky	3/23/2019	One week
Mild	5 ℃	Overcast	11/23/2019	One week

Table 2
Description of the datasets and their corresponding abbreviation.

Case (dataset)	Case description (excitation)	Period/Duration	Abbreviation
1	PRBS1	Week 1	W1-PRBS
2	PRBS2	Week 2	W2-PRBS
3	PRBS3	Week 3	W3-PRBS
4	PRBS4	Week 4	W4-PRBS
5	Intermittent on–off	Week 1	W1-Inter I/O
6	Intermittent on–off	Week 2	W2-Inter I/O
7	Intermittent on–off	Week 3	W3-Inter I/O
8	Intermittent on–off	Week 4	W4-Inter I/O
9	Intermittent on–off	Month 1	M1-Inter I/O
10	Intermittent on–off	Month 2	M2-Inter I/O
11	Intermittent on–off	Month 3	M3-Inter I/O
12	Intermittent on–off	Month 4	M4-Inter I/O
13	Intermittent on–off	Month 5	M5-Inter I/O
14	Intermittent on–off	Full heating season	FHS-Inter I/O
15	Intermittent PI	Month 1	M1-PI
16	Intermittent PI	Month 2	M2-PI
17	Intermittent PI	Month 3	M3-PI
18	Intermittent PI	Month 4	M4-PI
19	Intermittent PI	Month 5	M5-PI
20	Intermittent PI	Full heating season	FHS-PI

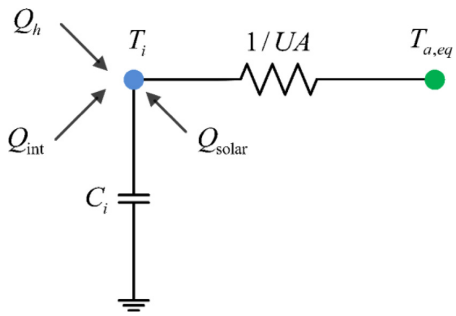

Fig. 4. First-order 1R1C model.

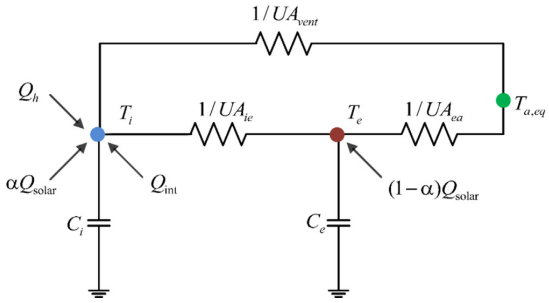

Fig. 5. Second-order 3R2C model.

3R2C model, only the coefficient α that distributes the solar gains between the two temperature nodes needs to be identified. In real applications, the gains are not known exactly. However, simplifying the problem enables us to emphasize the specific research questions in this paper. To obtain a more physical representation of the heat exchange between the building and its outdoor environment, an equivalent outdoor temperature is applied as described in Harb et al. [9]. This temperature is calculated using Equation (1) with a short-wave absorption coefficient of the exterior surface (a_f) of 0.5 and an exterior heat transfer coefficient (α_A) of 25 W/(m^{2}K):

$$T_{a,eq} = T_a + Q_{irrad}\frac{a_f}{\alpha_A} \tag{1}$$

The heat dynamics of the 1R1C model is expressed in the following differential equation:

$$C_i\frac{dT_i}{dt} = UA\,(T_{a,eq} - T_i) + Q_h + Q_{int} + Q_{solar} \tag{2}$$

The heat dynamics of the 3R2C model is expressed by the following differential equations:

$$C_i\frac{dT_i}{dt} = UA_{vent}\,(T_{a,eq} - T_i) + UA_{ie}\,(T_e - T_i) + Q_h + Q_{int} + \alpha\,Q_{solar} \tag{3}$$

$$C_e\frac{dT_e}{dt} = UA_{ea}\,(T_{a,eq} - T_e) + UA_{ie}\,(T_i - T_e) + (1-\alpha)\,Q_{solar} \tag{4}$$

3.2. Model identification tool and method

The MATLAB system identification toolbox is used in our study [37]. Madsen et al. [45] illustrated how stochastic models can be formulated as an extension of deterministic models. In the stochastic form, a system noise (or noise term) is added to the deterministic model equations to better account for the modelling approximations, unrecognized inputs and measurement of inputs corrupted by noise. The generic equations of the stochastic linear state-space model in innovation form can be expressed as:

$$\frac{dx}{dt} = Ax(t) + Bu(t) + Ke(t) \tag{5}$$

$$y(t) = Cx(t) + e(t) \tag{6}$$

where x is the state vector, A, B and C are the system matrices, u is the input vector (i.e. $T_{a,eq}$, Q_{solar}, Q_{int}, Q_h) and y is the output (i.e. indoor temperature, T_i). K is the disturbance matrix of the innovation form (Kalman gain) [46]. The matrices A, B, C and K are functions of the model parameters (θ), in our case defined by Equations (2) to (4). The continuous-time model is first discretized so that discrete measurement data can be used to identify the model parameters. Unlike IDA ICE, the time discretization in the MATLAB identification toolbox assumes piecewise-constant input data during each time interval (i.e. zero-order hold). For stochastic models, both the value and variance of the model parameters are identified. In the case of deterministic models, the K matrix is set to zero. The parameter variance is not clearly defined for the deterministic model in the MATLAB system identification toolbox. Therefore, it has been decided to only consider the parameter value.

At the beginning of the identification procedure, the initial guess of the model parameters and their region of feasibility (i.e. lower and upper bounds for each parameter) should be defined by the user as input parameters. Then, the optimizer iterates within the feasibility region to find the value of the parameters that minimize the prediction error criterion$f(x)$

$$f(x) = \sum_{k=1}^{N} ||y_k - \hat{y}_k(\theta)||^2 \tag{7}$$

where y_k is the measurement output while $\hat{y}_k(\theta)$ is the one-step ahead prediction.

The default function (*greyest*) in the MATLAB identification toolbox uses gradient-based optimizers. Four different iterative search methods are used in sequence. Consequently, the optimizer may

Table 3
The physical interpretation of the parameters of the grey-box models.

Parameters	Physical interpretation
T_i	Temperature of interior heat capacity [°C].
T_e	Temperature of the building envelope [°C].
T_a	The outdoor (or ambient) temperature [°C].
$T_{a,eq}$	The equivalent outdoor (or ambient) temperature [°C].
C_i	Heat capacity of the building combining the thermal mass of the air, the furniture, internal walls and, potentially, a fraction of the thermal capacitance of external walls: the first centimeters for the second-order model and a larger fraction for the first-order model [kWh/K].
C_e	Heat capacity of the node external wall for the second-order model [kWh/K].
UA	Overall heat transfer coefficient (HTC) between the building and its ambient, including ventilation [kW/K].
UA_{ie}	Heat conductance between the building envelope and the interior [kW/K].
UA_{ea}	Heat conductance between the ambient and the building envelope [kW/K].
UA_{vent}	Heat conductance between the ambient and the interior node [kW/K].
Q_{int}	Internal heat gain from artificial lighting, people and electric appliances [kW].
Q_{irrad}	Global solar irradiation on horizontal surface [K/m^2].
Q_{solar}	Heat gain from solar irradiation [kW].
Q_h	Heat gain from the electric heater [kW].
α	Fraction of solar gains to air node.

converge to a local optimum if the problem is not convex. As shown in Arendt et al. [47], Genetic Algorithm (GA) combined with a gradient-based method could be used to solve non-convex optimization problems used to identify the parameters of grey-box models. Likewise, a global optimization algorithm has been implemented in our work to avoid a local optimum. A metaheuristic Particle Swarm Optimization (PSO) is applied at the first stage, followed by the default *greyest* function to refine results during the second stage. The PSO algorithm begins by creating the initial particles and assigning them initial velocities. It evaluates the objective function at each particle location and determines the best (lowest) function value and the best location. In the next step, new velocities are chosen based on the current velocity, the particles' individual best locations, and the best locations of their neighbors. The optimizer then iterates the particle locations, velocities, and neighbors until the algorithm reaches a stopping criterion. Detailed information on the PSO algorithm can be found in [48,49]. For each test case, both optimization procedures are used in sequence: the default *greyest* and the global optimization. The method giving the lowest error for the prediction error criterion is selected to provide the model parameters. The flow chart of the identification routine is summarized in Fig. 6.

To determine the search space for the optimization, a first set of limits for the parameter values have been selected based on the thermal properties of the building in IDA ICE. Then, these minimum and maximum limits have been refined manually by trial and error. Several simulations (i.e. optimizations) have been run with different limits for the parameter values. It has been checked whether the solution (meaning the parameter values computed by the optimizer) hit the pre-defined parameter limits The limits of the parameter values leading to the smallest range without the optimizer hitting these limits have been selected. The PSO algorithm populates this range randomly to generate the initial condition. A sensitivity analysis has been done on the number of particles in the swarm as well as the number of iterations.

3.3. Data pre-processing method

Extended sampling time (T_s) can lead to a non-physical value and variance for the identified parameters of grey-box models (see e.g. [36]). In real-life applications, it can be seldom guaranteed that measurement data is recorded at a sampling time (T_s) shorter than the shortest time of the system (T_{min}). In our test case, T_{min} is related to the shortest period of the PRBS signal (T) as the other model inputs (namely the internal and solar gains) have a resolution of one hour. T_{min} is therefore 10 min and the sampling time (Ts) applied to the BPS data has been taken at 2.5 min to avoid aliasing. As $T_s < T_{min}$, it is therefore possible to identify the parameters of the grey-box model without facing the above-mentioned issues. However, the measurement data at 2.5 min can be resampled at longer sampling times, namely 15, 30 or 60 min, so that the case where $T_s < T_i$ can be directly compared to the cases where $T_s > T_i$. In real applications, it is difficult to guarantee that the data logging is done at a sampling time shorter than the system dynamics. In addition, the measurement data can be pre-processed before being logged at T_s. Two methods are considered here: low-pass filtering and *anti-causal shift*.

Regarding low-pass filtering, three approaches are compared:

- The first approach is direct sampling (DS) at T_s without pre-filtering. This may cause a high aliasing error.
- The second approach applies a moving-average (MA) filter of length T_s before sampling. With MA, the aliasing error is significantly decreased but, in theory, it can still occur.

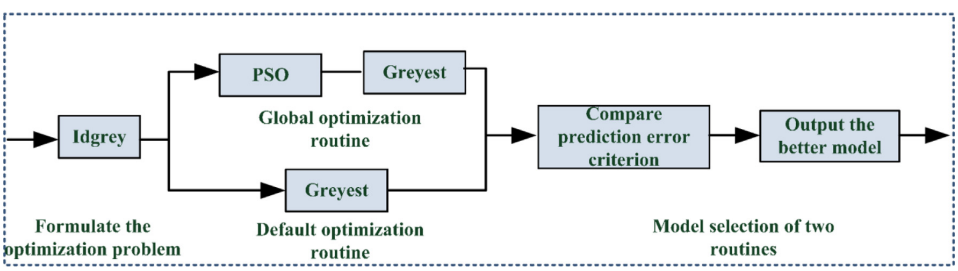

Fig. 6. Flow chart of the optimization procedure to identify the model parameters.

- The third approach applies a finite impulse response (FIR) filter with a cut-off frequency of $1/T_s$ before sampling. The FIR would lead to negligible aliasing error (if it is designed at a sufficient order).

By analyzing the performance of the three methods, it is possible to understand the influence of aliasing. It is known that these low-pass filters introduce a time delay [35]. However, as the low-pass filters are here applied to all input and output variables of the dataset, the delay does not affect the final identification results. In the paper, we don't distinguish between the low-pass filtering deliberately introduced by the data engineer before training the grey-box model and the low-pass filtering done internally in the sensor. If grey-box models of small residential buildings should be developed at low cost, there is most likely no time to take the technical specifications of each sensor into account. Therefore, the type of data pre-treatment performed by the sensor can be unknown. The analysis is thus generic.

Ljung and Wills [36] pointed out that time labeling plays a role in the alignment of inputs and outputs for the identification application. The results of Ljung and Wills's paper show that a time shift (ACS) of the input (Input Delay = -T_s) is beneficial for the model. The method is going to be tested with the data from IDA ICE model.

3.4. Key performance indicator

One main application of the grey-box model is MPC. In this context, the long-term prediction performance (i.e. the simulation performance) is paramount. In our work, the NRMSE fitting, defined in Equation (9), is taken as the key performance indicator (KPI) to evaluate the simulation performance. It is based on the normalized root mean squared error (NRMSE) quantifying how well the simulated or predicted model response matches the measurement data, see Equation (8). If the fitting is 100%, this means the model fits the measurement data perfectly, while a low or negative fitting corresponds to a worse model. There are no outliers in the measurement data that will skew the NRMSE KPI, so there is little reason to use KPIs handling outliers better, such as Mean Absolute Error (MAE).

$$NRMSE = \frac{||y_k - \hat{y_k}||}{||y_k - mean(y_k)||} \tag{8}$$

$$NRMSE_{fit} = (1 - NRMSE) \times 1\ 00\% \tag{9}$$

Regarding the characterization of the building thermal properties, the performance of the grey-box is evaluated using the physical plausibility of the identified parameters. The calibrated value of the model parameters should give a physically-reasonable estimate of the thermal building properties.

- The overall heat transfer coefficient (HTC) is the total heat loss of the building in a steady-state. Convective and long-wave radiative heat transfer are non-linear. However, in the case of a highly insulated building, the heat conduction is dominant and often assumed linear in BPS (like in IDA ICE). In addition, the heat recovery effectiveness is constant, making its model linear. Specifically, each resistance R (or conductance) of the grey-box model will be dependent on the excitation signal. However, their combination to form the HTC is a steady-state performance parameter. Consequently, the HTC does not depend much on the excitation signal used for the identification. For the first-order model, the HTC is equal to the conductance UA. For the second-order model, the formula of the HTC for the 3R2C model is defined by Equation (10). In conclusion, to be physically plausible, the identified HTC should be close to steady-state heat losses of the IDA ICE model. These losses have been evaluated at 85 W/K (identified by applying a step function of the space-heating to the IDA ICE model).

$$HTC = \frac{1}{1/UA_{ie} + 1/UA_{ea}} + UA_{vent} \tag{10}$$

- The capacitances (C_i and C_e) are strongly related to the building thermal dynamics. Defining their physical plausibility is more challenging because their value depends on the excitation signal. The effective heat capacitance of the building (C_{eff}) based on the ISO 13786:2017 [50] is taken as a reference value for the capacitances mostly related to the walls (meaning C_i in the 1R1C model and C_e in the 3R2C models). C_{eff} is evaluated assuming daily fluctuations (i.e. 24 h) and using the thermal properties of each layer in the building walls (i.e. physical-based approach). C_{eff} is here equal to 3.9 kWh/K. To be physically plausible, it is expected that the identified values, also considering their variance, have the same order of magnitude as C_{eff}. Indeed, none of the excitation signals used in our investigations have fluctuations significantly longer than one day. For the 3R2C model, there is no point of comparison for the identified value of C_i. However, as it is related to the fast dynamics of the building, it is expected to be smaller than C_{eff}. In addition, the value of C_i should decrease with increasing frequencies in the excitation signal.

4. Results

In this section, the model performance to characterize the building thermal properties is first discussed, followed by the analysis of the optimizer performance. Finally, the simulation performance, important for MPC applications, is investigated. The comparisons of this section are mainly based on the performance criteria defined in the previous section. However, there are 20 different training datasets (see Table 2), four different models, four different sampling times, two different optimizers and three pre-filtering methods of the virtual experiments, with and without a causal shift. It corresponds to a total of 4320 different test cases. Thus, only the most representative test cases are taken to illustrate the results and support the conclusions.

4.1. Characterization of the building thermal properties

The physical plausibility of the identified grey-box model parameters is verified. It means the ability to identify values for the parameters that are in line with physics. For the sake of the conciseness, we mainly focus on datasets 1 to 4 with a short training period but strong excitation as well as dataset 14 which has the largest amount of data, see Table 2. These datasets can be seen as extreme scenarios so that it makes them representative to illustrate the model performance. Other datasets are also occasionally used to better illustrate how the input data influences the identification results. As has been mentioned previously in Section 3.2, it has been demonstrated theoretically that ACS of the input signal can be beneficial for model identification [36]. Therefore, the influence of the ACS is tested. The 3R2C model is used to illustrate the results. Some of the results of the 1R1C model are given in Appendix A. Regarding the physical plausibility of parameters, the overall heat transfer coefficient (HTC) of the building and heat capacitances (C_e and C_i) are used to illustrate the results.

All the figures in this section are based on the same layout, see e.g. Fig. 7. In each figure, five cases or datasets are considered. The abbreviation for each case on the horizontal axis follows the

description given in Table 2. The influence of increasing sampling times on these five cases is reported from the left to the right of the figure. Each figure also distinguishes the cases as a function of the data pre-treatment. Firstly, the colors of markers correspond to the different pre-filtering techniques. The cases in red, blue and black represent the MA filter, the FIR filter and the direct sampling, respectively. Secondly, cases without ACS are shown by circles in normal colors while cases with ACS are shown by triangles in lighter colors.

4.1.1. Deterministic 3R2C model

In Fig. 7, the value of HTC is close to the reference value of 85 W/K. The same conclusion is obtained for the 1R1C deterministic model, see Fig. 18 in Appendix A. The sampling time (T_s) does not have a noticeable influence on the HTC. Likewise, the pre-filtering method and ACS have no significant impact on HTC.

As shown in Fig. 8, the training dataset has the largest influence on C_e while the sampling time, the pre-filtering technique and the ACS have a limited impact. The value of C_e is similar between the four datasets using PRBS excitation (i.e. cases 1 to 4) and is plausible compared to the C_{eff} of 3.9 kWh/K determined using standards. However, it differs for case 14 that generates a higher value, well above 3.9 kWh/K. Comparable results are observed for the 1R1C deterministic model (see Fig. 19 in Appendix A). To further illustrate the influence of the dataset, the values of C_e identified using an intermittent on–off excitation during each month of the space-heating season are compared, i.e. cases 9 to 13, in Fig. 9. Even though the excitation signal is generated from the same control (i.e. intermittent on–off control) and has the same duration of one month, the identified C_e strongly depends on the selected period used to train the model, meaning the specific month of the space-heating season.

As shown in Fig. 10, similar results are obtained for the values of C_i. The case with ACS shows a progressive increase of C_i with the sampling time. A possible reason is that C_i represents the thermal capacitance of the building combining the air, the furniture, internal walls and, potentially, the first centimeters of external walls. With increasing T_s, the high frequencies of the inputs and the output are reduced while the low frequencies, corresponding to a longer penetration depth in the walls, have more importance in the evaluation of the thermal capacitance. With longer penetration depths, more thermal mass is activated leading to a higher C_i.

Several conclusions can be drawn. Firstly, the value of the parameters strongly depends on the dataset selected to train the

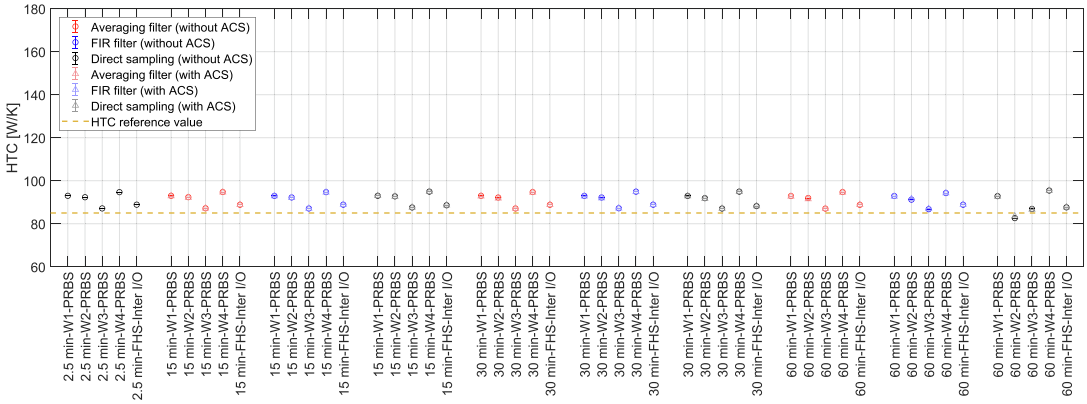

Fig. 7. Identified HTC of the 3R2C deterministic model for the cases 1,2,3,4 and 14, different sampling times and pre-filtering techniques; cases with ACS are shown by triangles in lighter colors.

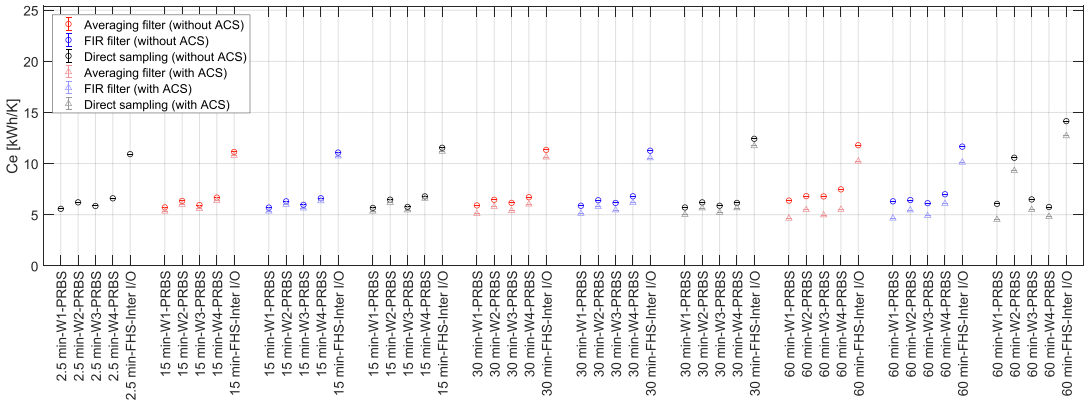

Fig. 8. Identified C_e of the 3R2C deterministic model for the cases 1,2,3,4 and 14, different sampling times and pre-filtering techniques; cases with ACS are shown by triangles in lighter colors.

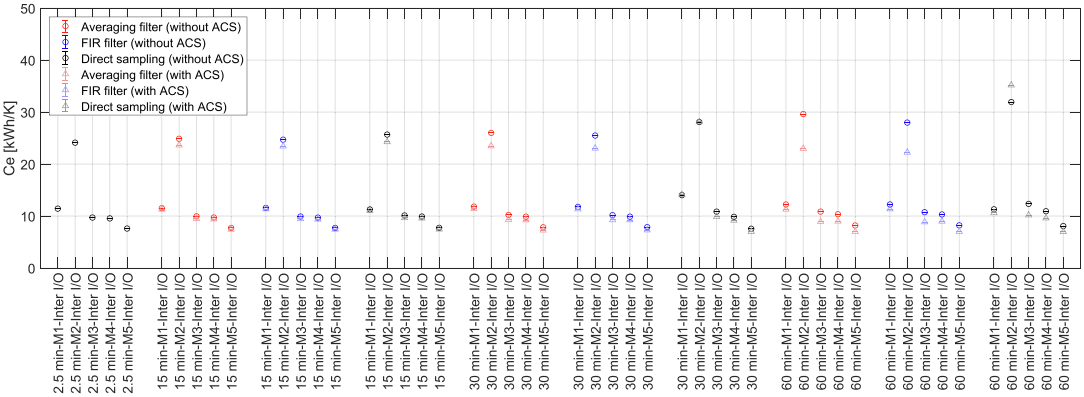

Fig. 9. Identified C_e of the 3R2C deterministic model for cases 9 to 13, different sampling times and pre-filtering techniques; cases with ACS are shown by triangles in lighter colors.

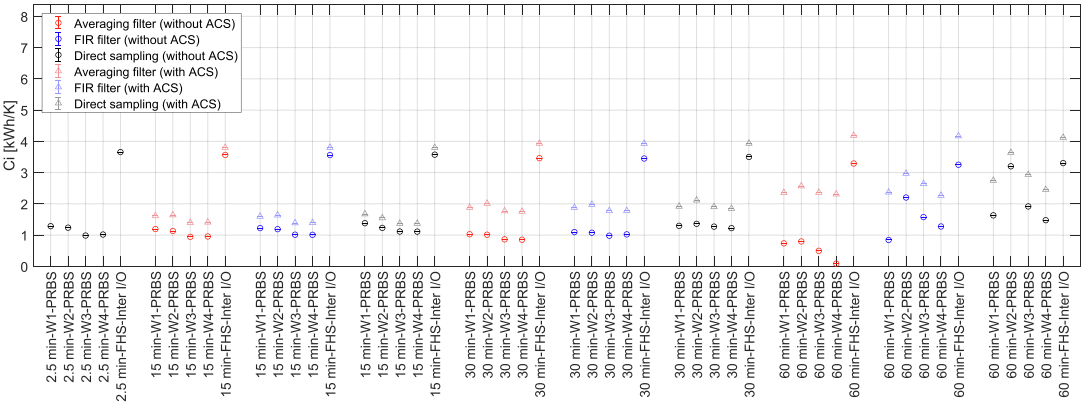

Fig. 10. Identified C_i of the 3R2C deterministic model for the cases 1,2,3,4 and 14, different sampling times and pre-filtering techniques; cases with ACS are shown by triangles in lighter colors.

model. Both the type of excitation (e.g. PRBS and on–off intermittent excitation) and the selected period during the space-heating season influence results. Secondly, the pre-processing of data does not have a large influence. Neither the ACS, the pre-filtering technique nor the sampling time leads to a significant change in the parameter values. The only exception appears with very large T_s. Then, the pre-filtering can prevent the parameter value from becoming non-physical. Finally, the HTC characterizing the steady-state performance of the building has rather stable values while the other parameters characterizing the thermal dynamics of the building, here C_e and C_i, are more strongly impacted by the training dataset and the sampling time.

4.1.2. Stochastic 3R2C model

For stochastic models, the value and variance of the model parameters are available. However, as the HTC is the combination of the three conductances in the 3R2C model, only the value of the HTC can be shown, not its variance. The value for HTC for the 3R2C stochastic model in Fig. 11 is similar to the deterministic model in Fig. 7. The same conclusion can be made for the 1R1C stochastic model, shown in Fig. 20 in Appendix A. As for the deterministic model, long sampling time can lead to a non-physical value of the HTC. While all the pre-filtering prevented the value to become non-physical for the deterministic model, only the moving-average filter and the ACS have the same effect for the stochastic model.

The value and variance of C_e are shown in Fig. 12. As long as the sampling time is shorter than the system dynamics (i.e. T_s equal 2.5 min), the value of C_e is independent of the training period and its variance is limited. Close to the C_{eff} of 3.9 kWh/K, the value of C_e is meaningful from a physical point of view. When the sampling time increases, the behavior should be distinguished with and without the application of an ACS. When the ACS is applied, the value and variance of C_e are regular even with long sampling time. The ACS has a strong positive effect on the physical plausibility of C_e. With ACS, pre-filtering has a limited influence on the results. Without ACS, the parameter value and variance become erratic with increasing T_s. Some values are so high that they fall outside the y-axis limit of the graph. In addition, no clear trend can be found on the influence of the pre-filtering and training period.

The same phenomenon is observed for the value and variance of C_i in Fig. 13. Nonetheless, there is one aspect that differs from C_e. As for the deterministic model with ACS, the values of C_i with the corresponding stochastic version also tends to increase with the sampling time. A possible explanation for this phenomenon has been given in the previous subsection.

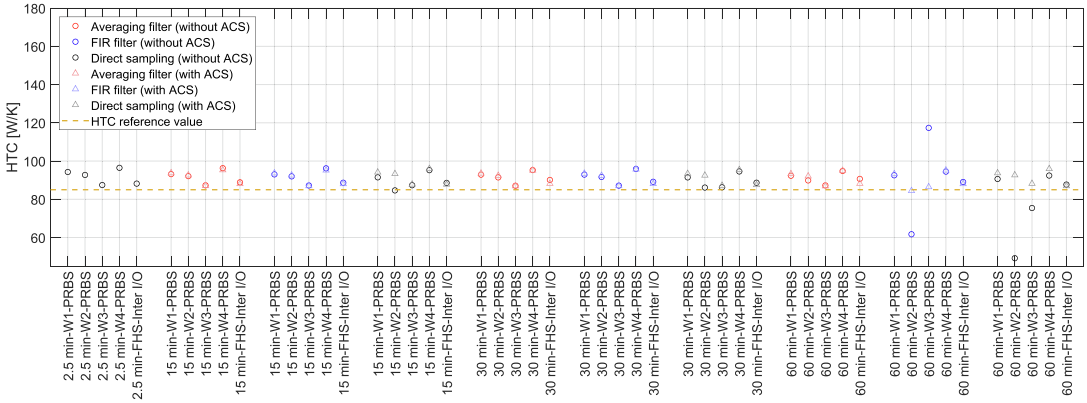

Fig. 11. Identified HTC of the 3R2C stochastic model for the cases 1,2,3,4 and 14, different sampling times and pre-filtering techniques; cases with ACS are shown by triangles in lighter colors.

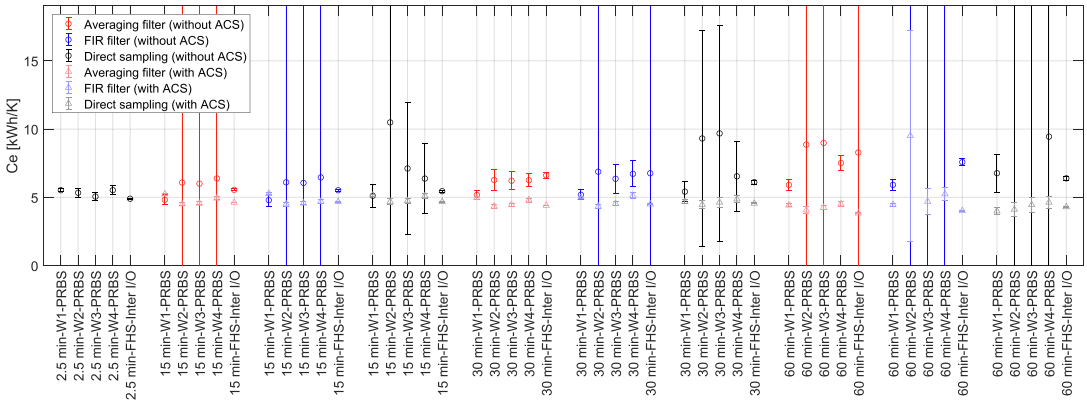

Fig. 12. Identified C_e of the 3R2C stochastic model for the cases 1,2,3,4 and 14, different sampling times and pre-filtering techniques; cases with ACS are shown by triangles in lighter colors.

From all the results of the stochastic models, several conclusions can also be drawn. First, the identified parameters are strongly dependent on the sampling time. The identified parameters are always consistent if the T_s is taken small compared to the shortest time of the system T_{min} (influenced by the excitation). It is only when T_s gets equivalent or larger than the building dynamics that the parameters are getting non-physical without ACS, especially the thermal capacitances. The second conclusion is that ACS prevents the parameter value and variance to get non-physical for large T_s. With ACS, the uncertainty of the parameters remains limited and their value remains physically plausible. Also with ACS, the values identified are mainly based on the training dataset but to a much smaller extent than the deterministic model. Pre-filtering only has limited influence with ACS while the pre-filtering influence without ACS does not show a clear trend, sometimes improving or degrading results. Finally, like the deterministic model, the steady-state characteristics HTC is less influenced by the dataset and pre-processing than the thermal capacitances.

4.2. Performance of the optimizer

The performance of both optimizers defined in Section 3.2 is compared for a selected number of datasets (i.e. cases 1 to 4 and 14), with and without ACS, for both deterministic and stochastic models. Table 4 shows the optimizer that leads to the lowest prediction error for each test case. The symbol "D" represents the default *greyest* function, "G" represents the two-stage global optimization algorithm and the symbol "≈" is used when both optimizers lead to extremely close results in terms of prediction error and estimation of the model parameters. Only results for the sampling times of 2.5 and 30 min are presented in Table 4. However, the same conclusions are found for the other two sampling times (i.e. 15 and 60 min).

It is observed that the two optimizers have identical results for all the cases using a deterministic model, regardless an ACS is applied or not. However, global optimization generally performs better than the default *greyest* optimization for stochastic models without ACS. On the contrary, both optimizers have similar performance when ACS is applied. It means that ACS tends to preserve the physical plausibility of the model parameters when T_s is large but it also positively influences the convexity of the optimization problem. In general, results confirm that it is better to use global optimization. Otherwise, the obtained sets of parameters are possibly located at a local minimum which mainly depends on the initial guess of the parameters.

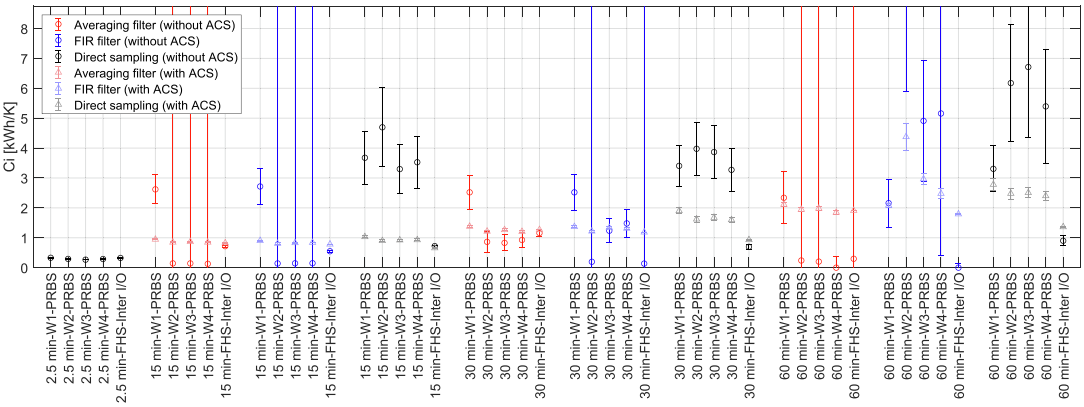

Fig. 13. Identified C_i of the 3R2C stochastic model for the cases 1,2,3,4 and 14, different sampling times and pre-filtering techniques; cases with ACS are shown by triangles in lighter colors.

Table 4
Optimizer leading to the lowest prediction error: each cell of the table has two symbols, one for the case without ACS (left) and the other with ACS (right); the symbol "D" means default greyest, "G" means global optimization and "≈" means equal performance.

Time (Ts)	Case	1R1C*DS* *(det)*	1R1CMA *(det)*	1R1C*FIR* *(det)*	3R2C*DS* *(det)*	3R2CMA *(det)*	3R2C*FIR* *(det)*	1R1C*DS* *(sto)*	1R1CMA *(sto)*	1R1C*FIR* *(sto)*	3R2C*DS* *(sto)*	3R2CMA *(sto)*	3R2CMA *(sto)*
2.5 min	1	≈/≈	–	–	≈/≈	–	–	G/≈	–	–	G/≈	–	–
	2	≈/≈	–	–	≈/≈	–	–	G/≈	–	–	G/≈	–	–
	3	≈/≈	–	–	≈/≈	–	–	G/≈	–	–	G/≈	–	–
	4	≈/≈	–	–	≈/≈	–	–	G/≈	–	–	G/≈	–	–
	14	≈/≈	–	–	≈/≈	–	–	G/≈	–	–	G/≈	–	–
30 min	1	≈/≈	≈/≈	≈/≈	≈/≈	≈/≈	≈/≈	G/≈	G/≈	G/≈	G/≈	G/≈	G/≈
	2	≈/≈	≈/≈	≈/≈	≈/≈	≈/≈	≈/≈	G/≈	G/≈	G/≈	G/≈	G/≈	G/≈
	3	≈/≈	≈/≈	≈/≈	≈/≈	≈/≈	≈/≈	G/≈	G/≈	G/≈	G/≈	G/≈	G/≈
	4	≈/≈	≈/≈	≈/≈	≈/≈	≈/≈	≈/≈	G/≈	G/≈	G/≈	G/≈	G/≈	G/≈
	14	≈/≈	≈/≈	≈/≈	≈/≈	≈/≈	≈/≈	G/≈	G/≈	G/≈	G/≈	G/≈	G/≈

4.3. Simulation performance of the models

The simulation performance of the grey-box models, analyzed here using the NRMSE fitting, is another important aspect of the system identification. As expected, the second-order 3R2C model has better simulation performance than the first-order model and is used to illustrate the results. Again, only a limited set of results can be shown. The simulation performance of the 3R2C model trained on the FHS intermittent on–off dataset (i.e. case 14) is taken. This training period covers the whole space-heating season and leads to the lowest variance of the identified parameters in Section 4.1. Then, the simulation performance of the model trained on the case 14 is evaluated on cases 1 to 4, as cross-validation test cases. In simulation, the full length of each dataset is taken as the prediction horizon for both the deterministic and stochastic models. Fig. 14 and Fig. 15 illustrate the influence of the number of steps ahead on the NRMSE fitting for the 3R2C stochastic model and datasets 1 and 2. The NRMSE fitting for long k-step ahead prediction (i.e. more than two days) is slightly higher than that in a simulation. To study the influence of the data pre-treatment, the 3R2C is trained on case 14 with different sampling times as well as with and without pre-filtering.

Fig. 16 compares the simulation performance of the deterministic and stochastic models without ACS. For different T_s and pre-filtering approaches, the deterministic model has a more constant simulation performance than the corresponding stochastic model. For the deterministic model, the NRMSE fitting tends to slightly decrease with increasing T_s while it tends to increase for the stochastic models (except for the PRBS3 case). The deterministic model has generally a better simulation performance than its corresponding model in stochastic form even though this difference tends to disappear for large T_s. This conclusion is noteworthy as for deterministic models the value of the parameters is significantly influenced by the training period and some of the values are even not physically plausible. In other words, identifying a model with parameters that have a more physical value does not necessarily lead to a model with better simulation performance. If one is not interested in the characterization of the thermal properties but rather the simulation performance (like in MPC), results suggest that deterministic models can be more robust than stochastic models. This makes the resolution of the optimization problem to calibrate the model easier (as both local and global optimizer lead to the same parameters). In addition, it has been shown that pre-filtering techniques and T_s have a limited effect on model performance. This conclusion is important in the context of the design of MPC for small residential buildings where a control model should be identified at a low cost, potentially using a fully automated procedure.

Fig. 17 compares the simulation performance of the stochastic model with and without ACS. While the ACS tends to improve the physical plausibility of the model parameters and positively influence the optimization problem, it has in general a negative influence on the simulation performance of the model. As already mentioned, the NMRSE fitting generally increases with T_s for the stochastic models without ACS. This increase is less pronounced for the stochastic model with ACS even though the physical plausibility of the parameters has been improved. Two conclusions can be given. Firstly, it confirms that parameters that are more physically plausible do not

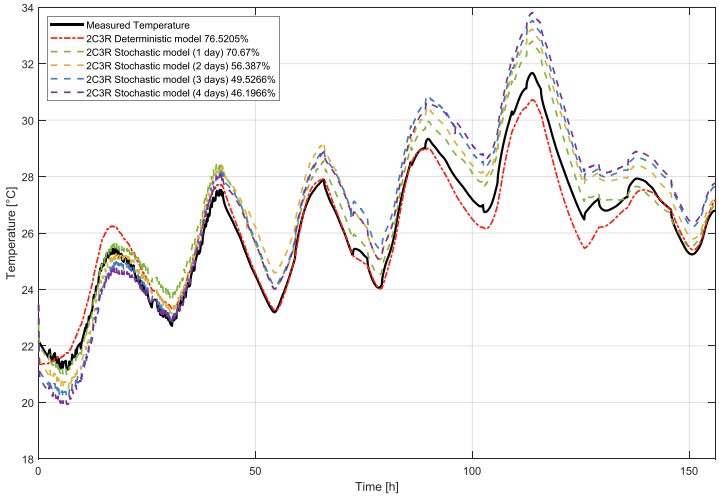

Fig. 14. Simulation performance of the deterministic and stochastic 3R2C models with different simulation length for the stochastic model, trained with the dataset 14 and validated with dataset 1.

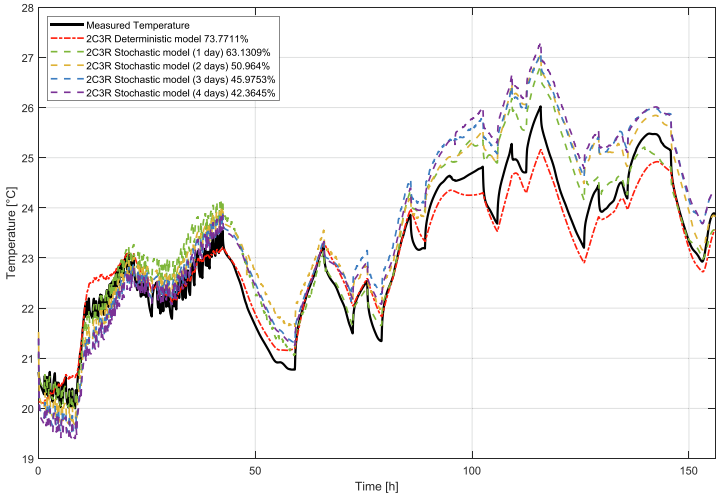

Fig. 15. Simulation performance of the deterministic and stochastic 3R2C models with different simulation length for the stochastic model, trained with the dataset 14 and validated with dataset 2.

necessarily lead to better simulation performance. Here, with large T_s and without ACS, the value of some parameters, such as C_e in Fig. 12, is non-physical but it nonetheless leads to better simulation performance. Secondly, the ACS showed to be a robust solution to characterize the thermal properties of the building and the resolution of the optimization problem. However, it appears from our investigations that the ACS comes at the price of lower simulation performance. Finally, none of the approaches investigated here manages to combine high physical plausibility and the highest simulation performance at large T_s.

5. Discussions

Based on the analysis of the results, some complementary discussions can be given:

- Even though ACS has a beneficial effect on the performance of the stochastic grey-box model, the fundamental reason for explaining this phenomenon is not given in the paper. From the authors' knowledge, no clear explanation has been given in the literature as well.

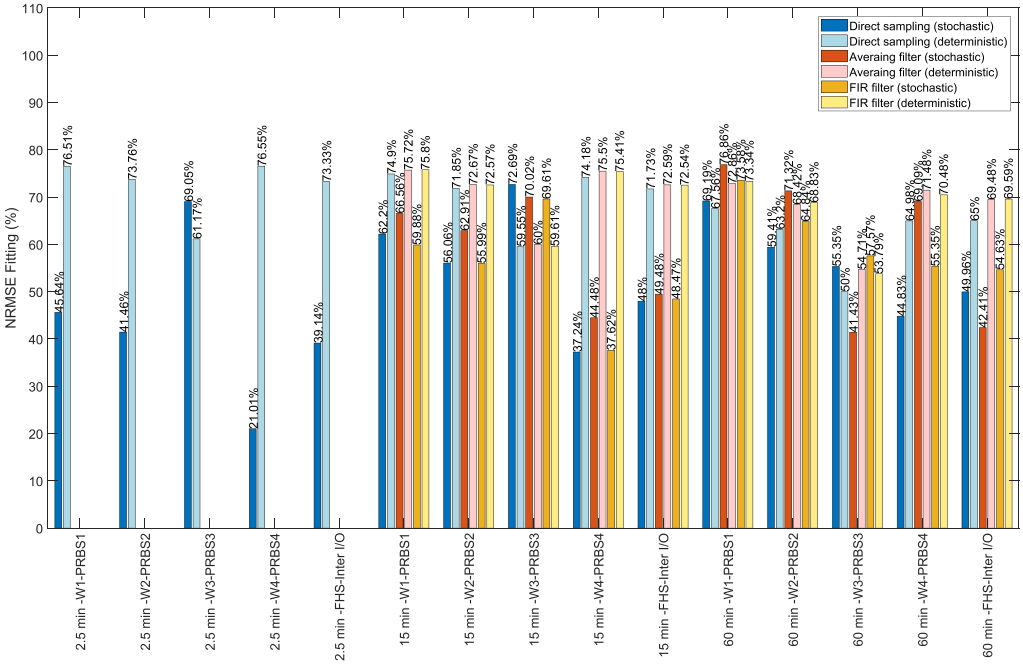

Fig. 16. Comparison of the simulation performance of the deterministic and stochastic 3R2C models trained on the dataset 14 without ACS and validated using the other datasets.

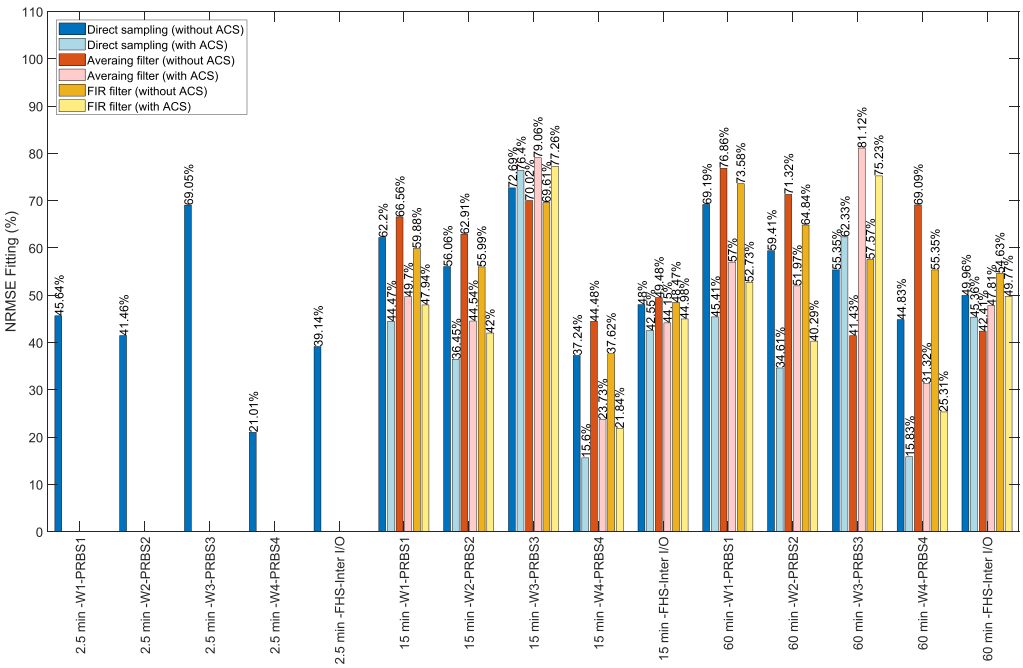

Fig. 17. Comparison of the simulation performance of the stochastic 3R2C model with and without ACS, trained with the dataset 14 and validated with datasets 1 to 4.

- The simulation performance is a good indicator of modeling accuracy in MPC applications. In Fig. 14, it can be seen that the k-step ahead prediction of two days (or more) has a NRMSE fitting close to simulation mode. It shows that the simulation performance is a good indicator even though the prediction horizon used in MPC is well shorter than the entire simulation period. However, even though it is a good indication, it is no mathematical proof that a model with higher simulation performance would systematically outperform another model with lower simulation performance when implemented in an MPC. It should be tested using an MPC test case and conclusions will most probably depend on the MPC test case selected.
- The results and conclusions of this paper are based on the stochastic grey-box model in innovation form. It is not proven that the results can be directly extrapolated to all formulations of the stochastic differential equations (for instance, the statistical grey-box modelling toolbox of CTSM-R [28]).
- The results and conclusions of this paper are based on the first- and second-order models. It is not guaranteed that the results can be extrapolated to a higher order. For instance, previous investigations have shown that overfitting may occur in third-order models which may lead to more complex analysis. In addition, the exact solar and internal gains have been applied to the grey-box models (i.e. they have not been identified). Furthermore, except for the solar gains, the distribution of the internal gains and the space-heating power between the two nodes of the 3R2C model has been fixed, based on the literature. If all these fixed parameters had also to be identified, it would have significantly increased the number of degrees of freedom and overfitting may have already appeared at second order [34].
- In real applications, the measurements would have some noise due to the sensor precision or the resolution of the data loggers. For some additional test cases not reported in the paper, artificial noise has been added to the IDA ICE measurements. For these cases, this artificial noise did not lead to changes in the conclusions. However, there are many different ways to define this measurement noise. For future work, a sensitivity analysis of the measurement noise should thus be performed in more systematic way to better understand how it affects the conclusions of this paper. Even though our study does not have measurement noise, it does have process noise. For instance, the IDA ICE model is multi-zone with a complex non-linear convective heat transfer between zones while the grey-box model is only mono-zone. Finally, in real applications, the air temperature measurements can be impacted by complex heat flows such as the building fabric, solar irradiation, low ventilation in the thermostat casing or occupant behavior. Such influences on the conclusions should also be analyzed in future work.
- The data series in this paper are based on virtual experiments using detailed dynamic simulations of one test case. As future work, it would be interesting to generalize results to other test cases and also using field measurements in real buildings.

6. Conclusions

The main objective of this paper is to investigate the influence of data pre-processing techniques and optimization approaches on the performance of grey-box models. Both the deterministic model and stochastic grey-box model in innovation form are investigated using the MATLAB system identification toolbox. The analysis is limited to first- and second-order grey-box models. Different excitation signals have been considered to generate input–output data. Three main aspects of grey-box models have been investigated: (1) the physical plausibility of the identified model parameters, (2) the performance of gradient-based compared to global optimizers and (3) the simulation performance. Among pre-processing techniques, the influence of the data pre-filtering (using an MA or an FIR), the sampling time (T_s) and the application of *anti-causal shift* (ACS) have been investigated. In general, it is shown that pre-filtering only has a limited influence so this is not discussed in detail in the conclusions. The conclusions appear to be distinct for the deterministic and stochastic models. Regarding the excitation signal, results also showed that the intermittent heating with on–off control of the electric radiators is a good excitation signal. It enables normal occupancy of the building and the collection of long data series as well as contain both slow daily and fast dynamics.

Regarding the physical plausibility of parameters:

- For deterministic models, the data pre-processing has a limited influence on the identified results. The identified parameters are strongly dependent on the types of excitation and the training period. The value taken by some of the parameters, especially the thermal capacitance, is not always physically plausible (even for the first-order model).
- For stochastic models, the identified parameters are physical if the sampling time (T_s) is much smaller than the higher frequency of the system to be identified.
- For large T_s and stochastic models, the parameters become non-physical without ACS (even for the first-order model). ACS is extremely beneficial to guarantee the physical plausibility of parameters, making the identified parameters not sensitive to the sampling time anymore.

Regarding the performance of the optimizer:

- For the deterministic and stochastic models, the sampling time (T_s) does not influence the optimizer performance.
- For the deterministic model, the identification results from the default gradient-based and global optimization routines are almost identical (with and without ACS). It seems non-convexity does not play a prominent role in this case.
- For the stochastic model, noticeable non-convexity effects already emerged from the first-order grey-box model (if ACS is not used). The two-stage global optimization leads to lower NRMSE than the default gradient-based optimizer and the resulting parameters have significantly different values. The non-convexity effects disappear if ACS is applied.

Regarding the simulation performance and the model application:

- The deterministic model has in general a higher simulation performance compared to the corresponding stochastic model. In our investigation, this difference tends to disappear for long sampling times. If one is not interested in the characterization of the thermal properties of the building but rather the simulation performance (important for MPC), results show that deterministic models can be a robust strategy as the simulation performance is not influenced much by the sampling time and the pre-filtering. In addition, the optimization problem appears more convex than the corresponding stochastic model. All these aspects can be valuable for the development of inexpensive control models for MPC applications where the identification procedure needs to be (partly) automated and where the information on the measurement accuracy and data acquisition system is limited. Finally, if the only focus is on simulation performance, it is worth questioning whether a grey-box model with parameters that have limited physical meaning have any added value compared to a black-box model. Therefore, in future work, it would be worth comparing the simulation performance of grey-box and black-box models.

- The ideal situation would be to combine physical plausibility with the highest simulation performance. Using stochastic models, a robust evaluation of the thermal properties requires the application of ACS which tends to reduce the simulation performance of the stochastic model. In this study, stochastic models appear more suitable for the characterization of the thermal performance of the building and results suggest this can be difficult to combine with the best simulation performance. However, it remains to be investigated whether the simulation performance of the stochastic model with ACS leads to acceptable accuracy when applied to an MPC.

CRediT authorship contribution statement

Xingji Yu: Conceptualization, Methodology, Software, Investigation, Validation, Visualization, Writing - original draft. **Laurent Georges:** Conceptualization, Methodology, Software, Validation, Investigation, Data curation, Visualization, Supervision, Project administration, Funding acquisition. **Lars Imsland:** Conceptualization, Writing - review & editing.

Declaration of Competing Interest

The authors declare that they have no known competing financial interests or personal relationships that could have appeared to influence the work reported in this paper.

Acknowledgments

This work is conducted in the framework of the Norwegian Research Centre on Zero Emission Neighbourhoods in Smart Cities (ZEN), co-funded by Research Council of Norway and industry partners. In addition, this reseach is also a contribution to IEA EBC Annex 81 on Data-Driven Smart Buildings. Finally, the authors would like to thanks Ning Guo that helped to review and edit the manuscript.

Appendix A

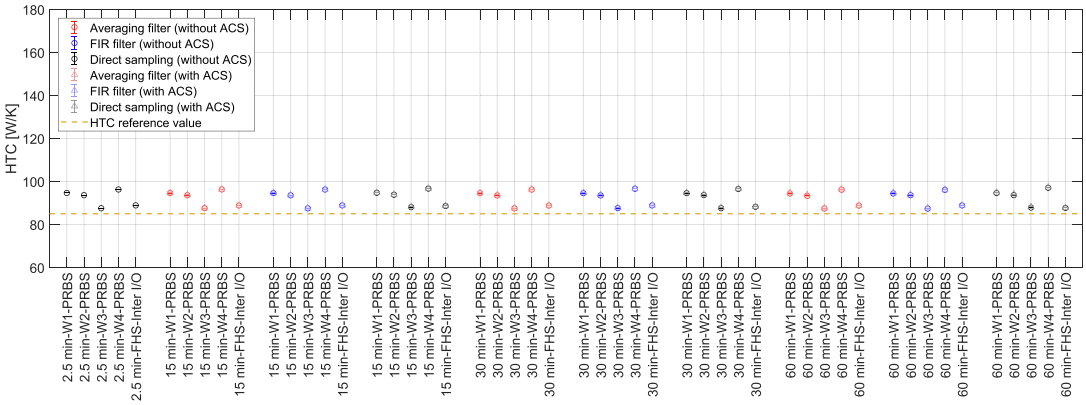

Fig. 18. Identified HTC of the 1R1C deterministic model for the cases 1,2,3,4 and 14, different sampling times and pre-filtering techniques; cases with ACS are shown by triangles in lighter color.

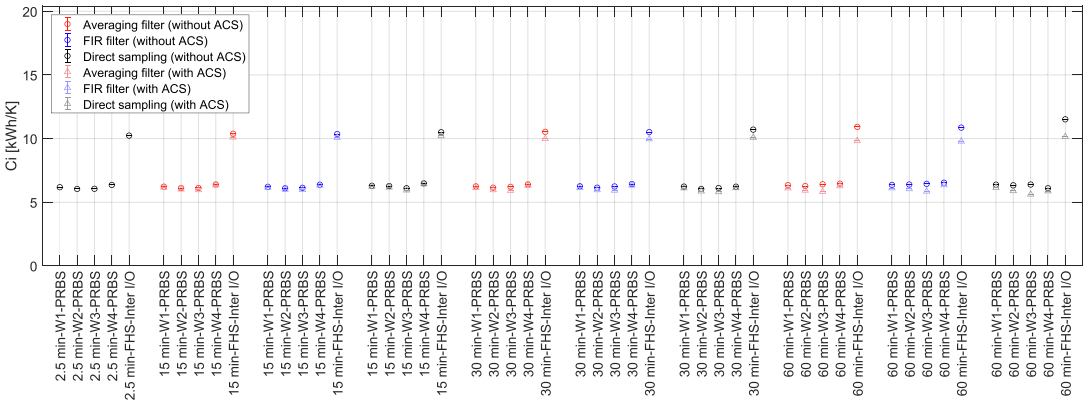

Fig. 19. Identified C_i of the 1R1C deterministic model for the cases 1,2,3,4 and 14, different sampling times and pre-filtering techniques; cases with ACS are shown by triangles in lighter colors.

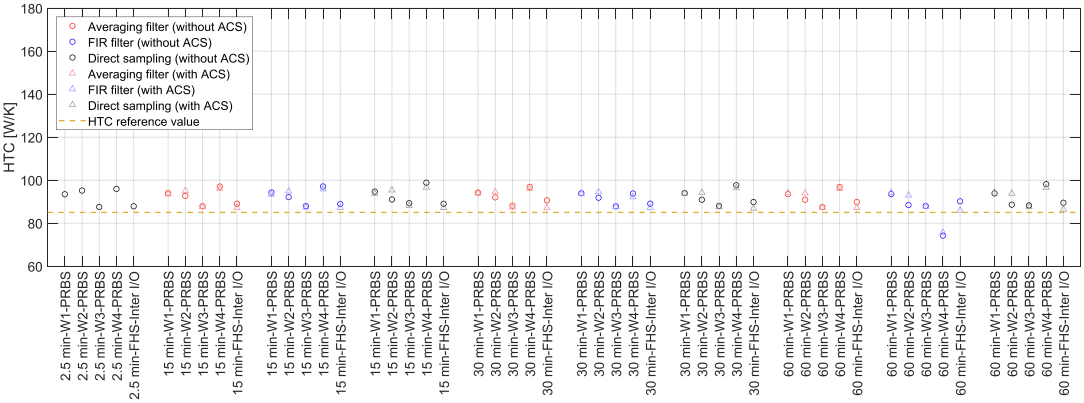

Fig. 20. Identified HTC of the 1R1C stochastic model for the cases 1,2,3,4 and 14, different sampling times and pre-filtering techniques; cases with ACS are shown by triangles in lighter colors.

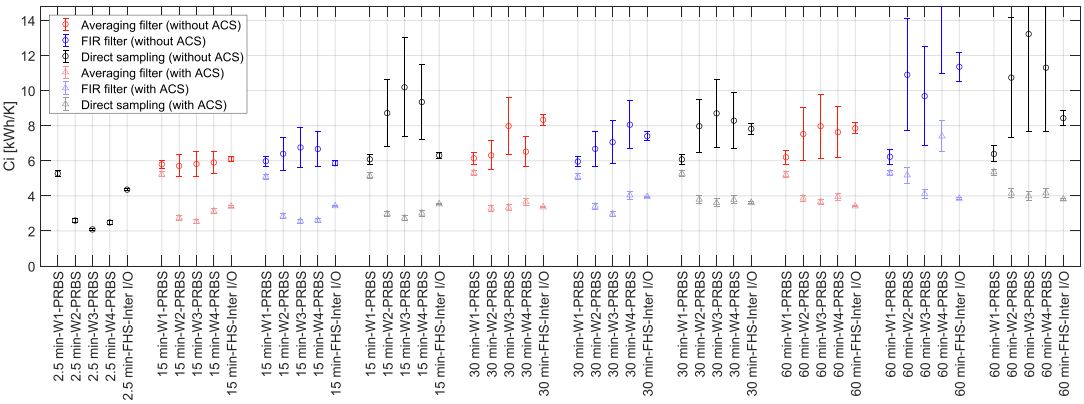

Fig. 21. Identified C_i of the 1R1C stochastic model for the cases 1,2,3,4 and 14, different sampling times and pre-filtering techniques; cases with ACS are shown by triangles in lighter colors.

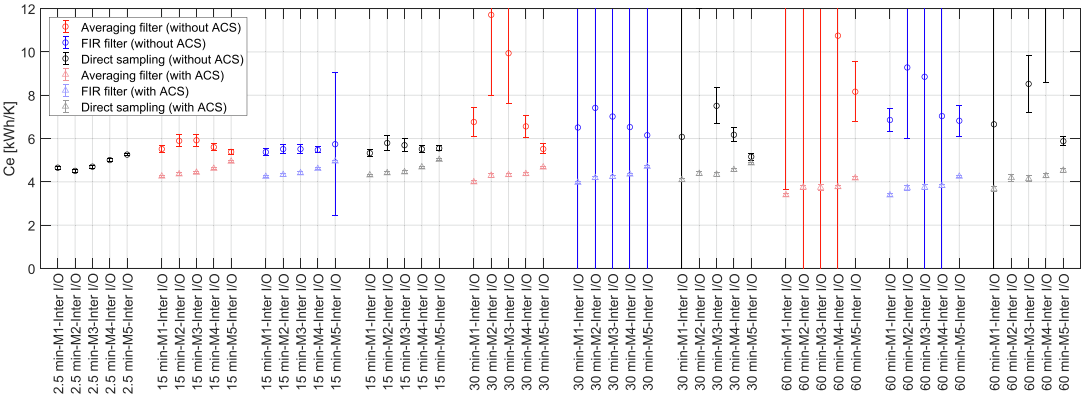

Fig. 22. Identified Ce of the 3R2C stochastic model for cases 9 to 13, different sampling times and pre-filtering techniques; cases with ACS are shown by triangles in lighter colors.

References

[1] M. Hu, F. Xiao, J.B. Jørgensen, S. Wang, Frequency control of air conditioners in response to real-time dynamic electricity prices in smart grids, Appl. Energy. 242 (2019) 92–106, https://doi.org/10.1016/j.apenergy.2019.03.127.

[2] S. Stinner, K. Huchtemann, D. Müller, Quantifying the operational flexibility of building energy systems with thermal energy storages, Appl. Energy. 181 (2016) 140–154, https://doi.org/10.1016/j.apenergy.2016.08.055.

[3] G. Steindl, W. Kastner, V. Stangl, Comparison of Data-Driven Thermal Building Models for Model Predictive Control, J. Sustain. Dev. Energy, Water Environ. Syst. 7 (2019) 730–742.

[4] P. Siano, Demand response and smart grids — A survey, Renew. Sustain. Energy Rev. 30 (2014) 461–478, https://doi.org/10.1016/j.rser.2013.10.022.

[5] A. Losi, P. Mancarella, A. Vicino, Integration of demand response into the electricity chain: challenges, opportunities, and Smart Grid solutions, John Wiley & Sons, 2015.

[6] E. Georges, B. Cornélusse, D. Ernst, V. Lemort, S. Mathieu, Residential heat pump as flexible load for direct control service with parametrized duration and rebound effect, Appl. Energy. 187 (2017) 140–153, https://doi.org/10.1016/j.apenergy.2016.11.012.

[7] J. Hu, H. Morais, T. Sousa, M. Lind, Electric vehicle fleet management in smart grids: A review of services, optimization and control aspects, Renew. Sustain. Energy Rev. 56 (2016) 1207–1226, https://doi.org/10.1016/j.rser.2015.12.014.

[8] L. Pérez-Lombard, J. Ortiz, C. Pout, A review on buildings energy consumption information, Energy Build. 40 (2008) 394–398, https://doi.org/10.1016/j.enbuild.2007.03.007.

[9] H. Harb, N. Boyanov, L. Hernandez, R. Streblow, D. Müller, Development and validation of grey-box models for forecasting the thermal response of occupied buildings, Energy Build. 117 (2016) 199–207, https://doi.org/10.1016/j.enbuild.2016.02.021.

[10] J. Le Dréau, P. Heiselberg, Energy flexibility of residential buildings using short term heat storage in the thermal mass, Energy. 111 (2016) 991–1002, https://doi.org/10.1016/j.energy.2016.05.076.

[11] G. Reynders, Quantifying the impact of building design on the potential of structural storage for active demand response in residential buildings, 2015. https://doi.org/10.13140/RG.2.1.3630.2805.

[12] S. Danov, J. Carbonell, J. Cipriano, J. Martí-Herrero, Approaches to evaluate building energy performance from daily consumption data considering dynamic and solar gain effects, Energy Build. 57 (2013) 110–118, https://doi.org/10.1016/j.enbuild.2012.10.050.

[13] Advanced Metering System (AMS) Status and plans for installation per Q2 2016, 2016. https://www.nve.no/energy-market-and-regulation/retail-market/smart-metering-ams/.

[14] K. Vortanz, P. Zayer, How energy providers can prepare for the rollout: Roadmap for the way into the future | Wie sich Energieversorger auf den Rollout vorbereiten können: Fahrplan für den Weg in die Zukunft, BWK-Energie-Fachmagazin. 67 (2015) 30–31.

[15] R. De Coninck, F. Magnusson, J. Åkesson, L. Helsen, Toolbox for development and validation of grey-box building models for forecasting and control, J. Build. Perform. Simul. 9 (2016) 288–303, https://doi.org/10.1080/19401493.2015.1046933.

[16] E. Atam, L. Helsen, Control-Oriented Thermal Modeling of Multizone Buildings: Methods and Issues: Intelligent Control of a Building System, IEEE Control Syst. 36 (2016) 86–111, https://doi.org/10.1109/MCS.2016.2535913.

[17] X. Pang, M. Wetter, P. Bhattacharya, P. Haves, A framework for simulation-based real-time whole building performance assessment, Build. Environ. 54 (2012) 100–108.

[18] D. Picard, J. Drgoňa, M. Kvasnica, L. Helsen, Impact of the controller model complexity on model predictive control performance for buildings, Energy Build. 152 (2017) 739–751, https://doi.org/10.1016/j.enbuild.2017.07.027.

[19] H. Wolisz, H. Harb, P. Matthes, R. Streblow, D. Müller, Dynamic simulation of thermal capacity and charging/discharging performance for sensible heat storage in building wall mass, in: Proc. Build. Simul. Conf., 2013.

[20] A.E. Ruano, E.M. Crispim, E.Z.E. Conceição, M.M.J.R. Lúcio, Prediction of building's temperature using neural networks models, Energy Build. 38 (2006) 682–694, https://doi.org/10.1016/j.enbuild.2005.09.007.

[21] A. Afram, F. Janabi-Sharifi, Review of modeling methods for HVAC systems, Appl. Therm. Eng. 67 (2014) 507–519, https://doi.org/10.1016/j.applthermaleng.2014.03.055.

[22] T.P. Bohlin, Practical Grey-box Process Identification, Springer, London (2006), https://doi.org/10.1007/1-84628-403-1.

[23] J.A. Crabb, N. Murdoch, J.M. Penman, A simplified thermal response model, Build. Serv. Eng. Res. Technol. 8 (1987) 13–19.

[24] R. De Coninck, L. Helsen, Practical implementation and evaluation of model predictive control for an office building in Brussels, Energy Build. 111 (2016) 290–298, https://doi.org/10.1016/j.enbuild.2015.11.014.

[25] Y. Zong, G.M. Böning, R.M. Santos, S. You, J. Hu, X. Han, Challenges of implementing economic model predictive control strategy for buildings interacting with smart energy systems, Appl. Therm. Eng. 114 (2017) 1476–1486, https://doi.org/10.1016/j.applthermaleng.2016.11.141.

[26] H. Viot, A. Sempey, L. Mora, J.C. Batsale, J. Malvestio, Model predictive control of a thermally activated building system to improve energy management of an experimental building: Part I—Modeling and measurements, Energy Build. 172 (2018) 94–103, https://doi.org/10.1016/j.enbuild.2018.04.055.

[27] S.F. Fux, A. Ashouri, M.J. Benz, L. Guzzella, EKF based self-adaptive thermal model for a passive house, Energy Build. 68 (2014) 811–817, https://doi.org/10.1016/j.enbuild.2012.06.016.

[28] P. Bacher, H. Madsen, Identifying suitable models for the heat dynamics of buildings, Energy Build. 43 (2011) 1511–1522, https://doi.org/10.1016/j.enbuild.2011.02.005.

[29] E. Palomo Del Barrio, G. Lefebvre, P. Behar, N. Bailly, Using model size reduction techniques for thermal control applications in buildings, Energy Build. 33 (2000) 1–14, https://doi.org/10.1016/S0378-7788(00)00060-8.

[30] G. Reynders, J. Diriken, D. Saelens, Quality of grey-box models and identified parameters as function of the accuracy of input and observation signals, Energy Build. 82 (2014) 263–274, https://doi.org/10.1016/j.enbuild.2014.07.025.

[31] X. Yu, L. Georges, M.D. Knudsen, I. Sartori, L. Imsland, Investigation of the Model Structure for Low-Order Grey-Box Modelling of Residential Buildings, in: Proc. Build. Simul. 2019 16th Conf. IBPSA, International Building Performance Simulation Association (IBPSA), 2019. https://doi.org/10.26868/25222708.2019.211209.

[32] German Association of Engineers. Calculation of transient thermal response of rooms and buildings e modelling of rooms. 91.140.10(VDI 6007), Düsseldorf: Beuth Verlag GmbH, 2012.

[33] International Organization for Standardization. Energy performance of buildings e calculation of energy use for space heating and cooling (ISO 13790:2008), Geneva, 2008.

[34] O.M. Brastein, D.W.U. Perera, C. Pfeifer, N.O. Skeie, Parameter estimation for grey-box models of building thermal behaviour, Energy Build. 169 (2018) 58–68, https://doi.org/10.1016/j.enbuild.2018.03.057.

[35] J.F. van Impe, P.A. Vanrolleghem, D.M. Iserentant, Advanced instrumentation, data interpretation, and control of biotechnological processes, Springer Science & Business Media, 2013.

[36] L. Ljung, A. Wills, Issues in sampling and estimating continuous-time models with stochastic disturbances, Automatica. 46 (2010) 925–931, https://doi.org/10.1016/j.automatica.2010.02.011.

[37] L. Ljung, System Identification Toolbox TM User ' s Guide, (2014)

[38] S. Norge, NS 3700: 2013 Criteria for passive houses and low energy buildings-Residential buildings, (2013)

[39] T. Johnsen, K. Taksdal, J. Clauß, X. Yu, L. Georges, Influence of thermal zoning and electric radiator control on the energy flexibility potential of Norwegian detached houses, E3S Web Conf. 111 (2019) 06030, https://doi.org/10.1051/e3sconf/201911106030.

[40] A.C. Bøeng, B. Halvorsen, B.M. Larsen, Kartlegging av oppvarmingsutstyr i husholdningene, Rapp. (2014/45. (2014).).

[41] S. Norge, SN/TS 3031: 2016 Energy performance of buildings, Calc, Energy Needs Energy Supply, 2016.

[42] L. Lennart, System identification: theory for the user, PTR Prentice Hall, NJ, Up. Saddle River, 1999, pp. 1–14.

[43] N.R. Kristensen, H. Madsen, S.B. Jørgensen, Parameter estimation in stochastic grey-box models, Automatica. 40 (2004) 225–237, https://doi.org/10.1016/j.automatica.2003.10.001.

[44] M.D. Knudsen, R.E. Hedegaard, T.H. Pedersen, S. Petersen, System identification of thermal building models for demand response - A practical approach, Energy Procedia. 122 (2017) 937–942, https://doi.org/10.1016/j.egypro.2017.07.426.

[45] H. Madsen, P. Bacher, G. Bauwens, A.-H. Deconinck, G. Reynders, S. Roels, E. Himpe, G. Lethé, IEA EBC Annex 58-Reliable building energy performance characterisation based on full scale dynamic measurements. Report of subtask 3, part 2: Thermal performance characterisation using time series data-statistical guidelines, (2016). https://www.iea-ebc.org/Data/publications/EBC_Annex_58_Final_Report_ST3b.pdf.

[46] K.J. Åström, Introduction to stochastic control theory, Courier Corporation (2012).

[47] K. Arendt, M. Jradi, M. Wetter, C.T. Veje, ModestPy: An Open-Source Python Tool for Parameter Estimation in Functional Mock-up Units, in: Proc. Am. Model. Conf. 2018, Oct. 9-10, Somb. Conf. Center, Cambridge MA, USA, 2019: pp. 121–130. https://doi.org/10.3384/ecp18154121.

[48] J. Kennedy, R. Eberhart, Particle swarm optimization, in: Proc. ICNN'95-International Conf. Neural Networks, IEEE, 1995: pp. 1942–1948.

[49] Particle Swarm Optimization Algorithm - MATLAB & Simulink - MathWorks, (n.d.). https://se.mathworks.com/help/gads/particle-swarm-optimization-algorithm.html#mw_522b9230-864b-47d1-a0db-1bf6c882d862.

[50] European Comittee for Standardization, ISO 13786:2017 - Thermal performance of building components - Dynamic thermal characteristics - Calculation methods, (2017).

PAPER 4

Yu X, Skeie KS, Knudsen MD, Ren Z, Imsland L, Georges L. Influence of data pre-processing and sensor dynamics on grey-box models for space-heating: Analysis using field measurements. *Building and Environment*, 2022; 108832.

RESEARCH PUBLICATIONS

Building and Environment 212 (2022) 108832

Contents lists available at ScienceDirect

Building and Environment

journal homepage: www.elsevier.com/locate/buildenv

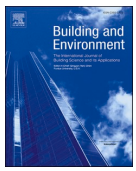

Influence of data pre-processing and sensor dynamics on grey-box models for space-heating: Analysis using field measurements

Xingji Yu [a,*], Kristian Stenerud Skeie [b], Michael Dahl Knudsen [c], Zhengru Ren [d], Lars Imsland [e], Laurent Georges [a]

[a] Department of Energy and Process Engineering, Faculty of Engineering, NTNU - Norwegian University of Science and Technology, Kolbjørn Hejes vei 1a, 7034, Trondheim, Norway
[b] Department of Architecture and Technology, Faculty of Architecture and Design, NTNU -Norwegian University of Science and Technology, Alfred Getz' vei 1, 7034, Trondheim, Norway
[c] Department of Civil and Architectural Engineering, Aarhus University, Inge Lehmanns Gade 10, 8000, Aarhus C, Denmark
[d] Department of Marine Technology, Marinteknisk senter, NTNU - Norwegian University of Science and Technology, Tyholt Otto Nielsens veg 10, 7052, Trondheim, Norway
[e] Department of Engineering Cybernetics, Faculty of Information Technology and Electrical Engineering, NTNU - Norwegian University of Science and Technology, O. S. Bragstads plass 2, 7034, Trondheim, Norway

ARTICLE INFO

Keywords:
Data pre-processing
Grey-box modeling
Building thermal mass
Model identifiability
Sensor measurement

ABSTRACT

A grey-box model is a combination of data-driven and physics-based approaches to modeling. For applications in buildings, grey-box models can be used as the control model in model predictive control (MPC) or to characterize the thermal properties of buildings. In a previous study using data generated from virtual experiments, the influence of data pre-treatment on the performance of grey-box models has been demonstrated. However, field measurement differs from data generated using building performance simulation (BPS). This is because the precision and accuracy, the location, and the dynamics of the sensors could be different. Consequently, this paper extends previous results and conclusions using a real test case of a highly-insulated residential building. The results confirm that data pre-processing has a minimal influence on the identified results (parameter values and simulation performance) for deterministic models. On the contrary, data pre-treatment influences the performance of stochastic models as follows. Firstly, large sampling time (T_s) can cause the parameters to become non-physical and can sometimes reduce the one-day ahead prediction performance. With large T_s, the anti-causal shift (ACS) proves to be beneficial to keep the parameters physically plausible while low-pass filtering can also contribute but to a lesser extent. With large T_s, ACS does not guarantee a higher one-day ahead prediction performance for stochastic models, whereas pre-filtering generally has a positive impact. Secondly, for the stochastic model, the sensor dynamics should be modeled if the sensor has a noticeable time constant to guarantee the physical plausibility of the parameters. Thirdly, the dynamics of the hydronic radiator do not need to be modeled if the time constant in the temperature sensors is larger than the radiator. These findings provide practical guidelines for grey-box modeling of buildings with field measurement data.

1. Introduction

The mathematical modeling of the thermal dynamics of a building is typically divided into three main categories [1]: white -, black-, and grey-box models. White-box models are based on physical laws (e.g. mass-, energy- and momentum balance equations). The white-box models are generally mathematically complex but have high accuracy. Black-box models are pure data-driven methods based on the measured time-series data from the system. This method needs sufficient training data to guarantee the accuracy of the model [2]. Grey-box modeling is a combination of these two techniques. This method takes the dominant physical processes to construct the model structure of the system and then fits the model parameters with the measurement data. Lumped resistance and capacitance models are used (i.e. RC models) to construct the grey-box model structure of a building, which means the thermal dynamics of the building are expressed by an electric circuit analogy [3,4]. Grey-box models are said to have better extrapolation properties

* Corresponding author.
E-mail address: xingji.yu@ntnu.no (X. Yu).

https://doi.org/10.1016/j.buildenv.2022.108832
Received 26 October 2021; Received in revised form 20 January 2022; Accepted 21 January 2022
Available online 26 January 2022

Nomenclature

RES	Renewable Energy Sources
DR	Demand Response
MPC	Model Predictive Control
BPS	Building Performance Simulation
RC	Resistance and Capacitance
SNR	Signal to Noise Ratio
PRBS	Pseudo-Random Binary Signal
PI	Proportional Integral
NRMSE	Normalized Root Mean Squared Error
MBE	Mean Bias Error
PSO	Particle Swarm Optimization
ACS	Anti-Causal Shift
DS	Direct Sampling
MA	Moving Average
FIR	Finite Impulse Response
Det	Deterministic Model
Sto	Stochastic Model
HTC	Heat Transfer Coefficient
HC	Heat Capacitance

than black-box models [5]. In addition, they have been widely applied to solve problems in building technologies, such as building load estimation, control and optimization, and building-grid integration [6,7]. The paper focuses on two main applications of grey-box models which are model predictive control (MPC) and characterization of the thermal properties of buildings using field measurements [6,8].

1. The emergence of MPC in buildings is related to the concept of energy flexibility and demand response (DR). The conventional electric energy system is undergoing dramatic changes due to the steadily rising share of renewable energy sources (RES). Power generation from RES is often decentralized and intermittent, which may cause considerable volatility to the electric grid. The power imbalance in the supply and demand sides can have severe implications for power quality and reliability [9]. Therefore, more flexible resources are needed to enable increasing penetration of intermittent RES. Demand response (DR) is gaining more attention in power system operations recently, driven by the smart grid concept [10]. Demand response means changes in energy use by the end-use customer from their normal consumption patterns in response to a specific penalty signal (e.g. price signal, CO_2 intensity factor for electricity signal) [10–13]. DR is closely related to the concept of energy flexibility defined by the IEA EBC Annex 67 as the ability of a building to manage its demand and generation according to local climate conditions, user needs and grid requirements [14]. Model predictive control (MPC) is considered a suitable technique for performing DR in a building [7,15] or for activating building energy flexibility [14]. Regarding space-heating, the thermal mass of a building can be a significant short-term heat storage to perform DR [16–20]. The exploitation of such thermal storage requires the indoor temperature to fluctuate within limits that are acceptable for the occupants. Previous studies have identified significant DR potential in using economic model predictive control (E-MPC) to exploit the thermal mass of residential buildings, see e.g. Refs. [21–23]. In these applications, grey-box models should enable adequate prediction to achieve good control performance.
2. Developing a suitable grey-box model with physically plausible (interpretable) parameters is appreciated from the building analysis point of view [19]. Physically reasonable parameters in grey-box models could contribute to characterizing the thermal properties of a building using field experiments, such as the overall heat transfer coefficient (HTC).

Data can be processed (or altered) by sensors, the data acquisition system (DAQ) or by the modeler before being used for model identification. Data pre-processing (or data pre-treatment) is acknowledged to have a key influence on the model identification results [24]. For instance, Ljung et al. [25] have analyzed this theoretically and demonstrated the strong influence of the sampling time. However, this topic has hardly been addressed in the specific field of grey-box models for building thermal dynamics. One exception is Madsen et al. [8] that mentioned the importance of data pre-processing in their guidelines, but they did not discuss the topic in detail in their report. Therefore, the main objective of the paper is to systematically investigate the influence of different data pre-processing techniques on the performance of grey-box models for the building thermal dynamics, with MPC and the physical plausibility of parameters in focus. In the past, this effect has been studied in Yu et al. [26] with deterministic and stochastic models. However, they used data generated by virtual experiments, namely multi-zone simulations using the building performance simulation (BPS) software IDA ICE [27]. The data pre-processing methods applied in this study are the sampling time, low-pass filtering and the anti-causal shift (ACS) [25]. ACS corresponds to a shift of the input data one step ahead (also equivalent to a backward shift of the output). Several main conclusions have been demonstrated in this previous study [26]:

- For deterministic models, the data pre-processing has limited influence on the identification results. However, the values of the parameters are strongly dependent on the training dataset and can sometimes be physically non-plausible.
- For stochastic models, the parameters are less dependent than the deterministic models on the training dataset. However, they become non-physical without ACS for large sampling time ($T_s > 15$ min). Large T_s does not alter the simulation performance of the stochastic model. ACS proved to be extremely beneficial to guarantee the physical plausibility of parameters with large T_s. Nevertheless, it generally has a negative influence on the simulation performance of the model.

As these important conclusions are based on virtual experiments, the first objective of the paper is to compare these conconclusions to a real test case based on field measurements. Field measurements deviate from virtual experiments in the following way:

- In reality, sensors have finite precision and accuracy, while the temperature and power data exported from BPS is perfect (i.e., noise-free observations).
- In most BPS software, the air volume of each room is supposed to be isothermal. In reality, the temperature field in a room is not uniform. Two important effects should be considered. Firstly, the room air can present significant temperature stratification, especially when the heat emitter is close to maximum power. Secondly, the sensors are usually mounted on a wall in a casing. For sudden changes in the indoor temperature, the measured value with a wall-mounted sensor may thus differ from the real air temperature. The thermal dynamics of the sensor due to the casing can also be seen as a form of implicit data pre-treatment if the sensor dynamics are not modeled.

This paper uses measurement data from an experimental building, the ZEB Living Lab [28,29] to compare the conclusions that were originally based on virtual experiments [26]. Three complete datasets of the indoor temperature corresponding to different sensor locations are available:

- Several temperature sensors without casing are mounted at different heights on a vertical bar located in the middle of different rooms. The

averaging of these measurements gives an approximation of the volume-averaged indoor air temperature, which is a good representation of the indoor air temperature T_i of a mono-zone model (i.e. one zone for the entire building). In addition, the volume-average indoor temperature is less sensitive to the vertical temperature stratification than the measurement from a single sensor.

- For market penetration, it is better to limit the number of temperature sensors to one in each room. Thus, it is important to investigate the possibility of identifying a proper grey-box model with measurements from a single temperature sensor. Firstly, one temperature sensor is located on a vertical bar at a medium height in the living room. The stratification effect at mid-height should be lower than the top and low locations in the room. Secondly and probably the most realistic configuration, another temperature sensor is mounted on a wall at the same mid-height location as the previous sensor (placed on the bar).

The second objective of the paper is to analyze how the type of indoor temperature measurement influences the performance of the grey-box models.

The main objective is to identify the specific influence of different data pre-processing techniques on the grey-box model performance. Other phenomena that could have an impact on the model performance, such as overfitting, should be removed from the analysis. Therefore, model structure selection is performed in detail in this paper before starting to analyze the influence of the data pre-treatment. It starts with a review of the literature regarding the structure of grey-box models. This results in the selection of a set of structures to be evaluated. The evaluation includes the analysis of structural and practical identifiability of the selected models, their prediction performance and physical plausibility of the parameters. Checking structural identifiability is the prerequisite in the model identification process [30,31]. This property guarantees that the parameters can be uniquely determined from the input-output data under ideal conditions of noise-free observations and error-free model structure. The structural identifiability of the candidate models in this study is verified using DAISY software [30]. However, field measurement data always contain noise and error, which challenges the practical identifiability of the model. Therefore, the prediction performance and the physical plausibility of parameters are taken as the criteria for the model selection. Finally, for stochastic models, a cumulative periodogram is used as an additional criterion to prove that the model is complex enough to capture the building dynamics.

The remainder of the paper is structured as follows. Section 2 provides information on the experimental setup, which includes the building geometry, measurement devices, the definition of test cases and the boundary conditions. Section 3 describes the methodology of this study, including the grey-box model structure and data pre-processing techniques used for this study. The algorithm to identify the grey-box model parameters is also outlined, followed by the definition of key performance indicators (KPIs). Section 4 gives the results and is divided into three main aspects. The most suitable model structure is selected with the original data with 5 min sampling time and the volume-averaged temperature. Then, the influence of data pre-processing and the sensor selection is presented. Finally, conclusions are presented in Section 5.

2. Description of experiments

2.1. Case building

The experiments performed in this study were carried out in the ZEB Living Lab, a single-family, zero-emission house with a heated floor area of about 100 m^2 on the campus of the Norwegian University of Science and Technology (NTNU) in Trondheim. The building envelope has a wooden frame with mineral wool measuring 35–40 cm and a glazing ratio of 0.2. The space-heating can be floor heating, a central radiator, or ventilation air. The ventilation system is equipped with a heat recovery unit. By operating the doors in the building, four zones can be created (bedroom west, bedroom east, bathroom, and living areas). The appearance of the building and the internal layout of the Living Lab is shown in Fig. 1. This study is based on two sets of experiments in this building with different space-heating emission systems and different periods of the space-heating season. Data from using two different heat emitters are used to make the conclusions more general.

The first set of experiments (from the 18th April to 15th May 2017) used an electric heater for space-heating. Detailed information on the measurement setup and data can be found in previous work [28,32]. The corresponding length of these three experiments are 6 days, 11 days and 7 days, respectively. The electric heater of 2.6 kW was placed in the center of the building (the heater is marked in red in Fig. 1 (b)). A pseudo-random binary signal (PRBS) has been applied to the electric heater to excite the thermal dynamics of the building. PRBS is a periodic and deterministic signal with white noise properties and a high signal-to-noise ratio (SNR). The PRBS signal activates the dynamic system at a broad range of frequencies.

Four experiments were carried out, and only the last three were successful. The successful experiments are named Experiments 2, 3, and 4 (i.e., Experiment 1 was discarded). The dataset has a time interval of 5 min. The measurements include the outdoor temperature, indoor air temperatures, global solar irradiation and electricity consumption, including the radiator power (Q_h). To avoid modeling the air-handling unit (AHU), the ventilation losses from the mechanical ventilation are introduced as one input to the grey-box model in this study. These ventilation losses are explicitly pre-calculated with the measured temperature difference between the supply and exhaust ventilation air combined with the measured airflow rate (constant air volume, CAV). The electric heating system has negligible thermal inertia compared to the building envelope, so it is assumed that the dynamics of the radiators play a limited role. Experiments 2 and 4 were conducted with internal doors opened, which theoretically should lead to a more uniform spatial distribution of the air temperature inside the building while all the doors were closed in Experiment 3. Air was pre-heated using a heating coil in Experiment 4 only. The building is unoccupied in all the experiments, but electric dummies operated by a control schedule have been used leading to realistic internal gains.

2.2. Experiment with the hydronic radiator

The experiment with the hydronic radiator was initially performed to investigate cost-effective MPC implementation (E-MPC) with control of the hydronic radiator in a Norwegian zero-emission building (Living Lab) [29]. The experiment lasted for approximately one month (from mid February to mid March 2017), with an 18-day excitation phase and an E-MPC operation phase of two weeks. A randomly generated binary signal switching the radiator temperature set-point between 21 °C and 24 °C was created to excite the thermal dynamics of the building and collect measurements for training the model. This new training dataset is based on six days in February and is named here as Experiment 5. The dataset has a time interval of 5 min.

The hydronic radiator has a rated power of 4.7 kW (at rated temperature 75 °C/65 °C) and was in the same place as the electric heater. The supply water temperature was maintained at about 55 °C leading to a maximum radiator power of 2.5 kW. The thermostatic valve in the radiator adjusts the mass flow using a proportional-integral (PI) controller to track the set-point temperature. Compared to the electric heater, the thermal mass of the hydronic radiator with 113 kg of steel cannot be neglected. The power delivered to the hydronic radiator (Q_h) is measured by an energy meter based on the difference between supply and return temperatures. When the hydronic radiator is switched on, the initial water temperature in the radiator is close to the indoor air temperature. Due to the thermal mass of the radiator, it takes time for the return temperature to heat up and reach steady-state (when the power

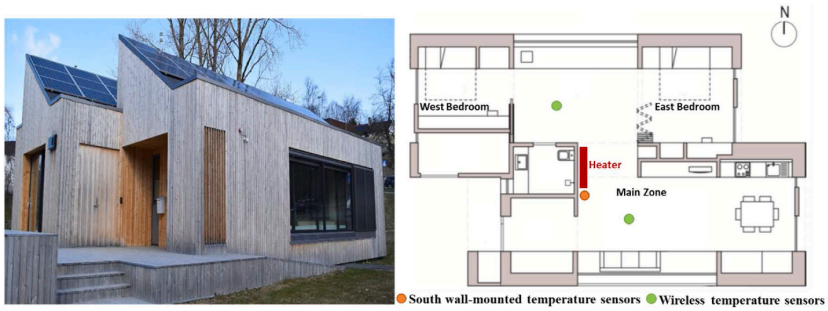

(a) (b)

Fig. 1. View of the ZEB Living Lab (a) and floor plan of the ZEB Living Lab with temperature sensor location (b).

delivered to and emitted by the radiator are equal). This makes a large difference in supply and return temperatures at the beginning, leading to a very high start-up peak for Q_h. The maximum emitted power of the radiator in steady-state is around 2.5 kW, while the maximum delivered power during start-up periods is around 4.0 kW. This confirms that the thermal dynamics of the hydronic radiator are significant. The summary of all the experiments used in this study is given in Table 1.

2.3. Indoor temperature measurement

In the experiments with the electric heater, PT100 sensors with an accuracy of ±0.1 K are placed at different locations in the building; see details in Ref. [28]. This leads to the definition of three datasets:

- Two available datasets correspond to different placement of PT100 temperature sensors without casing and with wireless transmitters. They are placed in a vertical bar in the middle of the two living rooms (see green dots in Fig. 1 (b) and Fig. 2 (a)). For each bar, the height of the six sensors is 0.18 m, 0.95 m, 1.6 m, 1.7 m, 2.3 m and 3.4 m, respectively. The *volume-averaged temperature* of the building is calculated using the measurement from all the sensors placed in the vertical bars and evaluated using the volume average at each horizontal layer. The *single sensor without casing* dataset corresponds to the measurement at 1.6 m in the living room south. The height of 1.6 m is close to the middle height of the building, where the influence of stratification is expected to be minimal (meaning that the measured temperature at 1.6 m is the closest to the volume-averaged temperature).
- The third dataset is based on PT100 sensors mounted on the wall in a casing (see the orange dot in Fig. 1 (b) and Fig. 2 (b)). The height of the wall-mounted sensors is 0.1 m, 0.8 m, 1.6 m, 2.4 m and 3.2 m, respectively. The third dataset corresponds to the measurement of a *single wall-mounted sensor* mounted in the south of the living room at the height of 1.6 m.

In the experiments with the hydronic radiator, only the temperature measurements from the wall-mounted temperature sensor are available.

Fig. 3 shows the temperature reading from the wireless temperature sensors with different heights (0.18 m, 1.6 m and 3.4 m) and the wall-mounted temperature sensor (1.6 m) against the volume-averaged temperature. The stratification of the temperature of the wireless temperature sensors at different heights can be observed. The stratification gets larger when the solar radiation or the radiator power is large. The reason for choosing the sensor in the south was to capture the influence of solar radiation. The thermal dynamics of the wall-mounted sensor can also be observed. The reading from the wall-mounted sensor is smoother compared to the volume-averaged temperature and the readings from the single wireless temperature sensors.

3. Methodology

3.1. Grey-box model structure

The structure of the grey-box models is derived from the conservation of energy. The physics modeled by the grey-box models is the heat transfer between the building and its outdoor environment, the solar radiation and internal gains.

The ZEB Living Lab is super-insulated with an efficient heat recovery of the ventilation air. These two points lead to limited temperature differences between rooms [33] (compared to the temperature difference between indoor and outdoor air) even if internal doors are closed. Consequently, the building can be modeled as one thermal zone (i.e., the mono-zone model with a unique node to represent the indoor temperature). Previous studies [29,32,34] confirmed that a mono-zone grey-box model is able to make an accurate prediction on the air temperature in the ZEB Living Lab, for closed and open internal doors.

Grey-box modeling is a very common approach and a considerable amount of research has already been applied to this method. In their study, Viot et al. [35] provided a comprehensive list of research papers on MPC that used RC models. Bacher and Madsen [36] identified a suitable model using data obtained from an unoccupied office building. The probability ratio tests were used to analyze models of different orders. The results showed that increasing the model order from the third-order does not substantially improve the results. In Ref. [37], Berthou et al. found that the second-order model performs best for occupied office buildings. Braun et al. [38], Hu et al. [39] and Goyal [40] used the second-order model as the base component for the multi-zone model of the building. It was concluded that the

Table 1
Summary of the four experiments, "Full set" means all measurements of volume-averaged, single sensor (no casing), wall-mounted sensor are available.

Experiments	Radiator	Door	Sampling time	Period	Use	Temperature Sensor
2	Electric	Open	5 min	18/04–24/04 (2017)	Validation	Full set
3	Electric	Closed	5 min	27/04–08/05 (2017)	Validation	Full set
4	Electric + AHU	Open	5 min	08/05–15/05 (2017)	Training	Full set
5	Hydronic	Open	5 min	22/02–27/02 (2019)	Training	Wall-mounted

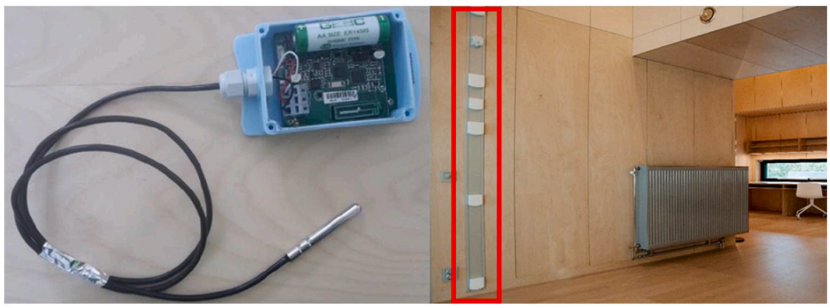

(a) (b)

Fig. 2. Wireless temperature sensors (a) and wall-mounted temperature sensors (b).

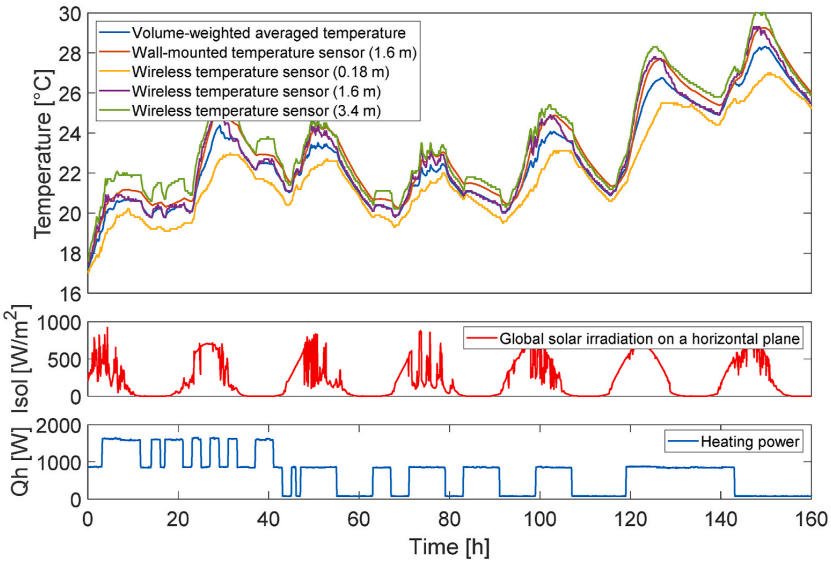

Fig. 3. Comparison of different indoor temperature sensors, global solar irradiation on a horizontal plane and heating power of the electric heater for Experiment 4.

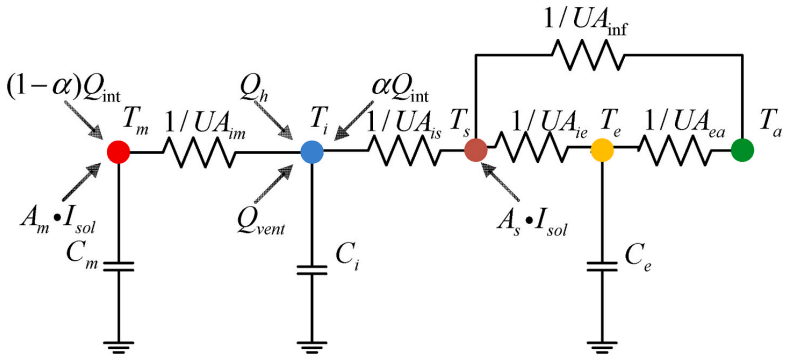

Fig. 4. Structure of the 5R3C model.

second-order model is sufficient for good prediction results for indoor temperature and heating power by Palomo Del Barrio et al. [41] and Reynders et al. [42]. Brastein et al. [43] showed that deterministic grey-box models at second-order could face the problem of practical identifiability. Yu et al. [34] proposed two grey-box model structures derived from VDI 6007 [44] and ISO 13790 [45]. The results were that with few measurements and a large number of unknown parameters, the identified parameters could easily become non-identifiable. Furthermore, due to overfitting and convergence issues, Reynders et al. [42] concluded that heat flux measurements were needed to ensure observability for higher-order models (i.e. fourth- and fifth-order models). Thus, based on these previous studies, our paper only considers the model structure up to the third-order.

As a result, seven mono-zone model structures limited to third-order have been taken from the existing literature [36,42,46]. The selection process will determine the best model structure to be used to investigate the specific influence of data pre-processing. These seven models correspond to different combinations of RC components and splitting factors for the distribution of internal gains between the nodes. According to report [28], some sensors in the ZEB Living Lab at specific locations were directly exposed to solar radiation at certain periods of the day, which makes some of the measurements an unsatisfactory representation of the air temperature. The dataset in Experiment 4 with open internal doors is chosen as the training dataset for the case with the electric heater. Only the 5 min dataset is used for the model selection to avoid aliasing errors. The datasets in Experiments 2 and 3 were used as the validation datasets to analyze the prediction performance of the models. Structural identifiability is a prerequisite for system identification [47], which refers to the theoretical possibility of determining the parameter values from the input and output data. Thus, the structural identifiability of the candidate model structures has been tested by the DAISY software [30,48] before implementing the identification process. The result is that all the seven grey-box model structures are structurally identifiable. The most complex structure is the 5R3C model and is shown in Fig. 4. Other model structures are obtained by simplification and can be found in the Appendix. The physical meaning of the model parameters is listed in Table 2.

The corresponding state-space model of Fig. 4 is given by:

Table 2
The physical interpretation of the parameters of all grey-box models.

Parameters	Physical interpretation and unit
T_i	Temperature of the internal node (i.e., indoor air, furniture) [°C].
T_e	Temperature of the external walls [°C].
T_s	Temperature of the internal wall surfaces of external walls [°C].
T_m	Temperature of the internal walls [°C].
T_a	The outdoor (or outdoor) temperature [°C].
C_i	Heat capacity including the thermal mass of the air, the furniture [kWh/K].
C_e	Heat capacity of the node external wall for the second-order and third-order models [kWh/K].
C_m	Heat capacity of the node internal wall for the third-order model [kWh/K].
UA	Overall heat transfer coefficient (HTC) between T_i and T_a [kW/K].
UA_{ie}	Heat conductance between the building envelope and the interior [kW/K].
UA_{ea}	Heat conductance between the outdoor and the building envelope [kW/K].
UA_{inf}	Heat conductance between the outddoor and the interior node (components with negligible thermal mass, like windows and doors) [kW/K].
UA_{im}	Heat resistance between the internal thermal mass and the interior node [kW/K].
UA_{is}	Heat resistance between the indoor wall surface and the interior node [kW/K].
Q_{int}	Internal heat gain from artificial lighting, people and electric appliances [kW].
Q_h	Heat gain delivered to the heat emitter [kW].
Q_{vent}	Heat gain from the ventilation (pre-computed using measurements) [kW].
I_{sol}	Global solar irradiation on a horizontal plane [W/m^2].
A_i	The effective window area of the building corresponding to T_i [m^2].
A_e	The effective window area of the building corresponding to T_e [m^2].
A_m	The effective window area of the building corresponding to T_m [m^2].
A_s	The effective window area of the building corresponding to T_s [m^2].
α	Fraction of internal gains injected to the internal node.

3.2. Model identification tool and optimization

Both the deterministic and stochastic models are investigated using the MATLAB system identification toolbox [49]. The stochastic models are formulated as an extension of deterministic models (K = 0) [8]. The generic equations of the stochastic linear state-space model in innovative form are expressed as:

$$\frac{dx}{dt} = Ax(t) + Bu(t) + Ke(t) \tag{3}$$

$$y(t) = Cx(t) + e(t) \tag{4}$$

$$\begin{bmatrix} \dot{T_e}(t) \\ \dot{T_i}(t) \\ \dot{T_m}(t) \end{bmatrix} = \begin{bmatrix} -\frac{(UA_{ie}+UA_{ea})}{C_e} + \frac{UA_{ie}^2}{C_e\cdot(UA_{is}+UA_{ie}+UA_{\inf})} & \frac{UA_{ie}\cdot UA_{is}}{C_e\cdot(UA_{is}+UA_{ie}+UA_{\inf})} & 0 \\ \frac{UA_{ie}\cdot UA_{is}}{C_i\cdot(UA_{is}+UA_{ie}+UA_{\inf})} & -\frac{(UA_{im}+UA_{is})}{C_i} + \frac{UA_{is}\cdot UA_{is}}{C_i\cdot(UA_{is}+UA_{ie}+UA_{\inf})} & \frac{UA_{im}}{C_i} \\ 0 & \frac{UA_{im}}{C_m} & -\frac{UA_{im}}{C_m} \end{bmatrix} \begin{bmatrix} T_e(t) \\ T_i(t) \\ T_m(t) \end{bmatrix} + \begin{bmatrix} \frac{UA_{ea}}{C_e} + \frac{UA_{ie}\cdot UA_{\inf}}{C_e\cdot(UA_{is}+UA_{ie}+UA_{\inf})} & \frac{UA_{ie}\cdot UA_{\inf}}{C_e\cdot(UA_{is}+UA_{ie}+UA_{\inf})} & 0 & 0 & 0 \\ \frac{UA_{is}\cdot UA_{ie}}{C_i\cdot(UA_{is}+UA_{ie}+UA_{\inf})} & \frac{UA_{is}\cdot A_s}{C_i\cdot(UA_{is}+UA_{ie}+UA_{\inf})} & \frac{\alpha}{C_i} & \frac{\alpha}{C_i} & \frac{1}{C_i} \\ 0 & \frac{A_m}{C_m} & \frac{1-\alpha}{C_m} & \frac{1-\alpha}{C_m} & 0 \end{bmatrix} \begin{bmatrix} T_a(t) \\ I_{sol}(t) \\ Q_{\text{int}}(t) \\ Q_{vent}(t) \\ Q_h(t) \end{bmatrix} \tag{1}$$

$$y(t) = \begin{bmatrix} 0 & 1 & 0 \end{bmatrix} \begin{bmatrix} T_e(t) \\ T_i(t) \\ T_m(t) \end{bmatrix} \tag{2}$$

where x is the state vector, A, B and C are the system matrices, u is the input vector (i.e. T_a, I_{sol}, Q_{int}, Q_h) and y is the output (i.e. indoor temperature, T_i). K is the disturbance matrix of the innovation form (Kalman gain) [50]. The matrices A, B, C and K are functions of the model parameters (θ). The continuous-time model is discretized to identify the model parameters using discrete-time series measurement. The time discretization in the MATLAB system identification toolbox assumes piecewise-constant input data during each time interval (i.e. zero-order hold).

Yu et al. [26] proved that the global optimization routine is more likely to avoid the local optimum compared to the pure gradient-based optimization routine. Wang et al. [51] successfully used the swarm-based optimization algorithm to estimate the parameters of thermal dynamic models. Thus, this paper also takes the global optimization routine to identify the parameters. The global optimization routine resorts to the heuristic particle swarm optimization (PSO) at the first stage. Then the default gradient-based optimization function (*greyest*) in the MATLAB identification toolbox is applied in the second stage to further polish the results. The objective function $f(x)$ of the optimization is defined as Equation (5).

$$f(x) = \sqrt{\frac{\sum_{k=1}^{N} ||y_k - \hat{y}_k(\theta)||^2}{N}} \tag{5}$$

where y_k is the measurement output, while $\hat{y}_k(\theta)$ is the prediction of the model (i.e., a simulation for the deterministic model and one-step ahead prediction for the stochastic model).

3.3. Data pre-processing techniques

Three distinct data pre-treatments are investigated in the paper. They are sampling, low-pass filtering and anti-causal shift (ACS). The original dataset has a sampling time (T_s) of 5 min which is faster than the highest frequency of the input signal (T_{min}), such as the PRBS signal. Ljung et al. [25] demonstrated that longer sampling time with $T_s > T_{min}$ can lead to non-physical value and variance for the identified parameters, as confirmed by Yu et al. [26] in the context of the thermal dynamics of the building. To investigate this effect, sampling times of increasing duration are considered in our investigations, namely 15, 30 and 60 min. Before resampling the data, a low-pass filter can be applied. This leads to three scenarios:

- *Direct sampling (DS)*: Sampling at T_s without pre-filtering, which may cause large aliasing errors for large T_s.
- *Moving-average (MA) filter*: The original 5 min data is averaged over a period T_s in the past before sampling. This can significantly decrease the aliasing error and it also conserves the integral of the physical quantity, such as energy.
- *Finite impulse response (FIR) filter*: A FIR with a cut-off frequency of $1/T_s$ is applied before sampling. The frequency content higher than the cut-off frequency is removed, which leads to a negligible aliasing error (if the FIR is designed at a sufficient order).

The low-pass filters are applied to all input and output variables in the dataset. Thus, theoretically, no delay will be introduced in the dataset, which could influence the final results. The conclusion would be different if the low-pass filter was applied to a subset of the input and output data.

Finally, time labeling plays a role in aligning inputs and outputs for the identification application [25]. As shown by Ljung et al. [25], a time shift, called anti-causal shift (ACS), of the input (Input Delay = $-T_s$) is beneficial for model identification with large T_s.

3.4. Dynamics of the wall-mounted sensor

Section 2.4 showed that the wall-mounted sensors have non-negligible thermal dynamics. Consequently, the grey-box model structures introduced in Section 3.1 should be adapted to account for the effect of the time constant of sensor dynamics and thus avoid potential mistakes in the model identification process. As proposed in Bacher et al. [36], it is possible to add an additional node for the temperature sensor, leading to an extra resistance (R_s) and capacitance (C_s). However, the authors also pointed out that it was not possible to give a physical interpretation for the value of C_s. This was also found from our preliminary tests based on our data. Therefore, we rather introduced an adaptation of the model with a single additional parameter, the time constant of the sensor $\tau = R_sC_s$. The model decreased the number of parameters compared to the version in the study [36] to increase the identifiability of the model. The dynamics for the sensor node is expressed by the following equation:

$$\frac{dT_{sensor}}{dt} = \frac{1}{\tau}(T_i - T_{sensor}) \tag{6}$$

where T_i is the temperature of the internal node, T_{sensor} is the temperature measurement from the wall-mounted temperature sensors.

3.5. Key performance indicator

Several key performance indicators (KPIs) are defined to evaluate the model performance. They can be divided into two categories: the physical plausibility of the identified parameters and the prediction performance of the model.

Physical plausibility means that the calibrated value of the model parameters should give a physically reasonable estimate of the thermal properties of the building. For conciseness in our study, it is not possible to report the value and variance of all the model parameters. However, the key parameters that are enough to support our conclusions will be presented: the overall heat transfer coefficient (HTC) and the capacitances (C_i and C_e). In addition, one parameter modeling the influence of the solar radiation, the effective window area (A_i), will also be taken as KPI when the influence of the data pre-processing is discussed.

The overall heat transfer coefficient (HTC) is the total heat loss of the building in steady-state. Heat transfer by convection and long-wave radiative heat transfer is nonlinear. However, heat conduction is dominant and has good linear properties if the building is highly insulated and airtight. The combination of several resistances of the grey-box model forms the HTC, which is defined by Equation (7) for the 3R2C model.

$$HTC = \frac{1}{1/UA_{ie} + 1/UA_{ea}} + UA_{inf} \tag{7}$$

Therefore, only the value of the HTC is shown in the later discussion, not its variance. Clauβ et al. [52] evaluated the HTC value of the ZEB Living Lab to be 83 W/K, which is used as the reference value for the HTC in this work.

It is challenging to define a physically plausible range for the capacitances (C_i and C_e) since their values strongly depend on the excitation signal. However, it is possible to obtain a rough indication of C_e. According to NS3031 (2016) [53], the effective heat capacitance (C_{eff}) of lightweight Norwegian buildings is typically within the range of 3.4–6.5 kWh/K. As the C_{eff} is based on daily excitations of the thermal mass of a building, it can be related to the thermal capacitance C_e (at least, up to second-order RC models without a node for internal walls, T_m).

The long-term prediction performance is of the utmost importance if the main application of the grey-box model is being employed in an MPC. Equation (8) gives the method of calculating the normalized root mean squared error (NRMSE).

$$NRMSE = \frac{||y_k - \hat{y}_k||}{||y_k - mean(y_k)||} \quad (8)$$

The NRMSE fitting, defined in Equation (9), is used to evaluate prediction performance. It translates how well the response of the predicted model matches measurement data. If the fit is 100%, the model perfectly matches the measurement data, whereas a low or negative fit is a model of lower quality. The NRMSE fitting value is calculated based on simulation for the deterministic model and one-day ahead prediction for the stochastic model. In other words, for the stochastic model, the model selection is done using the one-step ahead prediction while the ability to perform MPC is evaluated using a one-day ahead prediction.

$$NRMSE_{fit} = (1 - NRMSE) \times 100\% \quad (9)$$

In addition to the NRMSE fitting value, the mean bias error (MBE) defined by Equation (10) is also used as a complementary index. Theoretically, an MBE value close to zero is best as this means that the residual of the model has a lower mean bias error.

$$MBE = \frac{1}{n}\sum_{k=1}^{n}\left(y_k - \hat{y}_k\right) \quad (10)$$

In practice, the results show that all our models have good MBE properties. Therefore, this index has been used but is not reported in the paper.

4. Results

This section is divided into three parts. Firstly, the selection of the best model structure is presented and discussed. With the best model, the influence of data pre-processing and the type of indoor temperature measurement are then studied. Finally, the results are analyzed for deterministic and stochastic models. Most of the results presented are based on the datasets with the electric heaters (Experiments 2–4). The description of each case presented in this section is given in Table 3.

4.1. Model selection

The results for the electric radiator and the seven models using the volume-averaged temperature and the baseline T_s of 5 min are summarized in Table 6 in Appendix, while the key results are presented in Table 4.

- The first-order 1R1C model is not enough to describe the heat dynamics of the building for neither the deterministic nor the stochastic models. This is confirmed by the cumulative periodogram of the residuals in supplementary material. The cumulative periodogram falls largely outside the confidence interval, which indicates poor white noise properties of the residuals.
- The second-order models, 2R2C and 3R2C, show significant improvement in the NRMSE fitting compared to the first-order 1R1C model. The cumulative periodogram of the residuals also stays strictly within the confidence interval.
- Although the third-order models (3R3C to 5R3C) sometimes present better NRMSE fitting with the deterministic model, the identified parameters are not physically plausible for the stochastic model. The capacitance of the interior node C_i has a larger value than the value of the internal walls node C_m, which does not translate the actual physics. Furthermore, for the 4R3C and 5R3C stochastic models, the UA_{ea} value is identified close to 0, which also violates the reality (as external walls are not perfectly insulated). Regarding the cumulative periodogram of the residuals, the 5R3C is outside the confidence interval while the 3R3C and 4R3C models remain within the confidence interval but do not perform better than the second-order models. The variance of the key parameter C_e also shows that the third-order models could lead to large values with deterministic models, which implies that the third-order models may be overfitting. Further, the variance of C_e for the stochastic model also shows that the component UA_{inf} is necessary to be modeled. Finally, the objective function during the successive PSO iterations is plotted along with the parameter value. The scatter plots for parameters C_e and A_i for second-order and third-order models can also be found in supplementary material. It is observed from the scatter plots that the optimum are flatter with third-order models, which corresponds to lower practical identifiability of the models. It can be concluded that the third-order models are (or are close to being) overfitted. The fitting of validation NRMSE fitting also confirms that the second-order model is the best trade-off between model complexity and accuracy.

In conclusion, second-order grey-box models are most suitable for our study as the prediction performance and the physical plausibility are good. In addition, the dominant physical processes are properly modeled as proven by the cumulative periodogram. The second-order models are selected for the study as they are accurate but not overfitted. This guarantees that the conclusions will not be contaminated by overfitting. Among second-order models, the 3R2C model is taken as the baseline case in the remainder of the paper.

4.2. Influence of the temperature measurement

The model selection is based on the volume-averaged indoor temperature at 5 min. In the description of experiments, it has been shown that the indoor temperature is dependent on the type of measurement, see Section 2.4. Consequently, Fig. 5 and Fig. 6 compare the identified value of two key indicators (HTC and C_e) for the different types of temperature measurement, still using a sampling time of 5 min. For the deterministic model, the difference in temperature measurements has a limited influence on the identified model parameters. However, for the stochastic model, the identified HTC value using the baseline 3R2C model and the single wall-mounted temperature sensor is much larger than the reference HTC value. Furthermore, the variance of C_e is also extremely large. Thus, the time constant of the wall-mounted sensor dynamics has a large impact on the stochastic 3R2C model. This conclusion is also confirmed by the cumulative periodogram of the

Table 3
Description of the datasets and their corresponding abbreviations.

Case	Sensor	Sensor node in model	Dataset	Use
T1Exp2	Volume-averaged temperature (T1)	No	Experiment 2	Validation
T1Exp3	Volume-averaged temperature (T1)	No	Experiment 3	Validation
T1Exp4	Volume-averaged temperature (T1)	No	Experiment 4	Training
T2Exp4	Single temperature sensor in the air (T2)	No	Experiment 4	Training
T3Exp4	Single wall-mounted temperature sensor (T3)	No	Experiment 4	Training
T4Exp4	Single wall-mounted temperature sensor (T4)	Yes (τ)	Experiment 4	Training
T5Exp5	Single wall-mounted temperature sensor (T5)	No	Experiment 5	Training
T6Exp5	Single wall-mounted temperature sensor (T6)	Yes (τ)	Experiment 5	Training

Table 4
The values and the corresponding variance of C_e.

Model	C_e Value [kWh/K]	C_e Variance [kWh/K]	NRMSE Fitting (simulation)	NRMSE Fitting (validation)	Model	C_e Value [kWh/K]	C_e Variance [kWh/K]	NRMSE Fitting (1-step ahead)	NRMSE Fitting (validation)
1R1Cdet	5.62	**0.754**	72.7%	55.1%	**1R1Csto**	4.78	0.437	99.0%	65.7%
2R2Cdet	6.11	0.369	93.0%	75.3%	**2R2Csto**	6.37	**1.77**	99.2%	79.2%
3R2Cdet	5.28	0.284	93.6%	79.7%	**3R2Csto**	4.22	0.748	99.2%	81.8%
4R2Cdet	5.40	0.430	93.5%	72.4%	**4R2Csto**	4.28	0.726	99.2%	81.5%
3R3Cdet	6.08	**0.689**	95.0%	78.6%	**3R3Csto**	11.9	**3.92**	99.2%	71.1%
4R3Cdet	3.94	**0.609**	95.3%	75.6%	**4R3Csto**	4.02	0.709	99.2%	82.7%
5R3Cdet	3.99	**0.613**	95.3%	76.0%	**5R3Csto**	5.73	0.718	99.2%	79.8%

(For the first-order 1R1C model, Ce does not exist and the value reported in the table is the value of Ci. Bold values inside the table indicates unphysical parameters.)

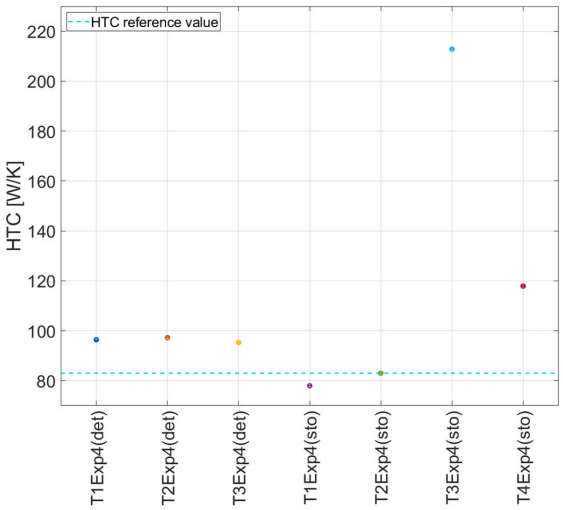

Fig. 5. Comparing the HTC of the 3R2C deterministic (det) and stochastic (sto) models using Experiment 4 and different types of temperature measurement (5 min).

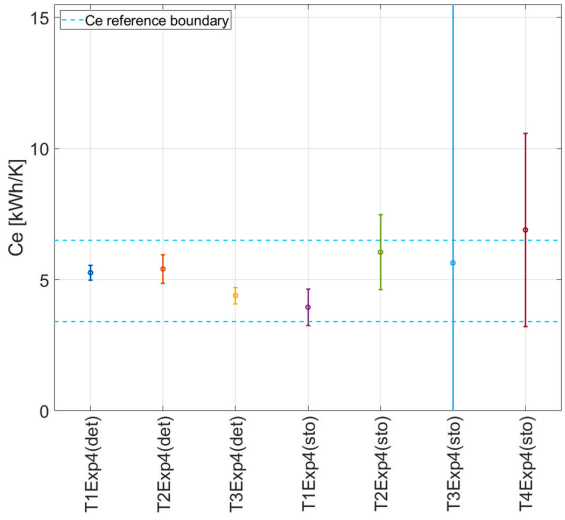

Fig. 6. Comparing the Ce of the 3R2C deterministic (det) and stochastic (sto) models using Experiment 4 and different types of temperature measurement (5 min).

residuals in Fig. 7, which shows that the baseline 3R2C model with the wall-mounted sensor does not describe the system dynamics (between 0.4–1.4 $\times$ 10^{-3} Hz). As introduced in Section 3.4, an adapted model with a time constant for the sensor is added to the original 3R2C model. This adapted model improves the results since the parameters become physically plausible again. In addition, the cumulative periodogram of the residuals confirms this conclusion (see dataset T4Exp4). Furthermore, the one-day ahead prediction comparison in Fig. 8 also shows the significant improvement from the adapted 3R2C compared to the original baseline 3R2C model. The identified time constant (τ) has a value of 8.28 min, thus is larger than the sampling time. For the remainder of the paper, the sensor node will only be analyzed for the stochastic model.

4.3. *Influence of data pre-processing on grey-box modeling*

Until now, the model performance has used a sampling time of 5 min without data pre-processing, which is faster than the Nyquist sampling frequency. The signal is sampled faster than the system dynamics so that it is guaranteed that it does not influence the results. Consequently, the specific influence of data-preprocessing can be identified in the present section. The analysis of deterministic and stochastic models should be clearly distinguished.

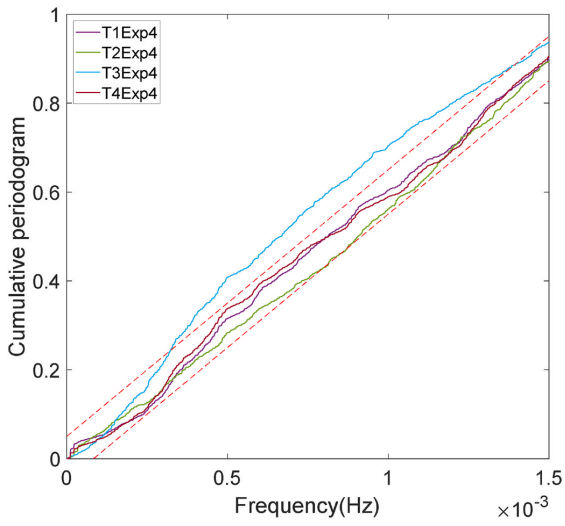

Fig. 7. Cumulative periodogram of the residuals of the model 3R2C for different types of indoor temperature measurement.

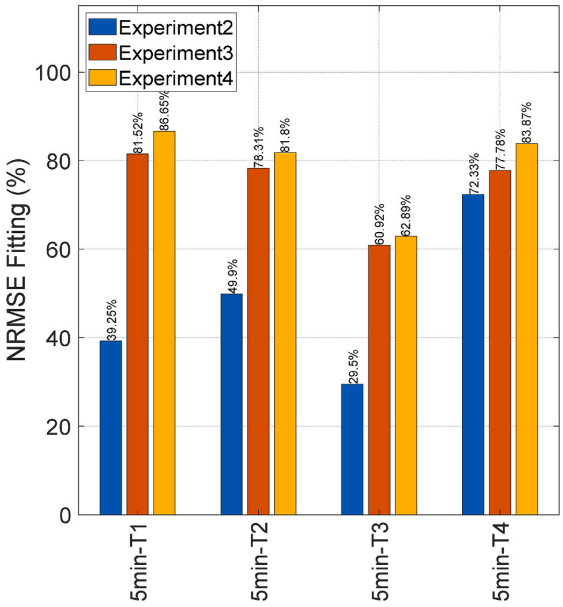

Fig. 8. Comparing the one-day ahead prediction of the 3R2C stochastic (sto) models with different types of temperature measurement, trained using Experiment 4 and validated using Experiments 2, 3.

4.3.1. *Influence of data-preprocessing on the deterministic model*

Fig. 9 presents the identified parameters results for the deterministic model using different types of temperature measurement and data pre-processing.

The identified values of HTC show that no matter which type of temperature is used for the identification, the HTC value is not significantly influenced by the pre-filtering method and ACS. The value is close to the reference value of ~83 W/K. The sampling time (Ts) does not have a noticeable impact on the HTC value.

The identified values of C_e give similar conclusions as the HTC value. The value of C_e is plausible for most of the cases since it is within the typical range (i.e., 3.4–6.5 kWh/K) given in standards [53]. The low-pass filtering and the ACS only have a slight impact on the results. With direct sampling, the C_e values are slightly outside the reference range when the sampling time is large (from 30 min). These conclusions are confirmed by the analysis of the effective window area A_i (related to the influence of solar radiation).

Regarding the simulation performance of the deterministic model, the influence of data pre-processing and the type of temperature measurement are also limited as are the identified parameters. Consequently, the simulation performance is only demonstrated for the volume-averaged temperature (see Fig. 10).

Several main conclusions can be drawn concerning the deterministic model. They are in good agreement with the findings of Yu et al. [26] using virtual experiments. Firstly, the pre-processing of data does not have a considerable influence on the deterministic model. Secondly, the pre-filtering technique could slightly contribute to a more stable estimation of the values if the sampling time T_s is large (>30 min). Thirdly, the influence of data pre-processing on simulation performance is negligible.

4.3.2. *Influence of data-preprocessing on the stochastic model*

As shown in Fig. 11, the data pre-processing has a more substantial influence on the identified HTC value for the stochastic model. The ACS can contribute to preventing the HTC value from becoming non-physical (stays close to the target reference value) for large sampling times. If the filter and the ACS are applied together, the identified HTC value remains stable and close to the reference value for the stochastic model. However, the identified HTC values are often non-physical using the baseline 3R2C model when the dynamics of the wall-mounted temperature sensors are not modeled, even when the sampling time becomes large. Again, only the adapted 3R2C model with a sensor node gives plausible HTC values. This result is counterintuitive. In Section 4.2, the time constant of the wall-mounted sensor has been estimated to be about 8 min. Therefore, it could be expected that the effect of the sensor dynamics would be filtered out by taking a larger sampling time (>15 min). However, this is not the case. This last conclusion is much clearer when analyzing C_e.

The identified C_e for the stochastic model without and with ACS are shown in Fig. 11, respectively. This confirms the positive effect of ACS for large sampling times. For cases without ACS, the identified C_e value and variance become non-physical when the sampling time is larger. The C_e values from volume-averaged temperature (T_1) and the single wireless temperature (T_2) sensors remain physically plausible for the large sampling times if the filter and ACS are applied simultaneously. Regarding the wall-mounted sensor, the baseline 3R2C model (T_3) does not give plausible C_e values even for large sampling times. The low-pass filtering or ACS does not improve the performance. This confirms that, even though the sensor time constant (~8 min) is significantly shorter than the sampling time, its influence is not filtered out and it still impacts the performance of the stochastic model. For the adapted model (T_4), the C_e value remains physically plausible for large sampling times when the ACS and the low-pass filter are applied, just like the datasets T_1 and T_2. It is worth mentioning that the C_e values from a single sensor are generally larger than those identified from the volume-averaged temperature.

At this stage, the influence of the ACS does not need to be further demonstrated. Therefore, the A_i values for the stochastic model are only shown in Fig. 11 with ACS. The results for A_i are consistent with the results for C_e and confirm the previous conclusions.

The identified τ values for the adapted 3R2C model with a sensor node can be found in Table 5. The sampling time (T_s) of 5 min is shorter than the identified time constant of about 8 min. However, when the T_s becomes significantly larger than 8 min, τ cannot understandably be identified at a lower value than T_s. In other words, a sound conclusion is that if the identified sensor time constant is to be physically plausible, the data should be sampled at a higher frequency than the sensor dynamics.

Fig. 12 compares the ability of the model to perform MPC using the one-day ahead prediction performance for the stochastic model identified using the volume-averaged temperature (T_1). Large sampling times have a limited effect on the one-day ahead prediction performance. The low-pass filter increases the one-day ahead prediction mainly for the validation datasets using Experiment 2. While the ACS improves the physical plausibility of the model parameters for large sampling times, its influence on the one-day ahead prediction performance is not systematic: it has a slightly positive impact on Experiments 3 and 4 but a negative influence on Experiment 2.

For the case of wall-mounted temperature sensors, the improvement from the adapted model for the one-day ahead prediction performance is significant. The results are shown in Fig. 13 and Fig. 14. If the same pre-processing is applied (i.e., sampling time and filtering method), the NRMSE fitting from the adapted 3R2C stochastic model with sensor node (T_4) is always higher than the baseline 3R2C stochastic model without sensor node (T_3). Using the wall-mounted sensor, the influence of large sampling time is considerable. However, this effect is reduced using low-pass filtering. The influence of ACS is still not systematic. Nevertheless, for the adapted model, the ACS systematically improves the prediction performance.

To sum up, except for wall-mounted sensors, large T_s have a limited effect on the prediction performance, which is in good agreement with

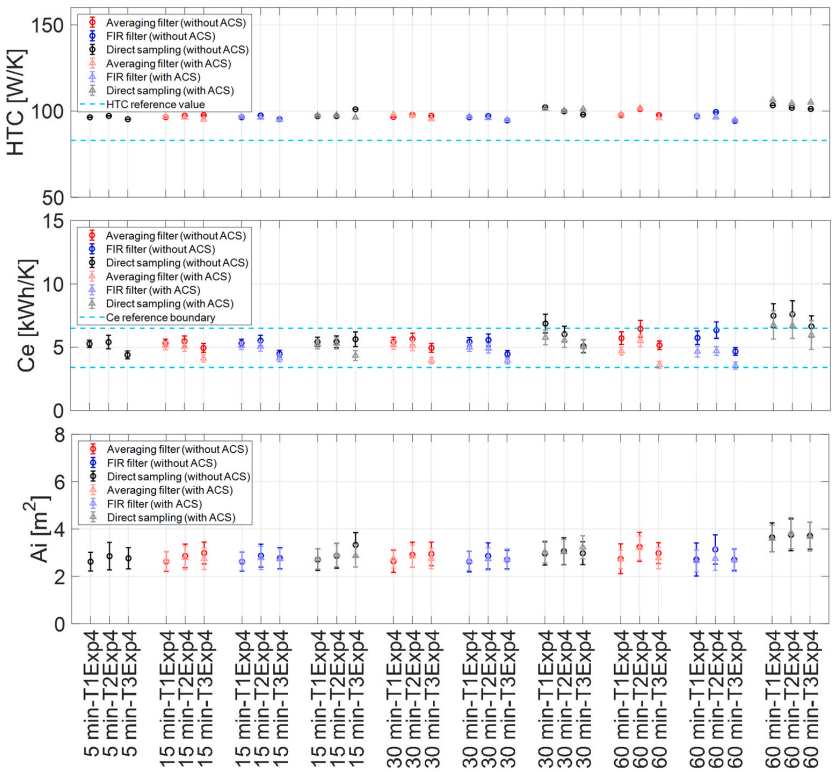

Fig. 9. Identified HTC, Ce and Ai of the 3R2C deterministic model for Experiment 4 with different types of temperature, data pre-processing techniques.

the findings of Yu et al. [26]. For the wall-mounted sensor, additional measures should be taken to conserve the prediction performance with large T_s. As for the physical plausibility, the low-pass filtering improves the prediction performance. However, the positive influence of the ACS for T_s is not as systematic for the prediction performance as it was for the physical plausibility of the parameters.

4.3.3. Stochastic model with hydronic radiator

As previously mentioned, the air temperature was only measured using the wall-mounted sensors for the experiment using the hydronic

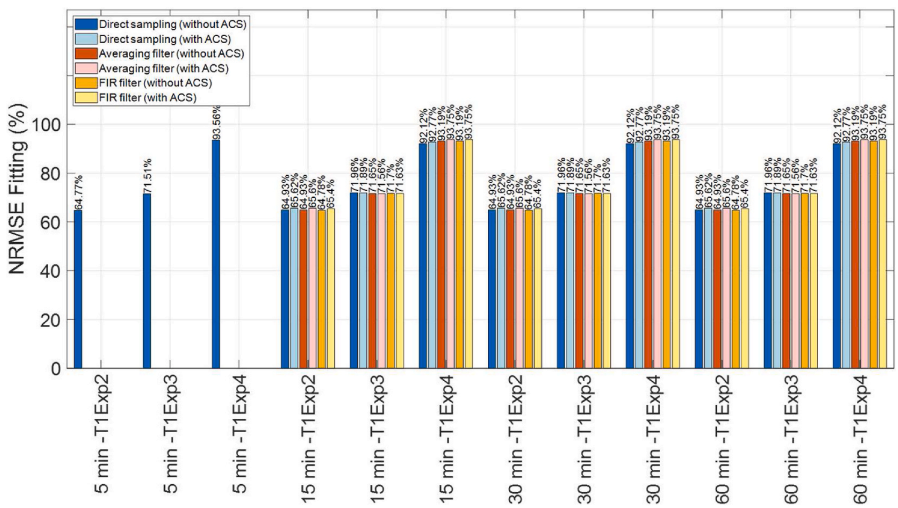

Fig. 10. Comparison of the simulation performance of the deterministic 3R2C model using the volume-averaged temperature (T1), trained using Experiment 4 and validated using Experiments 2, 3.

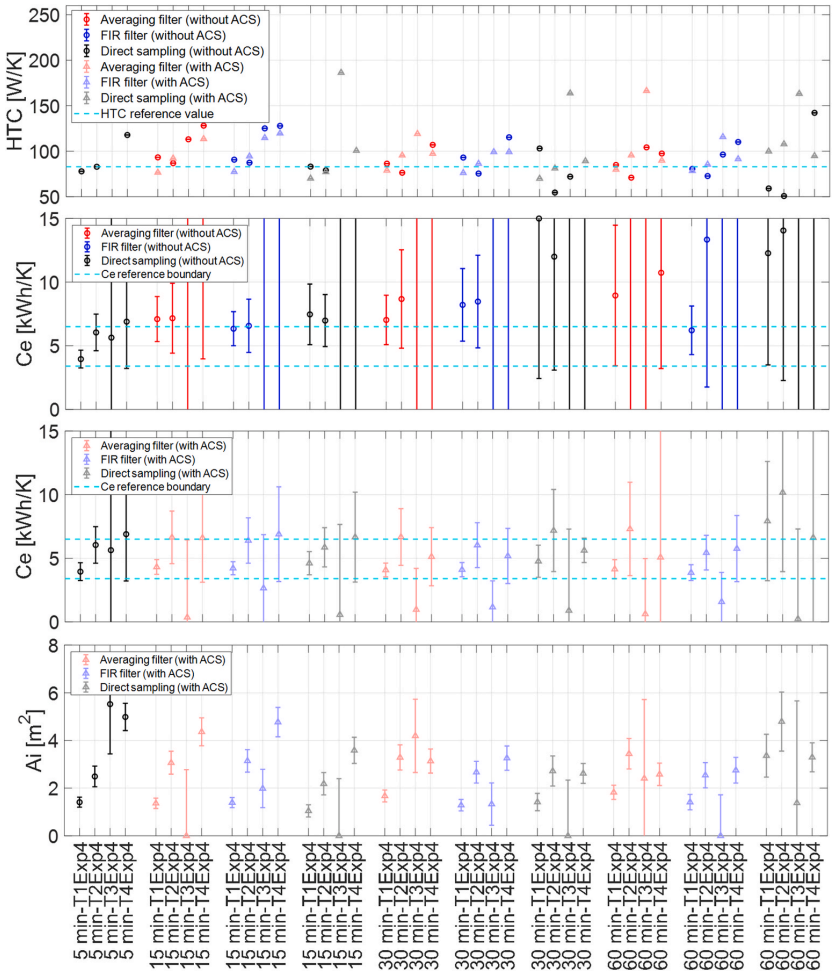

Fig. 11. Identified HTC, Ce and Ai of the 3R2C stochastic model for Experiment 4 with different types of temperature measurement and data pre-processing techniques.

radiator. As it has been proven that the sensor node was necessary for the modeling, only the performance of the adapted model is analyzed. Unlike the electric heater, the thermal dynamics of the hydronic radiator are significant (see Section 2.4). The analysis of the measured inlet and outlet temperatures of the hydronic radiator showed that its time constant is about 7 min. A priori, like the wall-sensor, it is expected that the hydronic radiator dynamics should influence the model performance, at least for a sampling time of 5 min (<7 min). However, the wall-mounted temperature sensor has a time constant of about 8 min. Consequently, the dynamics of the hydronic radiator cannot be properly captured by a grey-box model since the time constant of the wall-mounted sensor is comparable (or slightly larger) than the time constant of the hydronic radiator. The analysis of the cumulative periodogram (not reported here for the sake of the conciseness) shows that the adapted 3R2C can model the building heated using the hydronic radiator without the need to add a specific capacitance to model the hydronic radiator. In addition, preliminary results with an additional capacitance proved that the resulting model would be overfitted.

Table 5
Identified time constant (τ) of the 3R2C adapted stochastic model for Experiment 4 with different data pre-processing techniques.

Sampling time [min]	DS		MA		FIR	
	τ value [min]	τ variance [min]	τ value [min]	τ variance [min]	τ value [min]	τ variance [min]
5	8.28	0.420	–	–	–	–
15	16.4	1.82	12.9	1.21	11.6	1.04
30	67.9	62.1	26.2	3.59	27.6	4.08
60	97.6	19,465	79.1	1031	76.5	223

The experiments with the hydronic radiator and the electric heater have been performed in different years and different months of the heating season, leading to different sun elevations between the experiments. The identified effective window area A_i is thus expected to be significantly different for Experiment 5 and Experiments 2 to 4. Thermal properties that are intrinsic to the building fabric and less dependent on

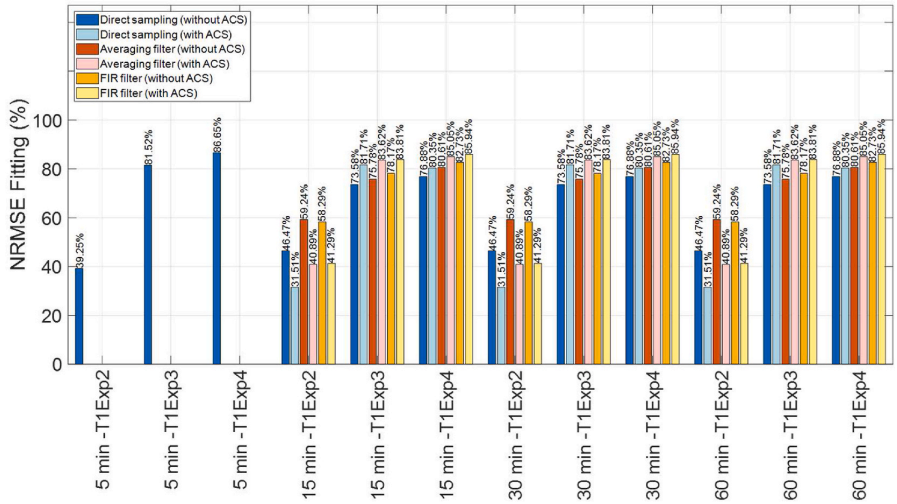

Fig. 12. One-day ahead prediction of the stochastic 3R2C model using the volume-averaged temperature (T1), trained using Experiment 4 and validated using Experiments 2, 3.

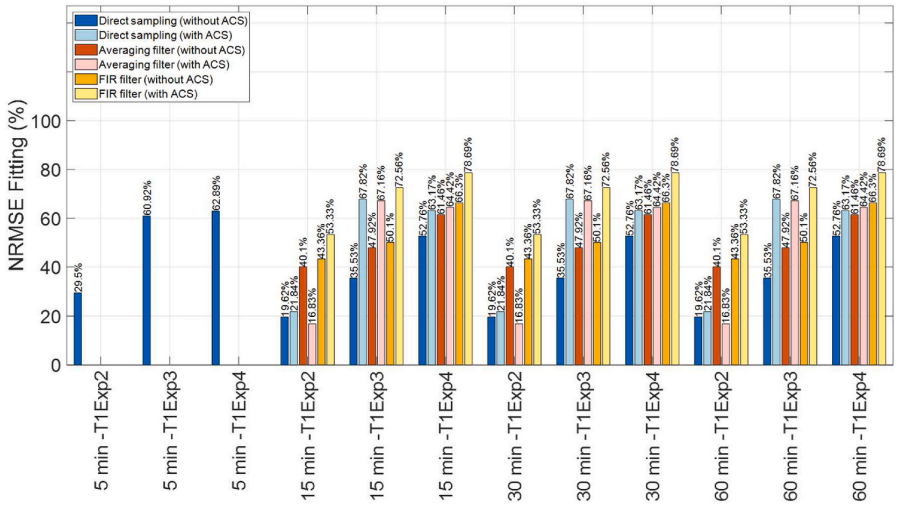

Fig. 13. One-day ahead prediction of the baseline stochastic 3R2C model using a single wall-mounted sensor (T3), trained using Experiment 4 and validated using Experiments 2, 3.

the outdoor conditions are used to analyze the model performance in Experiment 5, namely the HTC and C_e (Fig. 15). The identified HTC is still close to the reference value. Unlike the experiments with the electric heater, there is no significant difference between the baseline and adapted 3R2C models and the HTC remains plausible for large sampling times (with ACS).

However, the improvement resulting from the adapted model and ACS is more visible when analyzing C_e. Again, the HTC translates into a steady-state performance while the capacitances are inherently related to the building dynamics. Conclusions with the hydronic radiator are in line with the conclusions using Experiment 4 with the electric heater. With the baseline 3R2C model, the estimated C_e is entirely non-physical even using pre-filtering and ACS. The results are noticeably improved with the adapted 3R2C model with a sensor node. If the pre-filtering and ACS are applied, the C_e value strictly stays within the reference range no matter how large the sampling time is. For Experiment 5, it is worth mentioning that the quality of the adapted 3R2C model is marginal as the variance C_e is sometimes very large. Nevertheless, this does not impact the main conclusion. The experiment with the hydronic radiator confirms the positive influence of the adapted model with τ, the low-pass filtering and the ACS for large sampling times.

5. Discussion

This paper analyzes the influence of data pre-processing and sensor dynamics on the grey-box modeling of the building thermal dynamics using the MATLAB system identification toolbox. Some limitations to the work can be listed and discussed:

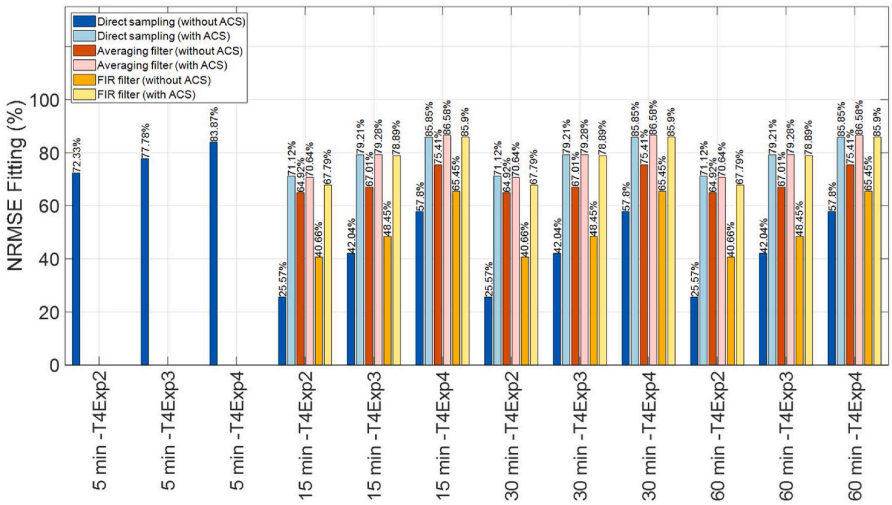

Fig. 14. One-day ahead prediction of the adapted stochastic 3R2C model using a single wall-mounted sensor (T4), trained using Experiment 4 and validated using Experiments 2, 3.

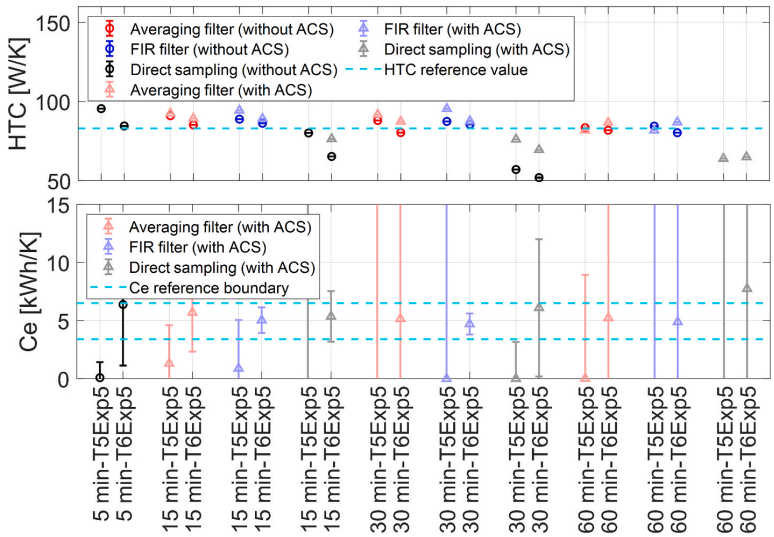

Fig. 15. HTC and C_e for the 3R2C stochastic model using Experiment 5 and different data pre-processing techniques.

- Important conclusions based on virtual experiments have already been drawn in the previous study of Yu et al. [26]. However, field measurements are different from virtual experiments. The paper succeeded in extending the conclusions from virtual experiments to a real test case with field measurements. However, more test cases are needed to have a generalization of the conclusions. It has been decided to limit the paper to a single test case. The experimental setup and the methodology should be sufficiently described to make the results transparent and reproducible. For the sake of conciseness, this limits the paper to a single test case.
- The test case is a super-insulated building with balanced mechanical ventilation and an energy-efficient heat recovery unit. This enabled the building to be modeled as a single thermal zone. This test case is relatively specific as most of the existing houses in the Norwegian building stock do not have these thermal properties. However, it is expected that the conclusions of the paper regarding data pre-treatment are not affected by the insulation level and type of ventilation.
- The paper considers that the data pre-treatment is performed equally for all input and output data. This is possible when the data pre-treatment is performed explicitly by the modeler. However, when the data pre-treatment is performed implicitly by the hardware (i.e., the sensor or the DAQ), this pre-treatment can affect the input and output data differently. In this case, additional data pre-treatment techniques should be considered (such as the identification of lag). The conclusions of the paper need to be extended to this case as well.

- The analysis is based on the MATLAB system identification toolbox, where the stochastic equations are written in innovation form. For the generalization, results should be reproduced in other system identification tools and formulations, such as CTSM-R [54].

6. Conclusion

This study is based on two experimental setups using two different space-heating emission systems, namely an electric heater and a hydronic radiator. The pre-processing techniques include low-pass filtering (using MA or FIR), the sampling time (T_s) and the application of *anti-causal shift* (ACS). Three different types of temperature measurements are analyzed to investigate the influence of the sensor selection and dynamics (i.e. volume-averaged air temperature, single temperature sensor without casing and single wall-mounted sensor).

To analyze the specific influence of the data pre-processing, it is important to ensure that the model performance is not polluted by other phenomena, such as overfitting or poor model fidelity. Therefore, the study starts by selecting a suitable structure for the grey-box model and proves that a mono-zone second-order model is an appropriate trade-off, with (1) a good prediction performance and (2) good interpretability of the physical parameters of the model (i.e., physical plausibility) (3) without beginning to be overfitted. Consequently, a mono-zone 3R2C model is taken as the baseline structure to illustrate the key research questions of the paper. Conclusions are presented separately between deterministic and stochastic models.

Deterministic model:

- Yu et al. [26] used virtual experiments and the data pre-processing has a limited influence on the model performance. This is confirmed using field experiments. In addition, the sensor thermal dynamics also has a limited influence on the deterministic model performance.

Stochastic model:

- Yu et al. [26] used virtual experiments and the parameters became non-physical without ACS for large sampling time (T_s). On the contrary, large sampling times did not alter the simulation performance significantly. Although the ACS tends to improve the physical plausibility of the model parameters with T_s, in general, it had a negative influence on the simulation performance of the model.
- These results are partly confirmed using field measurements. Like in Yu et al. [26], large T_s can cause the parameters to become non-physical without ACS. ACS is excessively beneficial to guarantee the physical plausibility of parameters, making the identified parameters insensitive to the sampling time. Like in Yu et al. [26], large T_s has a limited effect on the prediction performance for the temperature sensors without casing. However, for the wall-mounted sensor, pre-filtering and sometimes ACS should be used to converse the prediction performance at large T_s. Like Yu et al. [26] pre-filtering has a beneficial influence on the model performance but not in a dominant way. Unlike Yu et al. [26], the influence of ACS on prediction performance is most often beneficial in our study. At this stage, it can be concluded that the influence of the sampling time and ACS on the prediction performance is not systematic (i.e., sometimes positive or negative).
- The results for stochastic models depend on the type of temperature measurement. Firstly, the cases with temperature sensors with negligible thermal dynamics (i.e., free-standing air temperature sensor without casing) are analyzed. Even though the vertical thermal stratification is significant, there is only a slight reduction in the model performance when moving from a volume-averaged measurement to a single sensor located at mid-height in the room. Secondly, when the temperature sensor is the wall-mounted temperature sensor, an adapted model with time constant dynamics for the sensor is needed to obtain a physically plausible estimation of the parameters. This is an important conclusion as most buildings are equipped with wall-mounted temperature sensors. To limit the investment, the number of sensors should also be limited, making a volume-averaged measurement expensive.
- The dynamics of the hydronic radiator (with significant thermal mass) are not necessary to be modeled if the time constant of the measurement device is larger than that of the hydronic radiator.

As the article is based on a single test case, additional research on real buildings is needed to generalize the conclusions. These findings provide practical guidelines to identify the thermal dynamics of buildings using grey-box models and field measurement data.

CRediT authorship contribution statement

Xingji Yu: Conceptualization, Data curation, Formal analysis, Investigation, Methodology, Software, Validation, Visualization, Writing – original draft. **Kristian Stenerud Skeie:** Data curation, Writing – review & editing. **Michael Dahl Knudsen:** Writing – review & editing, Investigation. **Zhengru Ren:** Writing – review & editing, Validation. **Lars Imsland:** Conceptualization, Methodology, Supervision, Writing – review & editing. **Laurent Georges:** Writing – review & editing, Validation, Supervision, Methodology, Investigation, Funding acquisition.

Declaration of competing interest

The authors declare that they have no known competing financial interests or personal relationships that could have appeared to influence the work reported in this paper.

Acknowledgments

This work is conducted in the framework of the Norwegian Research Centre on Zero Emission Neighbourhoods in Smart Cities (ZEN), co-funded by the Research Council of Norway and industry partners. In addition, this research is also a contribution to IEA EBC Annex 81 on Data-Driven Smart Buildings.

Appendix A. Supplementary data

Supplementary data to this article can be found online at https://doi.org/10.1016/j.buildenv.2022.108832.

Appendix

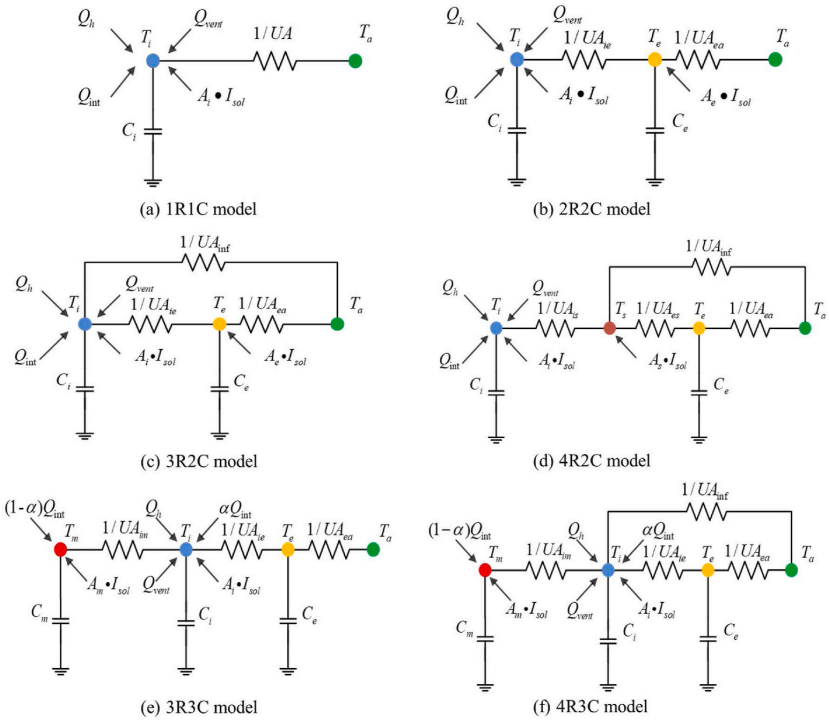

Fig. 16. Grey-box model structures except for the most complicated 5R3C model.

Table 6
Model identification results of the candidate models with 5 min data and volume-averaged temperature (T1), values highlighted with bold color are non-physical values.

Model	UA_{ea} [W/K]	UA_{ie} [W/K]	UA_{im} [W/K]	UA_{inf} [W/K]	UA [W/K]	UA_{as} [W/K]	UA_{es} [W/K]	UA_{is} [W/K]	C_e [kWh/K]	C_i [kWh/K]
1R1Cdet	–	–	–	–	106	–	–	–	–	5.62
2R2Cdet	114	826	–	–	–	–	–	–	6.11	0.749
3R2Cdet	80.2	876	–	23.0	–	–	–	–	5.28	0.767
4R2Cdet	52.1	–	–	51.5	–	–	2558	1345	5.40	0.781
3R3Cdet	153	404	565	–	–	–	–	–	6.08	0.961
4R3Cdet	104	303	687	26.5	–	–	–	–	3.94	0.909
5R3Cdet	102		686	–	–	28.1	331	4694	3.99	0.908
1R1Csto	–	–	–	–	109	–	–	–	–	4.78
2R2Csto	109	1058	–	–	–	–	–	–	6.37	1.24
3R2Csto	17.1	868	–	63.5	–	–	–	–	4.22	1.15
4R2Csto	**0.000**	1181	–	78.5	–	–	–	3342	4.28	1.11
3R3Csto	123	552	763	–	–	–	–	–	**11.9**	**1.23**
4R3Csto	5.40	692	346	71.4	–	–	–	–	**4.02**	**1.21**
5R3Csto	**0.000**	–	375	–	–	108	8492	1087	**5.73**	**1.19**

Model	C_m [kWh/K]	A_i [m^2]	A_e [m^2]	A_m [m^2]	A_s [m^2]	alpha [−]	MBE	NRMSE (one-step)	NRMSE (prediction)	HTC [W/K]
1R1Cdet	–	2.99	–	–	–	–	0.0010	–	72.7%	105
2R2Cdet	–	2.96	0.000	–	–	–	0.0007	–	93.0%	100
3R2Cdet	–	2.62	0.000	–	–	–	0.0008	–	93.6%	96.4
4R2Cdet	–	2.78	–	–	0.000	–	−0.0033	–	93.5%	103
3R3Cdet	2.09	3.82	–	0.000	–	0.500	−0.0017	–	95.0%	111
4R3Cdet	2.58	3.19	–	0.000	–	0.500	0.0025	–	95.3%	104
5R3Cdet	2.54	–	–	0.000	3.21	0.500	−0.0017	–	95.3%	106
1R1Csto	–	3.39	–	–	–	–	−0.0008	99.0%	73.4%	109
2R2Csto	–	3.07	0.000	–	–	–	0.0000	99.2%	87.3%	98.8
3R2Csto	–	1.56	0.122	–	–	–	0.0000	99.2%	87.2%	80.3
4R2Csto	–	1.09	–	–	0.686	–	0.0001	99.2%	86.6%	78.5
3R3Csto	**1.16**	3.07	–	0.819	–	0.500	0.0002	99.2%	80.6%	101
4R3Csto	**0.042**	1.44	–	0.000	–	0.500	0.0001	99.2%	86.1%	76.8
5R3Csto	**0.038**	–	–	0.078	2.67	0.500	0.0001	99.2%	88.9%	108

References

[1] J. Drgoňa, J. Arroyo, I. Cupeiro Figueroa, D. Blum, K. Arendt, D. Kim, E.P. Ollé, J. Oravec, M. Wetter, D.L. Vrabie, L. Helsen, All you need to know about model predictive control for buildings, Annu. Rev. Control 50 (2020) 190–232, https://doi.org/10.1016/j.arcontrol.2020.09.001.

[2] A.E. Ruano, E.M. Crispim, E.Z.E. Conceição, M.M.J.R. Lúcio, Prediction of building's temperature using neural networks models, Energy Build. 38 (2006) 682–694, https://doi.org/10.1016/j.enbuild.2005.09.007.

[3] J.A. Crabb, N. Murdoch, J.M. Penman, A simplified thermal response model, Build. Serv. Eng. Technol. 8 (1987) 13–19.

[4] L. Laret, Use of general models with a small number of parameters, Part 1: theoretical analysis, in: Proc. Conf. Clima, 2000, pp. 263–276.

[5] A. Afram, F. Janabi-Sharifi, Review of modeling methods for HVAC systems, Appl. Therm. Eng. 67 (2014) 507–519, https://doi.org/10.1016/j.applthermaleng.2014.03.055.

[6] Y. Li, Z. O'Neill, L. Zhang, J. Chen, P. Im, J. DeGraw, Grey-box modeling and application for building energy simulations - a critical review, Renew. Sustain. Energy Rev. 146 (2021) 111174, https://doi.org/10.1016/j.rser.2021.111174.

[7] Y. Yao, D.K. Shekhar, State of the art review on model predictive control (MPC) in Heating Ventilation and Air-conditioning (HVAC) field, Build. Environ. 200 (2021) 107952, https://doi.org/10.1016/j.buildenv.2021.107952.

[8] H. Madsen, P. Bacher, G. Bauwens, A.-H. Deconinck, G. Reynders, S. Roels, E. Himpe, G. Lethé, IEA EBC Annex 58-Reliable Building Energy Performance Characterisation Based on Full Scale Dynamic Measurements, Report of subtask 3, part 2: thermal performance characterisation using time series data-statistical guidelines, 2016, https://www.iea-ebc.org/Data/publications/EBC_Annex_58_Final_Report_ST3b.pdf.

[9] S. Stinner, K. Huchtemann, D. Müller, Quantifying the operational flexibility of building energy systems with thermal energy storages, Appl. Energy 181 (2016) 140–154, https://doi.org/10.1016/j.apenergy.2016.08.055.

[10] N.G. Paterakis, O. Erdinç, J.P.S. Catalão, An overview of Demand Response: key-elements and international experience, Renew. Sustain. Energy Rev. 69 (2017) 871–891, https://doi.org/10.1016/j.rser.2016.11.167.

[11] G. Steindl, W. Kastner, V. Stangl, Comparison of data-driven thermal building models for model predictive control, J. Sustain. Dev. Energy, Water Environ. Syst. 7 (2019) 730–742, https://doi.org/10.13044/j.sdewes.d7.0286.

[12] P. Siano, Demand response and smart grids — a survey, Renew. Sustain. Energy Rev. 30 (2014) 461–478, https://doi.org/10.1016/j.rser.2013.10.022.

[13] M. Dahl Knudsen, S. Petersen, Demand response potential of model predictive control of space heating based on price and carbon dioxide intensity signals, Energy Build. 125 (2016) 196–204, https://doi.org/10.1016/j.enbuild.2016.04.053.

[14] S.Ø. Jensen, A. Marszal-Pomianowska, R. Lollini, W. Pasut, A. Knotzer, P. Engelmann, A. Stafford, G. Reynders, IEA EBC Annex 67 energy flexible buildings, Energy Build. 155 (2017) 25–34, https://doi.org/10.1016/j.enbuild.2017.08.044.

[15] M. Killian, M. Kozek, Ten questions concerning model predictive control for energy efficient buildings, Build. Environ. 105 (2016) 403–412, https://doi.org/10.1016/j.buildenv.2016.05.034.

[16] H. Harb, N. Boyanov, L. Hernandez, R. Streblow, D. Müller, Development and validation of grey-box models for forecasting the thermal response of occupied buildings, Energy Build. 117 (2016) 199–207, https://doi.org/10.1016/j.enbuild.2016.02.021.

[17] J. Le Dréau, P. Heiselberg, Energy flexibility of residential buildings using short term heat storage in the thermal mass, Energy 111 (2016) 991–1002, https://doi.org/10.1016/j.energy.2016.05.076.

[18] R.E. Hedegaard, T.H. Pedersen, M.D. Knudsen, S. Petersen, Towards practical model predictive control of residential space heating: eliminating the need for weather measurements, Energy Build. 170 (2018) 206–216, https://doi.org/10.1016/j.enbuild.2018.04.014.

[19] S. Freund, G. Schmitz, Implementation of model predictive control in a large-sized, low-energy office building, Build. Environ. 197 (2021) 107830, https://doi.org/10.1016/j.buildenv.2021.107830.

[20] J. Wang, S. Li, H. Chen, Y. Yuan, Y. Huang, Data-driven model predictive control for building climate control: three case studies on different buildings, Build. Environ. 160 (2019) 106204, https://doi.org/10.1016/j.buildenv.2019.106204.

[21] R. Halvgaard, N.K. Poulsen, H. Madsen, J.B. Jørgensen, Economic model predictive control for building climate control in a smart grid, in: 2012 IEEE PES Innov. Smart Grid Technol., IEEE, 2012, pp. 1–6.

[22] M.D. Knudsen, R.E. Hedegaard, T.H. Pedersen, S. Petersen, System identification of thermal building models for demand response - a practical approach, Energy Proc. 122 (2017) 937–942, https://doi.org/10.1016/j.egypro.2017.07.426.

[23] M.A.A. Awadelrahman, Y. Zong, H. Li, C. Agert, Economic model predictive control for hot water based heating systems in smart buildings, Energy Power Eng. 9 (2017) 112–119.

[24] J.F. van Impe, P.A. Vanrolleghem, D.M. Iserentant, Advanced Instrumentation, Data Interpretation, and Control of Biotechnological Processes, Springer Science & Business Media, 2013.

[25] L. Ljung, A. Wills, Issues in sampling and estimating continuous-time models with stochastic disturbances, Automatica 46 (2010) 925–931, https://doi.org/10.1016/j.automatica.2010.02.011.

[26] X. Yu, L. Georges, L. Imsland, Data pre-processing and optimization techniques for stochastic and deterministic low-order grey-box models of residential buildings, Energy Build. 236 (2021) 110775, https://doi.org/10.1016/j.enbuild.2021.110775.

[27] T. Kalamees, IDA ICE: the simulation tool for making the whole building energy and HAM analysis, Annex 41 (2004) 12–14.

[28] P. Vogler-Finck, J. Clauß, L. Georges, A dataset to support dynamical modelling of the thermal dynamics of a super-insulated building. https://doi.org/10.5281/ZENODO.1034820, 2017.

[29] M.D. Knudsen, L. Georges, K.S. Skeie, S. Petersen, Experimental test of a black-box economic model predictive control for residential space heating, Appl. Energy 298 (2021) 117227, https://doi.org/10.1016/j.apenergy.2021.117227.

[30] G. Bellu, M.P. Saccomani, S. Audoly, L. D'Angiò, DAISY: a new software tool to test global identifiability of biological and physiological systems, Comput. Methods Progr. Biomed. 88 (2007) 52–61, https://doi.org/10.1016/j.cmpb.2007.07.002.

[31] M.P. Saccomani, S. Audoly, G. Bellu, L. D'Angiò, Examples of testing global identifiability of biological and biomedical models with the DAISY software, Comput. Biol. Med. 40 (2010) 402–407, https://doi.org/10.1016/j.compbiomed.2010.02.004.

[32] P.J.C. Vogler-Finck, J. Clauß, L. Georges, I. Sartori, R. Wisniewski, Inverse model identification of the thermal dynamics of a Norwegian zero emission house, in: Cold Clim. HVAC Conf., Springer, 2018, pp. 533–543.

[33] L. Georges, M.J. Alonso, R. Woods, K. Wen, F. Håheim, P. Liu, M. Berge, M. Thalfeldt, Evaluation of Simplified Space-Heating Hydronic Distribution for Norwegian Passive Houses, SINTEF akademisk forlag, 2017. https://www.sintefbok.no/book/index/1123/evaluation_of_simplified_space-heating_hydronic_distribution_for_norwegian_passive_houses#carousel.

[34] X. Yu, L. Georges, M.D. Knudsen, I. Sartori, L. Imsland, Investigation of the model structure for low-order grey-box modelling of residential buildings, in: Proc. Build. Simul. 2019 16th Conf. IBPSA, International Building Performance Simulation Association, IBPSA, 2019, https://doi.org/10.26868/25222708.2019.211209.

[35] H. Viot, A. Sempey, L. Mora, J.C. Batsale, J. Malvestio, Model predictive control of a thermally activated building system to improve energy management of an experimental building: Part I—modeling and measurements, Energy Build. 172 (2018) 94–103, https://doi.org/10.1016/j.enbuild.2018.04.055.

[36] P. Bacher, H. Madsen, Identifying suitable models for the heat dynamics of buildings, Energy Build. 43 (2011) 1511–1522, https://doi.org/10.1016/j.enbuild.2011.02.005.

[37] T. Berthou, P. Stabat, R. Salvazet, D. Marchio, Development and validation of a gray box model to predict thermal behavior of occupied office buildings, Energy Build. 74 (2014) 91–100, https://doi.org/10.1016/j.enbuild.2014.01.038.

[38] J.E. Braun, N. Chaturvedi, An inverse gray-box model for transient building load prediction, HVAC R Res. 8 (2002) 73–99, https://doi.org/10.1080/10789669.2002.10391290.

[39] J. Hu, P. Karava, A state-space modeling approach and multi-level optimization algorithm for predictive control of multi-zone buildings with mixed-mode cooling, Build. Environ. 80 (2014) 259–273, https://doi.org/10.1016/j.buildenv.2014.05.003.

[40] S. Goyal, P. Barooah, A method for model-reduction of non-linear thermal dynamics of multi-zone buildings, Energy Build. 47 (2012) 332–340, https://doi.org/10.1016/j.enbuild.2011.12.005.

[41] E. Palomo Del Barrio, G. Lefebvre, P. Behar, N. Bailly, Using model size reduction techniques for thermal control applications in buildings, Energy Build. 33 (2000) 1–14, https://doi.org/10.1016/S0378-7788(00)00060-8.

[42] G. Reynders, J. Diriken, D. Saelens, Quality of grey-box models and identified parameters as function of the accuracy of input and observation signals, Energy Build. 82 (2014) 263–274, https://doi.org/10.1016/j.enbuild.2014.07.025.

[43] O.M. Brastein, D.W.U. Perera, C. Pfeifer, N.O. Skeie, Parameter estimation for grey-box models of building thermal behaviour, Energy Build. 169 (2018) 58–68, https://doi.org/10.1016/j.enbuild.2018.03.057.

[44] German Association of Engineers, Calculation of Transient Thermal Response of Rooms and Buildings E Modelling Of Rooms, 91.140.10(VDI 6007), Beuth Verlag GmbH, Düsseldorf, 2012.

[45] International Organization for Standardization, Energy Performance of Buildings E Calculation of Energy Use for Space Heating and Cooling (ISO 13790:2008), Geneva, 2008.

[46] M. Hu, F. Xiao, L. Wang, Investigation of demand response potentials of residential air conditioners in smart grids using grey-box room thermal model, Appl. Energy 207 (2017) 324–335, https://doi.org/10.1016/j.apenergy.2017.05.099.

[47] A.F. Villaverde, A. Barreiro, A. Papachristodoulou, Structural identifiability of dynamic systems biology models, PLoS Comput. Biol. 12 (2016), e1005153.

[48] O. Chis, J.R. Banga, E. Balsa-Canto, Methods for checking structural identifiability of nonlinear biosystems: a critical comparison, IFAC (2011), https://doi.org/10.3182/20110828-6-IT-1002.00800.

[49] L. Ljung, System Identification Toolbox ™ User's Guide, 2014.

[50] K.J. Åström, Introduction to Stochastic Control Theory, Courier Corporation, 2012.

[51] J. Wang, H. Chen, Y. Yuan, Y. Huang, A novel efficient optimization algorithm for parameter estimation of building thermal dynamic models, Build. Environ. 153 (2019) 233–240, https://doi.org/10.1016/j.buildenv.2019.02.006.

[52] J. Clauß, P. Vogler-Finck, L. Georges, Calibration of a high-resolution dynamic model for detailed investigation of the energy flexibility of a zero emission residential building, in: Cold Clim. HVAC Conf., Springer, 2018, pp. 725–736.

[53] Standard Norge, NS 3031 Energy Performance of Buildings: Calculation of Energy Needs and Energy Supply, 2016.

[54] R. Juhl, J.K. Møller, H. Madsen, ctsmr-Continuous Time Stochastic Modeling in R, 2016. ArXiv Prepr, 1606.00242.

RESEARCH PUBLICATIONS

PAPER 5

Yu X, Georges L, Imsland L. Adaptive linear grey-box models for Model Predictive Controller of Residential Buildings. Accepted to *International Conference Organised by IBPSA-Nordic*, 22nd-23rd August 2022, Copenhagen, Denmark. BuildSIM-Nordic 2022 (BSN2022). (Accepted)

RESEARCH PUBLICATIONS

Adaptive Linear Grey-Box Models for Model Predictive Controller of Residential Buildings

Xingji Yu[1*], Laurent Georges[1], Lars Imsland[2]
[1]Department of Energy and Process Engineering, Faculty of Engineering, NTNU - Norwegian University of Science and Technology, 7034 Trondheim, Norway
[2]Department of Engineering Cybernetics, Faculty of Information Technology and Electrical Engineering, NTNU -Norwegian University of Science and Technology, 7034 Trondheim, Norway
* *corresponding author: xingji.yu@ntnu.no*

Abstract

Model predictive control (MPC) is an advanced optimal control technique to minimize a control objective while satisfying a set of constraints and is well suited to activate the building energy flexibility. The MPC controller performance depends on the accuracy of the model prediction. Inaccurate predictions can directly lead to low control performance. Linear time-invariant (LTI) models are often used in MPC in buildings. However, LTI models do not adapt to the weather conditions varying throughout the whole space-heating season, which makes the MPC based on LTI models not perform well over a long period of time. Therefore, this study introduces an adaptive MPC where the parameters of a linear grey-box model are continuously updated in real-time. Two alternative versions of this adaptive control are investigated. The first one, called partially adaptive MPC, only updates the effective window area of the grey-box model, while the second one, called fully adaptive MPC, updates all the parameters of the grey-box model. Results show that the partially adaptive MPC is not able to deliver satisfactory prediction performance. The fully adaptive MPC shows better performance compared to the other models when implemented in a MPC, especially in avoiding thermal comfort violation.

Introduction

The grid system today is facing new challenges due to the fastly increasing penetration of renewable energy resources (RES). The weather-dependent RES brings intermittent and is prone to uncertainty which makes the balance between the electricity supply and demand a challenging task. Thus, more flexibility is needed for the current energy system. Demand response (DR) is considered as a feasible solution on the demand side, which can adapt to volatile electricity generation (Esther & Kumar, 2016; Oconnell et al., 2014). Buildings account for a significant proportion of final energy consumption in developed countries (Pérez-Lombard et al., 2008) (20–40%). The thermal mass of building envelopes can be used as short-term heat storage to perform DR. This study mainly investigates model predictive control (MPC) to activate the flexibility of the building thermal mass. The MPC controller enables the indoor temperature to fluctuate within acceptable indoor temperature limits for the occupants while it optimizes the time profile of energy use by loading the building thermal mass at certain periods. The MPC controller performance strongly depends on the accuracy of the model prediction. Therefore, identifying an accurate prediction model is a key task for the deployment of MPC.

This study focuses on MPC using grey-box models as the prediction model. Grey-box models have a structure based on physical laws, while the model parameters are calibrated on measurement data (i.e., based on time-series data). The grey-box models are not as mathematically complex as white-box models, so they are less computationally expensive to solve. Grey-box models also have better extrapolation properties than black-box models (Madsen et al., 2016). In grey-box models, lumped resistance and capacitance (RC networks) are commonly used to represent the model structure of the building, which is also used in this study. Some existing studies have shown that linear time-invariant (LTI) models can approximate the thermal dynamics of buildings with sufficient accuracy for MPC purposes (Bacher & Madsen, 2011; M. D. Knudsen & Petersen, 2020; Michael Dahl Knudsen & Petersen, 2017; Prívara et al., 2013; Vogler-Finck et al., 2018). However, the performance of the MPC controller cannot be maintained if it is applied over a long period of time due to the time-varying weather conditions throughout the year. Thus, an MPC controller where the parameters of the grey-box model can be updated in real-time should provide satisfactory control performance over a long period of time. This paper uses virtual experiments (i.e., co-simulation) to compare the performance of a conventional MPC based on an LTI model to an adaptive MPC. IDA ICE is a detailed dynamic building performance simulation (BPS) software, which is used as the emulator for virtual experiments. The MPC controller is implemented in MATLAB with a co-simulation function in IDA-ICE provided by the company EQUA.

The data collected from IDA ICE simulations are used to train the parameters of the grey-box model. Then, the obtained model is used as the prediction model for the MPC controller. The adaptive MPC controller has two versions in this study. The first version, called partially adaptive MPC, only updates the effective window area of the grey-box model when the prediction error is large during the MPC operation. The reason is that solar radiation is the dominant factor that influences the model accuracy due to the cloud condition, changing altitude and zenith angles of the sun. The second version, called fully

adaptive MPC, updates all the parameters of the grey-box model when the prediction error is large during the MPC operation. The second version has more freedom to fit the model parameters compared to the first one. However, the second version of adaptive MPC theoretically takes more time to converge to a new set of parameters and may have the risk of obtaining a set of unphysical parameters due to insufficient training data. Both versions of the adaptive model use the full space-heating season data (here called full winter) to train the model parameters as the initial model to start the adaptive MPC. This study compares the performance of a conventional MPC based on an LTI grey-box model to the adaptive MPC.

Description of virtual experiments setup

This study uses a building model in IDA ICE developed in a previous study (Yu et al., 2021) as the emulator for the co-simulation. It is a detached house in Oslo. The floor area of the house is approximately 160 m^2 and is constructed in wood. The lightweight construction complies with Norwegian passive house standards (NS 3700 [15]) requirements. The appearance of the building is shown in Figure 1, while its floor plan is presented in Figure 2. The envelope of the building is the dominant heat dynamics to be modeled in this study, which has good linear properties. Thus, it is reasonable to use the linear grey-box model as the prediction model for the MPC controller design. The internal doors of the building are set to be open in the virtual experiments. Therefore, the mono-zone grey-box model is considered as the prediction model. The temperature of the indoor air node is represented by the volume-averaged temperature of the nine zones in IDA ICE. Electrical radiators are selected to be the space-heating system in the BPS since they are it is the most common for Norwegian residential buildings (Bøeng et al., 2014). The heat dynamics of electrical radiators are neglectable due to much smaller thermal inertia compared to the envelope. The profile for internal gains and occupancy is taken from the Norwegian technical standard TS3031:2016 (Norge, 2016).

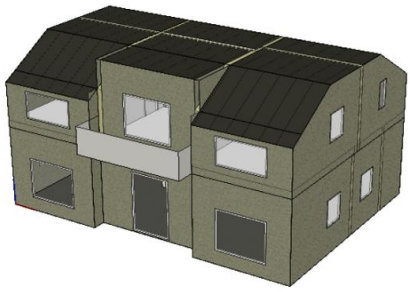

Figure 1: 3D geometry of the building model in IDA ICE (showing the southwest facade)

The heat dynamics of the building need to be perturbed to obtain the data for training the model parameters. The Pseudo-Random Binary Signal (PRBS) approximates white noise properties, which can excite the dynamic system in a large spectrum of frequencies (Kristensen et al., 2004; Lennart, 1999). The electrical radiator is the only controllable input of the system, so the PRBS signal is applied to the electrical radiator to obtain the training data. It is not always feasible to apply PRBS signal in real operation due to thermal discomfort caused by large variations of the indoor temperature for occupants. Therefore, the time of applying PRBS signal should also be limited. This study takes one week in November as the training week to apply PRBS signal to the heating system. It starts on November 23rd and lasts for one week (close to the middle of the whole experimental period). The outdoor temperature is mild with an average value of 5 °C. The data generated under typical operations are also used as training data. Intermittent heating with changing temperature setpoints is applied. The setpoint is shifted between daytime and nighttime (i.e. a night setback) and the local controller of the radiator is on-off. The model trained from the PRBS signal is only used for the LTI control model. The model trained from the full winter intermittent heating with changing temperature setpoints is also used as the initial model for the adaptive MPC.

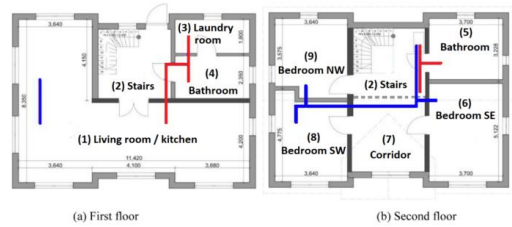

Figure 2: Floor plan of the test building (ducts for the supply ventilation air are in blue and in red for extraction)

In the co-simulation, the length of each MPC time step is set to 15 min. IDA ICE first sends the current calculated volume-averaged indoor temperature of the building to MATLAB. Then the MPC controller takes the prediction of the weather data and internal heat gains into the optimization to output the optimal control sequence for the heating system. However, only the first step decision of the control sequence is taken and sent back to IDA ICE. The heaters in the building will execute the calculated optimal power after receiving the control signal. When this time step is done in IDA ICE, the new state of the volume-averaged indoor temperature is sent back to MATLAB again; a new round starts. The process will keep iterating in time using this co-simulation setup until the pre-determined simulation period is finished. A similar co-simulation setup with IDA ICE has been applied in the study (Khatibi et al., 2022). A short initialization period is necessary for IDA ICE to come to realistic temperatures in each zone of the model, so PID control is applied at the beginning of co-simulation. The length of the initialization period in this study is set to be half-day.

In the co-simulation framework, there are variable constraints set in the MPC due to system limitations. In

the IDA ICE model, the total heating power of all the radiators is 3220W. The radiator in IDA ICE is assumed to be able to modulate its power by adjusting its part load ratio (PLR). Thus, the power constraint of the heating system in the MPC is from 0 to 3220W. The thermal comfort should also be considered and it is here considered using minimum and maximum indoor temperature limits. The minimum indoor temperature limit is set to be 20 °C and the maximum limit is set to be 24 °C. There is a night setback for the minimum temperature limilt decreasing from 20°C to 16 °C from 11PM to 7AM.

Methodology

Grey-box model

A grey-box model structure that has too many parameters may lead to overfitting and increase the calculation cost. Lower order models with few parameters can decrease the calculation cost for the MPC optimization but at the cost of unacceptable prediction performance. A considerable amount of research has already been done to find suitable mono-zone grey-box model structures to be applied to MPC of buildings (Bacher & Madsen, 2011; Berthou et al., 2014; Harb et al., 2016; Reynders et al., 2014; Viot et al., 2018). In the previous study (Yu et al., 2022), a 3R2C grey-box model has proven to be a suitable trade-off between model complexity and accuracy for the test case. Therefore, this model structure is used for the MPC controller in our work. The model structure and its parameters are given in Figure 3 and Table 1.

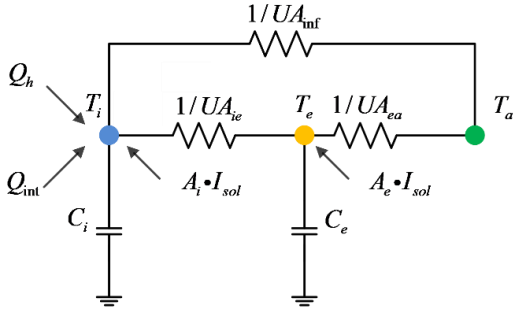

Figure 3: 3R2C grey-box model

Table 1: The physical interpretation of the parameters of the 3R2C grey-box model

Parameters	Physical interpretation and unit
T_i	Temperature of the internal node (i.e., indoor air, furniture) [°C].
T_e	Temperature of the external walls [°C].
T_a	The ambient (or outdoor) temperature [°C].
C_i	Heat capacity including the thermal mass of the air, the furniture [kWh/K].
C_e	Heat capacity of external wall [kWh/K].
UA_{ie}	Heat conductance between the building envelope and the interior [kW/K].
UA_{ea}	Heat conductance between the outdoor and the building envelope [kW/K].
UA_{inf}	Heat conductance between the outdoor and the interior node (components with negligible thermal mass, like windows and doors) [kW/K].
Q_{int}	Internal heat gain from artificial lighting, people and electric appliances [kW].
Q_h	Heat gain delivered to the heat emitter [kW].
I_{sol}	Global solar irradiation on a horizontal plane [W/m^2].
A_i	The effective window area of the building corresponding to T_i [m^2].
A_e	The effective window area of the building corresponding to T_e [m^2].

MATLAB system identification toolbox (Ljung, 2014) is used to calibrate the parameters of the grey-box model. This paper uses the global optimization routine of the previous study (Yu et al., 2021) to avoid the local optimum. The routine consists of two stages. The heuristic particle swarm optimization (PSO) is used at the first stage to give a general estimation of parameter values. Then the gradient-based optimization function (*greyest*) is applied in the second stage to further polish the parameter values. The objective function *f(x)* of the optimization is defined as Equation 1.

$$f(x) = \sqrt{\frac{\sum_{k=1}^{N} \| y_k - \hat{y}_k(\theta) \|^2}{N}} \quad (1)$$

Optimal Control Problem Formulation

The goal to implement MPC in the building varies between applications. The objective function of the MPC in our study is to minimize the total electricity use of the heating system while keeping the building within the thermal comfort temperature limits.

With the control objectives and constraints, the optimal control problem can be formulated. The time step of each control decision is 15 minutes. The prediction horizon of the MPC controller is set to be 24 hours (96 slots, N = 96). This duration of the prediction horizon is a typical value found in the literature. It keeps the computational time reasonable. The equations of the optimization problem are given below.

$$\min_{Q_h} \sum_{k=0}^{N-1} Q_h[k] + \varepsilon_1[k] L \varepsilon_1^{'}[k] + \varepsilon_2[k] L \varepsilon_2^{'}[k] \quad (2)$$

Subject to

$$x[k+1] = Fx[k] + Gu[k] + Ke[k], k \in N_0^{N-1} \quad (3)$$

$$T_{indoor}[k] = Cx[k], k \in N_0^{N-1} \quad (4)$$

$$T_{low}[k] - \varepsilon_1[k] \le T_{indoor}[k], k \in N_0^{N-1} \quad (5)$$

$$T_{indoor}[k] \le T_{up}[k] + \varepsilon_2[k], k \in N_0^{N-1} \quad (6)$$

$$0 \le Q_h[k] \le Q_{h,\max}[k], k \in N_0^{N-1} \quad (7)$$

$$0 \le \varepsilon_1[k]; 0 \le \varepsilon_2[k], k \in N_0^{N-1} \quad (8)$$

In the equations, $x[k]$ is the state vector in discrete-time, F, G and C are the discrete state space matrice obtained from the grey-box model identification process, $u[k]$ is the input vector in discrete-time and $y[k]$ is the output. K is the tunned steady Kalman gain. $Q_h[k]$ is the calculated optimal heat power at each step for the prediction horizon, while $Q_{h,max}[k]$ is the max power of the heating system. $\varepsilon_1[k]$ and $\varepsilon_2[k]$ are the slack variables of the soft constraints on the thermal comfort band. The existence of soft constraints can help the solver to avoid infeasible optimization problems by allowing thermal comfort limits to be violated. $T_{indoor}[k]$ is the predicted indoor temperature from the grey-box model. $T_{low}[k]$ and $T_{up}[k]$ are the corresponding temperature limits during the prediction horizon. The thermal discomfort (ε) is quantified in Kelvin hours outside the predefined thermal comfort limits. L is the penalty factor for discomfort in the objective function. For favor comparison of results, it has been decided that the thermal discomfort should be rare when using MPC so that a very high value of 10^8 is given to the penalty L. MPC resorts to a receding horizon. The above optimization problem is solved at each step to get the optimal control decision. Then, the initial states of the model and the weather forecasts are updated with the receded prediction horizon. Due to the quadratic form of the slack variables ε_1 and ε_2, a solver that can solve quadratic programming problems is needed. In this study, the toolbox YALMIP (Lofberg, 2004) in MATLAB is used for the formulation of the optimization problem, while Gurobi (Lofberg & Gurobi Optimization, 2004) is used to solve the optimization problem.

Conventional and Adaptive MPC

The baseline MPC is based on LTI models, which keep the value of the model parameters constant during simulation. The LTI model trained using the full winter experiments with intermittent heating is called *FullWinter*. The LTI model trained using the PRBS experiments of November is called *PRBSNOV*.

The partially adaptive MPC takes the FullWinter model to initialize the model, only the effective window area (A_i) parameter is updated during the simulation. The pseudo-code for updating the effective window area is presented in Algorithm 1. The fully adaptive MPC also starts with the FullWinter model but updates all the seven parameters of the model during simulation. The pseudo-code for fully adaptive MPC is presented in Algorithm 2.

The sliding accumulated error (ErrorS) is the index to detect when the parameters need to be updated. The sliding accumulated error sums up the absolute value of the prediction error (value difference between the measurement and the model prediction). The length of the sliding accumulated error is set to be 12 steps (i.e., 3 hours). When the ErrorS is larger than a predefined threshold, it actives the parameter updating routine. The threshold is called error_index and is set to be 5 in this study. It is unreasonable to use a short training period to update the model parameters as the parameters can be unphysical or with large uncertainty. On the opposite, taking a long period of historical data for training is also not optimal since the adaptive MPC should be able to adapt the parameters for changing operating conditions. Pushed to extremes, a very long training period will make the adaptive model converge to the LTI model. Thus, the two adaptive MPC take a training period of 7 days of data to update the model parameters. As a result, the adaptive MPC routines are not able to start the first model update during the first seven days of co-simulation.

Algorithm 1: Pseudo-code for the partially adaptive MPC

Algorithm 1: Partially Adaptive MPC

Initialize: Set FullWinter as the prediction model for the Partially Adaptive MPC;

Input: ErrorS;

if ErrorS> ErrorIndex

  Update the parameter A_i.

else

  Keep A_i unchanged.

end

Algorithm 2: Pseudo-code for the fully adaptive MPC

Algorithm 2: Fully Adaptive MPC

Initialize: Set FullWinter as the prediction model for the fully Adaptive MPC;

Input: ErrorS;

if ErrorS > ErrorIndex

  Update all parameters of the model.

else

  Keep parameters unchanged.

end

Results

The results using different MPCs are presented in this section. The virtual experiment starts from November 1st to December 31th (i.e., 61 days). The first 12 hours of simulation always start with a PID control to stabilize the co-simulation environment. Then, the control is switched to MPC. PRBSNOV MPC uses the LTI grey-box model trained using the data from one week of building operation with the PRBS excitation in November (PRBSNOV). FullWinter MPC uses the LTI grey-box

Table 2: Results summary of MPC controllers' performance

	FullWinter MPC	PRBSNOV MPC	Partially Adaptive MPC	Fully Adaptive MPC
Consumed Energy [kWh]	803.73	855.18	804.06	893.62
Thermal Discomfort [Kh]	534.39	194.37	528.87	72.04

model trained with the data from the intermittent heating with changing temperature setpoints during the full space-heating season (i.e., from November 1st to March 31th). The indoor temperature computed using co-simulation and the four MPC controllers are shown in Figure 4. Figure 5 is a close-up section of Figure 4 and the corresponding heating power of the radiator is also given. The aggregated results are given in Table 2. The history of the effective window area update is shown in Figure 6.

It can be seen that the FullWinter MPC can not make a satisfactory prediction, which causes the thermal comfort constraint to be significantly and frequently violated. The

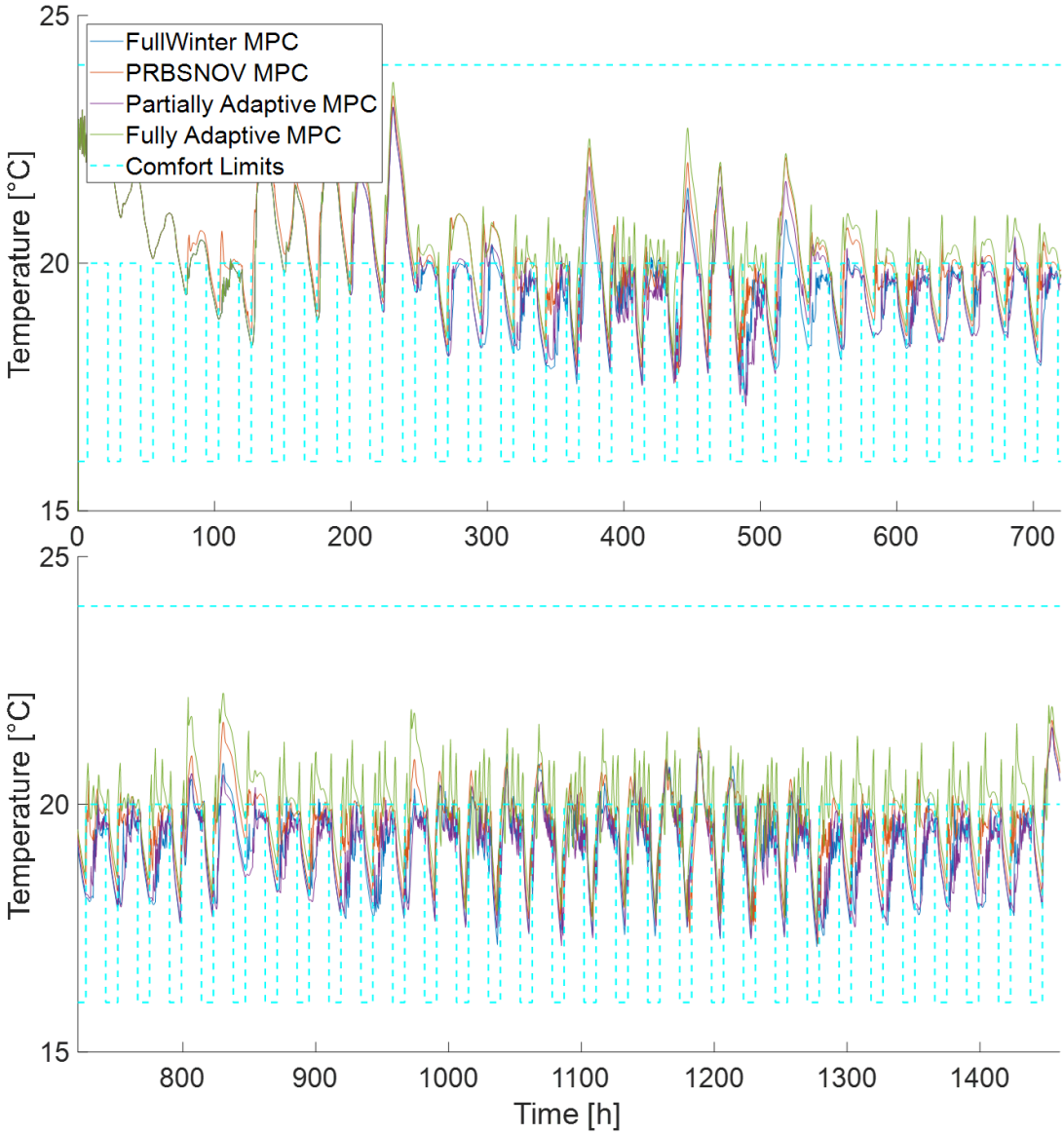

Figure 4: Indoor temperature profile under the operation of different MPC controllers with energy saving objective

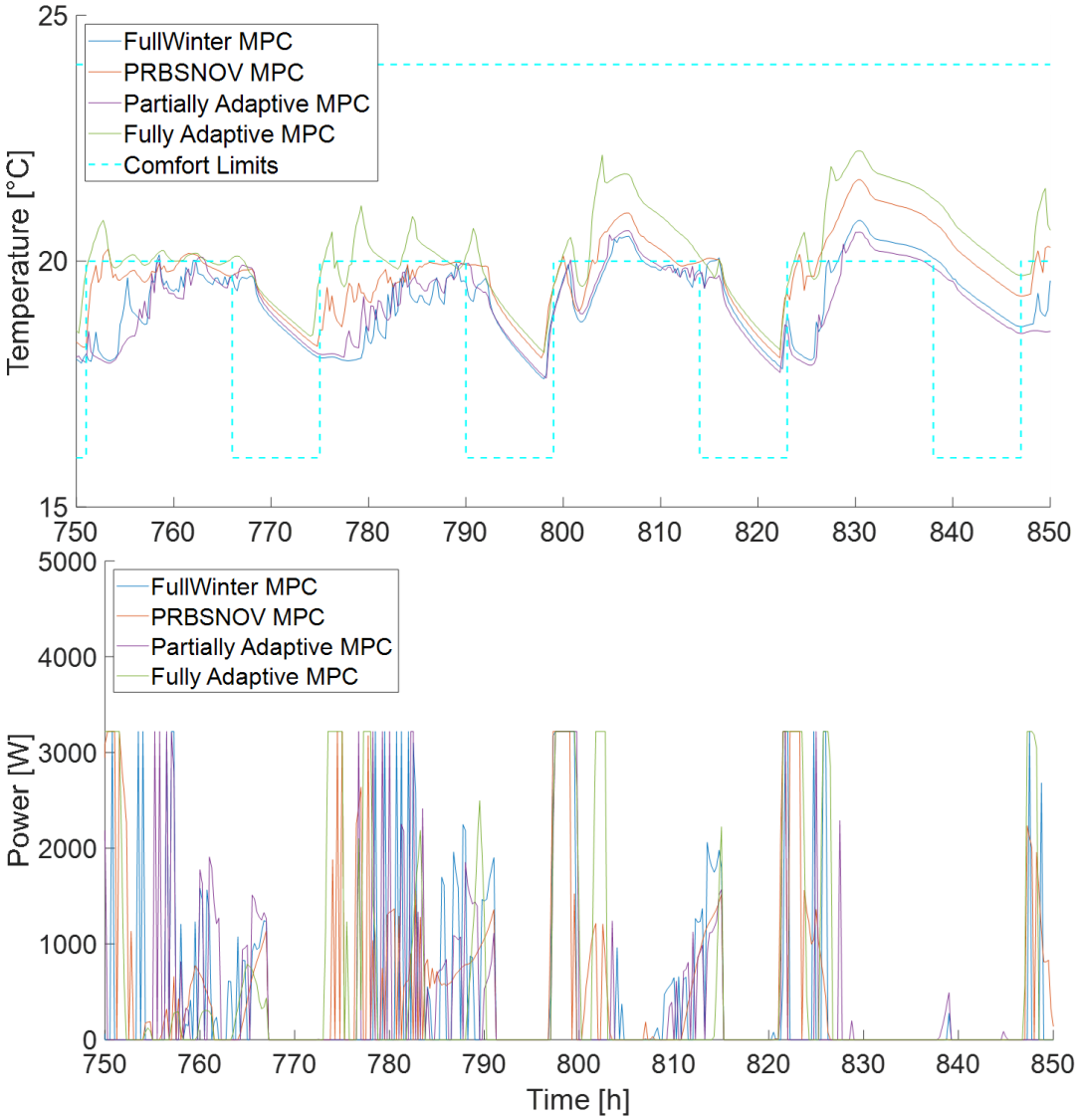

Figure 5: Close-up of the indoor temperature profile under the operation of different MPC controllers with energy saving objective

partially adaptive MPC shows only slightly better performance compared to the FullWinter MPC. The thermal comfort constraint is still frequently violated. These two models consume less energy compared to the other two models (i.e., the fully adaptive MPC and the PRBSNOV MPC). However, the MPC should first guarantee the thermal comfort of the occupants and then provide DR service to the grid. The FullWinter MPC and Partially Adaptive MPC consume less energy because they are less accurate, which causes the indoor temperature to drop below the minimum indoor temperature threshold. The heating system is switched on too late in the morning and causes large thermal discomfort. This indicates that the LTI grey-box model trained using the full winter data may not be suitable as the prediction model in MPC. Furthermore, quite surprisingly, only updating the effective window area of the model is not sufficient. This is also confirmed by the history of updates of the effective window area. The partially adaptive MPC updates the window area continuously, which means that the sliding accumulated error is always very large during simulation. The PRBSNOV MPC performs much better than the previous two models in terms of thermal discomfort. The resulting energy use of the PRBSNOV MPC is consequently higher. This result proves that it is necessary to use a model that is calibrated using a training period similar to the period when the MPC will be operated. The fully

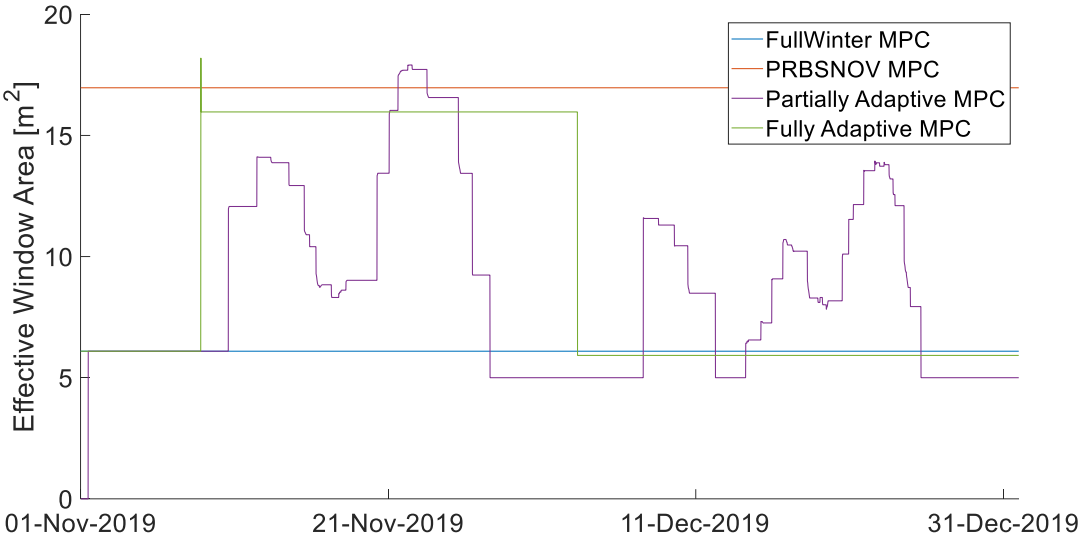

Figure 6: History of the effective window area update

adaptive MPC further reduces the thermal discomfort significantly compared to the PRBSNOV MPC. However, the consumed energy is even higher. The fully adaptive model performs better than the partially adaptive model mainly due to the extra degrees of freedom to adapt the model parameters. After the first update of the parameters done by the fully adaptive MPC, the violation of the indoor temperature constraint is significantly reduced. As shown in Figure 6, the effective window area is only updated three times during the simulation, which means that the obtained model is accurate and can deliver a decent prediction.

Conclusion

This study aims to assess different MPC controller performances using virtual experiments by coupling IDA ICE and MATLAB. The control objective of the MPC controller is to minimize the energy use with a high penalty on the thermal discomfort to give priority to thermal comfort over energy use.

Results show that the LTI grey-box model trained using the FullWinter data is not suitable as MPC prediction model. This model is too general and gives large prediction errors during specific periods of the winter. This is confirmed by the LTI grey-box model training using a PRBS excitation sequence for one week in November (PRBSNOV). The model is better calibrated to November than the FullWinter model and the resulting MPC gives better performance.

Although the effective window area is known to vary significantly during the space-heating season, only updating the window area of the model is surprisingly not enough to reach satisfactory MPC performance. The lower amount of indoor temperature violations of the fully adaptive MPC compared to the PRBSNOV MPC demonstrates the need to update all the model parameters during the space-heating season.

In future work, the performance of the four MPC controllers will be compared for different objective functions (e.g, minimization of the energy cost or the energy use during peak hours) and different magnitudes for the penalty coefficient weighting the thermal discomfort in the objective function.

Acknowledgment

This work is conducted in the framework of the Norwegian Research Centre on Zero Emission Neighbourhoods in Smart Cities (ZEN), funded by the Research Council of Norway and industry partners.

References

Bacher, P., & Madsen, H. (2011). Identifying suitable models for the heat dynamics of buildings. *Energy and Buildings*, *43*(7), 1511–1522. https://doi.org/10.1016/j.enbuild.2011.02.005

Berthou, T., Stabat, P., Salvazet, R., & Marchio, D. (2014). Development and validation of a gray box model to predict thermal behavior of occupied office buildings. *Energy and Buildings*, *74*, 91–100. https://doi.org/10.1016/j.enbuild.2014.01.038

Bøeng, A. C., Halvorsen, B., & Larsen, B. M. (2014). Kartlegging av oppvarmingsutstyr i husholdningene. In *Rapport 2014/45*. https://www.ssb.no/energi-og-industri/artikler-og-publikasjoner/kartlegging-av-oppvarmingsutstyr-i-husholdningene

Esther, B. P., & Kumar, K. S. (2016). A survey on residential Demand Side Management architecture, approaches, optimization models and methods. *Renewable and Sustainable Energy Reviews*, *59*,

342–351. https://doi.org/10.1016/J.RSER.2015.12.282

Harb, H., Boyanov, N., Hernandez, L., Streblow, R., & Müller, D. (2016). Development and validation of grey-box models for forecasting the thermal response of occupied buildings. *Energy and Buildings*, *117*, 199–207. https://doi.org/10.1016/j.enbuild.2016.02.021

Khatibi, M., Rahnama, S., Vogler-Finck, P., Bendtsen, J. D., & Afshari, A. (2022). Investigating the flexibility of a novel multi-zone air heating and ventilation system using model predictive control. *Journal of Building Engineering*, *49*(January), 104100. https://doi.org/10.1016/j.jobe.2022.104100

Knudsen, M. D., & Petersen, S. (2020). Economic model predictive control of space heating and dynamic solar shading. *Energy and Buildings*, *209*. https://doi.org/10.1016/j.enbuild.2019.109661

Knudsen, Michael Dahl, & Petersen, S. (2017). Model predictive control for demand response of domestic hot water preparation in ultra-low temperature district heating systems. *Energy and Buildings*, *146*, 55–64. https://doi.org/10.1016/j.enbuild.2017.04.023

Kristensen, N. R., Madsen, H., & Jørgensen, S. B. (2004). Parameter estimation in stochastic grey-box models. *Automatica*, *40*(2), 225–237. https://doi.org/10.1016/j.automatica.2003.10.001

Lennart, L. (1999). System identification: theory for the user. *PTR Prentice Hall, Upper Saddle River, NJ*, 1–14.

Ljung, L. (2014). *System Identification Toolbox ™ User ' s Guide*. *December*.

Lofberg, J. (2004). YALMIP: A toolbox for modeling and optimization in MATLAB. *2004 IEEE International Conference on Robotics and Automation (IEEE Cat. No. 04CH37508)*, 284–289.

Lofberg, J., & Gurobi Optimization, L. L. C. (2004). Gurobi optimizer reference manual. *2004 IEEE International Conference on Robotics and Automation (IEEE Cat. No. 04CH37508)*, 284–289.

Madsen, H., Bacher, P., Bauwens, G., Deconinck, A.-H., Reynders, G., Roels, S., Himpe, E., & Lethé, G. (2016). *IEA EBC Annex 58-Reliable building energy performance characterisation based on full scale dynamic measurements. Report of subtask 3, part 2: Thermal performance characterisation using time series data-statistical guidelines*. https://www.iea-ebc.org/Data/publications/EBC_Annex_58_Final_Report_ST3b.pdf

Norge, S. (2016). SN/TS 3031: 2016 Energy performance of buildings. In *Calculation of energy needs and energy supply*.

Oconnell, N., Pinson, P., Madsen, H., Omalley, M., Esther, B. P., & Kumar, K. S. (2014). Benefits and challenges of electrical demand response: A critical review. *Renewable and Sustainable Energy Reviews*, *39*, 686–699. https://doi.org/10.1016/j.rser.2014.07.098

Pérez-Lombard, L., Ortiz, J., & Pout, C. (2008). A review on buildings energy consumption information. *Energy and Buildings*, *40*(3), 394–398. https://doi.org/10.1016/j.enbuild.2007.03.007

Prívara, S., Cigler, J., Váňa, Z., Oldewurtel, F., Sagerschnig, C., & Žáčeková, E. (2013). Building modeling as a crucial part for building predictive control. *Energy and Buildings*, *56*, 8–22. https://doi.org/10.1016/j.enbuild.2012.10.024

Reynders, G., Diriken, J., & Saelens, D. (2014). Quality of grey-box models and identified parameters as function of the accuracy of input and observation signals. *Energy and Buildings*, *82*, 263–274. https://doi.org/10.1016/j.enbuild.2014.07.025

Viot, H., Sempey, A., Mora, L., Batsale, J. C., & Malvestio, J. (2018). Model predictive control of a thermally activated building system to improve energy management of an experimental building: Part I—Modeling and measurements. *Energy and Buildings*, *172*, 94–103. https://doi.org/10.1016/j.enbuild.2018.04.055

Vogler-Finck, P. J. C., Clauß, J., Georges, L., Sartori, I., & Wisniewski, R. (2018). Inverse Model Identification of the Thermal Dynamics of a Norwegian Zero Emission House. *Cold Climate HVAC Conference*, 533–543.

Yu, X., Georges, L., & Imsland, L. (2021). Data pre-processing and optimization techniques for stochastic and deterministic low-order grey-box models of residential buildings. *Energy and Buildings*, *236*, 110775. https://doi.org/10.1016/j.enbuild.2021.110775

Yu, X., Skeie, K. S., Knudsen, M. D., Ren, Z., Imsland, L., & Georges, L. (2022). Influence of data pre-processing and sensor dynamics on grey-box models for space-heating: Analysis using field measurements. *Building and Environment*, *212*(October 2021), 108832. https://doi.org/10.1016/j.buildenv.2022.108832

PAPER 6

Yu X, Ren Z, Georges L, Imsland L. Comparison of Time-Invariant and Adaptive Linear Grey-box Models for Model Predictive Control of Residential Buildings. Submitted to *Applied Energy* (Under review)

This paper is awaiting publication and is not included

RESEARCH PUBLICATIONS

PAPER 7

Erfani A, Yu X, Kull TM, Bacher P, Jafarinejad T, Roels S, Saelens D. Analysis of the impact of predictive models on the quality of the model predictive control for an experimental building. *Proceedings of Building Simulation 2021 17th Conference IBPSA*, International Building Performance Simulation Association (IBPSA), 1st-3rd September 2021, Bruges, Belgium.

RESEARCH PUBLICATIONS

Analysis of the impact of predictive models on the quality of the model predictive control for an experimental building

Arash Erfani[1], Xingji Yu[2], Tuule Mall Kull[3], Peder Bacher[4], Tohid Jafarinejad[1], Staf Roels[1], Dirk Saelens[1,5]
[1]KU Leuven, Department of Civil Engineering, Building Physics & Sustainable Design Section, Leuven, Belgium
[2]NTNU, Trondheim, Norway
[3]Tallinn University of Technology, Tallinn, Estonia
[4]DTU, Lyngby, Denmark
[5]EnergyVille, Genk, Belgium

Abstract

To increase energy efficiency of the building sector, many measures have been suggested which often require a predictive model of the building to function. Developing these models is one of the crucial challenges hampering pervasive use of these measures. Therefore, this study aims at assessing the impact of using different predictive models in an energy optimization application for an experimental building. First step in achieving this goal is developing various data-driven models for the investigated building in this study. Afterwards, a framework has been developed in which the performance of predictive models in the optimization strategy namely Model Predictive Control (MPC) could be evaluated. The results reveal that common indicators in the literature do no suffice to score the performance of models used in MPC, but another state-of-the-art indicator; multi-step ahead prediction error is more suitable for evaluating predictive models deployed in MPC.

Key innovations

- Finding a proper Key Performance Indicator (KPI) for evaluating various predictive models in an MPC framework
- Assessing the impact of one-step ahead prediction and multi-step ahead prediction accuracy on model's quality in MPC
- Applying Support Vector Machine as a powerful AI tool for building behavior identification

Practical implications

This paper could guide practitioners who work on building energy optimization in choosing a suitable model in their optimization algorithm .In addition; we suggest an appropriate criterion to assess the predictive models in terms of their performance in MPC, which could be instrumental for both researchers and practitioners.

Introduction

Surveys have shown that building stock has the highest potential in terms of energy saving to achieve *well below 2 ^{o}C* target by 2050 set in Paris agreement (EU Commission, 2018). Approximately 71% of all the final energy use in residential sector in Europe is used for space heating alone (EU Commission, 2018). Hence, there is a considerable potential of energy saving which could be activated by optimizing performance of existing HVAC systems. Several strategies have been proposed to increase existing building's energy efficiency such as RES integration (Haddadi et al., 2019), shading control (Da Silva et al., 2012), optimal control of HVAC systems (De Coninck & Helsen, 2016), heat recovery (Jafarinejad, et al., 2019), glazing improvement (Djamel & Noureddine, 2017), smart houses and etc. (Eicker et al., 2015; Guerra-Santin & Tweed, 2015). RES integration is one of the promising options. However, their uncertain nature affects all the energy users such as buildings (Reynders et al., 2017). One of these impacts is that the integration of RES in buildings renders performance of traditional control strategies non-optimal (Sangi et al., 2019). Hence, substantial attention has been paid to advanced control strategies recently (Afram & Janabi-Sharifi, 2014).

Amongst various control strategies suggested for optimization of building's thermal performance, Model Predictive Control (MPC) is one of the most promising ones. MPC is an active control strategy which optimizes the performance of a system over a given time horizon (Drgoňa et al., 2020). It has shown a considerable potential in optimizing the performance of HVAC systems along with facilitating the integration of RES in buildings (Atam & Helsen, 2016). MPC has the ability to handle slow moving dynamics, which matches the requirements for a good optimization strategy for buildings. To this end, MPC uses a model of the building to predict its thermal behavior in the future. This prediction feature gives MPC a crucial edge compared to other controllers (Reynders et al., 2014; Sourbron et al., 2013). Myriad studies have been carried out on application of MPC in buildings (Drgoňa et al., 2020). In spite of the abundance of such studies, MPC is still not used prevalently in buildings. One of the main issues hampering easy and cost-efficient implementation of MPC in buildings is developing a predictive model of the building (Sourbron et al., 2013).

This study aims at comparing different modeling techniques, which are used to identify a building's thermal characteristic and are integrated into the MPC framework as the predictive model. In this study, we place our focus on data-driven methods used for characterizing building's

thermal behavior since there is an ever-increasing interest in employing data-driven techniques for building energy optimization applications (Sepasgozar et al., 2020).

In general, data-driven methods could be divided into two categories, black box and grey-box models. In black box modeling techniques, the mapping between the input and the output is a mathematical one. These models have a wide range from a simple regression to complex AI-based methods such as deep learning methods (Drgoňa et al., 2020). As for grey-box models, they could be defined as a hybrid between mathematical (black-box) models and physics-based (white-box) models. In the most popular type of grey-box models used in buildings, structure of the model is determined by simplified physical laws governing building's dynamics. Next, , parameters of the model are estimated based on datasets (Afroz et al., 2018).

An important question, which comes up in the process of model selection and training, is how do I know which model would perform the best in my MPC? In other words, how to quantify the quality of different predictive models in the context of MPC. In this work, we endeavor to answer the above question by applying different KPIs to different models and assessing their suitability to score those models. We look into the one-step ahead prediction and multi-step-ahead prediction error (MSPE) of the models as two different KPIs for predictive models.

MSPE has been considered for quantifying predictive models in MPC before. The concept of Model predictive control Relevant Identification (MRI) for buildings was first introduced by (Žáčeková & Prívara, 2012) in which they developed a grey-box model based on MSPE minimization. Thereafter, some research studies in this field reported MSPE of their models in their work (Zhan & Chong, 2021). In one of the most relevant of these studies, (Picard et al., 2016) developed a detailed Modelica model for an office building. This Modelica model is then linearized into a state space model. Two grey-box models were developed in their study as well. One was identified based on measurements and the other one based on the proxy data obtained from the emulator. Performance of these three models are evaluated for 1 hour and 24 hours ahead. They showed that the most accurate model (linearized state space model) used 50% less energy while providing better thermal comfort. In a similar study, (Picard et al., 2017) applied model order reduction techniques to a white box model of a residential building and reported their model's quality based on both one-step ahead error and MSPE. They concluded that such models should be of higher order compared to their peer data-driven models to yield an MPC with good performance.

Although the concept of MSPE has been used before in the context of MPC design for a building, but a thorough analysis on its suitability for scoring different predictive models is lacking. In other words, previous studies did not consider various data-driven models in their structures. In addition, they did not distinguish between the impact of one-step and multi-step ahead prediction accuracy on the models and its impact on the controller's performance. In this paper, we take into account the MSPE associated with each model as a KPI and compare it to one-step ahead prediction error. In addition, Support Vector Machine (SVM) as a powerful tool in machine learning field has been applied for in the context of MPC.

The models developed for this study are AutoRegressive with eXogenous inputs (ARX), grey-box RC models with different orders, black-box State Space (SS) models with different orders, SVM and Artificial Neural network (ANN) with a Non-linear Auto-Regressive with eXogenous inputs (NARX) structure. The results of applying MPC with different models for 2 weeks in the heating season are presented. To be able to evaluate performance of these models in MPC, a framework has been considered. First, a simulation model of an experimental building equipped with an underfloor heating system has been developed. This simulation model replaces the real building in our simulations. This experimental building is one of the experimental buildings in the context of IEA Annex 71 project. MPC has been developed in MATLAB SIMULINK environment. The simulation model has been coupled to the controller using an Application Programming Interface (API). Furthermore, MPC results are compared to the ones of a well-tuned Rule-Based Controller (RBC) to show its superiority over traditional control methods.

First, framework of the study is described. Subsequently, predictive models developed for this study are described. Then, we proceed by presenting and analyzing the results of different MPCs. Last section concludes the paper.

Framework

In this section, various parts required for evaluating MPC for a building are described; starting with the building itself. Then, the API used in this study is briefly explained. Afterwards, structure of the MPC itself is explained. General schematic of the framework applied in this study is shown in Figure 1, which is explained in the rest of this section from top to bottom.

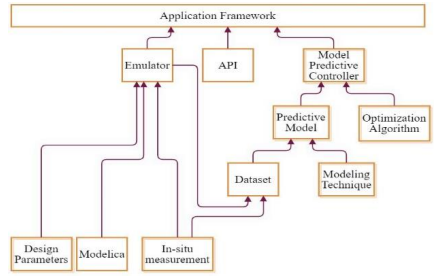

Figure 1: MPC framework for data-driven models

As it could be seen in Figure 1, one of the important components in simulating the performance of MPC in a building is to have a simulation model, which mimics the behaviour of the real building. Henceforth, this model is called the *emulator*. The emulator model is usually a complex white-box model, which due to its high computational load is not suitable to be deployed in real-time optimization applications (Afram & Janabi-Sharifi, 2014). Therefore, there is a need for simple and efficient model embedded in the MPC which is responsible for

predicting building's dynamics over a given time horizon. These models are called *predictive models.* The rest of this section is allocated to detailed description of different components of the framework shown in Figure 1.

Building

We first give a short description of the real building, which has been modelled using Modelica language in Dymola software using the OpenIDEAS library (Baetens et al., 2015). This simulation model serves as the emulator in this study. The building under study is one of the test cases of the IEA ANNEX 71 project titled: *"Building energy performance assessment based on in situ measurements."* Test building in this study is a two-storey experimental dwelling located in Holzkirchen, Germany. (See Figure 2)

Figure 2: Test Building

This building is equipped with multiple instruments for measuring and storing time-series data of different variables. Heating is provided by means of an air-to-water heat pump, which provides hot water for an underfloor heating system that is installed for both floors. (Figure 3). Occupants are introduced to the building using electrical heaters based on a pre-defined schedule. Thermometers are installed in all rooms to measure room's temperature. Ventilation system functions based on a pre-defined schedule and is equipped with measurement instruments both in exhaust and supply terminals.

Figure 3: Heat pump and the underfloor heating system

API

The controller in this study has been developed in SIMULINK, whereas the emulator is developed in Dymola. Hence, a way of communication is required to make the co-simulation between the two softwares possible. To tackle this issue, we use an interface, which facilitates the connection between Dymola and Matlab, which is called Functional Mock-up Interface (FMI).

The developed building model in Modelica is essentially composed of equations derived from physical laws. FMI translates these equations into binary format, which is supported by many simulation tools including MATLAB and Python. This binary file could be loaded and run by these softwares (Modelica Association Project "FMI," 2013). In this work, the emulator model of the building is compiled as a Functional Mock-up Unit (FMU). Then it is imported into SIMULINK using the FMU block of MATLAB. From there on, the FMU serves as the emulator model in our MPC framework and easily communicates with the controller in the Simulink environment.

Model Predictive Controller

MPC is composed of two main parts. A predictive model and an optimizer. Interested readers can refer to (Drgoňa et al., 2020) for further details on MPC formulation for buildings. The objective of the MPC here is to minimize the electricity use of the heat pump while minimizing indoor thermal discomfort. Total discomfort is calculated as Kelvin hours outside thermal comfort band. Heat pump's electricity use is obtained from the emulator model (FMU). A day-ahead electricity price profile from real-life implementation has been chosen as a way to reflect the integration of RES in the building load profile. Furthermore, to illustrate the suitability of MPC with respect to other common control methods, a well-tuned RBC has been designed and applied to our case study and the results of this RBC are compared to the ones of MPC. In addition, we investigate the propriety of two important KPIs in scoring predictive models in the context of MPC; namely one-step ahead and multi-step ahead prediction error. In the following, constraints acting on the system along with the optimizer used in this study are described.

Constraints

Constraints acting on the system are divided into two different types. First type of constraints are the ones imposed on the inputs. The manipulated inputs considered in this study are the heat pump's on/off status (u_1) and heat pump's supply water temperature (u_2). It should be mentioned that in this study the mass flow rate of the supply water is considered constant (when the heat pump is on) during the whole simulation. The issue with the constraints on the heat pump operation is the fact that if heat pump operates with low loads, it would have a low COP, which should be avoided. Determining the point that the efficiency of the heat pump deteriorates depends on many factors, including the modulation rate of the compressor, ambient temperature and supply water temperature. Hence, imposing an accurate bound for lower modulation of the heat pump is not straightforward and would complicate the optimization problem (Verhelst et al., 2012). To avoid these complexities, a lower band for supply water temperature is imposed to avoid performing with a low COP level. The upper limit of supply water temperature is extracted from the datasheet provided by the manufacturer. To wrap up, Equations (1)-(2) show the constraints on input signals of the heating system:

$$u_1 \epsilon [0,1] \tag{1}$$

$$28 \leq u_2 \leq 45 \tag{2}$$

In which u_1 is heat pump's on/off status and is a boolean variable, 1 means heat pump is on and 0 denotes that it is off. Here, u_2 is the supply water temperature provided by the heat pump. Second type of constraint applied in this study is indoor thermal comfort bands. Comfort band

considered in this study is [20 24] from 7:00 to 23:00 with a night setback of [18 22] from 23:00 to 7:00.

$$T_{low,t} \leq T_{in,t} \leq T_{up,t} \quad (3)$$

$T_{low,t}$ is equal to the lower limits of the bands defined above and $T_{up,t}$ corresponds to the upper limit of comfort bands. In this study, building is seen as one thermal zone and one temperature is used to represent the whole building, which is the volume-averaged temperature of all 10 thermal zones in Figure 2.

OCP formulation

Now having defined constraints and the objective function, the Optimal Control Problem (OCP) can be fully formulated. To avoid the high switching frequency of heat pump, time step chosen for this study is one hour. Furthermore, a control horizon of 12 hours (N=12) has been applied in this study which is sufficiently larger than the time constant of the building and the computational load does not become too large.

$$\underset{\vec{u}_1,\vec{u}_2,\ldots\vec{u}_{k+N-1}}{\text{Min}} \sum_{k=0}^{N-1} Lv_{k+i+1} + C_{el,k+i+1}\hat{P}_{el,k+i+1} \quad (4)$$

$$\hat{T}_{in,k+i+1} = f(\vec{x}_{k+i}, \vec{u}_{k+i}, \vec{d}_{k+i}) \quad (5)$$

$$\hat{P}_{el,k+i+1} = g(\vec{u}_{k+i}, \vec{d}_{k+i}) \quad (6)$$

$$\hat{T}_{in,k+i+1} + v_{k+i+1} \geq T_{low,k+i+1} \quad (7)$$

$$\hat{T}_{in,k+i+1} - v_{k+i+1} \leq T_{up,k+i+1} \quad (8)$$

$$u_1 \epsilon [0,1] \quad (9)$$

$$28 \leq u_2 \leq 45 \quad (10)$$

$$\vec{u} = [u_1, u_2] \quad (11)$$

$$v_{k+i+1} \geq 0 \quad , i=0,1,\ldots N-1 \quad (12)$$

In these equations, u_1 and u_2 indicate heat pump's status and its supply water temperature, d_k and x_k represent disturbances acting on the system and the systems states at time step k respectively. Equation (4) describes the objective function which is composed of two terms, one for the electricity cost and the other one penalizes thermal discomfort level, C_k is the electricity cost at each time step and $\hat{P}_{k+i}$ represents the estimation of heat pump's electricity use for i steps forward in time. In equation (5), $\hat{T}_{in,k+i}$ denotes the estimation of indoor temperature i steps ahead in time, f(.) is essentially the predictive model which provides the estimated temperature profile of the building throughout the control horizon (N) while g(.) represents the estimation of heat pump's electricity use. Heat pump's electricity consumption is estimated using a quadratic function of the supply water temperature (u_2) , return water temperature ($T_{w,ret}$) and ambient temperature (T_{amb}) which is multiplied by the status of the heat pump (u_1):

$$\hat{P}_{el,k+1} = u_1 * g_{quad}(u_2, T_{ret}, T_{amb}) \quad (13)$$

g_{quad} (.) represents the quadratic function on its three arguments. Equations (7-8) show the soft constraints on thermal comfort bands designated in Equation (3). These soft constraints help the solver in coming up with a feasible solution by allowing thermal comfort bands to be violated. The latter is achieved by introducing a slack variable (v_k). Its value is penalized in the objective function given a weight of L.

Solver

Now with the OCP defined we can choose a suitable type of solver for this case study. Looking at equations (13) and (4) we realize that the second term in the objective function is a non-linear function of decision variables ($u_{1,k}$, $u_{2,k}$). Hence, even in case that linear predictive models are deployed (equation (5)), we are dealing with a mixed integer non-linear programming problem, which is most likely to be non-convex. Therefore, the solver has to be able to handle non-convex mixed integer programming problems. In this study, we used Genetic Algorithm (GA) as the solver since it has proven to be able to deal with such programming problems (Afram & Janabi-Sharifi, 2014). To achieve the latter, Matlab's GA function has been deployed (*Global Optimization Toolbox*, 2021).

Predictive Model

As it could be seen in Figure 1, a data-driven predictive model has two important attributes: dataset and modelling technique. In this section, we are going to describe these two components of predictive models.

Dataset

To train and test the data-driven models datasets are essential. If we use data from in-situ measurements for training the models, quality of the models in the simulation environment would be influenced not only by the accuracy of the predictive model but also by the accuracy of the simulation model. Thus, it will not be possible to distinguish between the impact of the model quality and emulator's accuracy on the MPC results. Hence, with respect to the goal of this study, which is investigating the effect of different modelling techniques, proxy data generated from the emulator has been used for training data-driven models instead of in-situ measurements.

To create data for training models, we generated two random sequences for the heat pump's status and heat pump's supply temperature. The resulting temperature of the emulator is shown in Fig. 4. As it could be seen in Fig. 4, the indoor temperature varies between 15.5 and 25, which fully covers the full range of thermal comfort assigned in Equation (3). Throughout this paper, this dataset is used to train and validate data-driven models. To avoid the impact of dataset bias on modelling techniques, another dataset is used to test all the models, which has not been used in training process (explained later on).

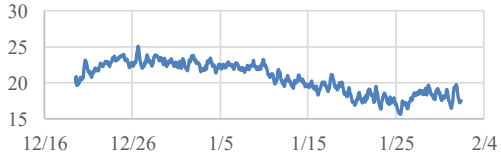

Figure 4: Temperature profile generated by feeding random sequence of inputs to emulator

Modelling technique

In this section, different modelling techniques applied for the purpose of this study are explained. Table 1 shows the general structure of these models.

Table 1- General description of the models

Model name	Model order	Inputs	R^2 (%) 1-step ahead
Grey-box 1	1	T_e, GHI, H_{in}	97.5
Grey-box 2	2	T_e, GHI, T_s, S_{hp}	97.8
State Space 1	1	T_e, GHI, T_s, S_{hp}, IHG,	97.5
State Space 2	7	T_e, GHI, T_s, S_{hp}, IHG, VFR_{av}	98
ARX	3	T_e, GHI, T_s*S_{hp}, DHI, VFR_{living}	97.5
NARX (ANN)	7	T_e, GHI, T_s, S_{hp}, IHG, VFR_{av}	98.8
SVM	---	T_e, GHI, T_s, S_{hp}, IHG, VFR_{av}	99.5

Input variables in the table are as follows:

T_e: Ambient temperature (°C)

GHI: Global horizontal irradiance (W/m^2)

T_s: Supply water temperature (u_2) (°C)

S_{hp}: Heat pump status (u_1)

H_{in}: Heat injected to building by underfloor heating (W)

IHG: Internal heat gains (W)

VFR: Volumetric flow rate of ventilation system (m^3/h)

DHI: Diffuse horizontal irradiance (W/m^2)

Grey-box Model 1

As a popular building identification method, grey-box models are included in this study. For the purpose of this study, we start with a simple structure for grey-box models (Figure 5) and we build up complexity onward. For each of the grey box models, first, the structure of the model is determined and then the parameters of the model are identified based on the training dataset. Interested readers are referred to Reynders et al., (2014) for more details on grey-box models. This grey-box model has only one state, which represents the average temperature of the indoor air.

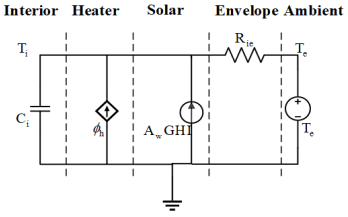

Figure 5: Grey-box model with one state

Grey-box Model 2

Another grey-box model used in this study has two states, one for the air temperature, while the other one represents the floor temperature (as the heating medium) of the building (Figure 6). Interested readers are referred to (Bacher & Madsen, 2011) for more details on this model.

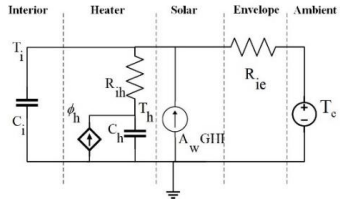

Figure 6: Grey-box model with two states

Autoregressive with exogenous inputs

One of the most common black box methods applied for building behaviour identification is Auto-Regressive with eXogenous input (ARX) models (Bourdeau et al., 2019). To develop this model, a Principle Component Analysis (PCA) has been carried out which led to the selection of optimal set of inputs (Table 1) as well as the number of output lags used for the building behaviour identification, which is three. The general structure of ARX models for identifying a multi input single output system is given in equation (14).

$$A(z)y(z) = B_1(z)u_1(z) + ...B_{n_u}(z)u_{n_u}(z) + C(z)e(z) \quad (14)$$

In this Equation, n_u stands for the number of input signals, which is five in this case (Table 1). A(), B() and C() are polynomials representing the parameter of the ARX model which are estimated using the training dataset.

State Space

Another popular modelling technique in the category of black-box models is state space identification, which has been successfully deployed for optimization of HVAC systems as well (Bourdeau et al., 2019). One of the advantages of linear state space models is the fact that most linear systems could be described using this formulation and most of the notations and theorems developed regarding MPC are based on state space representation of the systems (Maciejowski, 2002).

In this study, we focus on the Linear Time-Invariant (LTI) state space models. Two different state space models are deployed using Matlab's system Identification toolbox (*System Identification Toolbox*, 2021) .One only has one state, which is the simplest state space model possible; as for the other model, the number of states has been determined based on Singular Value Decomposition (SVD) of the Henkel Matrix for which 7 states is selected as the optimum number of states (Drgoňa et al., 2018). It should be noted that to identify this model 'Focus' is put on 'Simulation' rather than 'Prediction', which is an option provided in Matlab's system identification toolbox.

Artificial Neural Network

Artificial Neural networks (ANNs) are known as a powerful tool in machine learning. They are inspired by the structure of the brain (Abu-Mostafa, 1992). There is an ever-increasing interest in applying ANNs for HVAC system optimization applications. There are various architectures of ANNs available. One of the architectures deemed suitable for the application of building characterization is NARX which has proven successful in capturing dynamics of HVAC systems and it is selected

here as well (Bourdeau et al., 2019). These models have essentially the same input-output structure as ARX models. The main difference is that ANN-based NARX models use neurons for capturing system's dynamics instead of linear mapping in the ARX case. Interested readers can refer to (Erfani et al., 2018; Jafarinejad et al., 2019) for further details on NARX model.

Support Vector Machine

Support Vector Machine is a powerful method originally suggested for classification applications. Recently, it has been successfully applied in many regression applications as well, which is called Support Vector Regression (SVR). Like other non-linear regression techniques, SVM tries to find the function between the input and the output (*f(.)*). To carry out this task, SVM transforms the input-output space to a higher dimension space, which is called feature space. Function *f()* then would be in the form:

$$f(x) = < \omega, \Phi(x) > + b \qquad (15)$$

In which x is the input vector, Φ represents the higher dimension mapping and ω and b are parameters that are estimated by solving a convex optimization problem called the primal objective function. Operator < , > describes the kernel function in the feature space. Interested readers are referred to (Kumar & Kar, 2009) for more details on SVM.

Test Dataset

Since different combinations of the training dataset were used to train and validate the models, a second dataset was generated solely with the purpose of testing the models. As stated earlier, MPC solves an optimization problem over a given time horizon. Hence, predictive model used in the MPC should be able to provide acceptable predictions not only for one-step ahead in time but also throughout the whole control horizon. Therefore, here we are going to investigate whether one-step ahead prediction accuracy is a good enough indicator to reflect the quality of predictive models or should we look into multi-step ahead prediction accuracy. The results obtained by running the models against test dataset are presented in Figure 7.

This figure provides the boxplot accuracy of different modelling techniques used in this study. The maximum in each box corresponds to the one-step ahead prediction accuracy while the minimum corresponds to N (Control horizon) steps ahead prediction accuracy. As could be seen in Figure 7, NARX model and the SVR are the best performing models in terms of one-step ahead prediction accuracy but they are not the best models when looking into the multi-step ahead prediction.

Results

In this section, the results of deploying different predictive models in the context of MPC are brought out. The goal of this study is twofold. First, showing that integration of RES into the building energy structure is plausible by utilizing MPC. Integration of RES is considered here as a variable electricity pricing structure. The other goal of this study is finding a suitable KPI to score different predictive models, which are used in the MPC. The simulations have been carried out for a total duration of two weeks from 19th

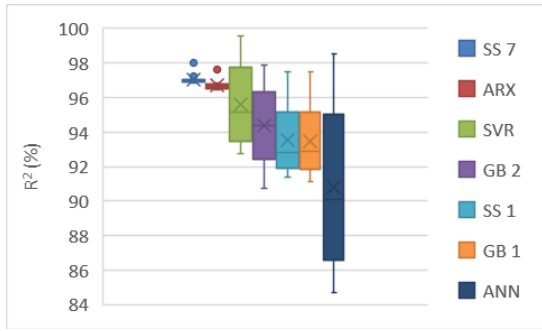

Figure 7: R^2 (%) of models against test dataset

of December to second of January. The weather data used for this study is from in-situ measurements of the building. Perfect forecast is considered for weather as well.

KPIs considered in this study based on which the MPCs are compared are total thermal discomfort level and the total electricity cost of the heating system. Attempting to analyze the results of different MPCs, we come across an impediment, which blocks the way of a straightforward comparison of the controllers. This barrier arises from the fact that the MPC aims at optimizing two objectives (thermal discomfort and electricity cost) which are not physically related to each other. Therefore, by changing the weight (L in Equation (4)) optimal performance of the controllers are obtained in a way that they yield similar discomfort levels as could be seen in Figure 8. By employing this method, we ensure that all controllers have a similar thermal discomfort so that we can compare the controllers only based on electricity cost. As could be seen in Figure 7, NARX model and the SVR are the best performing models in terms of one-step ahead prediction accuracy. Nevertheless, these two models are not the best performing models in our framework. This statement is especially more significant in the case of the NARX model since it leads to the highest electricity cost compared to the other models. Looking at MSPE, one can easily realize that, although the NARX model has the second highest one-step ahead R^2 (See Table 1), its multi-step ahead prediction performance is the poorest amongst all the models (see Figure 7). The reason for this observation is explained by the fact that ANNs easily become over-fit to training data if no regularization of some sort is used (Afroz et al., 2018). This issue should be tackled when using ANNs as predictive models otherwise one might end up with an ANN model, which is highly accurate for one-step ahead prediction but provides poor forecasts for multi-step ahead prediction.

Analyzing the results as illustrated in Figure 8, it could be concluded that the best performing MPC (deploying state space model with 7 states) compared to the RBC, reduces electricity cost from 11€ to 8.5 € which corresponds to 22.7%. Comparing different MPCs using Figure 8 we can deduce that the difference between electricity cost resulted from using different predictive models in the MPC is 7% (Electricity cost of 8.5 € in the SS7 model compared to 9.1 € achieved by using the NARX model). Considering the

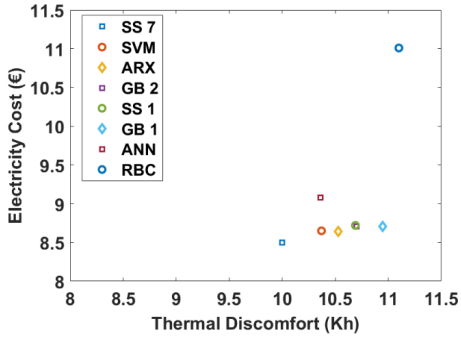

Figure 8: KPIs deploying different predictive models

22.7% as the highest potential of MPC achieved by our models for this case study, it could be inferred that the models used here vary by 24% in terms of activating the potential energy savings achieved by MPC, which demonstrates the importance of using models with high multi-step ahead prediction accuracy in the MPC.

Results obtained by applying state space model with 7 states, are presented in Figure 9 and Figure 10. It is illustrated in Figure 9 that the controller is able to maintain the temperature within the thermal comfort band although there are some minor violations. These violations could have two main causes. First, the magnitude of weight (L) scalar in the objective function, which allows thermal discomfort to some extent especially when the electricity cost is relatively high. The second reason behind the minor thermal discomfort could be the mismatch between the predictive model and the emulator. Electricity price shown in Figure 10 is based on time of use pricing structure from a supplier in Belgium. As seen in Figure 10, the load profile does not completely correspond with the time-of-use price. This observation is expected since the MPC does not optimize the building's behaviour only for one time-step but for the whole control horizon.

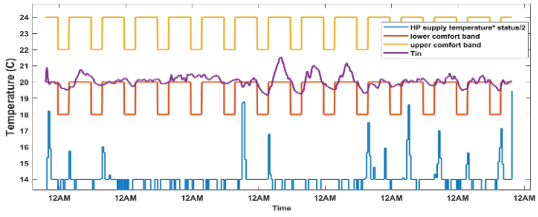

Figure 9: Building's temperature profile due to MPC

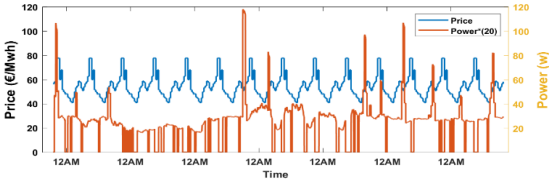

Figure 10: Electricity use against electricity price

Conclusion

Application of different data-driven models to serve as the predictor in a Model Predictive Control (MPC) are assessed. To score the predictive models in MPC, one-step ahead and Multi-Step ahead Prediction Error (MSPE) of the models are compared. Comparing performance of MPCs using different models shows that MSPE reflects the suitability of predictive models better; compared to one-step ahead accuracy. It has also been shown that models with similar one-step ahead accuracy could lead to 24% difference in terms of activating the potential cost savings achieved by MPC. On the other hand, ANN-based NARX model yielded the highest electricity cost, which is due to its poor multi-step ahead prediction performance. Furthermore, MPC is compared to a well-tuned Rule Based Controller (RBC). Best performing MPC (using state space model with 7 states) yielded 22.7% decrease in energy cost compared to the RBC.

It would be interesting to compare these models for longer simulation time and on other case studies to see whether the findings are valid or not. Another suggestion for future work is to train models based on MSPE and then check the suitability of each model. The impact of state estimator in case of grey-box and state space models have not been addressed yet and combining the dynamics of the estimator and the model might yield a better KPI for comparing these models.

Acknowledgement

This work has emerged from IEA-EBC Annex 71 project, an international project aimed at assessing building's energy performance based on in-situ measurements.

References

Abu-Mostafa, Y. S. (1992). Neural networks and learning. In *Institute of Physics Conference Series* (Vol. 127).

Afram, A., & Janabi-Sharifi, F. (2014). Theory and applications of HVAC control systems - A review of model predictive control (MPC). *Building and Environment*, *72*, 343–355.

Afroz, Z., Shafiullah, G. M., Urmee, T., & Higgins, G. (2018). Modeling techniques used in building HVAC control systems: A review. *Renewable and Sustainable Energy Reviews*, *83* (October 2017), 64–84.

Atam, E., & Helsen, L. (2016). Control-Oriented Thermal Modeling of Multizone Buildings: Methods and Issues. *IEEE Control Systems*, *36*(3), 86–111.

Bacher, P., & Madsen, H. (2011). Identifying suitable models for the heat dynamics of buildings. *Energy and Buildings*, *43*(7), 1511–1522.

Baetens, R., De Coninck, R., Jorissen, F., Picard, D., Helsen, L., & Saelens, D. (2015). Openideas - An open framework for integrated district energy simulations. *14th International Conference of IBPSA - Building Simulation 2015, BS 2015, Conference Proceedings*, 347–354.

Bourdeau, M., Zhai, X. qiang, Nefzaoui, E., Guo, X., & Chatellier, P. (2019). Modeling and forecasting building energy consumption: A review of data-driven techniques. *Sustainable Cities and Society*, *48*(April), 101533.

Da Silva, P. C., Leal, V., & Andersen, M. (2012). Influence of shading control patterns on the energy assessment of office spaces. *Energy and Buildings*, *50*, 35–48.

De Coninck, R., & Helsen, L. (2016). Practical implementation and evaluation of model predictive control for an office building in Brussels. *Energy and Buildings*, *111*, 290–298.

Djamel, Z., & Noureddine, Z. (2017). The Impact of Window Configuration on the Overall Building Energy Consumption under Specific Climate Conditions. *Energy Procedia*, *115*, 162–172.

Drgoňa, J., Arroyo, J., Cupeiro Figueroa, I., Blum, D., Arendt, K., Kim, D., Ollé, E. P., Oravec, J., Wetter, M., Vrabie, D. L., & Helsen, L. (2020). All you need to know about model predictive control for buildings. *Annual Reviews in Control*, *August*.

Drgoňa, J., Picard, D., Kvasnica, M., & Helsen, L. (2018). Approximate model predictive building control via machine learning. *Applied Energy*, *218*(March), 199–216.

Eicker, U., Demir, E., & Gürlich, D. (2015). Strategies for cost efficient refurbishment and solar energy integration in European Case Study buildings. *Energy and Buildings*, *102*, 237–249.

Erfani, A., Rajabi-Ghahnaviyeh, A., & Boroushaki, M. (2018). Design and construction of a non-linear model predictive controller for building's cooling system. *Building and Environment*, *133*(November 2017), 237–245.

EU Commission. (2018). *IN-DEPTH ANALYSIS IN SUPPORT OF THE COMMISSION COMMUNICATION* (Issue November).

Global Optimization Toolbox. (2021). https://nl.mathworks.com/help/gads/genetic-algorithm.html

Guerra-Santin, O., & Tweed, C. A. (2015). In-use monitoring of buildings: An overview of data collection methods. *Energy and Buildings*, *93*, 189–207. 2

Haddadi, M., Jafarinejad, T., & Badpar, F. (2019). Solar-hydrogen renewable supply system optimisation based on demand side management. *International Journal of Ambient Energy*, *0*(0), 1–10.

Jafarinejad, T., Erfani, A., Fathi, A., & Shafii, M. B. (2019). Bi-level energy-efficient occupancy profile optimization integrated with demand-driven control strategy: University building energy saving. *Sustainable Cities and Society*, *48*(November 2018).

Jafarinejad, T., Shafii, M. B., & Roshandel, R. (2019). Multistage recovering ventilated air heat through a heat recovery ventilator integrated with a condenser-side mixing box heat recovery system. *Journal of Building Engineering*, *24*(March), 100744.

Kumar, M., & Kar, I. N. (2009). Non-linear HVAC computations using least square support vector machines. *Energy Conversion and Management*, *50*(6), 1411–1418.

Maciejowski, J. M. (2002). *Predictive Control: With Constraints* (2nd ed.). Pearson Education.

Modelica Association Project "FMI." (2013). *Functional Mock-up Interface for Model Exchange and Co-Simulation*.

Picard, D., Drgoňa, J., Kvasnica, M., & Helsen, L. (2017). Impact of the controller model complexity on model predictive control performance for buildings. *Energy and Buildings*, *152*, 739–751.

Picard, D., Sourbron, M., Jorissen, F., Cigler, J., & Váňa, Z. (2016). Comparison of Model Predictive Control Performance Using Grey-Box and White-Box Controller Models of a Multi-zone Office Building. *4th International High Performance Buildings Conference*, 4.

Reynders, G., Diriken, J., & Saelens, D. (2014). Quality of grey-box models and identified parameters as function of the accuracy of input and observation signals. *Energy and Buildings*, *82*, 263–274.

Reynders, G., Diriken, J., & Saelens, D. (2017). Generic characterization method for energy flexibility: Applied to structural thermal storage in residential buildings. *Applied Energy*, *198*, 192–202.

Sangi, R., Kümpel, A., & Müller, D. (2019). Real-life implementation of a linear model predictive control in a building energy system. *Journal of Building Engineering*, *22*(January), 451–463.

Sepasgozar, S., Karimi, R., Farahzadi, L., Moezzi, F., Shirowzhan, S., Ebrahimzadeh, S. M., Hui, F., & Aye, L. (2020). A systematic content review of artificial intelligence and the internet of things applications in smart home. *Applied Sciences*

Sourbron, M., Verhelst, C., & Helsen, L. (2013). Building models for model predictive control of office buildings with concrete core activation. *Journal of Building Performance Simulation*, *6*(3), 175–198.

System Identification Toolbox. (2021). https://nl.mathworks.com/help/ident/index.html

Verhelst, C., Logist, F., Van Impe, J., & Helsen, L. (2012). Study of the optimal control problem formulation for modulating air-to-water heat pumps connected to a residential floor heating system. *Energy and Buildings*, *45*, 43–53.

Žáčeková, E., & Prívara, S. (2012). Control relevant identification and predictive control of a building. *Proceedings of the 2012 24th Chinese Control and Decision Conference, CCDC 2012*, 246–251.

Zhan, S., & Chong, A. (2021). Data requirements and performance evaluation of model predictive control in buildings : A modeling perspective. *Renewable and Sustainable Energy Reviews*, *January*, 110835.